Primary Biliary Cirrhosis, Macrophages and *NRAMP1*

Alexandra Mary Graham

PhD Thesis
The University of Edinburgh
1999

I hereby declare that this thesis has been composed by myself and has neither been presented or accepted in any previous application for a degree. All work presented in this thesis was, unless acknowledged, carried out by myself. All sources of information have been acknowledged by reference.

Alexandra M Graham
1999

THE UNIVERSITY OF EDINBURGH

ABSTRACT OF THESIS

(Regulation 3.5.13)

Name of Candidate Alexandra Mary Graham .....

Address .....

Degree PhD ..... *Date* 14th July 1999 .....

Title of Thesis Primary Biliary Cirrhosis, Macrophages and *NRAMP1* .....

.....

No. of words in the main text of Thesis 85000 .....

Macrophages (Mϕs) play a critical role in regulating and effecting both innate and acquired immune responses. Their presence in increased numbers and as epithelioid granulomas in the liver of patients with the chronic cholestatic liver disease primary biliary cirrhosis (PBC) suggests they may be important in the pathogenesis of this idiopathic disease. Biliary epithelial cells (BECs) of the small bile ducts are specifically targeted in this disease and their death is thought to occur via apoptosis, mediated by autoimmune mechanisms. A mycobacterial aetiology in association with specific genetic and environmental factors has been suggested in the initiation of PBC. The murine natural resistance-associated macrophage (*nramp1*) gene was identified as the gene responsible for susceptibility to a number of intracellular pathogens, including *Mycobacterium tuberculosis, Leishmania donovani* and *Salmonella typhimurium*, and has profound and pleiotropic effects on Mϕ activation and function. The gene is expressed specifically in Mϕs and granulocytes. Overexpression of the human homologue, *NRAMP1*, has been hypothesised to result in hyperstimulation of Mϕs, contributing to the pathogenesis of autoimmune and chronic diseases, while underexpression may contribute to susceptibility to infectious diseases. Rheumatoid arthritis (RA), like PBC, is an autoimmune disease in which Mϕs are propounded to play a destructive role and susceptibility has been associated with a specific microsatellite repeat polymorphic site in the 5' promoter region of *NRAMP1*. Alleles at this site affect levels of *NRAMP1* expression, the allele driving highest expression being associated with RA. Conversely, alleles at this site which fail to respond appropriately to immune stimuli, resulting in insufficient *NRAMP1* expression and incomplete Mϕ activation, have been associated with tuberculosis and leprosy. These findings support the theory that the balance of *NRAMP1* expression influences an individual's susceptibility to autoimmune or infectious disease.

This thesis reports the use of immunohistochemistry to identify increased expression of the pro-apoptotic proteins, bax and bcl-x, in BECs of PBC patients which suggests these cells are inherently susceptible to this form of programmed cell death supporting the belief that the cells die by apoptosis. An increased frequency of Ki-67 expression was also observed in BECs in PBC liver sections, showing these cells are capable of proliferation, but p53, bcl-2 and Fas/CD95 expression was similar to BECs of normal liver. Expression of *NRAMP1* was detected by reverse transcription-polymerase chain reaction (RT-PCR) in PBC and normal liver tissue. A genotyping strategy, based on restriction fragment length polymorphism (RFLP) analysis, was developed to genotype PBC and control groups for the 5' microsatellite repeat polymorphism to investigate if a similar association existed in PBC patients as RA patients. Two novel alleles were identified at this site, one of which was found at significantly increased frequency in the PBC population, though it was still uncommon. The allele driving the highest levels of expression, found at increased frequency in RA, was found at a similar frequency in the PBC population and control populations studied. To investigate the effect of overexpression of *NRAMP1*, MM6 and U937 cell lines were transfected with a plasmid constructed to drive high levels of *NRAMP1* expression. The presence and expression of plasmid sequence in transfectants was confirmed by PCR and RT-PCR, respectively. Analysis of the transfectants' divalent cation cellular content by inductively coupled plasma mass spectrometry (ICPMS) after culture in increased concentrations of manganese provide further evidence that the NRAMP1 protein is a divalent cation transporter protein, though the specificity of its substrate(s) requires further analysis.

I dedicate this thesis to my parents with love and thanks - and no, you don't have to understand it!

ACKNOWLEDGEMENTS

If due thanks were to be given to every individual by name who has been instrumental in the completion of this thesis, my acknowledgements run the risk of escalating towards a tome in themselves. I would, therefore, like to start by saying a huge thank you to all those who know they deserve to be mentioned, and also to the many who may not realise their actions have been greatly appreciated, but I feel should be acknowledged. Not one of you has been forgotten.

I feel privileged to have had the fortune of David Harrison's supervision throughout the course of this thesis. His breadth of knowledge, wisdom, inspiration and understanding have been a source of constant stimulation and admiration. How he succeeds in shedding new light on a negative situation never ceases to amaze me. I am greatly appreciative of the patience and understanding he has shown during this rather prolonged write up, and thank you seems insufficient to express my gratitude. The thought is there if not the words!!

I would also like to stress my appreciation for the help, advice and counselling Sarah Howie has provided, as she donned her 'many hats'. In her numerous guises I am indebted for her support and expertise.

How can I acknowledge the guidance, experience and friendship - not to mention those emergency supplies of dNTPs, oligo dT and *Taq* - which Frances Rae has provided? Her sympathetic ear and our mutual bewilderment as we attempted to explain the apparently inexplicable when PCRs were testing me to the limit, has been a source of comfort.

Thank you to both Stuart McKenzie and Steven Haig of the Imaging Unit for being so obliging on the photographic front. I shall never forget Steven risking body and limb for the sake of photographing those numerous gels!

Many thanks to Dr Marina Patriarca and Professor Peter Sadler for all their guidance and Marina's practical work and help with the ICPMS measurements. I appreciate all the time and effort which was so willingly given, not to mention the emails sent across the Channel from Italy.

My acknowledgements section would be incomplete without a word of thanks to my fellow scientists and students (at all levels), both past and present who have provided a stimulating and lively atmosphere in which to work. The infectious nature of the Pathology Department's innate desire to assist on all fronts spreads quickly and I shall never forget how helpful everyone has been.

Finally, I would like to acknowledge the constant support, love, patience and understanding which my parents have shown over the years. Without them none of this would have been possible. I am indebted for their long suffering nature and hope they receive due recognition.

CONTENTS

LIST OF FIGURES

LIST OF TABLES

ABBREVIATIONS AND SYMBOLS

Conventional abbreviations for the elements of the Periodic Table and the three letter abbreviations for the following amino acids have been used throughout the thesis used without defining them in the text i.e.

A	alanine	L	leucine
C	cysteine	P	proline
D	aspartic acid	Q	glutamine
E	glutamic acid	R	arginine
F	phenylalanine	S	serine
G	glycine	T	threonine
H	histidine	Y	tyrosine
K	lysine		

α	alpha
+alu	*NRAMP1* splice variant including *alu* sequence
-alu	*NRAMP1* splice variant without *alu* sequence
abc	ATP-binding cassette
aPBMC	adherent peripheral blood mononuclear cell
A. nidulans	*Aspergillus nidulans*
A. thaliana	*Arabidopsis thaliana*
A	adenine
A_x	absorbance at x nanometres
Aab	autoantibody
Ab	antibody
AB	avidin-biotin
ABComplex	avidin-biotin complex
ABComplex-HRP	horse radish peroxidase conjugated ABComplex
ADCC	antibody dependent cell cytotoxicity
ADP	adenosine diphosphate
AIC	autoimmune cholangitis
AIDS	acquired immune deficiency syndrome
AIF	apoptosis inducing factor
ALD	alcoholic liver disease
AMA	anti-mitochondrial antibody
Amp	ampicillin
Amp^R	ampicillin resistance gene
AP	alkaline phosphatase
Apaf-1	apoptosis protease-activating factor 1
APC	antigen presenting cell
APS	ammonium persulphate
ATP	adenosine triphosphate
A_x	absorbance at x nanometres
β	beta

β-gal	β-D-galactosidase
β-gal plasmid	pSV-β-galactosidase Control Vector
b	now designated rat *nramp2* locus (locus mutated in Belgrade rat)
bcg	now designated murine *nramp1* locus
bind silane	γ-methacryloxypropyltrimethoxysilane
bp	base pair
bsd2	bsd2 protein
B10R	resistant B10 mouse strain (wild type *nramp1*)
B10S	susceptible B10 mouse strain (mutated *nramp1*)
BALB/c	susceptible mouse strain (mutated *nramp1*)
BCIP	5-bromo-4-chloro-3-indolyl phosphate
BEC	biliary epithelial cell
BCG	Bacillus Calmette-Guréin
BH	bcl-2 homology domains
BSA	bovine serum albumin
BSD2	bsd2 gene
cdk	cyclin-dependent kinase
conserved transport motif	binding protein-dependent transport system inner membrane component signature
C	cytosine or carboxy for protein/peptide description
C57/Bl	C57/Black
C. spp.	*Candida species* except
C. elegans	*Caenorhabditis elegans*
cDNA	complementary DNA
cNOS	constitutive nitric oxide synthase (NOSI)
CAD	caspase activated deoxyribonuclease
CCl_4	carbon tetrachloride
CD	clusters of differentiation
CFA	complete Freund's Aadjuvant
CFU-GM	colony-forming unit, granulocyte-macrophage
CGD	chronic granulomatous disease
CHS	Chadiak-Higashi syndrome
CK	cytokeratin
CMI	cell mediated immune
CMC	chronic mucocutaneous candidiasis
CMV	cytomegalovirus
CNS	central nervous system
CNSDC	chronic non suppurative destructive cholangitis
CR	complement ereceptor
CREST	calcinosis, Reynaud's phenomenon, oesophageal dysfunction, sclerodactyl and telangiectasis
CSF	colony stimulating factor
CTL	cytotoxic T lymphocyte
CVID	common variable immunodeficiency
δ	delta
dATP	deoxyadenosine triphosphate

dCTP	deoxycytidine triphosphate
dGTP	deoxyguanosine triphosphate
dNTP	deoxynucleotide triphosphate
dTTP	deoxythymidine triphosphate
ddATP	dideoxyadenosine triphosphate
ddCTP	dideoxycytidine triphosphate
ddGTP	dideoxyguanosine triphosphate
ddTTP	dideoxythymidine triphosphate
dH_2O	distilled water
D. melanogaster	*Drosophila. melanogaster*
DAB	3,3'diaminobenzidine
DAT	Na^+- and Cl^--dependent dopamine reuptake carrier
DBA/2	resistant mouse strain (wild type *nramp1*)
DC	dendritic cell
DCT1	divalent cation transporter 1 (rat nramp2)
DEAE	diethylaminoethyl
DEPC	diethyl pyrocarbonate
DMS	dimethyl suberimidate
DMSO	dimethyl sulphoxide
DNA	deoxyribonucleic acid
DNase	deoxynuclease
DOPE	dioleoyl phosphotidylethanolamine
DOSPA	2,3-dioleyloxy-N-[2(sperminecarboxamido)ethyl]-N,N-dimethyl-1-propanaminium trifluoroacetate
DOSPER	1,3-di-oleoyloxy-2-(6-carboxy-spermyl)-propylamide
DOTMA	N-[1-(2-3-dioleyloxy)propyl]-n,n,n-trimethylammonium chloride
DTH	delayed type hypersensitivity
DTT	dithiothreitol
E. coli	*Escherichia coli*
EAE	experimental autoimmune encephalomyelitis
EAN	experimental autoimmune neuritis
EASY	Enhanced Analysis System
EDTA	ethylenediaminetetra acetic acid
EGTA	ethylene glycol-bis (β-aminoethyl ether)-N,N,N',N'-tetraacetic acid
ELISA	enzyme linked immunosorbant assay
EPR	electron paramagnetic resonance
ER	endoplasmic reticulum
EST	expressed sequence tag
EtBr	ethidium bromide
$F(ab')_2$	fragment antigen binding
FADD	Fas-associated death domain, also called Mort1
FAK	focal adhesion kinase
Fc	fragment crystallisable
FcR	Fc receptor
FCS	fetal calf serum

FIM	factor increasing monocytopoiesis
g	gramme or acceleration due to gravity
γ	gamma
γ-IRE	IFNγ response element
G	guanine
G418	G418 sulphate/Geneticin
GAPDH	glyceraldehyde-3-phosphate dehydrogenase and PCR for its detection described in **2.8.2**
GAS	IFNγ activating sequence
GBS	Guillain-Barré Syndrome
GM-CSF	granulocyte macrophage colony-stimulating factor
GMEM	Glasgow minimum essential medium
GSH	reduced glutathione
GST	glutathione S-transferase
GVHD	graft-versus-host disease
H^+	hydrogen ion
H_2O_2	hydrogen peroxide
HBS	HEPES-buffered saline
HBSS	Hanks' balanced salt solution
HIV	human immunodeficiency virus
HLA	human leukocyte antigen
HOME	Highly Optimised Microscope Environment
HRP	horse radish peroxidase
iNOS	inducible nitric oxide synthase (NOSII)
i.p.	intra peritoneal
i.v.	inta venous
IAP	inhibitor of apoptosis
IBD	inflammatory bowel disease
IBP-1	interferon binding protein-1
ICAM-1	intercellular adhesion molecule-1
ICPMS	inductively coupled plasma mass spectophotometry
IFA	incomplete Freund's adjuvant
IFN	interferon
IFNγR	interferon gamma receptor
Ig	immunoglobulin
IGF	insulin-like growth factor
IGF-BP3	insulin-like growth factor binding protein 3
I-κB	inhibitor of κB
IKK	inhibitor of κB kinase complex
IL	interleukin
Inr	initiator
IP_3	inositol triphosphate
IRE	iron-responsive element
IRP	iron regulatory protein
ISRE	interferon-stimulated response element
Ity	now designated murine *nramp1* locus
JNK	jun kinase

JNKK	JNK kinase
kb	kilo base
kDa	kilo dalton
KC	Kupffer cell
KLH	keyhole limpet haemocyanin
λ	wavelength
l	litre
lps^{n}	normal *lps* locus
lps^{d}	defective *lps* locus
L. spp.	*Leishmania species* except
L. monocytogenes	*Listeria monocytogenes*
L. pneumophilia	*Legionella pneumophilia*
lacZ	gene encoding β-D-galactosidase
LACK-Δ1	Leishmania activator of cell kinases
LAD	leucocyte adhesion deficiency
LAK	lymphokine activated killer
L-broth	Luria-Bertani broth
LBP	LPS binding protein
LDL	low density lipoprotein
LFA-1	lymphocyte function associated antigen 1
LOD	logarithm of the odds
LPS	lipopolysaccharide
LPG	lipophosphoglycan
Lsh	now designated murine *nramp1* locus
μg	microgramme
μl	microlitre
μm	micrometre
μM	micromolar
mA	milliampere
map	mitogen-activated protein
mg	milligramme
mk	now designated murine *nramp2* locus (locus mutated in mice with microcytic anaemia)
ml	millilitre
mM	millimolar
mRNA	messenger RNA
mvl	*malvolio* (*Drosophila nramp* homologue)
M. spp.	*Mycobacterium species*
Mϕ	macrophage
MAC	membrane attack complex
MAP	microtubule-associated protein
MBP	mannose binding protein
M-CSF	macrophage colony-stimulating factor
MEKK1	MAP/Erk kinase kinase-1
MHC	major histocompatibility complex
MIF	migration inhibitory factor

Milli-Q dH_2O	Ultrapure UV treated dH_2O from a Milli-U10 and Milli-Q_{plus} 185 system (Millipore, Watford UK)
MLR	mixed lymphocyte reaction
MM6	Mono Mac 6
Mn-SOD	manganese dependent superoxide dismutase
MPO	myeloperoxidase
MPS	mononuclear phagocyte system
MS	multiple sclerosis
neo	neomycin phosphotransferase gene
neoF1	PCR described in **2.8.5**
neoFexp	PCR described in **2.8.6**
nm	nanometre
nramp1	mouse natural resistance-associated macrophage protein 1 gene
nramp2	mouse natural resistance-associated macrophage protein 2 gene
nramp1	mouse natural resistance-associated macrophage protein 1protein
nramp2	mouse natural resistance-associated macrophage protein 2 protein
N	nolar or amino for protein/peptide description
NADPH	reduced form of nicotinamide adenine dinucleotide phosphate
NBT	nitro blue tetrazolium
NHS	normal human serum
NIK	NF-κB-inducing kinase
NK	natural killer
nm	nanometre
NMMA	N^G-monomethyl-L-arginine
NO	nitric oxide
NOS	nitric oxide synthase
NOSI	see cNOS
NOSII	see iNOS
NRAMP1	human natural resistance-associated macrophage protein 1 gene
NRAMP2	human natural resistance-associated macrophage protein 2 gene
NRAMP1	human natural resistance-associated macrophage protein 1 protein
NRAMP2	human natural resistance-associated macrophage protein 2 protein
NRAMPalu	PCR described in **2.8.3**
NRAMPpol	PCR described in **2.8.1**
NRpCI	PCR described in **2.8.4**
NRS	normal rabbit serum
NSS	normal swine serum
O. sativa	*Oryza sativa*

O_2^-	superoxide
OD	optical density
$^{\cdot}OH$	hydroxyl radical
OPD	o-phenylenediamine
ORF	open reading frame
OsNramp	OsNramp gene
OsNramp	OsNramp protein
pCIneo plasmid	pCI-neo Mammalian Expression Vector
pmol	picomole
PAK2	p21-activated kinase
PBC	primary biliary cirrhosis
PBL	peripheral blood lymphocyte
PBMC	peripheral blood mononuclear cell
PBS	phosphate buffered saline
PBST	PBS/0.05% Tween 20
PCD	programmed cell death
PCR	polymerase chain reaction
PDC	pyruvate dehydrogenase complex
PDC-E2	dihydrolipoamide acetyltransferase component of PDC
PDGF	platelet derived growth factor
PEP	processing enhancing protein
PGE_2	prostaglandin E_2
PHA	phytohaemagglutinin
PKC	protein kinase C
PLL	poly-L-lysine
PMA	phorbol-myristate-acetate
PMSF	phenyl methyl sulphonyl fluoride
PNS	peripheral nervous system
PPD	purified protein derivative
PSC	primary sclerosing cholangitis
PSS	progressive systemic sclerosis
rbc	red blood cell
rpm	revolutions per minute
RA	rheumatoid arthritis
RAIDD	RIP-associated Ich-1/CED3 homologous protein with a death domain
RAM-BIO	biotinylated rabbit anti-mouse Ig antibody
RAM-HRP	HRP conjugated rabbit anti-mouse Ig antibody
RE	reticuloendothelial system
RFLP	restriction fragment length polymorphism
RIP	receptor interacting protein
RNA	ribonucleic acid
RNase	deoxyribonuclease
ROI	reactive oxygen intermediate
RT	reverse transcriptase
s.c.	sub cutaneously
spp.	*species*

S. spp.	*Schistosoma species* except
S. aureus	*Staphylococcus aureus*
S. cerevisiae	*Sacharomyces cerevisiae*
S. dublin	*Salmonella dublin*
S. gordonii	*Streptococcus gordonii*
S. parasanguis	*Streptococcus parasanguis*
S. pneumoniae	*Streptococcus pneumoniae*
S. typhimurium	*Salmonella typhimurium*
SAR-BIO	biotinylated swine anti-rabbit Ig antibody
SAP	shrimp alkaline phosphatase
SAR-HRP	HRP conjugated swine anti-rabbit Ig antibody
SCID	severe combined immunodeficienct
SDS	sodium dodecyl sulphate
SDS-PAGE	SDS-polyacrylamide gel electrophoresis
SH3	src homology 3
SITS	4-acetamido-4'-isothyocyanatostibene-2,2'-disulphonic acid
SLE	systemic lupus erythematosus
SOD	superoxide dismutase
transpo	
T	thymine
T. spp.	*Toxoplasma species*
TAP	transporters associated with antigen processing protein
TBE	tris-borate EDTA
TB	tuberculosis
TBS	Tris buffered saline
TBST	TBS Tween
TCR	T cell receptor
TE	Tris-EDTA
TEMED	N,N,N',N',-tetramethylethylene diamine
Tf	transferrin
TfR	transferrin receptor
TGF	transforming growth factor
Th	T lymphocyte helper
Tm	melting temperature
TM	transmembrane
TMB	tetramethylbenzadine
TNF	tumour necrosis factor
TNFR	TNF receptor
TRADD	TNFR-associated death domain
TRAF2	TNFR-associated factor-2
Tween 20	polyoxyethylene-sorbitan monolaurate
U	unit
UDCA	ursodeoxycholic acid
UV	ultraviolet light
vATPase	vacuolar H+/ATPase
VCAM-1	vascular cell adhesion molecule-1

WAS	Wiskott-Aldrich syndrome
WHO	World Health Organisation
X-gal	5-bromo-4-chloro-3-indoyl- β-D-galactoside

1 INTRODUCTION

It is ninety one years since Elie Metchnikoff and Paul Ehrlich were awarded the Nobel Prize for Physiology and Medicine (Metchnikoff 1989) "in recognition of their work on immunity". Metchnikoff's observation, some twenty five years earlier in 1882, when he introduced small tangerine thorns into the larvae of *Bipinnaria* (starfish), of "a mass of moving cells surrounding the foreign bodies" was a turning point, not only in his own personal life, but for the discipline, and our understanding, of immunology. The eminent scientist, primarily an embryologist, has been associated with the terms "phagocytosis" to describe the engulfment of cellular or particulate matter, and "phagocyte" (cell eater) as the cell which undertakes the phagocytosis.

The great scientists working at the turn of the century laid the seeds which have flourished into modern day immunology. Though they could not reconcile all their observations, and a battle as vehement and ferocious as that between pathogen and immune system appeared to rage between the advocates of cellular and humoral immunity, it is fascinating to see how many of their theories of "amboceptor", "complement", "endolysis", "leukins" and "endotoxins", for example, have been elaborated and elucidated over the years. Perhaps one of the most important lessons we can learn since their polemics is the holistic nature of the immune system which we know to act as a concerted whole with cellular, humoral, innate and acquired components orchestrating an effective defence system. It will be important to remember through the course of this thesis, though the focus will be on the role of the macrophage (Mϕ) (synonymous with Metchnikoff's white corpuscle phagocyte), that the action of this cell, though of major importance, constitutes only one component of the complex system of interacting cells, chemicals and proteins we know as the immune system.

1.1 PRIMARY BILIARY CIRRHOSIS

Twenty eight percent of the first 227 orthotopic liver transplantations carried out by the Scottish Liver Transplantation Unit between 1992 and 1997 were for end stage

primary biliary cirrhosis (PBC), the greatest single reason for transplantation. (**Appendix A**). This statistic reflects, in part, amongst ethical considerations, favourable prognosis post transplantation, organ-patient compatibility etc., the paucity of effective treatment regimes for this disease making liver transplantation a necessity for the survival of sufferers with advanced disease.

PBC is an idiopathic, progressive, cholestatic liver disease and somewhat of a misnomer in so far as a presymptomatic and precirrhotic stage of the disease may last for many years before true cirrhosis is established as the disease progresses (Portmann and MacSween 1987). The term chronic non suppurative destructive cholangitis (CNSDC) may be a more accurate description of the initial lesions where destruction of biliary epithelial cells (BEC) of ducts between 30μm and 100μm diameter can be observed histologically.

PBC remains poorly understood, despite documentation of its symptoms as early as the 1800s (reviewed in Jorge and Leuschner 1996), but the bile duct damage is believed to be mediated by autoimmune mechanisms. Indeed PBC has been cited as the paradigm of organ-specific autoimmune diseases (Gershwin and Mackay 1997) where there is a breakdown of immunological self tolerance. In an organ specific disease of this sort the body's immune responses target self tissue and the reactions are limited to a particular organ, which in the case of PBC is the BECs of small to medium sized bile ducts in the liver.

1.1.1 Clinical Features

Patients with PBC usually present with intense pruritis, increasing skin pigmentation and eventually cholestatic jaundice, though icterus may not develop for months or years after the initial symptoms. 30% of patients exhibit xanthomas/xanthelasma. Weight loss and fatigue are other common symptoms and portal hypertension may manifest itself before cirrhosis is established. Asymptomatic patients may be identified due to hepatomegaly, raised serum alkaline phosphatase or anti-mitochondrial antibody (AMA) levels in the serum and it is possible for these

patients to experience a normal life expectancy. Symptomatic patients may survive for 5-15 years but the onset of jaundice heralds a worsening prognosis and clinical deterioration. Patients with advanced PBC may suffer pathologic fractures due to osteomalacia and osteoporosis. PBC is ultimately fatal, usually due to hepatocellular failure with approximately a third of cases suffering from bleeding from oesophageal varices (Portmann and MacSween 1987; Borum 1998).

1.1.2 Histology

Histologically PBC is divided into four stages (Scheuer 1988) though an individual biopsy section or biopsies taken from different areas of the same liver may show characteristics of more than one of these stages due to the chronic, segmental and progressive nature of the disease.

Stage I is characterised by florid bile duct lesions and necrotic bile ducts with BECs appearing shrunken and vacuolated. Granulomatous inflammation consisting of lymphocytes, plasma cells, histiocytes, eosinophils and giant cells surround the lesions and it is the presence of granulomas in PBC biopsy sections which is characteristic of the disease. Inflammation spreads out from the portal triads in stage II and biliary piecemeal necrosis characterised by vacuolated periportal hepatocytes, surrounded by foamy Mϕs is observed. The fibrosis progresses to scarring in stage III and fibrous septa link adjacent portal tracts. Cholestasis may be apparent due to the deposition of copper-associated protein. Stage IV is characterised by the presence of established cirrhosis.

1.1.3 Incidence of PBC

As with many autoimmune diseases there is a preponderance of female sufferers, with an incidence of approximately nine female sufferers per male sufferer (Borum 1998), though the disease is similar in both sexes. It has generally been postulated that hormonal differences are key to the different incidence of many autoimmune diseases between sexes, but an interesting theory has been proposed for the 90% female bias of systemic lupus erythematosus (SLE) sufferers which may also be applicable to PBC (Stewart 1998). X-chromosome inactivation in females leads to

two classes of cells differing in a subset of transcribed genes and hence, self proteins expressed and presented by these cells will also differ. A skew in X-inactivation of one of the X chromosomes in key antigen presenting cells (APC) such as dendritic cells (DC) could result in the evasion of tolerance induction of T lymphocytes in the thymus towards the silenced genes' products of the inactivated X chromosome.

PBC typically affects middle aged females with a peak incidence among 40-60 year olds, though onset in childhood has been reported which may or may not be a special paediatric form of PBC (Melegh *et al.* 1998). Estimates of disease prevalence vary between 20 and 240 cases per million population with an annual incidence between 4 and 30 per million (Hislop 1980; Triger 1980; Watson *et al.* 1995; reviewed in Kaplan 1996; reviewed in Metcalf and James 1997; reviewed in Neuberger 1997). The reported incidence of PBC is increasing but it is not known if this represents a true increase in disease prevalence or a greater awareness of the disease (reviewed in Neuberger 1997).

1.1.4 Aetiology

The aetiology of PBC remains a mystery. A geographical variation in incidence has been reported, with a low incidence in the Indian and African subcontinents (Portmann and MacSween 1987; Neuberger 1997) and a familial history of PBC is widely accepted as a predisposing factor to development of disease (Bach and Schnaffer 1994; Jorge and Leuschner 1996; reviewed in Neuberger 1997). This familial association suggests genetic factors may make certain individuals more susceptible to the effects of additional environmental and/or infectious agents, which together initiate the disease. To date studies to identify predisposing genotypes or mutations have failed to identify genes playing a major role and the search is still on to identify susceptibility loci.

A variety of infectious agents have been suggested which may trigger PBC initiation via a molecular mimicry mechanism (Burroughs *et al.* 1992; reviewed in Galperin and Gershwin 1996; reviewed in Jones 1996). PBC patients have been reported to have a higher incidence of urinary tract infections with *Escherichia coli (E. coli)*

which has been suggested to contribute to the onset of disease (Burroughs *et al.* 1984), though there is doubt whether this is prevalent across the whole PBC population (reviewed in O'Donohue and Williams 1996a). The sera from PBC patients has been shown to contain antibodies (Ab) reactive against *Mycobacterium. gordonae* (*M. spp.*) which cross react with the major mitochondrial autoantigens, to be discussed in **1.1.5.1** (Vilagut *et al.* 1994a). *M. gordonae* deoxyribonucleic acid (DNA) has also been detected in PBC liver sections (Vilagut *et al.* 1994b) though this has not been conclusively established (O'Donohue *et al.* 1998). Antigens cross-reactive with PBC specific autoantigens have also been found to be expressed in gram negative bacteria (*Enterobacteriacae* and *Salmonella*) and gram positive bacteria have been suggested as potential factors initiating disease (Hiramatsu *et al.* 1998) supporting the hypothesis of a bacterial aetiology (Stemerowicz *et al.*1988).

Using confocal laser scanning microscopy lipopolysaccharide (LPS) has been identified, by immunofluorescence, in BECs and to a lesser level in infiltrating cells around the bile ducts and hepatocytes (Sakisaka *et al.* 1997) and has been proposed to facilitate the expression of adhesion molecules by BECs, accelerating infiltration of inflammatory cells which may then target and attack the BECs. The endotoxin may also be released from BECs into the portal areas leading to infiltration of inflammatory cells around the bile ducts.

The association of viral infections with the onset of PBC has also been proposed and challenged (Podda *et al.* 1990; Le Cann *et al.* 1997; Malamud *et al.* 1997; reviewed in Neuberger 1997; Wang and Tschen 1997) and remains an area for continued study.

The familial association of PBC (Bach and Schaffner 1994) has led to many studies analysing particular genetic loci for an association with the disease. In the majority of cases these have failed to identify any strong association or where a positive association has been alleged to exist subsequent analysis has often proven controversial.

The most obvious candidate locus for association with an autoimmune mediated disease is the major histocompatibility complex (MHC) containing region of the genome. However, the existing data remains far from clear with possible associations with human leukocyte antigen (HLA)-DR3, HLA-DR8, HLA-DR2, HLA-DPB1, HLA-DRB4, HLA-DR8-DQB1*04, HLA-DRB1*0301-DQA1*0501-DQB1*0201 amongst others being reported (Ercilla *et al.* 1979; Clemente *et al.* 1998; reviewed in Leung *et al.* 1996; Lindgren *et al.* 1998). These and other studies (Santrach *et al.* 1990; Fugger *et al.* 1991; Morling *et al.* 1992; Underhill *et al.* 1992 and 1995; Gregory *et al.* 1993; Seki *et al.* 1993; Onishi *et al.* 1994; Zhang *et al.* 1994a; Mella *et al.* 1995) leave the possible HLA association unresolved. Based on circumstantial evidence a "three-way mimicry" hypothesis has been proposed to account for the role of MHC haplotypes in a number of autoimmune diseases, including PBC, and may be a possible explanation for the lack of strong HLA linkage to PBC (Baum and Staines 1997).

Studies to investigate polymorphisms at the tumour necrosis factor (TNF)-α (Fugger *et al.* 1989; Spengler *et al.* 1990; Messer *et al.* 1991; Gordon *et al.* 1996; Watt *et al.* 1997; Tanaka *et al.* 1998 and 1999; Jones *et al.* 1999), transporters associated with antigen processing protein (TAP)1 and TAP2 (Gregory *et al.* 1994), GSTM1 (Davies *et al.* 1993), interleukin (IL)-10 (Zappala *et al.* 1998), CTLA-4 (Agarwal *et al.* 1998) and C4B2 (Briggs *et al.* 1987) loci have been carried out but to date only weak or unconfirmed associations for TNFα and C4B2 have been reported.

1.1.5 Immunological Aspects

The autoimmune basis for PBC is supported by:

1. The frequent association of PBC with other immunological abnormalities or autoimmune disease including "sicca complex", CREST syndrome (calcinosis, Reynaud's phenomenon, oesophageal dysfunction, sclerodactyl and telangiectasis), rheumatoid arthritis (RA), polyarthritis, autoimmune thyroiditis,

renal tubular acidosis, coeliac disease, SLE and intestinal pulmonary fibrosis (reviewed in Kaplan 1996).

2. The increased frequency of certain MHC antigens i.e. HLA-DRW8, though these findings are inconsistent in different populations.

3. The presence of infiltrates containing T lymphocytes within the portal tract which show histological evidence of bile duct damage.

4. A number of immunological abnormalities including MHC Class II antigen expression and *in vitro* T cell proliferative responses.

5. The frequent association of numerous serum autoantibodies (AAb).

1.1.5.1 Autoantibodies

The first evidence suggesting PBC may have an autoimmune component arose in 1958 when complement fixing anti-tissue Abs were identified in patients' sera, with subsequent detection of Abs to cell mitochondria (reviewed in Mackay 1994). However, it took until the late 1980s to identify the dihydrolipoamide acetyltransferase component of the pyruvate dehydrogenase complex (PDC-E2) as the major autoantigen reacting with PBC sera and show that the AAbs were reacting against the non-catalytic, inner lipoyl domain of the E2 component (Fussey *et al.* 1990; reviewed in Neuberger 1997). Though the inner lipoyl domain of PDC-E2 may contain important B cell epitopes it appears that only a minority of PBC patients' T cells, which are responsive to PDC, respond to lipoylated recombinant PDC-E2 inner lipoyl domain or a lipoylated peptide of this domain (Palmer *et al.* 1999). In addition to antibodies reacting with PDC-E2 PBC patients frequently possess AAbs reactive against other components of the pyruvate dehydrogenase complex and the two other 2-oxoacid dehydrogenase enzyme complexes (2-oxoglutarate dehydrogenase and branched-chain 2-oxoacid dehydrogenase). Anti-nuclear (gp210, Sp100), anti-alpha-enolase, anti-platelet, anti-thyroid, anti-centromere and anti-DNA Abs amongst other

AAbs have also been identified in PBC sera (Akisawa *et al.* 1997; Feistauer *et al.* 1997; reviewed in Neuberger 1997; Tsuji *et al.* 1997; Luettig *et al.* 1998).

One of the presently accepted criteria for the diagnosis of PBC is the presence of anti-mitochondrial antibodies (AMA). Some advocate the presence of an AMA titre ≥1/40 is strongly suggestive of PBC, even in the absence of symptoms and the presence of normal alkaline phosphatase levels (Mitchison *et al.* 1986). However, there is a subset of patients presenting with "PBC symptoms" clinically and histologically, bar the presence of AMAs, who would previously have been diagnosed as suffering from PBC, but are now diagnosed with autoimmune cholangitis (AIC). The lack of AMAs in these patients initially appeared to be the only factor distinguishing them from PBC sufferers, questioning a genuine need for such a distinction and challenging the notion that the AMAs are truly pathogenic, at least in initiation of PBC, or even disease specific, as AMA are also found in the general population (though these may be of a different specificity). However, there is some evidence that there is a greater frequency of anti-nuclear antibodies, lower serum immunoglobulin (Ig) M levels, a lower frequency of the DR8 genotype and serum aspartate aminotransferase levels may differ in AIC patients compared to PBC patients (Czaja *et al.* 1998). Despite these observations it is still unclear whether AIC is a distinct disease. In fact it is probable that AIC is a cholestatic liver disease with a natural history similar to AMA positive PBC despite some differences in serology (reviewed in Heathcote 1997).

1.1.5.2 T lymphocytes

It has been postulated that clusters of differentiation (CD) 8+ cytotoxic T lymphocytes (CTL) mediate BEC damage in PBC. Indeed, a decrease in the number of CD8+ and CD28+ cells in peripheral blood of patients has been reported which may reflect infiltration of these cells into the liver (Moreno-Otero *et al.* 1994; Kurokohchi *et al.* 1998) and the lymphocytes observed in close contact with BECs have been reported to show similar morphology to that of cytotoxic lymphocytes observed in *in vitro* lymphocytotoxic systems (Bernuau *et al.* 1981). CD8+ lymphocytes have been observed infiltrating the damaged bile ducts over the

basement membrane (Deguchi *et al.*1998). As well as CD8+ T lymphocytes CD4+ cells are present in the lymphoid infiltrates within the liver, particularly around the portal tracts. The CD4+ T lymphocytes may partake in the destructive process via cytokine secretion, augmentation of CD8+ lymphocyte cytotoxicity mediated against BECs and/or enhancing B lymphocyte/plasma cell activity. There is evidence that T cell expansion in PBC patients is antigen driven and multiple T cell clones accumulate in the liver (Ohmoto *et al.* 1997; Okamoto *et al.* 1998). An increase in the memory ($CD4+CD45RA^{-}RO^{high}$) to naive ($CD4+CD45RA^{high}RO^{-}$) T lymphocyte ratio in peripheral blood lymphocytes and liver infiltrating lymphocytes has been reported implying cells of the former subset are functionally potent, requiring less stimulation to become activated (Björkland *et al.* 1991; Leon *et al.* 1995a). The literature regarding the T cell phenotype of the lymphocytes in PBC remains inconclusive and controversial (reviewed in Van de Water *et al.* 1997) exemplifying that the situation is complex and remains a conundrum for future study.

In the light of the infectious agent initiator hypothesis (**1.1.4**) it is interesting to note that expression of the CD1d antigen has been identified in periductal granulomas and early stage bile ducts in PBC liver (Tsuneyama *et al.* 1998). CD1d is one of a family of CD1 MHC Class I-like molecules which are believed to be important in non-Class I or -Class II antigen presentation pathways. The CD1 molecules can present microbial non-peptide lipid antigens to CD4-/CD8- T lymphocytes and it is possible that the CD1d molecules expressed in PBC granulomas and small bile ducts may be serving this purpose. Though CD1d expression was also observed in granulomas in the liver of patients with sarcoidosis the ductal epithelial staining was virtually unique to early stage PBC liver, the exception being one primary sclerosing cholangitis (PSC) case. The positive ducts in the PBC cases were all less than 100μm, i.e. those destined for destruction, and no late stage cases were positive. It is interesting to speculate whether this aberrant CD1d expression is involved in antigen presentation to surrounding T lymphocytes and what the nature of the antigen might be. Mycobacterial or bacterial components are prime candidates though modified

endogenous lipidic compounds related to bile ducts or biliary substance are other possibilities.

1.1.5.3 Cytokines

On the basis that PBC is an immunologically based disease analysis of the patients' cytokine expression profile and pattern may help elucidate the nature of the disease. However, this task is not an easy one because the majority of the patient liver material available for study represents late stage disease, by which point it may be argued that the immunological responses present are likely to have little bearing on those initiating the disease. Many early studies examined the cytokine expression profiles of peripheral blood mononuclear cells (PBMC), which may be unrepresentative of the situation in the liver, and the majority of studies have looked at mRNA levels which do not necessarily correspond to protein levels or give any indication of the origin of expression.

Individual T lymphocytes may express a variety of cytokines but chronic immune responses are often dominated by a T lymphocyte helper (Th) 1 (i.e. interferon (IFN) γ, IL-12, TNFα) or Th2 (IL-4, IL-5, IL-10) type cytokine profile (reviewed in Janeway and Travers 1994). Th1 and Th2 T lymphocytes develop from the same CD4+ T helper lymphocytes and the differentiation pathway is determined by the type of stimulation the precursor receives, in particular the cytokine environment present at the time of antigen recognition. The principal effector function of Th1 cells is in phagocyte and cell mediated immune (CMI) responses against infections. Th2 type responses are effective against extracellular pathogens such as helminths and arthropods and Th2 cytokines stimulate B lymphocytes to enhance antibody mediated responses. Though a Th1 mediated response is highly desirable in resolving a variety of infectious agents, under certain circumstances an inappropriate or exaggerated response may occur which proves detrimental to the host, resulting in self tissue damage and pathology. These undesirable responses are known as delayed type hypersensitivity (DTH) responses and are believed to be the pathological cause of many autoimmune diseases.

The differentiation of naive CD4+ lymphocytes into Th1 or Th2 cells is influenced by cytokines produced early in response to the initiating agent such that the orchestrators of the innate response have a profound effect on the evolution and development of the acquired response. Mϕs infected with *Listeria, Mycobacterium* or *Leishmania* produce IL-12 which initiates development of a Th1 response and natural killer (NK) cells can be stimulated by viruses, for instance, to produce IFNγ which acts on Mϕs to induce IL-12 secretion. This scenario illustrates an important link between an innate immunity mediator, IL-12, and a specific immune response and the central role of the Mϕ in development of the latter. IL-12 also enhances CTL and NK cell activity and IFNγ release, which inhibits development and enhancement of a Th2 response. When a response is initiated in the presence of IL-4 development of a Th2 response follows. As for the Th1 response there is a reciprocal inhibitory effect of the Th2 cytokine IL-10 on development of a Th1 response.

It would be helpful to determine whether the immune response mediating PBC is mainly a Th1 or Th2 response because there is the potential to manipulate these responses and hence, hopefully, alleviate the cellular destruction. When late stage liver biopsies and extracts have been analysed by RT-PCR there appears to be variations in patients' expression profiles between and within studies but IL-1 and TNFα levels have been reported to be negative or reduced compared with controls (Tovey *et al.* 1991; Shindo *et al.* 1996). In contrast, Yasoshima and colleagues identified increased expression of TNFα and IL-6, by immunohistochemistry and *in situ* hybridisation, in BECs of stage I and stage II PBC biopsies. Other hepatobiliary disease BECs showed mild or moderate expression while expression in normal liver samples was mild or absent. TNF receptor and IL-6 receptor α-chain were also detected on damaged bile ducts (Yasoshima *et al.* 1998). Analysis of IL-1β, IL-2, IL-6, IFNγ and transforming growth factor (TGF) β expression levels showed little difference between PBC patients and autoimmune chronic active hepatitis patients in one study, except for more frequent IFNγ expressing PBC patients. However, IL-5 mRNA expression was confined to PBC patients (Martinez *et al.* 1995). The elevated IL-5 levels may contribute to the high eosinophilia reported in PBC livers,

particularly in those showing stage I and II histology (Nakamura *et al.* 1996; Yamazaki *et al.* 1996). Some report that PBC patients exhibit elevated serum IFNγ levels (Galatola *et al.* 1998) while others report increased IL-1β and IFNγ expression in CAH compared with PBC (Napoli *et al.* 1994). Increased levels of IL-2, IL-6 and IL-8 have been detected by RT-PCR in PBC liver tissue of patients undergoing transplantation. However, as expected, this finding was common to other forms of cirrhosis and was not PBC-specific (Napoli *et al.* 1994). Shindo *et al.* failed to detect mRNA for IL-1, IL-2, IL-4, IL-5, IL-6 or TNFα from PBC liver biopsies, which contrasts with many of the above findings, but found IFNγ expression more frequently as disease progressed (Shindo *et al* 1996). Harada *et al.* have detected mRNA for both IFNγ and IL-4 in PBC livers with CD4+ cells being the predominant source of IFNγ. They observed a greater number of IFNγ positive cells than IL-4 positive cells and suggest a Th1 response predominates (Harada *et al.* 1997a). Analysis of individual liver-derived autoantigen-specific T cell clones suggest that both Th1- and Th2-like clones are present. This suggests both cell mediated and Ab mediated immune responses may co-exist (Van de Water *et al.* 1995; reviewed in Leung *et al.* 1996) though there are signs of defects in both Th1 and Th2 responses (Jones *et al.* 1997). It has been hypothesised that the destructive response in PBC is a Th1 mediated DTH type response and the Th2 like cells detected may be playing a regulatory role (reviewed in Berg *et al.* 1997), though much work remains to be done in this area before confirming or disproving this theory.

1.1.5.4 Macrophages and Kupffer Cells

The frequent incidence of epithelioid granulomas or epithelioid cell aggregation around damaged bile ducts, especially in the early histological stages of disease, is of particular interest and suggests Kupffer cells (KC), Mϕs and/or Mϕ derived cells (discussed in **1.3**), may be important players in the early lesions (Nakanuma and Ohta 1983; reviewed in Nakanuma *et al.* 1995). These granulomas are not restricted to the vicinity of the bile ducts and may also be observed in hepatic lobules (reviewed in Nakanuma *et al.* 1995). Mathew *et al.* have quantitatively analysed the Mϕ and KC distribution and morphology in PBC liver sections

immunohistochemically using the KP1 and EBM 11 anti-CD68 clones (Mathew *et al.* 1994). They observed larger cells showing increased cytoplasmic KP1 and EBM 11 staining in the PBC sections, with histological stage 3 sections showing the greatest numbers of positive cells. The authors believe that the expanded KC population mediates the stimulation of perisinusoidal cells, via release of factors such as TNFα, TGFα and TGF-β1, resulting in increased extracellular matrix protein synthesis and fibrosis. A histological study of twenty one stage I or stage II liver sections showed granulomas in the portal tract area of every section, frequently near damaged ducts, but additional interlobular granulomas were more frequent in AMA negative cases (Yunoye *et al.* 1984). Takezawa and Yamada report that the granulomas in PBC were closely related to interlobular bile duct lesions and suggest something derived from the ducts plays an important role in granuloma formation (Takezawa and Yamada 1984). The PBC patients analysed with granulomas were histologically of early stage, some being asymptomatic.

1.1.6 Therapy

UDCA (ursodeoxycholic acid) is gaining favour in managing the symptoms of PBC, improving patients' biochemical parameters, though whether it is effective in increasing life expectancy is unclear. It is one of the curiosities of PBC that, given its potentially autoimmune and immunological basis, the disease appears refractory to immunosuppressive therapies. The inevitable progression to cirrhosis and liver failure means that liver transplantation is presently the only therapeutic option for end stage cases (reviewed in Heathcote 1996) though graft rejection or recurrence of PBC following transplantation are serious problems (Van de Water *et al.* 1996).

1.1.7 Mechanisms of Cell Death

The exact mechanism by which the BECs are destroyed in PBC has not been fully elucidated. Before current knowledge of this subject is considered "cell death" in a more general form will be discussed.

Death is fundamentally as critical to living biological systems as life itself. A fine balance of cell proliferation and cell death exists continuously throughout life from

conception to death of the whole organism. Disruption of this homeostasis has major implications for health and may be the cause of conditions including cancer, psoriasis, autoimmune disease, neurodegeneration, Alzheimer's disease and congenital malformations to name a few. For maintenance of health, when faced with a plethora of pathogenic infectious agents, the body must adopt mechanisms to kill these exogenous pathogens while limiting damage to self tissue. Within the immune system death of self reactive thymocytes, during their development in the thymus, is the first level of regulation and control to prevent the emergence of autoreactive T lymphocytes.

The complexities of the mechanisms culminating in the demise of host and foreign cells are great, but are generally categorised to result in apoptosis or necrosis.

Apoptosis is a morphological description of a form of programmed cell death (PCD). The effector mechanisms appear to be similar in all cell types and are remarkably conserved between species. The characteristics of an apoptotic cell include chromatin condensation and cell shrinkage, cytoplasmic vacuolisation, blebbing of the plasma membrane and elaboration of apoptotic bodies (membrane-wrapped packets containing the cell's contents). Phagocytes subsequently take up the apoptotic bodies. Apoptosis epitomises a "tidy" removal of undesired material leaving no trace and, importantly, not initiating an inflammatory response. In contrast, a necrotic cell "leaves its mark". By spilling its contents, after lysis of the plasma membrane due to cell and organelle swelling, an inflammatory response follows shortly. Such a scenario is obviously undesirable as a mechanism of removal of effete body tissue or extensive infections.

1.1.7.1 Caspases

Initiation of the apoptotic process results in activation of cysteine aspartic acid-specific proteases known as caspases which disable key homeostatic and repair enzymes and bring about systematic destruction of the cell. Within the nucleus chromosomal DNA becomes degraded into nucleosomal sized fragments.

Caspases are a family of proteases whose members have distinct roles in inflammation and apoptosis (reviewed in Thornberry and Lazebnik 1998). The regulation of proteases is limited to control of their activity and substrate availability because proteolysis is irreversible. By synthesising caspases as inactive precursors large amounts of protein can accumulate which can be activated on demand by another protease or by regulated autocatalysis. Proteolytic processing of the caspases results in formation of heterodimers which themselves dimerise to form complexes with two active sites. Caspases are among the most specific proteases known and they cleave a select set of proteins in a co-ordinated manner during apoptosis. They can regulate their own activation by positive and negative feedback loops and can be inhibited by protease inhibitors e.g. the crmA, p35 and IAP (inhibitor of apoptosis) proteins.

The contribution of caspases to the events of apoptosis is not fully understood but some of their substrates have been identified. They inactivate proteins such as I^{CAD}/DFF45, which inhibits CAD (caspase activated deoxyribonuclease) releasing CAD's nuclease activity, and bcl-2 proteins (**1.1.7.5**), producing pro-apoptotic fragments. They cleave lamins causing collapse of nuclear lamina contributing to chromatin condensation and cleave proteins involved in cytoskeletal regulation e.g. gelosin, focal adhesion kinase (FAK) and p21-activated kinase (PAK2). Other caspase substrates include polyadenosine diphosphate (ADP) ribose polymerase, actin, rho-GDI and SREBP (reviewed in Nagata 1997). Caspases appear to cut off contact with surrounding cells, reorganise the cytoskeleton, shut down DNA replication and repair, interrupt splicing, destroy DNA, disrupt the nuclear structure, induce signals marking the cell for phagocytosis and disintegrate the cell into apoptotic bodies.

Activation of initiator caspases e.g. caspase-8 and caspase-9 leads to activation of effector caspases. By activating common effector caspases different signals leading to activation of different initiator caspases culminates in a common apoptotic sequellae.

1.1.7.2 Nitric oxide

Nitric oxide (NO) has been implicated as an inducer of apoptosis and may be an important factor initiating apotosis triggered by immune cells. High levels of NO produced by Mϕs generated by inducible NO synthase (iNOS) induce apoptotic death in a variety of cells (reviewed in Williams *et al.* 1998) and NO released from KCs has been shown to modulate the biological viability of cocultured hepatocytes and hepatoma cells, inducing apoptosis. Stimulation of the T cell receptor (TCR), under conditions which trigger PCD induces NO formation and inhibition of nitric oxide synthase (NOS) protects T lymphocytes from activation induced cell death (Williams *et al.* 1998). It has been suggested that NO and its metabolites react with amino acids in the target cells which may play a part in the induction of apoptosis (Higuchi *et al.* 1995; Kurose *et al.* 1995) and Fas ligand mRNA expression is known to be increased by reactive oxygen intermediates (ROI) (reviewed in Watson 1999). NO can induce necrosis as well as apoptosis and in some studies it has been shown to have a protective affect on apoptosis.

1.1.7.3 Reactive Oxygen Intermediates

Mitochondria are a major source of reactive oxygen intermediates (ROI) and excessive production of ROIs, i.e. oxidative stress, results in massive cellular damage associated with lipid peroxidation and protein and nucleic acid alterations leading to necrotic cell death. The hydroxyl ($^{\cdot}OH$) radical is believed to be responsible for most of the oxidative damage resulting in necrosis. ROIs can also act as signalling molecules and are believed to be central in the transduction pathways culminating in PCD. They have been implicated in activating PCD triggered by TNFα, ionising irradiation, anthracyclines, ceramides, glucocorticoids or survival factor withdrawal and may also be required for the execution of the death program itself. It is likely that the level of ROIs determines whether apoptosis, necrosis, or apoptosis converting to necrosis at the late stage of PCD occurs (reviewed in Mignotte and Vayssiere 1998).

1.1.7.4 Perforin and Granzymes

CTLs are known to induce apoptosis in their cellular targets which may be mediated through Fas/Fas ligand interaction (**1.1.7.5**) or perforin and granzymes. The CTLs' granules contain the pore-forming protein perforin and a family of serine proteinases termed granzymes. Perforin polymerises in the target cell membrane producing lesions analogous to those of the complement membrane attack complex (MAC), though perforin alone is incapable of producing the DNA fragmentation observed in CTL-mediated target cell death. Perforin is required for the primary lytic mechanism of antiviral, alloreactive peritoneal exudates and of NK effector cells. CTLs utilise the pore-forming capacity of perforin in conjunction with granzyme proteinases which are capable of fragmentation of target cell DNA (reviewed in Smyth and Trapani 1995).

1.1.7.5 Death Receptors

Death receptors are cell surface receptors which transmit apoptotic signals initiated by specific "death ligands" (reviewed in Ashkenazi and Dixit 1998). Within seconds of ligand binding, the receptors can activate death caspases resulting in death by apoptosis within hours. The receptors belong to the TNF receptor (TNFR) family and share a homologous cytoplasmic "death domain" sequence which enables the receptors to engage the cell's apoptotic machinery.

Fas

One of these receptor/ligand pairs is Fas (Apo1/CD95) and Fas ligand. The Fas/Fas ligand system is particularly important in peripheral deletion of activated mature T lymphocytes at the end of an immune response, killing of target cells such as virus infected or cancer cells by CTLs or NK cells and killing inflammatory cells at "immune privileged" sites such as the eye. Defects in Fas or Fas ligand in mice or humans can lead to the accumulation of peripheral lymphoid cells, enlargement of lymph nodes and a fatal autoimmune syndrome (reviewed in Nagata 1997).

When homotrimeric Fas ligand complexes bind trimeric Fas molecules an interaction of the Fas death domain with the death domain of the adapter protein FADD (Fas-

associated death domain, also called Mort1) follows. FADD also contains a "death domain" which binds an analogous tandem repeated domain within the zymogen form of caspase-8 (FLICE/MACH). The FADD mediated oligomerisation of caspase-8 initiates the latter's self cleavage and activation which results in activation of downstream effector caspases such as caspase-9, the functional homologue of *Caenorhabditis elegans'* (*C. elegans*) CED 3, and execution of the apoptotic pathway (reviewed in Nagata 1997; reviewed in Ashkenazi and Dixit 1998; reviewed in Faubion and Gores 1999). Other cytoplasmic proteins besides FADD may recognise the Fas death domain e.g. Daxx and FLIP and regulate apoptotic signals through Fas. Fas/Fas ligand interaction may also activate caspase-2 using receptor interacting protein (RIP) and RAIDD (RIP-associated Ich-1/CED3 homologous protein with a death domain), as the adapter molecules, via pathways distinct from those involving cytochrome c release from mitochondria (discussed in **1.1.7.6**) and are not inhibited by bcl-2 (discussed in **1.1.7.8**) (reviewed in Watson 1999). FADD not only transduces a death signal on Fas ligation but is also essential for mitogen or antigen induced proliferation of T lymphocytes and B lymphocyte production (reviewed in Strasser and Newton 1999).

Tumour Necrosis Factor

Mϕs and T lymphocytes are the major source of TNF and its ligation with TNFRI (p55) activates the NF-κB and AP-1 transcription factors and induction of pro-inflammatory and immunomodulatory genes. TNF may also induce apoptosis through TNFRI, though this is usually dependent on a block in protein synthesis, suggestive of synthesis of suppressive factors thought to be mediated through NF-κB and JNK (jun kinase)/AP-1. As for Fas, trimeric complexes of TNF interact with TNFRI and the adapter protein TRADD (TNFR-associated death domain) binds TNFRI recruiting a number of signalling molecules to the complex (reviewed in Nagata 1997; reviewed in Ashkenazi and Dixit 1998; reviewed in Faubion and Gores 1999). Recruitment of TRAF2 (TNFR-associated factor-2) and RIP activates NF-κB-inducing kinase (NIK) which activates the inhibitor of κB (I-κB) kinase complex (IKK). IKK phosphorylates I-κB resulting in its degradation which allows NF-κB to

enter the nucleus and activate transcription. The TRAF2 and RIP recruitment also activates JNK/AP-1 through a signalling cascade involving the mitogen-activated protein (map) kinases MEKK1 (map/Erk kinase kinase-1), JNKK (JNK kinase) and JNK. TNFRI-TRADD-FADD interaction results in caspase-8 interaction and apoptosis induction while apoptosis can also be induced through a TNFRI-TRADD-RIP-RAIDD interaction, initiated through the binding of RAIDD to caspase-2.

The TNF and TNFR families are extensive and also include Apo2L (TRAIL), Apo3L, DR3 (Apo3), DR4 and DR5, as well as several decoy receptors which inhibit Apo2L-DR4 or DR5 mediated signalling. Thus, multiple physiological apoptosis initiators exist which may endow specificity or redundancy to the critical regulatory system.

1.1.7.6 Mitochondria and Apoptosis

Apoptosis is independent of oxidative phosphorylation and does not require mitochondrial DNA, though mitochondria play a central role in apoptosis in many systems. There is evidence for a caspase-independent commitment to death and some pro-apoptotic proteins such as bax (discussed in **1.1.7.8**), which target mitochondrial membranes, can induce mitochondrial damage and cell death when caspases are inactivated (reviewed in Green and Reed 1998). At least three general mechanisms, whose effects may be interrelated, are known of how mitochondria control life and death. These include:

1) Disruption of electron transport (probably at the cytochrome b-c_1/cytochrome c step), oxidation, phosphorylation and adenosine triphosphate (ATP) production.

2) Release of proteins which trigger caspase activation (i.e. cytochrome c, procaspase-3, apoptosis inducing factor (AIF)).

3) Alteration of the cell's redox potential.

Cytosolic cytochrome c forms part of the vertebrate "apoptosome" which is composed of cytochrome c, apoptosis protease-activating factor 1 (Apaf-1) and

procaspase-9, resulting in caspase-9 activation and subsequent apoptosis. This is a rapid process but release of cytochrome c may also result in necrosis due to collapse of electron transport, generation of oxygen free radicals and decreased ATP production. Release of cytochrome c from the mitochondria is likely to be mediated through opening of a large conductance channel, the mitochondrial permeability transition pore, which results in dissipation of the membrane potential, matrix swelling and disruption of the outer membrane. However, it has also been suggested that the outer membrane disruption may involve hyperpolarization.

Many bcl-2 family members (discussed in **1.1.7.8**) are situated in the outer mitochondrial membrane, orientated towards the cytosol. Bcl-2, bcl-x and bax can form ion channels in synthetic membranes and they may communicate functionally or physically with inner membrane proteins governing ion transport or they may regulate the intermembrane space pH. The anti-apoptotic bcl-2 family members' role is much more complex than merely suppressers of caspase-activated proteins, which is considered in **1.1.7.8**.

1.1.7.7 p53

p53 is a tumour suppressor transcription factor (reviewed in Evan and Littlewood 1998) which is normally maintained in abeyance at low levels through its interaction with Mdm-2, which signals its degradation. Phosphorylation of p53 or Mdm-2, induced by DNA damage, prevents their interaction, resulting in stabilisation and activation of p53. p53 activation may lead to growth arrest in the G1 and G2 stage of the cell cycle, mediated through the cyclin-dependent kinase (cdk) inhibitor p21, or to apoptosis. Genes implicated as p53 targets involved in apoptosis include those coding for bax, insulin-like growth factor (IGF) 1 receptor, IGF binding protein 3 (IGF-BP3), proteins regulating angiogenesis and components of the renin-angiotensin system. p53 may also trans-repress anti-apoptotic genes and p53 has been shown to upregulate Fas and Fas ligand (reviewed in Watson 1999). Responses to other stimuli such as physical damage, metabolic deprivation, heat shock, hypoxia and expression of certain oncogenes (e.g. *myc* and *EIA*) may involve p53.

1.1.7.8 The bcl-2 Family Members

Bcl-2 was the first mammalian regulator of apoptosis identified, due to a chromosomal translocation in a human follicular lymphoma which resulted in *bcl-2* gene activation and cytokine independent survival of cytokine dependent haematopoietic cells. *Bcl-2* is a functional homologue of *C elegans' Ced-9* and inhibits apoptosis induced by many physiological and experimental stimuli. The protein acts as a dominant repressor of apoptosis at a point where several independent signal transduction pathways converge. However, some apoptotic inducers, including antigen-receptor activation induced cell death and cytotoxic T lymphocyte and TNF-mediated cytolysis are not inhibited by *bcl-2* (Strasser 1995). Proliferation promotes apoptosis and suppression of apoptosis appears to suppress proliferation in certain circumstances. Elevated *bcl-2* expression suppresses apoptosis but the cells have difficulty entering the cell cycle (Evan and Littlewood 1998).

Apoptosis is regulated by a fine balance between pro- and anti-apoptotic members of the *bcl-2* family (reviewed in Adams and Cory 1998). At least fifteen members have been identified in mammalian cells. Bcl-2 is structurally and functionally homologous to *Caenorhabditis elegans' (C. elegans)* Ced-9 and their survival function is opposed by proteins such as bax, mammalian bik (or Nbk) and nematode EGL-1. Structurally the proteins most similar to bcl-2 which contain all four or the first two of the conserved motifs known as bcl-2 homology domains (BH1-BH4), are anti-apoptotic. The pro-apoptotic members fall into two subfamilies possessing BH1, 2 and 3 (i.e. bax, bak, bok) or only BH3 (i.e. bik, blk, bad, bid). The BH1, 2 and 3 domains are involved in homo- and hetero-dimerisation of the family members, which regulates their function. Post translational phosphorylation events also affect their activity. The effector mechanisms of these proteins is still being elucidated but bcl-x_l (the larger product of two splice variants of *bcl-x* mRNA) may prevent caspase-9 activation by inhibiting Apaf-1/caspase-9 interaction and bcl-2 may act in part by preventing cytochrome c release from mitochondria (discussed in **1.1.7.6**). These proteins may also protect cells from apoptosis by shifting the cellular redox

potential to a more reduced state and inhibiting the availability of cytochrome c in the cytosol (reviewed in Mignotte and Vayssiere 1998). The ability of the BH1 and BH2 containing proteins to insert into membranes and their resemblance to bacterial toxins suggests the proteins may form channels in organelles but their substrates or role in killing remains to be established. In particular the ability of bax to initiate caspase-independent death has been hypothesised to be mediated via channel forming activity promoting mitochondrial permeability or puncturing the mitochondrial outer membrane.

The anti-apoptotic effect of bcl-2 is active in response against a diverse range of cytotoxic insults (γ radiation, ultraviolet (UV) radiation, cytokine withdrawal, dexamethasone, staurosporin, cytotoxic drugs), but provides little protection against Fas mediated apoptosis of lymphocytes or death of autoreactive T lymphocytes in the thymus.

1.1.7.9 Macrophages and Apoptosis

Mϕs have been implicated in playing the role of passive scavenger of apoptotic cells in regression of a variety of tissues, but they seem to play a more active role in certain situations as Mϕ ablation studies show their apparent requirement for cell death during regression of ocular capillaries (Aliprantis *et al.* 1996). Mϕ derived TNFα may be central in induction of apoptosis, particularly the membrane-bound form of TNFα which activates TNFRII (p75), consistent with the observation that cell-to-cell contact appears essential in Mϕ-mediated apoptosis.

1.1.7.10 Cell Death in the Context of PBC

Electron microscopy studies have shown BECs in PBC patients to display various abnormalities including irregular shaped nuclei, dilated endoplasmic reticulum (ER), swollen mitochondria and numerous cytoplasmic cytolysosomes. This form of necrosis has been described as cytoplasmic focal necrosis and has also been observed in many other cholestatic liver diseases (Bernuau *et al.* 1981). Of particular interest in the above study was the report of *"..particular type of necrosis....fragmentation of the nuclear chromatin and condensation of the cytoplasm in which closely packed*

organelles were still recognizable." This is a classic description of a cell undergoing apoptosis and apoptotic bodies were also identified within cytoplasmic vacuoles of BECs. Though only some BECs in a few of the cases studied exhibited this phenotype it provides good evidence for apoptosis contributing to the loss of BECs in PBC. Nakanuma *et al.* reported four types of biliary epithelial injury suggesting cell death in the ducts; coagulative necrosis; lytic necrosis without detachment of affected cells from the biliary epithelial layer; apoptosis; and detachment of several adjoining biliary cells from the basement membrane and neighbouring biliary cells (Nakanuma *et al.* 1983). Apoptotic cells were rare and affected cells were most frequently those of bile ductules (structures containing not more than five nuclei). These studies and others (Kuroki *et al.* 1996; Harada *et al.* 1997b; Koga *et al.* 1997) suggest that death of the BECs may be mediated by multiple mechanisms, including apoptosis, and further investigation is warranted to elucidate the extent and potential for manipulation of the pathways involved.

Kuroki *et al.* report that cell death and cell proliferation were simultaneous in the same affected bile duct and their findings indicate that the cell death was faster than the proliferation (Kuroki *et al.* 1996). The balance between cell death and proliferation during the course of this chronic disease is clearly an important determinant of the net number of viable BECs as a small imbalance, biased towards death, will lead to a cumulative large deficit of cells. It is widely accepted that within the liver of PBC patients there is proliferation of hepatocytes and cells which take on the form of BECs, but the progenitor of the latter is uncertain. The so called "ductular metaplasia" observed may originate from pre-existing BECs, from hepatocytes or from a stem cell proposed to reside within the duct of Hering (Aterman 1992; Marucci *et al.* 1993; Nakanuma and Harada 1993; Rubin *et al.* 1995; Rudi *et al.* 1995). Bcl-2 expression in small interlobular bile ducts of normal liver and in cirrhotic livers was found to be more prominent in ductules at the borders of cirrhotic nodules (Koukoulis *et al.* 1995) and may influence the extent of viability loss of these cells.

Extensive hepatocyte injury does not appear to be prominent in the early evolution of PBC (Klion and Schaffneer 1966) and the liver cell damage observed as disease progresses is thus likely to be the result of secondary damage in the organ.

Using *in situ* nick-end labelling an increased frequency of BECs positive for DNA fragmentation was seen in PBC sections compared with chronic viral hepatitis C and normal controls, and in PBC and hepatitis C hepatocytes compared with normal controls (Sakisaka *et al.* 1997). Though not specific for apoptosis this method for detecting DNA fragmentation suggests that cellular injury of BECs and hepatocytes in PBC may be the result of apoptosis. In contrast Ballardini *et al.* found apoptosis, measured by a DNA fragmentation assay, to be a rare event in early stage PBC liver sections (Ballardini *et al.* 1998). They found only four positive BECs in three biopsies, but this low incidence is not surprising due to the short duration of apoptotic events (2-4 hours) which extrapolated to an 5% apoptosis rate implies a daily death rate as high as 40%. Koga *et al.* report increased DNA fragmentation and bcl-2 expression in BECs and hepatocytes which may reflect apoptotic stress in the PBC cases they analysed (Koga *et al.* 1997).

Immunohistochemistry studies have shown increased expression of Fas in BECs and more frequent Fas ligand expressing CD4+ and CD8+ T lymphocytes around bile ducts in PBC liver sections compared with those from hepatitis C patients (Koga *et al.* 1998) which may suggest Fas mediated apoptosis contributes to BEC loss.

1.1.8 Pathogenesis

The pathogenesis of PBC remains an enigma, with various ideas and possible mechanisms having been proposed without substantial evidence to support them. A major problem in the understanding of PBC is the lack of a suitable animal model for the disease. Though attempts have been made to induce PBC in animals by administrating AMAs; attempting to induce these antibodies in a variety of ways such as immunisation with the antigen; or immunising severe combined immunodeficient (SCID) mice with peripheral blood lymphocytes (PBL) from PBC patients, the results are a poor attempt at replicating the human disease (Krams *et al.*

1989a and 1989b; Kobashi *et al.* 1994; Abedi *et al.* 1996). PBC and graft-versus-host disease (GVHD) share a number of features which has led people to suggest understanding one of these phenomena may further our understanding of the other (Bernuau *et al.* 1981; Shulman *et al.* 1988; reviewed in Czaja 1994). However, these hopes have yet to be realised and stark differences are apparent between GVHD and PBC including the lack of AMA in the sera of GVHD sufferers (Quaranta *et al.* 1998) and lack of response of PBC to immunosuppressive therapy. Murine GVHD systems, which are sometimes used as a model for PBC, are far from ideal and may actually be misleading regarding the pathogenesis of PBC.

The following observations may give some insight into potential defects or abnormalities suffered by PBC patients which may have some bearing on the manifestation of disease.

1.1.8.1 Immunological Abnormalities

Numerous reports of intrinsic abnormalities or differential behaviour/responses of components of PBC patients' immune systems have been published. These observations reinforce the immunological basis for this disease but fail to provide definitive proof of the precise abnormality which patients suffer. However, some of the findings may reflect secondary effects of the disease process, or results of *in vitro* studies may be due to the differential activation status of the cells in question at the time of collection from the patients. A by no means exhaustive collection of reported observations on this topic shall be mentioned to emphasise the breadth of studies in this area.

DCs from PBC patients are reported to have a lower stimulatory capacity but higher NO levels compared to controls in allogeneic mixed lymphocyte reactions (MLR) (Yamamoto *et al.* 1998a and 1998b) yet the NO level measurements of whole blood venous specimens from PBC patients showed an inverse correlation with disease progression (Battista *et al.* 1997). S100 positive cells with DC morphology have been identified inside the basement membrane between BECs of septal bile ducts in early, but not late, stage PBC liver sections and may partake in initiation and/or

progression of the disease. It is interesting to note that these S100 positive cells were found less frequently in other chronic inflammatory liver diseases studied (Demetris *et al.* 1989).

T lymphocytes from PBC patients appear deficient in their responsiveness to IL-2 (Menéndez *et al.* 1992) and their mitogen-induced production of TNFα, TNFβ and IFNγ (Spengler *et al.* 1992).

Monocytes derived from PBC patients have been reported to exhibit markedly reduced production of IL-1 (Saibara *et al.* 1984) yet increased levels of superoxide (O_2^-) production, both when unstimulated or stimulated with phorbol-myristate-acetate (PMA) (Sipos *et al.* 1995). They have also been reported to produce approximately threefold more prostaglandin E_2 (PGE_2) than monocytes from normal or alcoholic cirrhosis controls when stimulated with phytohaemagglutinin (PHA) which may account for the reduced proliferation of PBC cultures observed by others (Chiricolo *et al.* 1989). Ultrastructural examination of PBC liver biopsies by electron microscopy has shown Mϕs surrounding bile ducts, especially in the later stages of disease, though their role in destruction of the BECs is uncertain (Chedid *et al.* 1974).

In vitro spontaneous and LPS-stimulated TNF production by cultured mononuclear cells from PBC patients is significantly lower than that of cells from PSC patients (Broomé *et al.* 1992). PBLs from PBC patients show reduced NK activity (James and Jones 1985) and a defect in the spontaneous cytotoxic function of surface Ig negative, Ig fragment crystallisable (Fc) receptor (FcR) positive lymphocytes against Chang cells (Vierling *et al.* 1977).

Though elevated levels of γδ T lymphocytes have been associated with autoimmune disease it appears that in end stage PBC cases there is a significant reduction in the proportion of hepatic lymphocytes expressing the γδ TCR (Curry *et al.* 1998). The altered balance between γδ and αβ TCR+ T lymphocytes is likely to reflect the

infiltration of circulating αβ TCR+ T lymphocytes and may affect the immune homeostasis provided by the former T cell subset.

The eosinophilia observed in portal tracts in the vicinity of damaged bile ducts, particularly during the histologically early stages of PBC, the deposition of major basic protein and increased IL-5 mRNA levels discussed previously (**1.1.5.3**) suggest eosinophils may be involved in the pathogenesis of bile duct damage (reviewed in Nakanuma *et al.* 1995; Nakamura *et al.* 1996; Yamazaki *et al.* 1996). *In vitro* studies of the effect of bile acids (taurochenodeoxycholic acid (TCDCA) and tauroursodeoxycholic acid (TUDCA)) on these cells have shown a dose dependent activation or cytotoxic effect which may contribute to the cholangiocyte injury (Yamazaki *et al.* 1998).

Both MHC Class I and II molecules have been found to be expressed by BECs and hepatocytes in PBC liver sections which has led to suggestions that these cells could partake in antigen presentation (Ballardini *et al.* 1984; Tsuneyama *et al.* 1995a and 1995b; reviewed in O'Donohue and Williams 1996a). However, for effective antigen presentation to CD4+ T lymphocytes additional costimulatory molecules must be expressed on the APC in addition to the MHC molecules (reviewed in Harlan *et al.* 1995). It has been shown that B7-1 (CD80) and B7-2 (CD86) expression on BECs can only be detected in sections showing histological late stage disease (Tsuneyama *et al.* 1995a; Spengler *et al.* 1997) and *in vitro* studies suggest it is unlikely that human intrahepatic BECs play a direct role in activation of antigen specific CD4+ T lymphocytes (Leon *et al.* 1996) and their ability to express B7 is questionable (Leon *et al.* 1995b). Thus, a role of the BECs acting as "professional APCs" for the infiltrating T lymphocytes is unlikely to be an initiator of disease. However, they may contribute to the pathology as disease progresses, in combination with the observed intercellular adhesion molecule-1 (ICAM-1) and vascular cell adhesion molecule-1 (VCAM-1) expression of these cells in PBC which are not detected on ducts in normal livers (reviewed in Leung *et al.* 1996; Nakanuma *et al.* 1997). Though elevated or aberrant expression of surface molecules, such as ICAM-1, MHC

Class I and MHC Class II, on interlobular bile ducts has been observed in PBC liver sections it is not disease specific as this expression pattern is also seen in other immune-mediated liver disease states and the data regarding ICAM-1 expression is inconsistent (Spengler *et al.* 1988; Hashimoto *et al.* 1993; Tsuneyama *et al.* 1995a and 1995b; reviewed in Broomé *et al.* 1996; Kamegaya *et al.* 1997; reviewed in Nakanuma *et al.* 1997).

The presence of secretory IgA anti-PDC antibodies in the saliva of PBC patients has led to suggestions that these antibodies may be present in the liver and partake in the BEC damage. By trafficking through the BECs the antibodies could bind PDC intracellularly, depleting the cells of PDC causing metabolic cell damage. The complex would then be secreted into the lumen of the ducts (Palmer *et al.* 1998). In support of this theory PBC liver sections show high levels of IgA staining in the luminal region of bile duct epithelium which is not seen in controls (Van de Water *et al.* 1993), though other cholestatic diseases also show the presence of IgA in bile ducts (reviewed in Krams *et al.* 1990). There is evidence for abnormal expression of either PDC-E2, a PDC-E2 peptide or a possible cross-reactive molecule by BECs (as well as salivary epithelium) in PBC and AIC patients which may contribute to disease initiation or progression should this molecule be the focus of immunological attack (Tsuneyama *et al.* 1995a, 1995b and 1997; Cha *et al.* 1996; reviewed in Leung *et al.* 1996; reviewed in O'Donohue and Williams 1996b). However, it is also possible that these or other antigens may be absorbed from bile or periductal tissue into the BECs. Odin and colleagues suggested that apoptosis might modify PDC-E2 and propose high levels of reduced PDC-E2 after large scale BEC apoptosis may prompt the autoantibody response (Odin *et al.* 1999). The PDC-E2 (or cross-reactive molecule) expression observed in PBC BECs precedes Class II expression, the latter seldom being found in liver sections of early stage disease (Tsuneyama *et al.* 1995a and 1995b) suggesting antigen presentation by BECs of PDC or a cross reactive antigen is unlikely to occur at the onset of disease. An observation of significant interest regards the expression of PDC-E2 mRNA in liver determined by *in situ* hybridisation (Harada *et al.* 1997c). This revealed that the aberrant apical staining

pattern on interlobular bile ducts seen in PBC but not control liver, using an antibody against PDC-E2, is not reflected by the expression levels of the mRNA. The control cases included a variety of hepatic diseases and tissue showing no significant change histologically. The majority of cases (over 88%) showed PDC-E2 mRNA expression in periportal hepatocytes whereas less than 24% and less than 38% of cases showed expression in interlobular and septal bile ducts, respectively. Proliferating bile ductules, in contrast, showed expression of the mRNA in over 80% of cases. These findings appear to support the view that the molecule which the anti-PDC-E2 antibody reacts with showing the aberrant apical staining pattern in PBC interlobular bile ducts is not actually PDC-E2 but a cross reactive molecule.

BECs in PBC biopsy sections appear to have an impairment in high junctions with increased paracellular permeability, which may allow toxic bile acids or various antigens to leak into the periductal area from the bile duct lumen (Sakisaka *et al.* 1997). Whether this is a primary or secondary event in the pathogenesis of PBC is not clear. Lymphoid and liver cells of PBC patients show altered mRNA and protein expression of anion exchange genes which has been suggested to play a role in the cholestasis, exocrine failure and immunodysfunction associated with the disease (Prieto *et al.* 1993; Medina *et al.* 1997). The basement membrane of bile ducts in PBC liver sections is disrupted, sometimes with multilayering and loss of continuity (Chedid *et al.* 1974).

1.1.8.2 The Role of the Macrophage in PBC

As has been alluded to previously the presence of epithelioid cells and granulomas in PBC liver sections is one of the few distinguishing histological observations when various chronic biliary diseases are compared. In some patients epithelioid granulomas are also found in lymph nodes, spleen and lungs. Within the liver the number of epithelioid granulomas correlates with the presence of bile ducts such that granulomas are less predominant in cases with extensive bile duct loss, suggesting their subsequent disappearance after BEC destruction. Granulomas are not confined to the bile duct lesions and epithelioid cells and granulomatous necrosis may be predominant within the hepatic parenchyma. The inciting agent(s) inducing the

granuloma formation is unknown but a number of suggestions have been made including bacterial/mycobacterial infection, the absorption by Mϕs of biliary fats or bile pigments which have leaked from the hyperpermeable biliary epithelial layer, a hypersensitivity reaction against altered bile proteins or tissue proteins due to tissue-damaging biliary substances, the effect of cytokines released by infiltrating mononuclear cells or the presence of undigested immune complexes (Nakanuma and Ohta 1983; reviewed in Nakanuma *et al.* 1995). Whatever its origin the epithelioid granuloma formation is a fundamental lesion of PBC. Bearing this in mind the Mϕ and its role in health and disease will be discussed in more detail (**1.2** and **1.3**) before considering the influence and effect of the *natural resistance-associated macrophage protein (NRAMP1)* gene on this cell type and PBC (**1.8**).

1.2 THE MACROPHAGE AND THE IMMUNE SYSTEM

The human immune system has evolved and adapted effective and efficient mechanisms to protect the body from infectious and harmful agents. The innate immune system offers a first line of defence, employing non-antigen-specific attack mechanisms which hold the pathogen in check while an antigen specific response is mounted. Mϕs and neutrophils/granulocytes are central effector cells of the early non-specific response, and Mϕ participation during this stage equips them for the role of APCs. Antigen presentation to antigen specific T lymphocytes is a pre-requisite for the highly specific acquired immune response involving T and B lymphocytes. Their activation and products should effectively result in elimination of infectious agents which have survived the innate immune response. Again the Mϕ comes into play during a cell mediated response and it plays additional roles during a humoral response, emphasising the cell's multifunctional role from the earliest stages of infection to the final demise of the offending agent.

1.3 THE MACROPHAGE

The mononuclear phagocyte system (MPS) (reviewed in Auger and Ross 1992) comprises bone marrow monoblasts and promonocytes, peripheral blood monocytes, tissue Mϕs and DCs. It constitutes the second major cell population of the immune

system. Metchnikoff coined the term Mϕ or "big eater" in 1892, though we are still faced with many questions concerning the origin and function of these cells. Throughout the body Mϕs are widely distributed and display great functional and structural heterogeneity. They are found in lymphoid organs, the liver, lungs, gastrointestinal tract, central nervous system (CNS), serous cavities, bone synovium and skin.

Mϕs were originally assigned to the reticuloendothelial (RE) system in 1924 by Aschoff. However, this did not constitute a true system as it included cells of non-Mϕ lineage which were capable of taking up "vital dyes", hence the introduction of the MPS in 1969 to encompass cells of the Mϕ lineage sharing functional characteristics *in vivo,* including high phagocytic capacity, and being of monocyte origin (van Furth *et al.* 1972).

1.3.1 Origin of the Macrophage

The Mϕ originates initially, ontogenetically in the yolk sac (Moore and Metcalf 1970), then the fetal liver and subsequently in the bone marrow (reviewed in Auger and Ross 1992) from a common progenitor of the monocyte and neutrophil/granulocyte known as the colony-forming unit, granulocyte-macrophage (CFU-GM) (Metcalf 1971). The decision of commitment to the monocytic or granulocytic pathway is likely to take place at a stage preceding the promonocyte and promyelocyte stage. However, the HL-60 human promyelocytic leukaemia cell line can be differentiated *in vitro* down either path in the presence of certain phorbol esters (to monocyte/Mϕ) or dimethyl sulphoxide (DMSO) (to neutrophil) (reviewed in Auger and Ross 1992). This suggests the switch may be at a later stage, but as with all observations of cell lines the transposition of findings *in vitro* of a malignant/mutant cell to a physiological, *in vivo* situation must be considered with caution.

Monoblasts are the least mature cell of the MPS. They contain relatively small quantities of lysozyme and non-specific esterase and possess limited phagocytic

capacity. Monoblasts divide to form two promonocytes which contain lysozyme, non-specific esterase and granules of peroxidase. Promonocytes phagocytose to a large extent and are capable of phagocytosing opsonised bacteria, which the monoblast can not, as well as IgG coated red blood cells (rbc), but relatively few C3b-coated rbcs. The promonocytes give rise to monocytes, which remain in the bone marrow for less than 24 hours, in the mouse, before entering the circulation, where they remain for between 36 and 104 hours. The monocytes subsequently migrate into extravascular tissue to become Mϕs. Migration involves adherence to endothelium, migration between endothelial cells and through endothelial structures, utilising high molecular weight glycoproteins on the monocyte, lymphocyte function associated antigen 1 (LFA-1 or CD11a/CD18), which interacts with ICAM-1 on vascular endothelial cells. IFNγ and IL-1 can augment ICAM-1 expression, facilitating monocyte migration to inflammatory sites. Once monocytes have left the peripheral blood they do not return.

The epithelioid cell is believed to be a terminal stage of development of the Mϕ system. These cells develop abundant cytoplasm and a morphological resemblance to skin epithelial cells. Epithelioid cells can fuse to form multinucleated giant cells and these cell types are common in granulomatous lesions, which will be discussed later (**1.4**). They have lower levels of cell surface Ig and complement receptors (CR) and are poorly phagocytic but exhibit increased lysosomal and respiratory enzyme activity.

Monocytes and older resident tissue Mϕs generally have limited functional potential. Mϕs from sites of inflammation (inflammatory Mϕs) have greatly increased properties for endocytosis, digestion and secretion of neutral proteases, acid hydrolases and regulatory proteins. Fully activated Mϕs which have been exposed to microorganisms and/or products of sensitised T lymphocytes have in addition to the properties of inflammatory Mϕs the ability to act as professional APCs, secrete large amounts of ROIs and kill microbes and tumour cells efficiently.

More than 95% of tissue Mϕs originate from blood monocytes while the remaining 5% appear to derive from the local division of mononuclear phagocytes which have arrived in the tissues and body cavities from the bone marrow within the previous 24 hours, before completion of cell division. The fate of the tissue Mϕ is unclear. They may die *in situ* in the tissue or in local draining lymph nodes. Wherever or however they die, the number of dying cells must be considerable, based on statistics from the mouse, where approximately 1.5 x 10^6 monocytes are produced every 24 hours which will eventually leave the bone marrow to become tissue Mϕs.

Our knowledge of the factors regulating monocytopoiesis *in vivo* is relatively sparse. Macrophage colony-stimulating factor (M-CSF) and granulocyte macrophage colony-stimulating factor (GM-CSF) are haematopoietic growth factors produced by Mϕs themselves and their production is stimulated by exposure to external stimuli including phagocytosable particles and endotoxin. Mϕ derived IL-1 and TNF can induce non-haematopoietic cells, such as fibroblasts and endothelial cells, to produce M-CSF and GM-CSF, and hence mononuclear phagocyte development. T lymphocyte derived GM-CSF and IL-3 are likely to contribute to Mϕ activity in DTH reactions, and serum derived factor increasing monocytopoiesis (FIM) stimulates monocytopoiesis in mice and rabbit bone marrow. M-CSF is likely to regulate steady state monocytopoiesis while GM-CSF and IL-3 may play a greater role in the regulation during an inflammatory response.

1.3.2 Functions of the Macrophage

Mononuclear phagocytes encompass the clearest example of a cell population which is critical for natural immunity but has additionally adapted to play a central role in specific acquired immunity. Their principal functions in natural immunity include the following (reviewed in Abbas *et al.* 1994):

1) Mϕs function as the principal scavenger cells of the body, phagocytosing foreign and potentially harmful particles including microbes, macromolecules, antigens and injured or dead self tissue. Recognition of these substances involves cell

surface receptors, possibly for phospholipids and sugars. Once internalised, lysosomal enzymes degrade the substances. Mϕs also secrete enzymes, reactive oxygen species, NO and lipid derived mediators, e.g. prostaglandins, which kill microbes and control the spread of infections but they are also capable of injuring normal tissue in the immediate vicinity.

2) Mϕs secrete a wide range of cytokines, enzymes and biologically active substances: over 100 have been reported ranging from superoxide anions to fibronectin, growth factors to mediators of cell death. They release cytokines which attract neutrophils and other inflammatory cells to a site of inflammation and are responsible for many of the systemic effects of inflammation e.g. fever.

Functioning as accessory cells in immune responses, Mϕs play an important role in the cognitive, activation and effector phase of specific immunity including:

1) Mϕs function as accessory cells in lymphocyte activation by presenting antigen to T lymphocytes and expressing proteins promoting T lymphocyte activation.

2) During CMI responses antigen stimulated T lymphocytes secrete cytokines which activate Mϕs, enhancing the latter's phagocytic, degradative and cytocidal functions. In an activated state Mϕs play a principal part in cell mediated immunity.

3) Mϕs also partake in the elimination of foreign antigens by humoral responses by taking up antibody or complement opsonized particles much more efficiently than uncoated particles. Mϕs themselves are an important source of complement components.

1.3.3 Activation and Signal Transduction

At least three distinct signal transduction pathways have been identified during the induction of Mϕ activation which are related and interact. Within seconds to minutes

after a given activating molecule ligates its receptor, a series of rapid events occur. Intermediate events occur within minutes to 4 hours and slow events occur within hours to days. IFNγ initiates intermediate events, termed cascade I, including generation of slow Ca^{2+} fluxes and changes in protein kinase C (PKC) potential. LPS is an endotoxin derived from gram negative bacteria which is a potent activator of Mϕs. It forms a complex with the LPS-biding protein (LBP), an acute phase reactant present in serum, and the LPS-LBP complex is the ligand for CD14 (Wright *et al.* 1990). CD14 is a well known marker for monocytes and Mϕs and its ligation can stimulate production of TNFα, IL-1, IL-6 and IL-8. LPS initiates events collectively termed cascade II which comprise the breakdown of polyphosphoinositides, diacylglycerol generation, PKC stimulation and protein phosphorylation, as well as the generation of inositol triphosphate (IP_3) isomers and subsequent Ca^{2+} fluxes. A distinct cascade of events, cascade III, also initiated by LPS, results in synthesis of a distinct set of polypeptides, which are likely to have a regulatory role, and transcription of the competence KC gene.

1.3.4 Macrophage Heterogeneity

There is no evidence that the tissue destination of monocytes is pre-programmed and seeding to different tissues is thought to be random. In the absence of inflammatory signals resident Mϕs are widely distributed and display regional heterogeneity with regards to functional, morphological and phenotypic characteristics, which are likely to result from the local environment of the Mϕ. These heterogeneous populations include alveolar Mϕs of the lung, KCs of the liver, red pulp Mϕs of the spleen, histiocytes of connective tissue, microglia of the CNS and Mϕs of the intestine to name a few. It is the role of the KC, in particular, which is of most interest with respect to pathology of the liver and will be considered in more detail.

Named after the pathologist C. von Kupffer, Kupffer cells (KC) are the resident Mϕs of the liver and comprise the largest component of tissue Mϕs in the body, constituting 80-90% of the total fixed Mϕs (reviewed in te Velde 1994). They are located in the liver sinusoid in close contact with the fenestrated sinusoidal

endothelium. Non-parenchymal sinusoidal cells constitute 10% of the liver mass, of which 30% are KCs, 60% endothelial cells and 10% Ito cells. KCs of the periportal area are usually larger, have a higher endocytic and lysosomal enzyme activity and are at a higher density than those of the venous area. Their location in the hepatic sinusoid makes KCs the first Mϕs to contact products reaching the circulation via the portal vein. KCs remove potentially harmful materials such as viruses, bacteria, microorganisms, tumour cells, immune complexes and portal antigens and hence form a protective barrier for the systemic circulation. To assign KCs to the role as mere scavengers of these agents understates their true potential. Once activated, after exposure to endotoxins or circulating cytokines from the portal circulation, KCs function as inflammatory Mϕs. They release cytokines, lysosmal enzymes and ROIs, and display enhanced chemotaxis and phagocytosis. Upregulation of MHC Class II antigens on their surface and IL-1 production makes them capable of presenting antigens to T lymphocytes. Though the liver plays a predominant role in clearing systemic bacterial infections it is rarely infected itself. The clearance of infections from the portal vein is highly dependent on KCs but it has been suggested that the demise of these infections may be a concerted effort of the KC binding the bacteria extracellularly and recruited neutrophils killing the extracellular bacteria, rather than the KCs acting alone (Gregory and Wing 1998).

1.4 GRANULOMATOUS INFLAMMATION

Granulomas (reviewed in Adams and Hamilton 1989) are a characteristic feature of many human diseases including tuberculosis, sarcoidosis and leprosy. They represent focal, organised, chronic inflammation in which the Mϕ is the predominant constituent but other cells, including T and B lymphocytes, eosinophils, mast cells and fibroblasts may be present and play important roles. Within the granuloma the mononuclear phagocytes (small mononuclear cells, Mϕs, epithelioid cells and giant cells) have either migrated into the tissue or divided within the lesion.

There are two distinct kinetic types of granuloma, high turnover granulomas which tend to be induced by toxic substances such as mycobacteria, and low turnover

granulomas which are usually induced by inert substances such as foreign materials. High turnover granulomas contain many epithelioid cells and the irritant is usually contained within a small number of Mϕs in the granuloma, whereas in low turnover granulomas the irritant is distributed within most of the Mϕs throughout the granuloma. As the irritant is digested and degraded in high turnover granulomas these generally evolve into low turnover granulomas. The "turnover" refers to the rate of death and replacement of Mϕs in the granulomas.

Granulomas are generally evoked by relatively high concentrations of indigestible or poorly degradable, persistent, inanimate or living substances, which are frequently particulate. Microorganisms which evoke granulomas often induce a strong DTH response and the accompanying T lymphocytes' secretion of factors, including migration inhibitory factor (MIF), chemotactic agents, IFNγ, and TNF, promotes the accumulation and activation of Mϕs within the granulomas and expansion of the lymphocyte population. The extent and duration of the granulomatous inflammation can be dampened by Th2 lymphocytes suppressing the Th1 population and a fine balance between host inflammatory responses and the nature of the inciting agent determines the progression of the granuloma. The granuloma is further regulated by monokines and other factors released by cellular components other than T lymphocytes. These can include pro-inflammatory factors, anti-inflammatory agents, factors stimulating fibroblast activity and fibrosis, inducers of acute phase reactants and factors promoting leukocyte production in the bone marrow. The development of mononuclear phagocytes in granulomas mirrors that of monocytes through to activated Mϕs described earlier (**1.3.1**).

1.5 DEFENCE MECHANISMS MEDIATED BY MACROPHAGES

1.5.1 Phagocytosis

As mentioned previously, Mϕs and neutrophils are highly phagocytic (**1.3**) and this defence mechanism can be very effective in limiting and curtailing infections. Opsonized particles which have been coated with complement or Ab are taken up

most efficiently but the phagocytes also express receptors which recognise microbe surface components, ligation of which enhances phagocytosis. Mϕ phagocytic receptors include FcγRI, FcγRII FcγRIII, Fcα, CR1, CR3, C1qR, CD14 and mannosyl/fucosyl receptors (reviewed in Speert 1992). The receptors for opsonized material provides a way of recognising and phagocytosing a wide array of species with broad heterogeneity in surface characteristics, using a limited number of receptors. The surface expresssion of these receptors is influenced by local conditions, cytokines and the differentiation state of the phagocytes. Formation of the phogososme initiates a complex biochemical signalling pathway activating a unique reduced form of nicotinamide adenine dinucleotide phosphate (NADPH)-dependent oxidase complex which reduces oxygen (O_2) to superoxide (O_2^-). The O_2^- is secreted into the phagosome and dismutased to hydrogen peroxide (H_2O_2). The phagocyte's primary (or azurophilic) cytoplasmic granules fuse with the phogosome. These contain myeloperoxidase (MPO), hydrolases (acid hydrolases, lysozyme, neutral proteases, deoxyribonucleases (RNase)), elastase, cathepsin G and defensins. Secondary (or specific) cytoplasmic granules, which contain lactoferrin, lysozyme, vitamin B_{12}-binding protein and the membrane proteins CD11b/CD18 (Mac-1), cytochrome b_{558} and formyl-methionyl-leucyl-phenylalanine, fuse with the plasma membrane releasing their contents (Calafat *et al.* 1993). Lysozyme is present in relatively high concentrations in Mϕs, however its bactericidal function has been questioned and it has been suggested that its principal role may be digestive. Other lysosomal enzymes produced by Mϕs (including plasminogen activator, elastase, collagenase, lipoprotein lipase, phospholipase, lysosomal acid hydrolases, arginase, RNase, deoxynucleases (DNase), acid phosphatase and cathepsin) are able to lyse bacteria and digest bacterial cell walls, but their direct role in antibacterial defence has not been established clearly.

1.5.2 Reactive Oxygen Intermediates

Reactive oxygen intermediates (ROI) exhibit a broad spectrum of biotoxicity and the optimal microbicidal activity of phagocytic cells, such as Mϕs, depends on these substances i.e. O_2^-, H_2O_2, $^{\cdot}OH$, hypochlorous acids (HOX; X=halide ion).

Microorganisms have evolved mechanisms to avoid contact with, and protect themselves from, phagocyte derived oxidants. Likewise, host cells have developed similar mechanisms to protect themselves from exposure to oxidants. The O_2^- ion is moderately reactive and can act as an oxidant or reductant in biological systems. Due to its relative inactivity it can diffuse for considerable distances before exerting its toxic effects and extracellularly generated O_2^- (or a substance with similar properties) can access intracellular targets via cellular ion channels (Roos *et al.* 1984). At low pH (e.g. inflammatory sites and inside phagolysosomes) O_2^- is protonated to form $^{\cdot}HO_2$ which is more membrane permeable and likely to react with itself to form H_2O_2. H_2O_2 is more reactive than O_2^- and readily diffuses across cell membranes. In the presence of catalytically active iron the Haber Weiss reaction can occur resulting in $^{\cdot}OH$ and OH^- species. The $^{\cdot}OH$ is a more potent oxidant than the O_2^- ion and H_2O_2 and may in fact be mediating injury in cases where the latter species have been implicated, however, its high reactivity limits diffusion and it is unlikely to travel far before oxidising a substrate. It must, therefore, be generated in close proximity to its target, and targets at a distant site may be injured by initiation of a free radical cascade (Weiss 1986; Buettner 1993). These ROIs cause damage to cellular membranes, enzymes and DNA, inhibit membrane transport processes and are effective antimicrobial agents. Stimulated monocytes and neutrophils release MPO which interacts with H_2O_2 to form HOCl, and chloramines, tyrosyl radical and $^{\cdot}OH$ are also produced by activated monocytes and neutrophils via an MPO-dependent pathway adding to the defensive arsenal of these cells. The developmental stage of the cells of the MPS determines their respiratory burst capacity and *in vitro* cultured human monocytes show decreased MPO content and cytocidal activity compared to freshly isolated monocytes (Locksley *et al.* 1987).

1.5.3 Reactive Nitrogen Intermediates

Nitric oxide (NO) is a gaseous free radical (i.e. an uncharged molecule with an unpaired electron) generated by the five-electron oxidation of one of the terminal guanidine nitrogen atoms of L-arginine to L-citrulline by NOSs (Vladutui 1995). At least three NOS isoenzymes have been cloned. cNOS (NOSI) is constitutively

expressed in neurones and certain epithelial cells. iNOS (NOSII) is transcriptionally regulated and expressed in many cell types including Mϕs, hepatocytes and respiratory epithelium. The activity of iNOS is dependent on fluctuations in intracellular Ca^{2+} and microorganisms, microbial products and cytokines modulate iNOS levels. NOSIII is also constitutively expressed, mostly in endothelial cells, but its expression can be upregulated (e.g. by stress). NO can act as an oxidising agent or interact with O_2^- to generate peroxynitrite ($ONOO^-$) and ultimately $^{\cdot}OH$ via $ONOO^-$ formation and decomposition. NO's cytostatic and cytotoxic effects involve its interaction with iron containing key enzymes of the respiratory cycle (e.g. glyceraldehyde-3-phosphate dehydrogenase (GAPDH)) and DNA synthesis, formation of nitrosothiol groups on proteins and formation of toxic alkylating agents. $ONOO^-$ may be more important in mediating cytotoxicity by oxidising sulfhydryl groups and DNA bases, catalysing iron dependent membrane lipid peroxidation and reacting with metals or metaloproteins e.g. superoxide dismutase (SOD) to form the toxic nitronium ion NO_2^-. NO may mediate cell death by apoptosis or necrosis, depending on the cell type investigated, and convincing demonstrations of a protective role for NO in oxidative stress have been reported (reviewed in Kröncke *et al.* 1997).

1.5.4 Factors Augmenting Macrophage Function

Complement enhances Mϕs' antimicrobial activity, which may be mediated by its chemotactic properties for mononuclear phagocytes and neutrophils and its roles as an opsonin enhancing phagocytosis (reviewed in Speert 1992). It may also facilitate the lysis of gram negative bacteria. Fibronectin is a widely distributed glycoprotein which enhances the capacity of human monocyte derived Mϕs to ingest complement coated particles and kill ingested bacteria. In the lung surfactant protein A may act as an opsonin. It has similarities to the C1q complement factor and mannose binding protein (MBP) which enables it to bind C1qR, enhancing phagocytosis by mononuclear phagocytes. MBP can act in a similar fashion. 1,25 (OH)-vitamin D enhances the anti-tuberculosis activity of human monocyte derived Mϕs, particularly

in the presence of autologous serum, and may explain the enhanced natural resistance to infection with *M. tuberculosis* offered by sunlight.

1.6 MONONUCLEAR PHAGOCYTES IN HEALTH AND DISEASE

Monocytes and Mϕs play an extensive role in health and disease. Their role in innate immunity is crucial to hold infections at bay until an antigen specific acquired immune response is mounted and initiation of this response may be Mϕ mediated through antigen presentation to T lymphocytes. During a cell mediated response they again take on the role of effector cells. Defects in any of their immune functions are likely to be to the detriment of the host. Their activity, however, may not always be beneficial to the host when damage to host tissue, hyperactivation of Mϕs and inappropriate immune responses occur.

Impairment of Mϕ function can be primary, where it is the cause of the pathology, or secondary, where it is a consequence of other immune cells' dysfunction, but may facilitate the development and progression of disease. Mϕs may exert their effect on an immune response either directly or indirectly, by providing induction signals for other immune cells. Due to the common lineage of Mϕs and granulocytes/neutrophils defects observed in the function of Mϕs may also manifest themselves in the function of granulocytes/neutrophils, and *visa versa*. Hence, many syndromes and disease with a Mϕ component may also be the result of granulocyte/neutrophil dysfunction.

1.6.1 Immune Functions and Role in Disease of Macrophages

In response to injurious stimuli or immunological disorders, there is a rapid adjustment of plasma protein composition known as the acute phase response (reviewed in Auger and Ross 1992). The liver is the major organ synthesising acute phase proteins however, it is the monocyte/Mϕ which plays a central role in regulating the response by secreting the cytokines IL-1, TNFα and in particular IL-6. IL-1α and IL-1β (reviewed in Rees and Parry 1992) act as endogenous pyrogens, lymphocyte activation factors and inducers of acute phase proteins. IL-1β is the predominant form found in activated monocytes and up to 5% of the total mRNA in

these cells codes for it. IL-1β is the major secreted form with IL-1α predominantly functioning as a membrane bound cytokine. IL-1 increases the ability of NK cells to bind to their target tumour cells and synergises with IL-2 to induce lymphokine activated killer (LAK) activity. IL-1 induces IL-2 secretion and expression of high affinity IL-2 receptors on activated T lymphocytes and is chemotactic for CD3+ T lymphocytes. TNFα (reviewed in Rees and Parry 1992) occurs naturally as a dimer, secreted or membrane bound. It is linked to septic shock and its synthesis is induced by PMA, LPS, IL-1, IL-2, IFNγ and TNFα itself. TNFα can exhibit growth inhibitory and promoting activity and is important in the activation and differentiation of cells of the immune system. It induces MHC Class I expression and Class I and Class II expression when it synergises with IFNγ. As discussed previously it can be a potent inducer of apoptosis (**1.1.7.5**). IL-6 (reviewed in Auger and Ross 1992) acts as a B cell differentiation and growth factor and as a co-signal for IL-2 production and proliferation of T lymphocytes.

The Mϕ employs both oxygen dependent and oxygen independent mechanisms to destroy infectious agents, including viruses, bacteria, protozoa and parasites. Mϕs are attracted to sites of infection and phagocytose the infectious agent. The mechanisms employed to destroy different agents vary and the battle between 'prey and predator' is continually evolving as microorganisms evolve mechanisms to avoid the mononuclear phagocytes' potent microbicidal activity (discussed in **1.7**). The oxygen dependent defence mechanism is often referred to as the respiratory burst and includes the production and intracellular release of reactive oxygen species such as $O_2^{\cdot-}$, H_2O_2, $^{\cdot}OH$ as discussed previously (**1.5.2**). Oxidized halogens can kill bacteria and destroy many of their components, including redox enzymes and nucleotides. The oxygen independent acidification of the phagolysosome to a pH of 4.5-5 provides optimal conditions for the activity of lysosomal acid hydrolases, which kill a number of species.

Rheumatoid arthritis (RA) (reviewed in Pollack and Etzioni 1992) is an inflammatory joint disease affecting the wrists and small joints of the hands and feet,

but may also present as a systemic disease. Rheumatic nodules consist of necrotic material which is surrounded predominantly by Mϕs which often have epithelioid characteristics. RA sufferers have high levels of activated monocytes in their peripheral blood which produce elevated prostaglandin E_2 (PGE_2) levels. Two main hypotheses have been proposed to explain the pathogenesis of RA: Mϕ-fibroblast interactions and Mϕ-T cell interactions (reviewed in Kingsley. and Panayi 1997), both of which involve Mϕs as central players in joint destruction. The role of the Mϕ/granulocyte-specific gene *NRAMP1* and pathogenesis of RA will be discussed in more detail later.

Mϕs have been cited as playing a contributory role in the immune responses resulting in a number of diseases including systemic lupus erythematosus (SLE) (reviewed in Pollack and Etzioni 1992), scleroderma (reviewed in Pollack and Etzioni 1992), Guillain-Barré Syndrome (GBS) (Hartung *et al.* 1995), multiple sclerosis (MS) (Bauer *et al.* 1996) and sarcoidosis (Chilosi *et al.* 1988). They also play a role in wound healing, haemostasis (reviewed in Auger and Ross 1992) and atherosclerosis (reviewed in Parums 1992).

1.6.2 Macrophages and Mycobacterial Infection

The re-emergence of tuberculosis (TB) as a serious threat to human health throughout the world, after a period of relative "Western World freedom" from this scourge, has been widely publicised throughout the medical profession and media. However, the true scale of the problem may not be fully appreciated. At the 1993 symposium on "Immunology of Tuberculosis" in Berlin it was predicted that by the year 2000, ten million people will freshly acquire active disease annually, of which a third will die (Ehlers *et al.* 1994).

The course of TB can be divided into four stages. In stage 1 there is no bacillary growth, and the organism is usually destroyed or inhibited by mature resident alveolar Mϕs which ingest it. If it is not destroyed the tubercle bacillus grows in non activated Mϕs and destroys them. In stage 2 the bacilli grow logarithmically within

immature Mϕs from the blood stream and early lesions form. During stage 3 the number of viable bacilli becomes stationary due to the cell mediated and DTH responses which are mounted and inhibit bacilli growth. The tubercle forms with a solid caseous centre, and extracellular bacilli within it can not multiply due to the anoxic conditions, low pH and inhibitory fatty acids. By killing the non-activated Mϕs, in which the bacilli are growing, by the CMI and DTH responses, the host eliminates the intracellular environment favourable for bacilli growth. Bacilli present in immature Mϕs around the caseous centre are able to multiply, but in hosts which have mounted a good DTH response, multiplication is inhibited and bacilli are destroyed in highly activated Mϕs and epithelioid cells. These ingest and destroy bacilli escaping from the caseum and can arrest the disease. However, in severely infected and highly immunocompromised hosts, and in some cases even if the CMI response is well developed, the bacillus evades the host defences and in stage 4 the caseous centres may liquify resulting in unrestricted growth of the bacilli in the liquified mestruum. In the lung DTH responses against the extensive bacilli growth cause necrosis of the surrounding tissues and erosion of the walls of small bronchi, resulting in cavity formation and spread of the bacilli to adjacent tissues and the environment.

At the stage 3 point in the disease progression the difference in Mϕ activation determines the subsequent course of the disease. In resistant rabbits and most immunocompetent adult humans the lesion becomes surrounded by numerous microbicidal Mϕs, activated by T lymphocyte derived lymphokines. Bacilli escaping the caseous centre are ingested and destroyed, the tubercle becomes walled off and disease arrests. In susceptible rabbits, infants and immunocompromised adults many poorly activated Mϕs, which permit intracellular bacilli growth, surround the lesion. The DTH response kills these Mϕs, enlarging the caseous centre. Bacilli lodging in the draining tracheobronchial lymph nodes are not destroyed and multiple uncontrolled tubercles with extensive caseation form throughout the body ultimately leading to death.

1.6.3 Macrophages and Parasite Infections

The outcome of many parasitic infections is dependent on mounting an appropriate Th1 or Th2 response to eradicate or contain the pathogen. The Mϕ appears to be instrumental in the outcome of a number of parasite infections and is likely to influence the type of response mounted. In many cases resulting pathology is due to an inappropriate host response. Extracellular parasites of the helminth family *Schistosoma* (*S. spp.*): *S. japonicum, S. mekongi, S. mansoni* and *S. haematobium*) cause disease world wide (reviewed in Sadick 1992). *Leishmania* (*L. spp.*) is an obligate intra-macrophage parasite in the mammalian host and *L. major, L. donovani, L. donovani chagasi, L. mexicana* and *L. braziliensis* are responsible for Leishmaniasis in humans (reviewed in Sadick 1992). In schistosomiasis a granulomatous response to the schistosome eggs is common. In this infection a Th1 response is protective and a Th2 response results in disease. In leishmaniasis the reverse is true and the genetic effect of the gene *nramp1* on innate immunity to *Leishmania* infection in mice will be considered in more detail later (**1.8**).

1.6.4 Macrophages and Viral Infections

Blood monocytes, tissue Mϕs and DCs are the major cellular elements in the clearance and inactivation of many viral pathogens (reviewed in Gendelman and Morahan 1992). However, they are also the major target cell and infectious reservoir for many viruses, particularly lentiviruses. The phagocytic capacity of mononuclear phagocytes enables them to eliminate blood borne virus from the circulation. Mϕs can also restrict virus infection or replication in other cells by Mϕ mediated antibody dependent cell cytotoxicity (ADCC) when virus induced antibodies are present which can neutralise and bind to infected cells. Mϕs may initiate immune reactions, increasing the host's antiviral defence activity through release of cytokines (e.g. IFNα, IFNβ, TNFα, colony stimulating factors (CSF) and platelet derived growth factor (PDGF)) and may themselves be activated to an antiviral state by the action of cytokines released by virus specific T lymphocytes. Mϕs may also release factors with antiviral potential e.g. complement factors, arachidonic acid metabolites and neutral proteases. By acting as APCs and inducing specific antiviral T lymphocyte

mediated responses they initiate the second specific phase of the immune response. If a primary infection has not been successfully prevented they may act as a permissive target cell for viral latency and persistence.

The classic example of the effect of the hosts' genotype influencing infectivity of a virus is resistance to HIV infection in individuals who do not express the chemokine receptor CCR5, which acts as a co-receptor with CD4 for the virus. HIV not only infects CD4+T lymphocytes but Mϕs and DCs as well and the effect of the virus within these cells is likely to have major implications on the course of infection and transition to AIDS.

1.6.5 Macrophages and Primary Immunodeficiencies

The broad range of functions which Mϕs partake (i.e. inflammatory responses, antigen presentation, immunomodulatory networks) results in their dysfunction being involved in a wide variety of cellular and humoral immunodeficiency conditions. However, the fact that no condition has been reported to date where there is complete lack of the Mϕ cell population supports the indispensable role of this cell lineage. Mononuclear phagocytes are not only central to the immune system but during embryogenesis they clear the developing body of apoptotic cells which have died by PCD as the body form and organs of the foetus develop.

Mϕs or monocytes have been shown to be defective in a variety of ways in patients suffering from a number of diseases including chronic granulomatous disease (CGD) (Donowitz and Mandell 1982), chronic mucocutaneous candidiasis (CMC) (reviewed in Pollack and Etzioni 1992), common variable immunodeficiency (CVID) (Arala-Chaves *et al.* 1982; Eibl *et al.* 1982a, 1982b and 1983; Pollack *et al.* 1985), Wiskott-Aldrich syndrome (WAS) (reviewed in Pollack and Etzioni 1992), leucocyte adhesion deficiency (LAD) (reviewed in Pollack and Etzioni 1992) and Chadiak-Higashi syndrome (CHS) (Gallin *et al.* 1975; Komiyama *et al.* 1986; reviewed in Griffiths 1995). Such conditions render sufferers to succumb to frequent

infections including *Staphylococcus aureus* (*S. aureus*), enteric gram negative rods, *Aspergillus spp.* and *Candida spp.* and pyrogenic bacteria.

A number of primary familial monocyte disorders have been documented where patients' monocytes exhibit reduced phagocytic activity and accessory cell function (Prieto *et al.* 1990) and abnormal mobility and phagocytosis-killing ability against *C. albicans* (Yamazaki *et al.* 1984).

Protective immunity to intracellular bacteria such as *Mycobacterium* and *Salmonella* is dependent on CMI, a major effector mechanism of which is believed to be activation of infected Mϕs by type 1 cytokines including IFNγ. IFNγ is produced by Th1 lymphocytes and NK cells, and regulated by IL-12, which is released by Mϕs and DCs. Severe and selective susceptibilty to infection with *Mycobacteria* of low grade virulence, and sometimes *Salmonella*, occurs in individuals with complete IFNγ receptor (IFNγR) 1 deficiencies (Ottenhoff *et al.* 1998). Poorly differentiated mycobacterial granulomata develop with many scattered Mϕs, but a lack of epithelioid cells, giant cells and surrounding lymphocytes. The immunodeficiency is often fatal. The IFNγR1 gene has been identified as harbouring a mutation hot spot for deletions which result in dominant negative mutations inferring susceptibility to the same pathogens as the complete IFNγR1 mutations (reviewed in Foote 1999; Jouanguy *et al.* 1999). Partial IFNγR1 deficiency has also been reported which impairs, but does not abrogate, IFNγR affinity for its ligand (Ottenhoff *et al.* 1998). The deficiency appears to predispose individuals to curable "tuberculoid-like" mycobacterial infections. A single case of complete IFNγR2 deficiency has been identified which clinically, immunologically and histopathologically closely resembles the cases of complete IFNγR1 deficiency (Ottenhoff *et al.* 1998). Individuals with IL-12 p40 and IL-12Rβ1 deficiencies have also been described who show similar clinical syndromes to partial IFNγR1 deficiency (Ottenhoff *et al.* 1998). The selectivity of the infections with poorly pathogenic mycobacteria, and in some cases *Salmonella*, in the absence of other severe microbial infections suggests the type 1 cytokine pathway and its effect on Mϕ function is essential in controlling

these infections and there is no redundant protective immune response in these individuals.

This collection of examples of human disease syndromes associated with Mϕ dysfunction serve to highlight their importance in the maintenance of health and resistance to infection. It is apparent that their function and activity may be regulated and affected, either subtly or significantly, by genetic factors and determining these loci may help extend our understanding of how Mϕs perform effectively.

1.7 INTRACELLULAR EVASION MECHANISMS AGAINST MACROPHAGE DEFENCE

The Mϕ is the target cell for a large and diverse range of microorganisms demonstrating an obligate requirement for an intracellular environment in which to survive and replicate. In order to survive they need to overcome the defence mechanisms of the Mϕ which include the oxygen dependent production of ROIs and reactive nitrogen intermediates (RNI) and the oxygen independent acidification of the phagolysosmal vacuole and action of hydrolytic lysosomal enzymes, nutrient deprivation, defensins and other antimicrobial proteins. The complexity and multi-layered make up of the host defence means there are many levels where parasites may interfere with development of the response. Intracellular pathogens can actively alter cell signalling leading to Mϕ deactivation and deactivation can also result from the induction of auto-inhibitory cytokines such as IL-10 and TGFβ. A number of infectious agents including *Leishmania, Mycobacterium*, *Plasmodium*, *Yersinia* and HIV can result in Mϕ dysfunction. Many microbes secrete toxins to kill the phagocyte which include streptolysin of *Streptococcus spp.* and leukocidin of *S. aureus*. *Neisseria meningitidis* and *pnemococci* cover their surface with a hydrophobic capsule to resist phagocytosis. Organisms including *Chlamydia*, *Legionella pneumophilia* (*L. pneumophilia*), *Leishmania*, *Mycobacterium*, *Toxoplasma gondii* (*T. gondii*) and *Trypanosome cruzi* have adopted strategies to survive the hostile phagolysosome e.g. inhibition of its acidification or phagosome-

lysosome fusion or escape from the vacuole (reviewed in Hall and Joiner 1991; reviewed in Sadick 1992; reviewed in Speert 1992; reviewed in Reiner 1994).

Having discussed the Mϕ, its actions and importance in the maintenance of well being our present knowledge about a gene of particular importance in the function of this cell lineage will now be considered in detail and the possible role the gene may play in human disease.

1.8 NATURAL RESISTANCE-ASSOCIATED MACROPHAGE PROTEIN

1.8.1 History and Isolation of the *Nramp* Gene

As mentioned previously, intracellular bacterial parasite infections represent a serious problem and genetic analysis of mice showing distinct phenotypic differences in their response to such infections is one approach to understanding the natural response against these pathogens. Gros *et al.* reported that, in mice, natural resistance to the intracellular BCG (Bacillus Calmette-Guréin) parasite is controlled by a single, dominant, autosomal gene, which is not linked to the H-2 locus (Gros *et al.* 1981). Phenotypic expression of the gene, defined as *Bcg*, could be detected as early as 24 hours after infection and susceptible strains of mice showed active multiplication of BCG up to 3 weeks, after which bacterial counts started to decline. *Bcg* exerts its effect during the early innate immune response and appears to control early *in vivo* multiplication of the bacilli, rather than their elimination. Independently a similar observation was made with respect to susceptibility and resistance to *L. donovani* with susceptible mice unable to contain growth of the parasite during the early stage of infection and the locus responsible was named *Lsh* (Bradley 1974). The same pattern of resistance and susceptibility was observed with *Salmonella typhimurium* (*S. typhimurium*) infection, the phenotype being inherited in a single, autosomal, recessive Mendelian fashion (Plant and Glynn 1976). The locus responsible was termed *Ity*. However, unlike with the *Bcg/Lsh* genotype, and mycobacterial/leishmanial infections, *S. typhimurium* infection in susceptible animals is fatal by day 10-16 post infection. The difference is due to the highly

virulent nature of this mouse pathogen, which replicates very rapidly in RE organs producing an overwhelming, lethal infection before a specific immune response has been established.

Significant evidence existed which suggested the *Bcg, Lsh* and *Ity* loci were one and the same (Plant *et al.* 1982; Skamene *et al.* 1982). This was confirmed when a candidate gene, which had been mapped to mouse chromosome 1 (Schurr *et al.* 1989) was cloned (Vidal *et al.* 1993) and named natural resistance-associated macrophage protein (*nramp*).

Evidence from a variety of sources, including silica treatment, radio-resistance, explantation of Mϕs from resistant to susceptible mice and the cellular tropism of the infectious agents, indicated that the Mϕ was the cell type expressing the genetic differences between the resistant and susceptible strains of mice. In addition, *in vitro* stimulated Mϕs from resistant and susceptible mice show temporal, qualitative and quantitative differences in mRNA expression of early response genes including *c-fos, c-myc, JE* and *KC*. The microbistatic effect against *L. donovani* is most pronounced in KCs: however, it and the antimycobacterial activity of activated Mϕs is independent of the respiratory burst. Though differences in the latter are observed in resistant and susceptible strains this appears to be a marker of the activation state of the Mϕs, rather than mediating the antimicrobial effect of the cells. Killing of *Leishmania* in resistant strains does appear, however, to be dependent on NO production mediated through a TNFα autocrine fashion (Blackwell *et al.* 1991). It is important to note that the early resistance/susceptibility controlled by the *Bcg/Lsh/Ity* locus is independent of a functional T cell population. However, the genotypic status may have "knock on" effects on the course of infection due to upregulation of MHC Class II antigens in resistant Mϕs and more efficient antigen presentation to CD4+ T lymphocytes. For instance CD4+ splenic T lymphocytes from resistant mice infected with *L. donovani* retain an enhanced and increased ability to generate IFNγ in response to *in vitro* re-stimulation with leishmanial antigen which is not seen in susceptible mice. Similar findings have been observed following *M. bovis* BCG

infection (reviewed in Lang *et al.* 1997). Thymic, euthymic and athymic nude mice of the *Ity*-resistant phenotype showed no difference in *S. typhimurium* growth during the early innate stage of infection (O'Brien and Metcalf 1982). There have also been reports showing that BALB/c (susceptible) mice are actually more resistant to the virulent H37Rv strain of *M. tuberculosis* than DBA/2 (resistant) mice, emphasising that the ultimate outcome of such infections is regulated by additional genetic loci to *nramp* (Medina and North 1996 and 1998; Medina *et al.* 1996). Studies using NOSII knockout mice have identified iNOS to be of paramount importance in controlling *M. tuberculosis* infection in mice (MacMicking *et al.* 1997). The $NOSII^{-/-}$ mice did not appear affected with respect to many cellular components of the immune response considered important i.e. CD4+ and CD8+ T lymphocyte populations, Th1 proliferative responses to other intracellular pathogens, IFNγ induced MHC Class II upregulation, respiratory burst and IFNγ and TNFα elaboration, yet the mice succumbed to infection and died. The susceptibility was independent of *nramp* genotype. However, it is important to point out that the end points and responses measured in this study were taken at times beyond those where *nramp* dependent responses are measurable. iNOS and NO production are obviously critically important in influencing the end outcome and chronicity of *M. tuberculosis* infection, and may well be a point of convergence of IFNγ and TNFα signals. *Nramp*, though pivotal in orchestrating the early innate response, may not be able to override the regulation and effect of determinants of the specific immune response, which is the final death knell of such infections.

Penninger *et al.* have shown that ligand recognition of γδ transgenic T cell hybridomas, which was dependent on the γδ TCR, but independent of TAP-2 and MHC Class I or II, was influenced by the *nramp* gene. The hybridomas did not respond against Mϕs from susceptible mice but the role of *nramp* in the recognition by the γδ T lymphocytes is not clear nor the implication of this finding in physiological situations and infections (Penninger *et al.* 1995).

Vidal *et al.* isolated *nramp* as a candidate for the *Bcg/Lsh/Ity* gene by a positional cloning approach (Vidal *et al.* 1993). The gene was later renamed *nramp1* when further homologous genes were isolated. Its expression was found to be restricted to RE organs, populations enriched in Mϕs and a Mϕ cell line. This expression profile has subsequently been confirmed and the gene is expressed specifically in Mϕs and granulocytes (Vidal *et al.* 1993; Govoni *et al.* 1997).

1.8.2 Nramp1 Protein

Computer assisted analysis of the predicted amino acid sequence translation of the *nramp1* gene identified ten or twelve hydrophobic potential transmembrane (TM) domains (now believed to be twelve), two potential N-linked glycosylation sites, five potential PKC phosphorylation sites and a putative src homology 3 (SH3) binding domain (Vidal *et al.* 1993; Barton *et al.* 1994). The latter two are not conserved in all the other family members of this protein, which will be discussed later (**1.8.3**), suggesting a lack of functional importance or differences in regulation of the different proteins across species. A twenty amino acid transport motif, initially identified in a group of bacterial proteins (including the histidine, maltose and oligopeptide transporters of *E. coli*), known as the "binding protein-dependent transport system inner membrane component signature" (which will be referred to as the conserved transport motif) was also present in *nramp1*. This motif has the sequence (E,Q) $(S,T,)_2$ 3X G 6X (L,I,V,M,Y,F,A) N4X (F,L,I,V) (P,K) where residues in brackets are alternative residues and X represents any residue (Gruenheid *et al.* 1995). Bacterial permeases containing this motif are multi-subunit transporters composed of a periplasmic substrate-binding protein, one or two homologous highly hydrophobic inner membrane proteins believed to participate in substrate translocation and one or two peripheral ATP-binding energy coupling subunits. They are members of the ATP-binding cassette (abc) superfamily of membrane transporters and the motif is postulated to mediate the interaction of peripheral ATP binding subunits with the membrane components to energise transport (reviewed in Belouchi *et al.* 1997). Eukaryotic abc transporters have not retained the conserved transport motif, having integrated ATP binding subunits and membrane anchors in

the same polypeptide. However, certain eukaryotic transport proteins i.e. (Na^+, K^+) ATPase of *Drosophila melanogaster* (*D. melanogaster*), uracil permease of *Sacharomyces cerevisiae* (*S. cerevisiae*), *Aspergillus nidulans'* (*A. nidulans*) nitrate uptake protein, murine and human nramp2 proteins, *Oryza sativa* (*O. sativa*) nramp proteins and sequences from *C. elegans* and *M. leprae* show high sequence identity and similarity which is most marked in the motif and hydrophobic core of the proteins (33-75% identity). This degree of conservation is remarkable for membrane proteins separated by up to a billion years (reviewed in Cellier *et al.* 1995). The most conserved region of the nramp family member proteins shares several invariant residues (T M T $(X)_4$ G (D,Q) $(X)_4$ G F notation as for the conserved transport motif described above) with a highly conserved region of animal voltage-gated K^+ channels and a pattern of conserved residues with the proteolipid subunit of the vacuolar H^+/ATPase family (vATPase) (reviewed in Skamene *et al.* 1998). Human NRAMP1 (discussed in **1.8.8**) and mouse nramp1 proteins are 89% homologous and share the same characteristic features including potentially charged residues in six of the TM domains, which are also highly conserved in the other family members analysed. This may suggest that the proteins function as water-filled pores or hydrophilic conducting channels. The TM segments are believed to form helical structures which form a bundle with the more conserved face of the helices, containing the invariant polar/charged residues, positioned towards the interior of the channel and the hydrophobic exterior towards the lipid membrane.

Substantial evidence that *nramp1* was responsible for the *Bcg/Lsh/Ity* phenotype came from the identification of a single g>a transition present in the *nramp1* gene of seven susceptible strains, but none of the twenty resistant strains, of mice analysed (Vidal *et al.* 1995a). Based on the predicted multispanning transporter model this would result in substitution of glycine (G), a small flexible residue, with aspartic acid (D), a negatively charged residue, at position 169 on a strongly hydrophobic face of the proposed helix within TM 4. Such a change would be expected to have profound effects on the physical properties of the domain. Vidal *et al.* have failed to identify mature nramp protein in susceptible mice by Western blotting, suggesting

this single amino acid change prevents proper folding and/or causes aberrant targeting to the Golgi and subsequent degradation of the mutant protein (Vidal *et al.* 1996). In fact the G>D mutation is a null allele in mice. These mutants have the same phenotype as that of *nramp1*$^{-/-}$ mice (Vidal 1995a and 1995b), showing the profound impact a single base change can have.

Definitive proof that *nramp1* was the *Bcg/Lsh/Ity* gene was provided by targeted gene disruption of *nramp1* and transfer of the wild type allele onto a susceptible background (Vidal *et al.* 1995a and 1995b; Govoni *et al.* 1996). Vidal and colleagues also showed that an intact *nramp1* gene is not necessary to mount cellular responses against BCG, for granuloma formation, to contain bacterial dissemination or to trigger Mϕ differentiation into cells capable of killing ingested mycobacteria, supporting the view that *nramp1* does not appear to play a major role in elimination of intracellular parasites by activated Mϕs but prevents their proliferation.

1.8.3 Nramp Family Members

Sequence analysis of *nramp1* has identified a number of genes and proteins which have been collectively classified as members of the *nramp* family. These have been found in many phylogenically distinct organisms suggesting the fundamental importance of these proteins throughout evolution. Before murine *nramp1* (**1.8.4-1.8.6**) and human *NRAMP1* (**1.8.8**) are discussed in detail a selection of other members of their family will be considered. Studying and elucidating the function of these homologues has enhanced our understanding of the nramp1 proteins.

1.8.3.1 Other Mammalian *Nramp* Genes

In 1995 a murine gene named *nramp2* was reported which mapped to chromosome 15 and had been isolated by cross hybridisation of *nramp1* complementary DNA (cDNA) clones. The predicted structure of the nramp2 protein is very similar to that of nramp1, with the proteins having 63% identical (78% similar) residues and the genes being 86% identical (Gruenheid *et al.* 1995). A second human *NRAMP* gene (*NRAMP2*) was identified in 1995, which mapped to 12q13. The full length *NRAMP2* cDNA was published in 1997, the coding region of which was 64%

identical to human *NRAMP1* (Kishi and Tabuchi 1997). Two splice variants of the gene have been identified with the shorter (*NRAMP2 non IRE*) differing at the 3' end, lacking a classical iron-responsive element (IRE) and substituting twenty five novel amino acids for the C-terminal eighteen amino acids of the *NRAMP2 IRE* form (Lee *et al.* 1998). The human *NRAMP2* promoter region contains two CCAAT boxes, three potential Sp1 binding sites, a potential IRE and five potential metal response elements but no TATA box.

Electrophysiological studies in *Xenopus* oocytes demonstrated that nramp2 functions as a pH dependent divalent cation transporter (reviewed in Atkinson and Barton 1998; reviewed in Hackman *et al.* 1998). The high level of sequence conservation between the nramp1 and nramp2 proteins reinforced the predicted role of this family of proteins as multispanning transport proteins. A view substantiated by Fleming and colleagues when they identified *nramp2*, using linkage analysis, genetic mapping and candidate gene approaches, to be the gene responsible for microcytic anaemia (*mk*) in mice (Fleming *et al.* 1997; reviewed in Vulpe and Gitschier 1997). These mice show defects in intestinal iron absorption and erythroid iron utilisation. Analysis of *nramp2* sequence identified a g>a transition at a CpG dinucleotide in strains of *mk* mice from two independent origins, resulting in a glycine (G) to arginine (R) substitution. This mutation, like the nramp1 G>D mutation, is situated in TM 4, two helical turns away from the equivalent position of the nramp1 mutation. Again, a charged residue replaces a flexible glycine residue with extremely detrimental consequences for affected mice. This same mutation has also been identified in the *nramp2* gene of the Belgrade rat (*b*) which has an autosomal, recessively inherited, microcytic, hypochromic anaemia associated with abnormal reticulocyte iron uptake and gastrointestinal iron absorption. These rats represent an animal model for deficiency in intestinal iron uptake (Fleming *et al.* 1998). This rat homologue was initially identified as a divalent cation transporter with a broad substrate range including Fe^{2+}, Zn^{2+}, Mn^{2+}, Co^{2+}, Cd^{2+}, Cu^{2+}, Ni^{2+} and Pb^{2+} and was named *DCT* (divalent cation transporter) *1* (Gunshin *et al.* 1997). It is interesting to note, when hypothesising the specificity of *nramp1* from studies of its homologues, and potential

for a shared or similar function of nramp1 and nramp2 that nramp1's affinity for Fe^{2+} was much lower than that of DCT1 and nramp2 transfection of RAW264.7 cells was unable to overcome the *nramp1* susceptible phenotype (Govoni *et al.* 1999). *DCT1* maps to a region of rat chromosome 7 exhibiting syntenic homology to the distal portion of mouse chromosome 15, where murine *nramp2* maps. Both rat and murine genes generate alternatively spliced mRNAs which encode 561 or 568 amino acid proteins. DCT1's amino acid sequence is 73% identical to human NRAMP1 and 92% identical to human NRAMP2. It is expressed in a wide range of tissues, with particularly high levels in the intestine at the sites responsible for intestinal absorption of most divalent cations, in the S3 proximal tube segments and collecting ducts of the kidney, in the cortex of the thymus and neurones in the brain. Nramp2 is an integral membrane protein which is extensively modified by N-linked glycosylation which contributes more than 40% of its molecular mass (Gruenheid *et al.* 1999). The protein has been localised to the plasma membrane and recycling endosomes which contrasts to the lysosome location of nramp1 (discussed in **1.8.6**) (Gruenheid *et al.* 1997). Nramp2 co-localises with Tf and may be responsible for transporting Fe^{2+} into the cytoplasm after acidification of the Tf-positive endosome. Both release of iron from Tf and iron transport by nramp2 require conditions of low pH. *DCT1* mRNA levels appear to be regulated by iron, with diet induced iron deficiency resulting in dramatically enhanced expression. This may be due to stabilisation of the mRNA as the message has a stem-loop-structure in the 3' untranslated region similar to the iron regulatory element-binding protein site which mediates stability of the TfR mRNA during iron deficiency (reviewed in Fleet 1998). It has been suggested that DCT1 may be responsible for non-receptor mediated iron uptake in the intestine. Though Tf receptor (TfR) mediated endocytosis of iron is likely to partake in iron uptake, the level of apo-transferrin in the intestinal lumen is insufficient to account for the total dietary iron absorption, necessitating another uptake mechanism. It is likely that the phenotypic abnormalities exhibited by the *mk* and *b* animals result from the cumulative effect of metabolic disorders of divalent cations such as Mn^{2+}, Zn^{2+} or Co^{2+} in addition to those mediated by iron. Complementation studies in yeast, where *nramp2* was capable of complementing the

smf1/smf2 mutant (discussed in **1.8.3.5**), suggest *nramp2* encodes a protein which is capable of transporting Mn^{2+} in yeast and that residues Q384 and G394 in nramp2 were necessary for this complementation (Pinner *et al.* 1997; reviewed in Govoni and Gros 1998).

In the human *NRAMP2* gene five polymorphic sites and a single nucleotide mutation have been identified but no observed linkage disequilibrium of haemochromatosis patients with either mutant or normal *HFE* genes and a particular haplotype has been found (Lee *et al.* 1998), though this does not eliminate *NRAMP2* as a potential contributor to human iron transport pathologies. Zoller *et al.* propose decreased amounts of low molecular weight iron in duodenal crypt cells of hereditary haemochromotosis patients, due to the *HFE* mutation, may activate the IRE binding affinities of iron regulatory protein (IRP)-1 and IRP-2 resulting in increased TfR and *NRAMP2* mRNA levels. Increased NRAMP2 expression at the apical site of the duodenal mucosa would then promote uptake of iron leading to iron overload of the duodenal cells (Zoller *et al.* 1999).

The most striking difference between nramp1 and nramp2 is the ubiquitous expression of the latter compared to the highly specific Mϕ and granulocyte restricted pattern seen for nramp1. Isotype specific antibodies raised against murine nramp1 and nramp2 have shown Mϕs to co-express both nramp proteins (Gruenheid *et al.* 1999). In addition nramp2 does not contain the putative SH3 binding domain of nramp1. Two *nramp* genes have been identified in mice, rats and humans; three have been found in swine and birds; a putative third gene in mice has been mapped to chromosome 17; and *nramp* genes have been cloned from sheep and apes (Bussmann *et al.* 1998; Roger *et al.* 1998).

1.8.3.2 *Malvolio*

Shakespeare's Malvolio in "Twelfth Night" lives on in namesake in a group of *Drosophila* mutants who, likewise, "*tast'd with distemper'd appetite*" (Rodrigues *et al.* 1995). These *mvl* mutants showed a reduced preference for sugars and increased acceptance of low salt concentrations. The mutants' abnormal taste behaviour could

be suppressed by Mn^{2+} and Fe^{2+} supplementation and the *mvl* mutation appears to affect a signal transduction pathway underlying taste perception rather than a requirement for correct development of the nervous system components involved in taste perception (Orgad *et al.* 1998). The amino acid sequence of the protein responsible for the abnormal taste behaviour is 64%/65% identical and 78%/79% similar to the mouse nramp1/human NRAMP1 sequences. *Mvl* is expressed in fully differentiated neurones in the CNS, and neurones in the PNS and Mϕs throughout development. Its function is not known but Supek *et al* suggest it may be involved in Mn^{2+} transport on the basis of preliminary experiments in which Mn^{2+} ions reversed the taste behaviour phenotype (Supek *et al.* 1997).

1.8.3.3 Fish

Recent reports have identified *nramp1* (*OmNramp alpha*) and *nramp2* (*OmNramp beta*) homologues, in rainbow trout (a teleost) and smelt. The latter are diploid relatives of the ancestral tetraploid teleost supporting the hypothesis that *OmNramp alpha* and *OmNramp beta* are independent loci which were present before chromosomal duplication of salmonids, and the trout loci do not represent a recent duplication (Dorschner and Philips 1999).

1.8.3.4 *crnA*

crnA mutants of *A. nidulans* were discovered which retained wild type growth on nitrate as a sole source of nitrogen but showed reduced nitrate uptake (Unkles *et al.* 1991). The *crnA* gene, which encodes a nitrate transporter, was identified via these mutants and when *nramp1* was subsequently isolated the striking sequence conservation attracted much interest and speculation of a similar function for the nramp1 protein, a view which has now fallen out of favour.

1.8.3.5 *SMF*

SMF1 and *SMF2* were identified as *S. cerevisiae* genes capable of suppressing the *mif1* mutant, which has a defective processing enhancing protein (PEP) of mitochondria (West *et al.* 1992). A mutation in the *CDC1* gene was also found which prevented growth of the yeast in the presence of ethylene glycol-bis (β-

aminoethyl ether)-N,N,N',N'-tetraacetic acid (EGTA) and the mutant could be suppressed by overexpression of the *SMF1* gene. *SMF1* appears to be involved in high affinity Mn^{2+} and/or Zn^{2+} uptake and is located in the plasma membrane (Supek *et al.* 1996). *SMF2* has been identified as a possible low affinity Mn^{2+} transporter (Supek *et al.* 1997) and a third yeast gene of this family has also been identified. As well as these substrates the SMF1 and SMF2 proteins participate in transport of Cu^{2+}, $Co^{2+}$and Cd^{2+} (reviewed in Liu and Culotta 1999a).

The amino acid sequence of SMF1 is 30%, and SMF2 29%, identical to human and mouse nramp1 proteins with between 53% and 58% overall similarity. The greatest sequence conservation is over the conserved transport motif (Blackwell *et al.* 1995). These findings introduce the possibility that nramp1 may function as a Mn^{2+} and/or Zn^{2+} transporter. A gene has been identified which negatively regulates the SMF1 and SMF2 metal transport systems called *BSD2.* The gene product is situated in the ER and was postulated to retain the metal ion transporter proteins in the ER preventing their over accumulation in the plasma membrane and resulting over accumulation of metal ions (reviewed in Orgad *et al.* 1998). Recent reports have elucidated the control of SMF1 and SMF2, mediated by the *BSD2* gene product, to include regulation via manganese and to a lesser extent iron as well. Under normal situations the bulk of the SMF protein is targeted to the vacuole for degradation, however, in *BSD2* mutants the transporter remains within the secretory pathway and fails to arrive at the vacuole. Physiological concentrations of manganese induces the degradation of SMF2 in a bsd2-dependent manner while under conditions of metal starvation the protein fails to arrive at the vacuole, accumulating at the cell surface in a bsd2 independent way (Liu and Culotta 1999a). A functional metal transporter is a prerequisite for movement to the plasma membrane and sequences in the conserved transport motif and TM4 domains are needed for SMF1 to respond to metal starvation (Liu and Culotta 1999b). A similar system regulated by the cellular metal ion concentration is likely to exist controlling the mammalian homologues and it has been speculated that the haemochromatosis *HFE* gene may produce an analogous protein to the bsd2 protein (reviewed in Orgad *et al.* 1998). SMF1 and SMF2 do not

share the SH3 binding domain structure suggesting that this domain may be a recent addition to the nramp1 molecule related to its Mϕ/granulocyte restricted function.

1.8.3.6 *OsNramp*

Using the predicted amino acid sequences of the mammalian nramp1 proteins a database search identified several expressed sequence tags (EST) with significant homology to *nramp1* (Belouchi *et al.* 1995). Two of these originated from *O. sativa* (rice) and led to identification of a gene named *OsNramp1* which encodes a protein with 60% overall homology to *nramp1*. As for the other *nramp* family members the highest degree of sequence conservation is in the regions of predicted functional importance, the conserved transport motifs, twelve predicted TM domains (including the charged residues) and N-linked glycosylation sites, though the SH3 binding domain in nramp1 is not conserved. *OsNramp1* is expressed primarily in roots and only at very low levels in leaves/stems. Based on hybridisation studies two further members of the family, *OsNramp2* and *OsNramp3*, have also been identified and several homologues are believed to exist in other plant species including corn, wheat and possibly potatoes, tomatoes, cabbage and field beans (Belouchi *et al.* 1997). *OsNramp2* is primarily expressed in leaves and *OsNramp3* in roots and leaves and the proteins are 69% and 60% similar to nramp1, respectively. Divalent cations such as Mg^{2+}, Mn^{2+}, Co^{2+} and Zn^{2+} are essential cofactors for many metabolic enzymes and the OsNramp proteins may be plant transporters of such ions. The three members may transport similar metal ions in different plant tissues with the differences in the proteins reflecting differences in their regulation or their ability to function in a specific cellular environment. It has also been suggested that these *nramp* homologues may be implicated in the ethylene response pathway based on identification of an *Arabidopsis thaliana* (*A. thaliana*) homologue which complemented *A. thaliana* mutants defective in the ethylene respiratory pathway.

1.8.3.7 *Caenorhabditis elegans*

Genomic sequencing of *C. elegans* has revealed two tandem genes encoding peptides 85% identical and 66-70% identical to mammalian *nramp,* though their function is unknown (reviewed in Cellier *et al.* 1996).

1.8.3.8 *Mycobacteria*

An *nramp* family member has been found in *M. leprae* which shares 37% identity with its mammalian counterpart and it has been suggested the two proteins may compete for a common substrate vital for the intracellular survival of the bacteria (reviewed in Cellier *et al.* 1996). Additional *nramp* related sequences have also been identified in the genomes of *M. tuberculosis, M. avium* and *M. smegmatis* as well as some gram negative and gram positive bacteria (reviewed in Govoni and Gros 1998; reviewed in Skamene *et al.* 1998).

Gene	Source	Amino acid identity with nramp1	Function
NRAMP1	Human	88%	DCT
nramp2	Mouse	78%	DCT (Fe^{2+})
DCT1	Rat	63%	DCT (Fe^{2+})
Mvl1	*Drosophila*	70%	DCT (Mn^{2+})
crnA	*A. nidulans*		nitrate transporter
SMF1/SMF2/ SMF3	*S. cerevisiae*	29-30%	DCT (Mn^{2+}, Zn^{2+})
OsNramp1/ OsNramp2/ OsNramp3	*O. satavia*	46-57%	
	C. elegans	68%	
	Mycobacterium	37%	

Table 1.1 Table showing the amino acid identity of a selection of nramp1 family members with the nramp1 sequence. Where known the proposed protein function is given; DCT divalent cation transporter with the cation of highest affinity given in brackets. Reference sources are as in the text of **1.8.3**.

1.8.4 *Nramp1* Regulation

Murine *nramp1* is constitutively expressed in Mϕs but the level is dramatically enhanced by IFNγ, LPS and GM-CSF suggesting it has a function in both resting and activated Mϕs (Atkinson *et al.* 1997; Brown *et al.* 1995). Treatment with corticosterone increases *M. avium* growth in susceptible but not resistant mice and suppressed *in vitro nramp1* mRNA expression in susceptible Mϕs, suggesting a role of hormones in the gene's regulation (Brown *et al.* 1995). *Nramp1* has been shown to

be expressed in granulocytes at very high levels and *in vivo* or *in vitro* maturation of monocytes to Mϕs upregulates its expression (Govoni *et al.* 1997).

Upstream of the two predicted transcription initiation sites in the murine *nramp1* gene no TATA or CAAT sequences associated with RNA polymerase II transcription have been found, but a potential initiator (Inr) element exists. The region contains a GC rich region, two putative AP-2 sites, one AP-1 site, one AP-3 site, a PU-1 binding site, two NF-IL6 sites, five IFNγ response elements (γ-IRE), an interferon-stimulated response element, (ISRE), an IFNγ activating sequence (GAS) element, an interferon binding protein-1 (IBP-1) binding site, two NF-IL6 binding sequences and a Sp1 binding site. The latter has been shown to augment transcription of the IL-8 and *Ha-ras* genes during Mϕ activation (Blackwell *et al.* 1995; Govoni *et al.* 1995). The presence of these elements is consistent with a Mϕ expression profile regulated by LPS and/or IFNγ. Govoni and colleagues have shown murine *nramp1* expression can be strongly upregulated by LPS in RAW264.7 cells in a dose and time dependent fashion, which requires active protein synthesis. Pre-treatment with IFNγ prior to LPS administration increased *nramp1* induction, showing a synergistic effect of these stimuli, though IFNγ treatment alone did not have a strong modulatory effect on *nramp1* mRNA expression. *In vivo* experiments using intraperitoneal injection of LPS or thioglycollate also induced *nramp1* mRNA expression in splenic Mϕs (Govoni *et al.* 1997).

1.8.5 Nramp Function and Phenotypic Effects

The role of NO in controlling intra-Mϕ infections and its regulation by *nramp1* is unclear. From the sequence similarity of *nramp1* and *crnA*, the *A. nidulan's* nitrate transporter (**1.8.3.4**), a similar function was proposed, whereby *nramp1* mediated transportation of nitrate or nitrite into the phagosome/phagolysosome might augment NO production in the acidic environment, with potential anti-pathogen activity. Blackwell *et al.* have reported a requirement for NO in the anti-leishmania response (Blackwell *et al.* 1991), though Brown and colleagues have ruled out a role for NO as an effector molecule in *Bcg*-mediated resistance based on *in vitro M. avium*

infections (Brown *et al.* 1995). Though N^G-monomethyl-L-arginine (NMMA) inhibited the antimycobacterial response in Mϕs from both resistant and susceptible mice, corticosterone suppressed NO production in resistant Mϕs but did not affect *M. avium* growth.

Doherty and Sher (Doherty and Sher 1997) have reported that the mechanism of control of *M. avium* appears distinct from that triggered by other intracellular infections such as *M. tuberculosis* and *T. gondii*, being *nramp1* independent. The mycobacteria appear to escape the innate phase of the response and TNFα and NO induction do not seem to be necessary for control of the infection but may actually contribute to the pathology. The NO resistance has been ascribed to the unusual nature of the mycobacterium's cell wall. Thus, the phenotypic effect of the *nramp1* genotype does not seem to be generalised over all members of a species reflecting a highly specific defence mechanism and pathogen interaction which may account for the above discrepancies. Indeed the complex interaction of the genotype of both host and pathogen has been highlighted by a study of susceptible and resistant mice which were infected with *S. dublin*, which contains a virulence plasmid, and the isogenic plasmid-cured strain LD842. Both strains of mice were resistant to the LD842 bacteria but when mice with the *nramp1* mutation were made neutropenic they succumbed to the infection. Mice of both strains, however, were susceptible to the virulent *S. dublin*. The authors of this study suggest that *Salmonella* have adapted to grow inside Mϕs, sheltered from neutrophils with neutrophils being the primary host defence against non typhoid *Salmonella* carrying virulence plasmids (Vassiloyanakopoulos *et al.* 1998).

Nramp1 mutations have been reported to have a dramatic effect on the growth rate of *L. donovani, M. bovis, M. intracellulare, M. lepraemurium, S. typhimurium, Brucella abortus, T. gondii* as well as *M. avium* (in contrast to the findings of Doherty and Sher mentioned above (Doherty and Sher 1997)) in RE organs but the growth of other intracellular parasites such as *L. monocytogenes, L. pneumophilia, Pseudomonas aeruginosa, S. aureus* and *Bacillus subtilis* does not appear to be under

nramp1 control (reviewed in Gruenheid *et al.* 1997; reviewed in Govoni and Gros 1998). The impact of *nramp1* on *M. avium* growth is controversial.

Resistant and susceptible congenic strains of mice infected with an attenuated vaccine strain Rv6 of *Salmonella abortusovis* showed marked differences in their specific antibody response (Gautier *et al.* 1998). These responses, particularly IgM and IgG3 titres, were significantly higher in susceptible mice and may reflect the higher bacterial load and longer persistence of the bacteria in these mice which would provide a stronger stimulation for the humoral response. In contrast, in resistant mice the alternative defence mechanism involving IFNγ and TNFα synthesis and intracellular killing of pathogens by Mϕs is likely to predominate. Despite IgM and IgG3 being good activators of the complement cascade no difference in the complement response to infection was seen.

The *in vitro* effects of LPS/IFNγ mediated Mϕ priming or activation influenced by *nramp1* include regulation of the C-X-C neutrophil chemoattractant KC, IL-1β, iNOS, MHC Class II, 5' nucleotidase, AcM-1, TNFα, NO, L-arginine flux, respiratory burst and tumouricidal activity. The gene clearly has many pleiotropic effects and it is hard to reconcile its proposed functions as a phagosomal/phagolysosomal nitrate transporter, based on homology with *crnA* (**1.8.3.4**), with this multitude. From the sequence similarity of nramp1 with the SMF1 and SMF2 proteins (**1.8.3.5**) and the mistaken view initially that SMF1 and SMF2 resided in the mitochondrial membrane it was proposed *nramp1* may play a role in mitochondrial function. Mitochondrial derived ROIs and NF-κB activation are involved in the apoptotic and gene inductive effects of TNFα which some have suggested *nramp1* may regulate (Barton *et al.* 1995). An increase in respiratory burst, nitrite release and L-arginine transport has been observed in susceptible Mϕs transfected with the resistant *nramp1* allele, and the respiratory burst in response to BCG infection in resistant mice and their splenic adherent cells is superior to that of their susceptible counterparts (Denis *et al.* 1988). *Nramp1* has been proposed to modulate mitochondrial activity and ROI generation via the electron transport

system which can lead to NF-κB activation (Barton *et al.* 1995). It has been suggested that the respiratory burst, influenced by *NRAMP1*, may be a more prominent effector mechanism of human Mϕs, in which NO does not appear to play a major antimicrobial role, than in murine Mϕs.

It has also been speculated that collaboration between nramp1 and the IFNγ receptor may occur to achieve efficient signal transduction. This could be mediated through the SH3 binding domain of the nramp1 protein, and/or an integrin-mediated tyrosine kinase signal transduction pathway (Formica *et al.* 1994).

Olivier *et al.* have shown differences in PKC activity between resistant and susceptible Mϕ cell lines which is consistent with the involvement of PKC in the biochemical pathways inducing several Mϕ functions e.g. phagocytosis, MHC Class II expression and *c-fos* mRNA accumulation. These differences may account, in part, for the pleiotropic effects which have been ascribed to *nramp1* (Olivier *et al.* 1998).

The ability of Mϕs from resistant mice to exhibit increased Class II expression over their susceptible counterparts has been widely accepted to correspond to effective and defective antigen presentation to T lymphocytes in the resistant and susceptible mice, respectively, and to contribute to the latter's inability to curtail infection. Sírová and colleagues question this assumption and suggest that *in vivo* the activity of other APCs mask the effect of the *nramp1* allele on antigen presentation. For instance, DCs from resistant and susceptible mice possess equivalent antigen presentation capacity. They found no association with the *nramp1* allele and *in vivo* antibody responses to exogenous antigens despite the splenic adherent cells from resistant mice inducing higher levels of antigen-specific-T cell-proliferation (Sírová *et al.* 1997). However, Lang *et al.* have shown Mϕ clones transfected with wild type *nramp1* demonstrate enhanced LPS-dependent antigen processing and IFNγ-induced MHC Class II expression compared to the mutant allele-bearing parent cell line or clones transfected with the mutant allele (Lang *et al.* 1997). The influence of *nramp1* on antigen processing was only seen with a recombinant leishmania activator of cell

kinases (LACK-Δ1) antigen and not with chicken egg ovalbumin, human chorionic gonadotrophin or bacteriophage lambda cI protein, suggesting the processing effect was specific to particular amino acid sequences in the LACK-Δ1 antigen. None of the antigens used by Sírová and colleagues (Sírová *et al.* 1997) were derived from bacteria or parasites associated with the *nramp1* phenotype and this processing specificity may help explain their findings. It is of significant importance, in the light of the development of human vaccination strategies, to note that *nramp1* wild type and mutant strains of mice showed differential responses to vaccination with attenuated *S. typhimurium* mutants carrying recombinant tetanus toxoid and leishmanial gp63. The wild type strains developed a Th1 protective response when subsequently challenged with *L. major* while the mutant mice showed signs of bias towards a Th2 response and exacerbated disease (Soo *et al.* 1998).

Measurements of the acidity of susceptible and resistant Mϕs' phagosomes infected with live *M. tuberculosis* (Hackam *et al.* 1998) or *S. typhimurium* (Govoni *et al.* 1999) have shown that the phagosomes of wild type or *nramp1* transfected cell lines are significantly more acidic than those from susceptible mice. This may have a direct bacteriostatic effect, activate microbicidal enzymes, favour the protonation of nitrite to nitrous acid leading to RNIs or promote the dismutation of O_2^- to H_2O_2, all of which may contribute to restricting the replication of intracellular pathogens.

In a carbon tetrachloride (CCl_4) model of liver inflammation and fibrosis *nramp1* null mice showed significantly higher fibrosis scores compared with their wild type counterparts (Thompson *et al.* 1998). KCs are thought to play a pivotal role in this system and the activity of *nramp1* in these cells may be an important determinant in the resulting tissue damage. It is an interesting possibility that human *NRAMP1* genotype or expression levels may contribute in determining the severity and extent of fibrosis and cirrhosis in human hepatic diseases.

Using two-dimensional gel electrophoresis coupled with multivariate analysis of cellular proteins prepared from murine B10R (resistant), B10S (susceptible) and

B10R-Rb (resistant transfected with *nramp*-ribozyme) cell lines Kovárová *et al.* have identified four proteins which were differentially expressed in the cell lines with resistant or susceptible phenotypes (Kovárová *et al.* 1998). Two of these were unidentified but the authors have identified the third as manganese dependent superoxide dismutase (Mn-SOD) and a candidate for the fourth as bcl-2. These proteins were more abundant in the resistant cell extracts. This group has also shown expression of these proteins to be differentially regulated by IFNγ or LPS stimulation in mice with the wild type or mutated *nramp1* gene and mice with the normal (lps^n) or defective (lps^d) allele of the *lps* gene. The *lps* locus affects the natural resistance of mice to a number of pathogenic organisms, including *Francisella tularensis*, and its product is believed to be involved in LPS recognition and/or LPS signalling. In mice with mutated *nramp1* neither IFNγ nor LPS reconstituted the low levels of Mn-SOD or the bcl-2 candidate. However, in the lps^d mice Mn-SOD levels were fully restored with either IFNγ or LPS stimulation and the levels of the bcl-2 candidate were partially restored (Kovárová *et al.* 1997). Mn-SOD expression is regulated by ROIs and thiol modulation and it is possible nramp1 may be involved in modulating the intracellular redox balance, membrane potential, osmomolarity or contributing to the induction of complementary anti-oxidant protective systems, such as Mn-SOD. The authors speculate that resistant phagocytes may be better suited to coping with oxidative stress, which may be reflected in attenuation of the apoptotic pathway and their survival, enabling them to act as APCs (Kovárová *et al.* 1998). Bcl-2 regulates the apoptotic pathway which is intricately related to the cell's redox state and may account for the elevated bcl-2 expression observed. However, this theory is not supported by the findings of Rojas *et al.* who have used resistant and susceptible Mϕ cell lines to show the resistant Mϕs were more sensitive to undergo apoptosis when infected with *M. tuberculosis* H37Rv or stimulated with purified protein derivative (PPD) or IFNγ than the susceptible Mϕs (Rojas *et al.* 1997). The observed increased apoptosis of the resistant Mϕs is dependent on the production of NO, which is generated at higher levels in the resistant cells, but is independent of ROIs (Rojas *et al.* 1998). These workers also found NO, but not ROIs, played a role in the antimycobacterial activity of murine Mϕs. Further studies suggest there may be at

least two pathways capable of inducing Mϕ apoptosis in *M. tuberculosis* infected cells, activation of caspase 1 and the production of NO, which seem to be parallel but independent events (Rojas *et al.* 1999). It seems that the *nramp1* background controls the production of TNFα and IL-10 and it is the relative amounts of these which determine the balance between apoptosis and Mϕ survival in the infected cells with TNFα inducing apoptosis, NO production, caspase 1 activation, p53 expression and down regulation of bcl-2 while IL-10 had opposing effects.

Ectopic expression of *nramp1* in COS-1 cells has been shown to modulate cellular iron levels following loading with low molecular iron chelates such that reduced cellular iron loads were observed in the transfectants (Atkinson and Barton 1998). Based on this observation it has been proposed that nramp1 may play a role in a salvage pathway of iron recycling. The role of nramp1 in iron transport has also been investigated using a murine *in vivo* iron-loading system followed by infection with *M. avium* (Gomes and Appelberg 1998). These experiments showed a dose dependent effect on *M. avium* growth, with increased iron levels increasing proliferation of the pathogen and decreasing the difference in mycobacterial growth between resistant and susceptible mice. A number of studies (Barrera *et al.* 1997; Brown *et al.* 1997) have shown that differences in resistance to mycobacterial growth mediated by *nramp1* correlates with mRNA stability of IFNγ-induced genes and corticosterone treatment increased the decay of mRNA in Mϕs from susceptible mice. These findings led them to contemplate a role of *nramp1* in controlling iron transport thereby regulating levels of intracellular iron and mRNA stabilisation because iron is known to modulate mRNA stability.

Dissecting the physiological function and effects of *nramp1* is an ongoing project. Comparison of the different *in vivo* responses of susceptible and resistant mice to infection is a complex exercise. It is difficult to determine which phenotypic differences observed are a direct effect of functional nramp1 protein and which are secondary or downstream events (despite being nramp1 dependent) and not the direct result of nramp1 activity/function. *In vitro* systems, though less physiological,

can simplify matters to some extent but the problems still remain. Differences observed may be a consequence of an overall increased activation state of resistant Mϕs rather than a specific nramp1 function, which should be taken into account when considering the information known.

1.8.6 Cellular Location and Characteristics of Nramp1

As for nramp1 protein function, opinions regarding its cellular location are varied and sometimes contradictory. A major stumbling point has been the development of specific antisera against the protein, which remain few and far between, with some doubt as to absolute specificity. Speculative suggestions have been made for a mitochondrial membrane location and a role in transportation of substrates regulating the redox state of the organelles. Other suggestions include localisation to the nuclear envelope where it may regulate translocation of DNA binding proteins (Blackwell 1996) or a plasma membrane localisation and role in signal transduction leading to Mϕ activation (Barton 1994; Kishi and Nobumoto 1995).

Gruenheid *et al.* generated rabbit anti-mouse nramp1 polyclonal antisera against a glutathione S-transferase (GST)-nramp1 fusion protein which they used to report localisation of nramp1 to late endosomes/lysosomes in resting Mϕs (Gruenheid *et al.* 1997). Upon phagocytosis they found the sera was reactive with the phagosome membrane and remained so during its maturation to phagolysosome. They showed no evidence for a nuclear or plasma membrane location. The authors suggest that nramp1 is targeted to the membrane of maturing phagosomes where it either directly or indirectly modifies the intraphagosomal environment, affecting replication of intracellular parasites. They hypothesise transportation of a cytocidal or cytostsatic agent into the phagososme or elimination of a factor vital for parasite proliferation via the nramp1 protein. Based on this idea they have tried to explain the species-specific effect of nramp1 on a number of pathogens, all of which have their own defence mechanisms to protect them against their host. For instance *L. donovani* synthesises SOD which neutralises reactive oxygen species and *M. tuberculosis* blocks acidification of the phagosome by preventing fusion of the phagosome to

vATPase positive vesicles. *S. typhimurium* containing phagosomes acquire lysosomal glycoproteins and lysosomal acid phosphatase but not mannose-6-phosphate receptors (a marker for late endosomes), have decreased cathepsin D levels, show decreased fusion with late endocytic compartments and delayed and attenuated acidification. However, the three organisms transit through and remain associated with the phagosome which acquires Lamp1 at some stage. Lamp1 and nramp1 co-localise and it is this mutual accumulation of defence molecule and pathogen which may be of critical importance. In contrast, the entry of *L. pneumophilia* into Mϕs involves a unique 'coiled phagosome' which does not acidify or become Lamp1 positive and *L. monocytogenes* secretes listeriolysin leading to its escape from the phagosome. Gruinheid *et al.* suggest that this escape may occur before a significant amount of nramp1 protein is delivered to the *L. monocytogenes* containing phagosomes as escape occurs within twenty minutes (Govoni and Gros 1998) explaining the indifference of these pathogens to their host's *nramp1* genotype.

Schmidt and Ernst report the generation of rabbit antisera to human NRAMP1 using N and C termini oligopeptides. Using the antisera and *NRAMP1* transfected COS-1 cells a distinctive intracellular vesicular pattern of immunoreactivity was observed and a subpopulation of the positive staining organelles appeared to fuse with endosomes. However, human monocyte-derived Mϕs showed a less obviously vesicular staining pattern with the sera and the authors conclude neither these cells nor the COS-1 transfectants showed distribution of NRAMP1 in early endosomes, lysosomes or mitochondria (Schmidt and Ernst 1996).

Polyclonal rabbit sera has been raised against a C terminal peptide of the human NRAMP1 sequence (CHFLYGLLEEDQKGETSG) coupled to keyhole limpet haemocyanin (KLH) via the NH_2 terminal cysteine which is not present in the NRAMP1 sequence (Kishi *et al.* 1996a). This sera was reactive against a 60kDa protein in human PBLs, HL-60 (promyelocytic leukaemia cell line), U937 (histiocytic lymphoma cell line), ARH-77 (multiple myeloma cell line), CCRF-CEM (T cell leukaemia cell line), K562 (myelogenous leukaemia cell line), Raji (B-

lymphoblstoid cell line) and MOLT-4 (T-lymphoblastoid cell line) cells. These findings contrast with the Mϕ/granulocyte specific expression profile reported by others (Cellier *et al.* 1997) and could reflect the immortalisation/transformation or different stage of differentiation of the cultured T and B cell lines, or a lack of specificity of the antisera. The NRAMP1 open reading frame is predicted to encode a 550 amino acid protein with a molecular weight of 59880, consistent with the weight of the protein the polyclonal sera reacts against. This protein would, therefore, represent a post-translationally unmodified NRAMP1 protein, despite the observation of a number of putative phosphorylation and glycosylation sites and evidence that the murine homologue is heavily glycosylated with a molecular weight in the range of 90-100kDa (Vidal *et al.* 1996). Kishi *et al.* also identified a 120kDa reactive product which they suggest may represent dimerisation of the protein, an interaction maintained under the reducing conditions of the experimental procedure (Kishi and Nobumoto 1995). It is surprising, based on the increased level of NRAMP1 mRNA expression after LPS and/or IFNγ stimulation and the phenotypic effects of these stimuli believed to be mediated through, or in part by, NRAMP1 that no detectable increase in expression of the 60kDa immunoreactant was observed using this sera when PBLs were stimulated with LPS and/or IFNγ (Kishi and Nobumoto 1995), further querying the specificity of this antisera.

The same sera was used to immunocytochemically localise the reactive material to the plasma membrane of the U937 cell line (Kishi *et al.* 1996a). Electron microscopy of the stained U937 cells confirmed reactivity with the plasma membrane but not other cellular organelles and the authors concluded the human NRAMP1 molecule resides on the plasma membrane in contrast to the findings outlined above.

The NH_2-terminal region of NRAMP1 shares structural homology with the proline, serine and threonine rich microtubule-associated protein (MAP)-4 which led Kishi *et al.* to speculate a possible cytoskeletal-NRAMP1 interaction. Using an NRAMP1-GST fusion protein and affinity purification α- and β-tubulin were found to associate with the NH_2-terminal cytoplasmic domain of NRAMP1 (Kishi *et al.* 1996a). This

finding and the plasma membrane localisation led the authors to suggest that NRAMP1 may act as a membrane-anchor and bind microtubules, promoting microtubule-mediated vesicle transport, important in phagocytosis of microorganisms and/or sorting of internalised vesicles. Based on competition studies for microtuble-binding activity the group subsequently reported that NRAMP1 might be a new microtubule-associated protein with unique characteristics, forming a new category of MAPs (Tokuraku *et al.* 1998).

Nramp1 has been shown to behave as an integral membrane protein, resistant to urea extraction, as predicted from its sequence. It is phosphorylated and heavily glycosylated with up to 40% of its mass resulting from post translational addition of complex carbohydrate side chains (Vidal *et al.* 1996).

1.8.7 Metal Homeostasis

When studying living, biological systems, it is tempting to neglect how crucial inorganic chemistry is to organic life. The homeostasis of mineral nutrients within a cell and the various cellular compartments is maintained by a fine balance of transport across plasma and organelle membranes, metabolic effects and chelating agents. Metal ions are generally maintained at low concentrations in the cytoplasm, which vary depending on the cell's metabolic state, while the organelles often serve as storage compartments.

Metal ions, particularly of the transition series are vital for the function of countless cellular enzymes and overall well being. Everyone is aware of the debilitating effects of iron deficiency and anaemia. Iron imbalances also account for a variety of other conditions including haemochromatosis, while defects in copper storage in the liver is the cause of Wilson's disease. Zinc is central to the function of zinc finger transcription factors and equally important is the toxic effect of high levels of many metals, including aluminium, which affects the brain.

Maintenance of cellular iron homeostasis is a prerequisite for growth and proliferation of cells. However, it is also of central importance in regulating immune

functions, playing a role in lymphocyte proliferation and cell mediated immune responses involving Mϕs. Increased free, non-ferritin-bound, intracellular iron concentrations diminish the effectivity of IFNγ towards monocytes via reduced MHC Class II expression, neopterin formation, TNFα production and cytotoxicity towards intracellular pathogens. A regulatory feedback exists between iron and NO within the cell. Iron reduces iNOS mRNA transcription and NO formation, and NO in turn influences the regulation of cellular iron metabolism.

Cellular uptake, storage and consumption of iron are regulated post-transcriptionally by IRP-1 and IRP-2, which interact with IREs within mRNAs such that iron uptake is promoted during iron deficiency or oxidative stress and iron storage and consumption is stimulated when the levels of cellular iron is increased.

Immunostimulatory cytokines (e.g. IL-1, IL-2, IL-6, TNFα and IFNγ) influence iron metabolism via IRE/IRP independent mechanisms. However, IL-4 and IL-13 enhance expression of molecules involved in iron uptake and storage by Mϕs by regulating IRP activity. This is mediated by the suppressive effects of the cytokines on NO formation and by antagonising the IFNγ mediated blockage of TfR mRNA expression. IL-4 nad IL-13 may, therefore, increase iron uptake and storage by Mϕs which may negatively affect the cells' effector functions and antimicrobial activity as iron down regulates NO formation and decreases the effectivity of IFNγ towards Mϕs. The IL-4 and IL-13 mediated uptake and storage of iron in Mϕs might also act as a control mechanism during chronic inflammation by reducing the formation of toxic hydroxyl radicals via the iron mediated Haber Weiss reaction (discussed in **1.5.2**).

The TfR mediated uptake mechanism of iron by mammalian cells has been widely documented. The pathway involves the adsorption of iron onto Tf, which has two binding sites for the ions, followed by binding of iron-transferrin (Fe-Tf) to the TfR on the plasma membrane. The receptor-ligand complex is internalised into endosomes within which the low pH, generated by vATPase, results in release of

iron, which is subsequently transported across the endosomal membrane into the cytoplasm. Though of major significance this is not the sole iron uptake mechanism by mammalian cells as Tf independent pathways exist, exemplified by the recent reports and speculations of the function of nramp1 and nramp2 (Fleming *et al.* 1997 and 1998; Gunshin *et al.* 1997; Atkinson and Barton 1998; Gomes and Appelberg 1998). It is an attractive proposition that nramp1's effects on immune responses and intracellular pathogens may be, in part, due to regulation of cellular iron levels. However, our present understanding whether this transport system would be unidirectional into or out of the phagolysosome, or potentially bi-directional, remains unresolved (reviewed in Blackwell and Searle 1999). In comparison to iron, our knowledge of the mechanisms of uptake of metals such as manganese is in its infancy and the possibility that nramp1 may play a role based on the activity of other nramp family members (**1.8**) is an exciting area for research.

1.8.8 Human *NRAMP1*

In 1994 partial (Kishi 1994) and complete (Cellier *et al.* 1994) cDNA sequences of *NRAMP1*, the human homologue of murine *nramp1*, were published.

1.8.8.1 Human *NRAMP1* Gene and Protein

The predicted human NRAMP1 protein sequence shares 88% identity and 93% similarity to the murine sequence with the extreme NH_2- and COOH- terminal ends showing the least cross species sequence conservation (66% and 74% identity, respectively). The human protein contains 550 amino acids, two more than the murine protein. The two predicted N-linked glycosylation sites, the SH3 binding domain and two of the five PKC phosphorylation sites (those in the NH_2 terminal region of the sequence) found in the murine sequence are conserved. The conserved transport motif between TM6 and TM7 is highly conserved, incorporating one conservative substitution, as are eight of the TM domains, which are identical except for one conservative substitution (Cellier *et al.* 1994). This remarkable sequence conservation suggests key structural and/or functional roles of these domains in the proteins.

The human *NRAMP1* gene spans 16kb and was mapped to human chromosome 2q35 within a syntenic region encompassing the equivalent region of murine chromosome 1, which contains *nramp1*. As for the murine gene 15 exons have been identified (Cellier *et al.* 1994).

Interestingly a splice variant of the human mRNA was identified which contained 74bp of an *Alu* element belonging to the *Sx Alu* family mRNA (Cellier *et al.* 1994). The *Alu* element is inserted in the genomic DNA in an inverted orientation relative to the direction of gene transcription. The alternatively spliced sequence is present at the position corresponding to intron 4 and was found to be expressed in the U937, THP-1, KG-1 and HL-60 cell lines at an approximately 1:5 ratio in favour of the species lacking the *Alu* sequence. The 74bp insertion introduces a frame shift which results in the appearance of a stop codon in exon 5. Should such a message be translated the predicted protein would be truncated prematurely, lacking the majority of the TM domains and the conserved transport motif, and as such is unlikely to play a function as a transport protein. It is possible that such a truncated NRAMP1 protein which would contain the NH_2 terminal SH3 binding domain could retain signal transduction capacity or sequester cellular SH3 domain containing proteins and hence have a functional role in this respect. However, it is more likely that such a protein would be targeted for degradation based on evidence that the murine *nramp1* gene containing the g>a point mutation does not generate detectable nramp1 protein (Vidal *et al.* 1996).

Northern blot analysis of the human *NRAMP1* mRNA expression pattern showed tissue specific expression of the gene in PBLs, lung, spleen and liver, with liver showing the lowest level of expression. Two hybridising species of about 2kb and 4kb were co-expressed. The smaller species may be the result of alternative polyadenylation sites but this is not certain (Cellier *et al.* 1994).

The transcription start site of the human gene is 148bp 5' of the ATG initiation codon and a series of predicted promoter region elements 5' of the transcription start

site have been identified. These include thirteen IFNγ response elements, three W-elements, two AP-1 sites, three NF-κB binding sites, two GM-CSF elements, one NF-IL6 site and several PU-1 binding sites, a number of which create PEA-3 motifs. No TATA, GC or CCAAT boxes were identified. Thus the murine (**1.8.4**) and human promoter regions share many regulatory elements which support the inducible and myeloid specific expression pattern observed (Blackwell 1995; Kishi *et al.* 1996b; Searle and Blackwell 1999).

1.8.8.2 Human *NRAMP1* Polymorphisms

Of particular interest in the human *NRAMP1* promoter region is a polymorphic microsatellite repeat region located from -317bp to -274bp 5' of the transcription start site. The alleles at this site have been inconsistently reported. Blackwell *et al.* report four alleles but they have allocated different sequences to allele 4 following their initial publication. The sequence of these alleles are shown below (* Blackwell. 1996; Shaw *et al.* 1996 and 1997: $ Blackwell *et al.* 1995: # Searle and Blackwell 1999):

Allele 1*$	$t(gt)_5ac(gt)_5ac(gt)_{11}ggcaga(g)_6$
Allele 2*$	$t(gt)_5ac(gt)_5ac(gt)_{10}ggcaga(g)_6$
Allele 3*$	$t(gt)_5ac(gt)_5ac(gt)_9ggcaga(g)_6$
Allele 4*	$t(gt)_5ac(gt)_{10}ggcaga(g)_6$
Allele 4$	$t(gt)_5ac(gt)_5ac(gt)_4ggcaga(g)_6$
Allele 4#	$t(gt)_5ac(gt)_9ggcaga(g)$

Liu *et al.* identified three alleles at this site, which they allocated alleles 1, 2 and 3 with 2bp increments of increasing size and allele 1 having the sequence $t(gt)_7ac(gt)_5ac(gt)_9g$ (Liu *et al.* 1995).

The frequencies of the alleles were determined by the two groups in a number of ethnic populations and in all cases the allele present at highest frequency contained $(gt)_9$ at the 3' position of the repeat region.

This promoter region polymorphic microsatellite repeat is of great interest because it is a putative Z-DNA forming dinucleotide repeat. DNA in the Z-conformation can interact with a distinct class of eukaryotic DNA binding proteins which may negatively or positively regulate gene transcription. Gene reporter studies using the polymorphic promoter regions of the human *NRAMP1* gene provide evidence that this is a functional polymorphism. Blackwell's allele 3 has been reported to drive the highest levels of expression and as such an individual's genotype at this locus could affect the levels of *NRAMP1* expressed and Mϕ function and activity (Blackwell 1995; Bellamy and Hill 1998). The microsatellite repeat is flanked by other promoter region response elements and there is, therefore, scope for both a direct effect on transcription through the interaction of transcription factors with the Z-DNA as well as the potential to influence the juxtaposition of other response elements. Compared with other microsatellite repeat polymorphisms the number of alleles identified is small which may suggest that the generation of further polymorphic variants of this repeat is intolerable in evolutionary terms.

Using a variety of methods to search for mutations in the human *NRAMP1* gene, including single-strand conformation analysis, Southern analysis and direct sequencing, Liu and colleagues identified nine polymorphic sites/mutations by analysing native Canadian kindred and Hong Kong families (Liu *et al.* 1995). Of these, four sites were in coding sequence: two were silent substitutions in exons 3 and 8 and the other two an A>V conservative substitution (A318V) in exon 9 within the region between TM5 and TM6 and a D>N substitution (D543N) in exon 15 within the cytoplasmic COOH terminal which could be functional. The remaining variants were in non coding sequence: a g>a in intron 5 and intron 13, a g>c in intron 4, a 4bp deletion downstream of the last codon in intron 15 and the previously discussed microsatellite repeat. At the latter site three alleles were identified with 2bp increments of increasing size for alleles 1 to 3 and allele 3 was assigned the sequence $(gt)_7ac(gt)_5ac(gt)_9$. The discrepancy between the size of Liu's and Blackwell's first (gt) repeat of this polymorphic site (Blackwell *et al* 1995) is likely to be due to difficulties in sequencing repetitive DNA. A further polymorphic 4bp

(CAAA) insertion/deletion at the poly A tail of an *Alu* element of the *Alu J* family situated in the 3' untranslated region of the gene has been identified but the physiological effect or function of these polymorphisms, except the 5' promoter region microsatellite repeat, has not been reported or fully understood (Buu *et al.* 1995).

There is no evidence to date for existence of an analogous mutation in the human *NRAMP1* gene to that found in the susceptible strains of mice. Such a mutation would be expected to have a profound functional effect on the role of the protein. The only potentially detrimental polymorphism identified to date in the human gene, an amino acid triplet repeat in exon 2 encoding the putative SH3 binding domain, occurs at a frequency of less than 0.001 (Blackwell and Searle 1999).

1.8.8.3 Human *NRAMP1* Expression

Northern analysis of PBMCs and their fractionation into the granulocyte and non granulocyte containing fractions identified granulocytes to be the source of the highest levels of *NRAMP1* expression (Cellier *et al.* 1997). Alveolar Mϕs and adherent monocytes both expressed *NRAMP1*. The level of *NRAMP1* expressed by adherent monocytes was lower than that of the alveolar Mϕs but could be increased to those of the latter by long term culture. The HL-60 cell line showed induction of NRAMP1 expression when it was differentiated towards either the monocytic or granulocytic pathway and it appears that expression of *NRAMP1* increases during maturation of mononuclear phagocytes. The high level of expression by granulocytes is of interest in the context of the importance of granulocytes in control of virulent *S. dublin* infection in wild type mice (Vassiloyanakopoulos *et al.* 1998). However, this expression pattern is in contrast to that observed by Yoshida and Kishi using their rabbit polyclonal anti-human NRAMP1 sera in a flow cytometry study of human PBLs (Yoshida and Kishi 1997). They report expression of NRAMP1 in 52.9% of CD14+ monocytes/Mϕs, 22.2% of CD2+ T lymphocytes, 26.6% of CD19+ B lymphocytes but only 3.2% of CD16+ neutrophils/granulocytes. The authors suggest the discrepancy between the widely accepted murine Mϕ, monocyte/granulocyte

specific pattern and their observation could be due to a species difference but this does not account for the inconsistency between their results and those of Cellier *et al.* above (Cellier *et al.* 1997).

1.8.8.4 Infectious Disease and Human *NRAMP1*

The lack of reliable tools to investigate human NRAMP1 protein expression or function in physiological or disease situations has meant the major avenue, to date, for human studies has been genetic and polymorphic analysis of the *NRAMP1* gene. From knowledge of the phenotypic effect of the murine mutation the human homologue represented an obvious candidate to have an important effect on the course of human *M. tuberculosis* and/or *M. leprae* infection.

Leprosy is the result of chronic *M. leprae* infection affecting an estimated 5-6 million people worldwide and susceptibility has a significant genetic component. Abel and colleagues have studied sixteen Vietnamese and four Chinese multiplex leprosy families for a number of *NRAMP1* intragenic haplotypes and extended haplotypes in the immediate vicinity of *NRAMP1* (Abel *et al.* 1998). They found a significant non random segregation to affected individuals of a small chromosomal segment carrying *NRAMP1*. Though it can not be ruled out that another gene in linkage with *NRAMP1* might be the cause of the haplotype sharing, the study suggests that susceptibility to leprosy is a genetically heterogeneous trait with *NRAMP1* playing a more pronounced role in certain ethnic populations and more than one susceptibility locus being involved.

Despite estimates that a third of the world's population is infected with *M. tuberculosis* only 10% will develop clinical disease. It is clear that although the mycobacterium is necessary for development of tuberculosis it is not sufficient and there is significant evidence that the host genotype is important in determining the outcome of infection. In situations such as tuberculosis where several genes are likely to play a role in the aetiology of disease both family-based linkage and association-based case control studies are required to complement each other when trying to identify the relevant genes. Association studies are useful to detect genes

exerting a moderate effect on disease susceptibility, which would be missed by linkage studies, but can only be used to detect association over short genetic distances. Such studies often rely on the existence of a candidate gene in the region of the genome of interest.

Associations between tuberculosis and MHC class II antigens, most frequently HLA DR2, have been reported, but inconsistently, and are only likely to account for a relatively small percentage of the total genetic influence. Analysis of a number of candidate genes including those encoding NRAMP1, TNF, MBP, vitamin D receptor, IFNγ, IL-1α, IL-1β, IL-1 receptor antagonist, IL-4, IL-9, IL-10, CR1, ICAM-1, iNOS, and chemokine receptors is underway to try to determine which, if any, of these which have the potential to affect the course of tuberculosis, have a genetic association with disease (reviewed in Bellamy and Hill 1998).

In the context of this thesis studies of a potential genetic association of *NRAMP1* with tuberculosis is of interest. In a Gambian case-control study four of six polymorphic sites within the *NRAMP1* gene analysed were found to be strongly associated with smear positive pulmonary tuberculosis (Bellamy and Hill 1998; Bellamy *et al.* 1998). Of the loci analysed the 5' microsatellite repeat region and the intron 4 g>c transversion were in linkage disequilibrium, as were the exon 15 D543N and the 4bp deletion downstream of exon 15 polymorphisms, hence these results are not independent. Individuals who are heterozygous for both the intron 4 g>c transversion and deletion downstream of exon 15 were significantly over represented among tuberculosis cases compared to those who do not possess either variant allele (odds ratio=4.07, confidence interval=1.86-9.12). The allelic association between the 5' promoter region and the 3' region of the gene with disease susceptibility were independent indicating multiple *NRAMP1* polymorphisms influence tuberculosis in the population studied. Other reports of an association between the promoter region microsatellite repeat and tuberculosis exist (Bellamy and Hill 1998). With respect to an *NRAMP1* resistant genotype allele 3 homozygotes have been reported to be most resistant to the development of tuberculosis (Bellamy and Hill 1998). These findings

are of great interest as they show it is possible to identify host genetic factors leading to increased risk of disease, but it is not known yet how important these genetic variants are in different populations and environments or what functional effects the genetic variants have on the NRAMP1 gene product. The proviso that different genes contribute to or influence tuberculosis or leprosy susceptibility or outcome in different races may partially account for the findings of a study of Bolem tuberculosis multicase families which showed only weak linkage of 2q35, the *NRAMP1* locus, with disease (Blackwell 1998). Liu *et al.* have failed to find association between susceptibility to tuberculosis and the nine polymorphic sites they analysed (Liu *et al.* 1995). This lack of association may be genuine but may also be due to the very small number of cases they tested or their choice of cases. It has been suggested that human *NRAMP1* is more likely to be important in the development of overt disease in contrast to murine *nramp1*, which determines the ability to control proliferation of mycobacteria in the early stages of infection.

A presently favoured hypothesis of NRAMP1 function in relation to innate resistance to mycobacterium proposes NRAMP1 is located in the membrane of the mycobacterial phagosome where it transports iron out of the vacuole. Where a non-functional NRAMP1 protein exists, bacteria may multiply faster because they have more iron and other metal ions necessary for growth and proliferation, whereas a functional NRAMP1 protein effectively starves the pathogen. Metal ions have a plethora of cellular functions and effects and the pleiotropic effects on Mϕ activation attributed to NRAMP1 may be related to the requirement for metal ions transported into the cytoplasm from vacuoles. This theory could help explain the iNOS independent mechanism slowing down bacterial replication observed in mouse systems prior to Mϕ activation. The subsequent killing of the pathogen may also be due to the effect of NRAMP1 on Mϕ activation.

1.8.8.5 Autoimmune Disease and Human *NRAMP1*

The murine phenotypic studies related to *nramp1* genotypic status are based on a binary outcome - susceptibility/death or resistance/survival - to infection of the

relevant intracellular pathogens. However, the consequence for a host with less extreme genotypic variants of the *NRAMP1* gene could be hypothesised to have significant or subtle effects on Mϕ function. Enhanced NRAMP1 function or expression might result in increased resistance to infectious diseases where Mϕs play an important role in defence. However, such a situation may also be detrimental to the host, as Blackwell proposes (Blackwell 1996), resulting in hyperactivation and stimulation of Mϕs and an exaggerated, undesirable immune response, due to enhanced TNFα, IL-1β, MHC Class II etc. expression, leading to induction and/or maintenance of chronic inflammatory or autoimmune disease. This idea has prompted a number of studies to investigate a possible association of human *NRAMP1* genotypes with human autoimmune/chronic inflammatory diseases in which Mϕs are believed to play a detrimental role and/or mycobacterial/bacterial agents are suspected to be important in the aetiology of the disease.

RA is an autoimmune disease for which there is evidence of bacterial/mycobacterial aetiology, either as a trigger for autoimmunity or as an agent perpetuating disease. A study of multicase RA affected families supports *NRAMP1* as a candidate for disease susceptibility. The families were typed for the 5' promoter region microsatellite repeat in *NRAMP1* and four close marker genes and the data analysed by a method based on maximal likelihood of identity-by-descent in affected sib pairs and transmission disequilibrium testing. The likelihood ratio chi-squared test statistic was 4.66 and maximum logarithm of the odds (LOD) score was 1.01 for *NRAMP1*. There was a significant bias towards transmission of allele 3 in affected offspring. This allele drives most efficient *NRAMP1* expression and this polymorphism may be one of, or the, disease associated genetic factor in these RA families (Shaw *et al.* 1996 and 1997). An association between allele 3 and juvenile RA sufferers and diabetic patients with a first or second degree relative with RA has also been identified (reviewed in Blackwell and Searle 1999).

Crohn's disease and ulceritive colitis come under the umbrella of inflammatory bowel disease (IBD) and genetic factors are believed to contribute to the

pathogenesis of these diseases. Evidence exists suggesting mycobacteria/bacteria may contribute to the initiation or maintenance of Crohn's disease and a number of studies have investigated whether *NRAMP1* may play a role in IBD. IBD appears to be complex, displaying genetic heterogeneity, multilocus inheritance and/or multifactorial inheritance.

Using two DNA markers (D2S434 and D2S1323) in the vicinity of *NRAMP1* on chromosome 2q35 Crohn's disease and ulceritive colitis sufferers have been genotyped and the allelic, genotypic and haplotypic distributions compared to those of normal controls (Hofmeister *et al.* 1997). The authors of the study suggest two individual haplotypes were present at a significantly different frequency in patients with Crohn's disease compared to the control group ($p=0.023$ and $p=0.001$). However, further analysis of larger numbers of patients will be necessary to determine if there is a difference between the Crohn's disease and ulceritive colitis frequencies. This study is contentious due to the large number of possible haplotypes generated from the two DNA markers and hence the "chance" finding of an association. Closer analysis of the *NRAMP1* gene itself will be necessary before definitive evidence for a genuine association of the gene with IBD can be accepted.

Neibergs *et al.* have claimed in a separate report that *NRAMP1* is a major susceptibility locus for ulceritive colitis based on analysis of the same two DNA markers mentioned above (Neibergs *et al.* 1997). However, analysis of 60 Crohn's disease patients, 52 ulcerative colitis patients, 11 PSC patients and 238 normal controls for the exon 8 c (allele 1)>t (allele 2) transition failed to find an association with this polymorphic site and IBD, but identified an increased frequency of allele 2 in the small group of PSC patients genotyped; 18.2% for PSC versus 5.5% for controls compared to Liu *et al's* frequencies of 2% for Caucasians ($n=120$) and 15% for Asians ($n=40$) (Liu *et al.* 1995; Stokkers *et al.* 1997).

1.9 AIMS OF THIS PROJECT

Based on the themes I have discussed the aims of this project were to 1) immunostain PBC and normal liver biopsy sections for markers of apoptosis; 2a) genotype PBC sufferers for the 5' polymorphic microsatellite repeat in the *NRAMP1* gene; 2b) investigate *NRAMP1* expression in the liver; 2c) investigate the effect of *in vitro* overexpression of *NRAMP1*, as expanded on below:

1) To investigate liver biopsy sections of early and late stage PBC and normal control tissue for the phenotype of the BECs with respect to indicators suggesting the capacity for, or activation of, execution of the apoptotic pathway. I wished to determine if there is evidence of abnormal protein expression in the PBC BECs of a variety of factors known to be important in regulating the apoptotic pathway, namely bcl-2, bax, bcl-x, p53 and Fas/CD95. Members of the bcl-2 family have been shown to interact with each other forming homo- and hetero-dimers and p53 transcriptionally regulates Fas/CD95 and bax (Miyashita *et al.* 1994; Selvakumaran *et al.* 1994; reviewed in Wyllie 1994; Owen-Schaub *et al.* 1995). It is possible that the BECs in PBC patients show altered susceptibility to apoptosis, which might be exhibited by expression of such factors. I also wished to determine the proliferative status of the BECs using the MIB-1 antibody against Ki-67 (Gerdes *et al.* 1991) to see whether the cells were capable of proliferation because a lack of this regenerative capacity could be a potential contributing factor resulting in the net loss of biliary structures in the liver of PBC sufferers.

2a) Despite extensive research the aetiology of PBC remains unclear but I was interested in investigating the reported familial association and genetic predisposition of the disease with respect to the *NRAMP1* gene. Though most effort has been directed towards unravelling the acquired and T cell immune responses of PBC patients, little work has been done to determine the early initiating influences culminating in these responses. In the light of the apparent participation of Mϕs in the pathology of PBC, I was particularly interested in

investigating whether characteristics of these cells may be contributing to disease susceptibility in PBC sufferers. By understanding early host factors and events which may be central in initiation of these responses, such as the activity of Mϕs, and identifying those at risk of PBC the ultimate aim of disease prevention becomes tangible. To this end I wished to analyse the 5' polymorphic promoter region microsatellite repeat in the human *NRAMP1* gene in PBC patients to determine if there is evidence that this gene may play a similar role in influencing susceptibility to PBC as has been postulated in RA patients, causing a hyperstimulated Mϕ population to exist. Normal controls, alcoholic liver disease (ALD) and hepatitis C patients were chosen as control populations with which to compare the allele frequencies of the PBC population. The ALD population represent a form of chemically induced cirrhosis while the hepatitis C group represent cirrhosis induced by a virus with tropism for Mϕs. At present there is no evidence that *NRAMP1* genotype affects the course of viral infections or any reason to suppose it is influential in the pathogenesis of ALD.

2b) I also wished to investigate the expression pattern of the *NRAMP1* gene and protein in the liver of PBC patients compared with control tissue to determine if there is evidence of abnormal expression in the disease tissue which might be influential in generation of the characteristic granulomas in PBC patients and the chronic immune response. Such responses require an ongoing stimulus, which could take the form of a hyperactivated Mϕ perpetuating and maintaining the response.

2c) Based on the proposal that hyperactivation of Mϕs mediated by overexpression of *NRAMP1* could be an important factor determining human pathology, I wished to construct a mammalian expression vector containing human *NRAMP1* cDNA which would result in overexpression of the gene when transfected into human Mϕs. After developing an assay to determine expression of the transfected gene, differences in phenotypic effects of overexpression of

NRAMP1, a gene central to Mϕ function, could be analysed in successful transfectants in the hope of gaining an insight into the function of the NRAMP1 protein.

2 MATERIALS AND METHODS

All chemical reagents were purchased from Sigma, Poole UK, unless otherwise stated. Phosphate buffered saline (PBS) used throughout this project for procedures except tissue culture was purchased from Oxoid, Basingstoke UK. PBS for tissue culture use was purchased from Life Technologies, Paisley UK.

Nunc sterile plasticware (Life Technologies, Paisley UK) was used for tissue culture work, unless otherwise stated. Sterile technique and equipment was used for all tissue culture work which was carried out in a BIO2+ Class II microbiological safety cabinet (Envair, Lancashire UK) and cells cultured in a Gallenkamp CO_2 incubator (Fisher Scientific, Loughborough UK) at 37°C, 5% CO_2. Where necessary solutions were filter sterilised using a 0.2μm syringe filter (Sartorious, Surrey UK).

1.5 millilitre (ml) tubes were purchased from Life Sciences International, Hampshire UK and thin walled 0.75ml tubes used for polymerase chain reactions (PCR) were purchased from Advanced Biotechnologies, Epsom UK. RNase free 1.5ml tubes for RNA work were purchased from Anachem, Luton UK.

A Life Technologies Model No 3000 (Life Technologies, Paisley UK) power supply, a Bio-Rad Power Pac 3000 (Bio-Rad, Hemel Hempstead UK) or a MPSU-125/200 power supply (Anachem, Luton UK) were used throughout this project. Microcentrifugation was carried out using a Micro Centaur, centrifugation was carried out using a Coolspin 2 or Mistral 2000R centrifuge and 96 well plates were centrifuged in a Centaur 2 bench top centrifuge (all MSE, Sussex UK).

2.1 SELECTION OF PATIENT AND CONTROL MATERIAL

2.1.1 Paraffin Embedded Liver Tissue for Immunohistochemistry and DNA Extraction

The diagnosis of PBC was made after full clinical, serological and histological assessment with the help of a trained pathologist. Fifteen cases showed

predominantly histological features seen in Stage I or II (14 female, 1 male) and 14 showed Stage III or IV (13 female, 1 male) according to the proposed model of disease progression reported by Scheuer (Scheuer 1987). Fifteen control liver samples were obtained from patients during routine lymphoma staging, psoriasis patients prior to commencing methotrexate therapy, or laparotomy during resection of colon cancer (6 female, 9 male). All liver tissue in the control group was reported as histologically normal and there was normal liver biochemical and synthetic function. Clinical details of the PBC cases are shown in **Table 2.1**.

	Bilirubin	Alanine amino-transferase	Alkaline phosphatase	Albumin
Normal range	5–17μM	<35U/l	<130U/l	40-50g/l
Histological early disease (Stage I, II)	11 [5-60]	69.5 [27-194]	200 [104-891]	41.5 [29-44]
Histological late disease (Stage III, IV)	56.5 [13-256]	87 [20-945]	402.5 [115-1368]	32 [22-43]

Table 2.1 Clinical data assessing liver function of PBC patients at the time of liver biopsy compared with the normal range. The median and [range] values of bilirubin, alanine aminotransferase, alkaline phosphatase and albumin of PBC patients whose biopsy tissue was used for immunohistochemistry are shown. μM: micromolar, U/l: units per litre, g/l: grammes per litre.

2.1.2 Human Material for *NRAMP1* Polymorphism Study

The diagnosis of PBC, hepatitis C and ALD was based on clinical and serological parameters and on histological assessment of routine liver biopsies. Normal controls were obtained from the Blood Transfusion Service and have been previously described (Cantlay *et al.* 1994). Standard ethylenediaminetetra acetic acid (EDTA)-blood samples were obtained from 78 normal controls, 76 ALD, 46 PBC and 39 hepatitis C cases. Paraffin embedded liver material, fixed in 10% buffered formalin, from explanted liver taken at the time of orthotopic liver transplantation (described in **2.1.1**) was obtained from 9 PBC cases, for two of these blood samples were also available.

2.2 IMMUNOHISTOCHEMISTRY PROTOCOLS

Immunohistochemistry procedures were carried out using a humidified chamber, the semi-automated Sequenza wet chamber (Shandon, Basingstoke UK) or a DAKO Techmate™ 500 automated immunocytochemistry stainer (DAKO, Cambridge UK). The Sequenza system utilises plastic clips which hold the slides in a rack in a position allowing 100µl of liquid to be held by capillary action between the slide and clip in an even film. Addition of more fluid to the reservoir at the top of the clip displaces the fluid held against the section allowing standardisation of volumes and incubation times. The DAKO Techmate™ 500 automated immunocytochemistry stainer utilises a robotic arm to move slide holders from location to location during the staining procedure, increasing throughput, improving accuracy and enhancing reproducibility. A state-of-the art capillary process is used to ensure reagents are gently drawn up over the tissue sections. The Techmate™ 500 stainer is linked to computer software.

3µm sections of tissue, fixed in 10% buffered formalin and processed to paraffin were cut using a Reichert-Jung Biocut 2030 microtome (Zeiss, Welwyn Garden City, UK) onto poly-L-lysine (PLL) coated Twin Micro Slides (Blue Star, Warley UK) or, for automated staining, onto DAKO ChemMate Capillary Gap Microscope Slides (75mm) (DAKO, Cambridge UK). Sections were dewaxed in xylene (Genta Medical, York UK) and rehydrated through descending alcohols (absolute to 74% to 64%) (Genta Medical, York UK) to water.

When the chromogen 3,3-diaminobenzide (DAB) was used for visualisation, with the humidified chamber or Sequenza, endogenous peroxidase was blocked in 1% w/v H_2O_2 in dH_2O for 15 minutes then washed in running tap water prior to antigen retrieval as described below (**2.2.1**).

2.2.1 Antigen Retrieval

All antibodies or antisera for which the conditions for immunohistochemistry had not been previously optimised were initially tested over a range of concentrations on

paraffin embedded tonsil and/or liver tissue sections which received either no pre-treatment, had been pre-treated with trypsin or had received microwave antigen retrieval in citrate buffer to determine the most suitable working conditions. It was subsequently reported that microwave pre-treatment in EDTA proved a highly effective form of antigen retrieval (Pileri *et al.* 1997) and this procedure was used for a subset of antibodies towards the end of the project. Antigen retrieval procedures are required for certain antigens due to the paraffin embedding process causing crosslinking, which may mask certain epitopes. Antigen retrieval was performed as follows:

1. **Trypsin digestion**: Sections were incubated at 37°C for 17 minutes in 0.1% trypsin (ICN Biomedicals Inc., Basingstoke UK), 0.1% calcium chloride pH7.8 then washed in running tap water.

2. **Microwave in citrate buffer**: Sections were microwaved for 10 minutes at 1000W in 1.05 grammes (g) citric acid/500ml H_2O pH6.0, allowed to cool until tepid then washed in running tap water.

3. **Microwave in EDTA**: Sections were microwaved for 5-10 minutes at 650W in 0.01M EDTA pH8.0, and cooled under running tap water.

The optimal antigen retrieval procedure for the antibodies used, the working concentrations and the antibody suppliers are shown in **Table 2.2**.

2.2.2 Procedure for use with the Humidified Chambers or Sequenza

The following procedures apply to staining procedures using humidified chambers or the Sequenza. When the Sequenza was used the sections were clipped into the racks after antigen retrieval and all fluids were added into the reservoir at the top of the clip. When the humidified chamber was used fluids were gently pipetted to cover the tissue sections and removed by gently tapping the long edge of the slides on absorbent paper towel. Washes were carried out in Coppling jars.

Sections were washed with Tris buffered saline pH7.6 (TBS) and incubated in blocking serum of the species in which the secondary antibody was raised to reduce non specific binding i.e. either 20% normal rabbit serum (NRS) (SAPU, Lanarkshire UK) or normal swine serum (NSS) (Harlan Sera-Lab, Loughborough UK) prepared in TBS. Sections were then incubated in the appropriate dilution of primary antibody, prepared in the blocking serum, for an hour at room temperature. Sections were washed three times for 5 minutes in TBS then incubated in biotinylated secondary antibody (rabbit anti-mouse (RAM-BIO) (DAKO, Cambridge UK) at 1/400 for monoclonal primary antibodies) or swine anti-rabbit (SAR-BIO) (DAKO, Cambridge UK) at 1/500 for rabbit polyclonal primary antisera) diluted in blocking serum, for 30 minutes at room temperature. The sections were washed, as previously, before incubation for 30 minutes in horse radish peroxidase conjugated avidin-biotin complex (ABComplex-HRP) (DAKO, Cambridge UK) (for DAB chromogen) (**Appendix B**) or alkaline phosphatase conjugated avidin biotin complex (ABComplex-AP) (DAKO, Cambridge UK) (for Fast Red or Vector Red visualisation) (**Appendix B**) then washed again before visualisation with either DAB (**2.2.2.1**), Fast Red (**2.2.2.2**) or Vector Red (**2.2.2.3**).

2.2.2.1 DAB Visualisation

Sections incubated in HRP conjugated secondary antibodies were visualised with DAB as chromogen. DAB at a final concentration of 0.5 milligramme (mg)/ml (prepared by adding 4.8ml Tris-HCl buffer pH7.6 and 0.1ml of freshly prepared 1% H_2O_2 to 0.1ml of 25mg/ml DAB) was added to the sections and left for 3-5 minutes for a brown colour change to occur. The sections were washed thoroughly in TBS then water, removed from the Sequenza racks and clips where necessary, counterstained in haematoxylin (Shandon, Basingstoke UK) for about 20 seconds, washed in tap water and 'blued up' in Scott's Tap water substitute (**Appendix B**) for about 20 seconds. The sections were dehydrated through ascending alcohols (64% to 74% to absolute) (Genta Medical, York UK) then xylene (Genta Medical, York UK) and mounted in pertex (Cellpath, Hemel Hempstead UK).

2.2.2.2 Fast Red Visualisation

Sections incubated in AP conjugated secondary antibodies were visualised with Fast Red as chromogen. All reagents were weighed or measured out ready for rapid preparation. 4mg naphthol AS MX phosphate was dissolved in 0.4ml N,N dimethylformamide in a glass beaker. 19.6ml alkaline phosphatase (AP) buffer (**Appendix B**) was added with 20µl 1M levamisole, to block endogenous AP. Immediately prior to use 20mg Fast Red TR was added and dissolved and the mixture was run through filter paper in a conical funnel. 500µl was added to each slide in the Sequenza racks and incubated in the dark for about 30 minutes until a pink colour had developed. The sections were washed thoroughly in tap water, counterstained and 'blued up', as for DAB visualised sections (**2.2.2.1**), then mounted in Aquamount Improved (Merck, Leicester UK).

2.2.2.3 Vector Red Visualisation

Sections incubated in AP conjugated secondary antibodies were visualised with Vector Red as chromogen. Vector Red (Vector Laboratories, Peterborough UK) was prepared according to the manufacturer's instructions. Two drops of Reagent 1 was added to 5ml of 100 millimolar (mM) Tris-HCl pH8.2 and mixed well. Two drops of Reagent 2 was added, mixed well, followed by two drops of Reagent 3 and mixed well. The tissue sections were incubated with the substrate at room temperature for 20-30 minutes until suitable staining had developed. The sections were then washed, counterstained and mounted as described above for the DAB visualised sections (**2.2.2.1**).

2.2.3 Procedure for use with the DAKO Techmate™ 500 Automated Immunocytochemistry Stainer

Sections, pre-treated where necessary as described above (**2.2.1**), were washed in PBS/0.1% polyoxyethylene-sorbitan monolaurate (Tween 20) prior to loading onto a DAKO Techmate™ 500 automated immunocytochemistry stainer (DAKO, Cambridge UK) according to manufacturer's instructions. Initial runs were carried out using the manufacturer's recommended programme with subsequent runs detecting CD68 expression using an altered protocol incorporating an additional

water wash before staining the sections in haematoxylin. The detection system was based on streptavidin/biotin complexes and horseradish peroxidase with 3'3'diaminobenzidine as chromogen and was suitable for use with primary monoclonal antibodies and polyclonal sera. Negative controls omitting the primary antibody were included. After completion of the immunohistochemistry and haemotoxylin staining sections were washed in running tap water and taken through ascending alcohols (64% to 74% to absolute) (Genta Medical, York UK) to xylene (Genta Medical, York UK) prior to mounting using a Bayer Tissue-Tek automated cover slip mounter (Bayer, Newbury UK).

Antigen	Clone	Supplier	Pre-treatment	Dilution	Protocol
bcl-x	polyclonal	Autogen Bioclear UK Ltd., Calne UK	Trypsin	1/100	Automated
bax	polyclonal	Autogen Bioclear UK Ltd., Calne UK	Trypsin	1/200	Automated
bcl-2	124	DAKO, Cambridge UK	MW Citrate	1/50	Automated
Fas/CD95	UB2	Coulter, Luton UK	MW Citrate	1/200	Automated
Ki-67	MIB-1	Coulter, Luton UK	MW Citrate	1/50	Automated
p53	DO-7	DAKO, Cambridge UK	None	1/100	Automated
CD68	PGM1	DAKO, Cambridge UK	Trypsin	1/100	Sequenza
CD68	PGM1	DAKO, Cambridge UK	MW EDTA	1/300	Automated

Table 2.2 Details of antibodies used for immunohistochemistry. The antibodies' antigen, the antibody clones and suppliers, the antigen retrieval method and optimal dilution and the immunohistochemistry procedure used during this study are shown. The antigen retrieval procedures are described in **2.2.1**; Trypsin: trypsin digestion; MW citrate: microwave in citrate buffer; MW EDTA: microwave in EDTA. The automated and Sequenza protocols are described in **2.2.3** and **2.2.2** respectively.

2.2.4 Cytospin Preparation and Immunostaining

2.2.4.1 Preparation of Cytospins

1 x 10^6 viable cells, determined by trypan blue exclusion (**2.18.2**), were centrifuged at 1000 revolutions per minute (rpm) for 10 minutes and the supernatant discarded. The cell pellet was resuspended in 1ml PBS containing 10% fetal calf serum (FCS) and 100µl (1 x 10^5 cells) of the cell suspension was pipetted into the funnel of prepared cytospin chambers, assembled as described by the manufacturer, which had been placed in a Cytospin 2 (Shandon, Basingstoke UK). The chambers were spun at 300rpm for 3 minutes and carefully dismantled to avoid scraping the cells adhered to the glass slide with the filter paper separating the slide from the plastic chamber. The cytospins were air dried and fixed for 3 minutes in 4% paraformaldehyde prepared in PBS then washed twice in ethanol (Genta Medical, York UK).

2.2.4.2 Immunostaining Cytospins

The prepared cytospins were immunostained using the Sequenza wet chamber as described in **2.2.2** using DAB visualisation (**2.2.2.1**) with the following alteration to the previously described protocol. The cytospins were blocked in TBS containing 1% bovine serum albumin (BSA) for 20 minutes then incubated in the test rabbit sera diluted 1/125, 1/250 and 1/500 for 30 minutes. Negative control sections were incubated in 1% BSA in TBS. After washing in TBS the cytospins were incubated for 30 minutes in (SAR-HRP) (DAKO, Cambridge UK) diluted 1/125 in 1% BSA in TBS, washed in TBS then visualised with DAB chromogen as described in **2.2.2.1**.

2.3 GENERATION OF ANTI-PEPTIDE SERA

2.3.1 NRAMP1 Peptide Synthesis

The human and murine NRAMP1 protein sequences (Cellier *et al.* 1994) were analysed to identify regions of sequence heterogeneity and structural moieties most suitable for use as synthetic peptides against which an anti-human NRAMP1 antibody response might be raised. The extremely high degree of sequence conservation between the two species and the intracellular location of regions of the

molecule severely limited the possible peptides of appropriate length for immunisation protocols. Two possible candidate peptides were identified, one at the amino (N) terminus, amino acids 41-58, and the other at the carboxy (C) terminus, amino acids 532-546 (Cellier *et al.* 1994). Of these, the C terminal peptide was chosen because antibodies successfully raised against this epitope of the whole NRAMP1 protein should only detect full length protein molecules, whereas the N terminal peptide had the potential to elicit antibodies capable of detecting truncated NRAMP1 protein molecules, resulting from the +alu mRNA splice variant (discussed in **1.8.8.1**), should these be translated.

The chosen peptide sequence is shown below with the murine sequence variations denoted underneath where present.

H H H F L Y G L L E E D Q K G E T S G
K P N E G V Q G S

20mg of the peptide was synthesised by the Department of Chemistry, University of Edinburgh, in collaboration with Professor Robert Rammage, using an Applied Biosynthesis 430A automated peptide synthesiser. The peptide was stored at 4°C as lyophilised protein. For immunisations of peptide without adjuvant the peptide was dissolved in PBS to give a concentration of 100μg/ml.

2.3.2 Preparation of Peptide for Immunisation using Imject Alum as Adjuvant

Lyophilised peptide was dissolved in PBS to give a concentration of 200μg/ml. An equal volume of Imject Alum (Pierce and Warriner, Chester UK) was added dropwise to the peptide solution, inverting to mix between additions, to give a final peptide concentration of 100μg/ml. Prior to immunisation the emulsion was rotated on a SR2 roller mixer (Stuart Scientific, Staffordshire UK) to ensure it was completely mixed and at room temperature.

2.3.3 Preparation of Peptide for Immunisation using Nitrocellulose as Adjuvant

50μg of peptide solution at 1mg/ml prepared in PBS was pipetted onto a small piece of Hybond-C nitrocellulose (Amersham Pharmacia Biotech, Little Chalfont UK) of about 5mm x 6mm. The nitrocellulose was dried at 37°C then placed in a glass bijou. DMSO was added dropwise until the nitrocellulose completely dissolved, then PBS was added dropwise until a fine suspension was obtained.

2.3.4 Enrichment of Dendritic Cells By Plastic Adherence and Pulsing the Cells with Peptide

A standard protocol (Coligan *et al.* 1995) for the enrichment of DCs from splenic cells followed by pulsing these cells with peptide prior to immunising mice of the same MHC haplotype as the isolated DCs was followed making minor adjustments to the protocol where necessary. All collagenase H solutions were prepared in Glasgow minimum essential medium (GMEM) (**Appendix B**), filter sterilised before use and kept on ice. The supplemented RPMI-1640 medium was as described in **Appendix B** with additional mercaptoethanol at 50μM. Where RPMI-1640 is described in the protocol the medium had no supplements added.

Collagenase Digestion of Spleen

Four female BALB/c mice which had been immunised as described in **5.2.9.1**, but had failed to generate a detectable anti-NRAMP1 peptide response, were killed and the spleens removed to GMEM (**Appendix B**). About 5ml of filter sterilised 0.25mg/ml collagenase H was added to a sterile 100mm tissue culture grade Petri dish. The spleens were held with forceps over a second 100mm tissue culture grade Petri dish. Using a 5ml syringe (Becton Dickinson UK Ltd., Oxford UK) with a 23½G needle (Becton Dickinson UK Ltd., Oxford UK) 1ml of the collagenase was injected in 100μl aliquots into each spleen, starting at the narrowest end of the spleen and pushing the needle further into the spleen by a few millimetres between injections, until the needle emerged at the other end of the spleen. The spleens were torn open using the needle and transferred to the Petri dish containing the 0.25mg/ml

collagenase H. The cell suspension in the second Petri dish over which the injections were carried out was collected into a 50ml centrifuge tube (Sterelin, Staffordshire UK) and placed on ice. The dish was rinsed with about 1.5ml of 0.25mg/ml collagenase H, adding the washings to the centrifuge tube. A further 1.5ml of 0.25mg/ml collagenase H was added to this dish and the spleens transferred one by one, using two forceps to tease them into small fragments. After all the spleens had been fragmented the contents of the dish were pipetted vigorously with a 5ml sterile plastic Pasteur pipette. The resulting cell suspension was transferred to the 50ml centrifuge tube on ice, leaving any large fragments in the Petri dish. The dish was rinsed with 0.25mg/ml of collagenase H and the fine suspension collected and added to the centrifuge tube.

5ml of 1mg/ml collagenase H was added to the spleen fragments, pipetting several times, and the fragments were incubated at 37°C, 5% CO_2 for 1 hour. The spleen fragments were pipetted vigorously and transferred to a sterile tea strainer over a sterile 100mm tissue culture grade Petri dish. The fragments were rinsed with a few millilitres of 0.25mg/ml collagenase H and mashed with the plunger from a sterile 5ml syringe (Becton Dickinson UK Ltd., Oxford UK) until any trace of red colour was removed. The sieve was rinsed with a few millilitres of 0.25mg/ml collagenase H and the contents of the sieve discarded. The fine suspension was pipetted vigorously and transferred to the 50ml centrifuge tube. The dish was rinsed with 0.25mg/ml collagenase H and the washing transferred to the centrifuge tube.

Preparation of Low Density Splenocytes

The collagenase H digested splenocytes were centrifuged at 280g (acceleration due to gravity) for 10 minutes at 4°C and the supernatant carefully removed with a pipette to avoid disturbing the pellet. The pellet was resuspended in 4ml of dense BSA (**Appendix B**), transferred to a 15ml conical tube and carefully overlayed with 1ml of RPMI-1640 at 4°C. The column was centrifuged at 5500g for 15 minutes at 4°C, with the brakes turned off. The cells at the interface, all the RPMI-1640 medium and about 1ml BSA solution from the top of the BSA layer were transferred

to a clean 50ml centrifuge tube. The tube was filled with RPMI-1640, mixed by gentle inversion then centrifuged at 280g for 10 minutes at 4°C. The supernatant was removed with a pipette and the cell pellet resuspended in RPMI-1640 and placed on ice. The cells were counted for viability, by trypan blue exclusion (**2.18.2**), which should be approximately 10^7 low density splenocytes per spleen.

Dendritic Cell Enrichment by Plastic Adherence and Pulsing with Peptide

5ml of low density splenocytes at about 10^7 cells/ml were plated on a 60mm sterile tissue culture grade Petri dish and incubated at 37°C, 5% CO_2 for 1½ hours. The cell density should not be greater than $4x10^7$ cells/dish as this reduces adherence and yield. After incubation the non adherent cells were removed with a pipette and the dish washed gently several times with RPMI-1640 medium, which had been pre-warmed to 37°C. A further 4ml of 37°C RPMI-1640 medium was added to the dish, which was incubated at 37°C, 5% CO_2 for 30 minutes. The dish was washed as described above and viewed by phase contrast under an inverted microscope to determine the proportion of dark, stellate DCs relative to bright, flattened Mϕs and round lymphocytes and monocytes. The half hour incubations and washes were continued until the dark, stellate DCs predominated. 4ml of filter sterilised supplemented RPMI-1640 containing 100μg/ml NRAMP1 peptide (**2.3.1**) was added to the washed dish and the dish cultured at 37°C, 5% CO_2 overnight. The surface of the dish was washed with supplemented RPMI-1640 medium and the eluted cells transferred to a universal tube (Rosslabs, Cheshire UK). The dish was rinsed with about 2ml of supplemented RPMI-1640 and the washings transferred to the universal which was centrifuged at 280g for 5 minutes at 4°C. The supernatant was discarded and the cells resuspended in 1ml of PBS. The viable cells were counted by trypan blue exclusion (**2.18.2**). Each spleen is expected to yield 0.5×10^6 - 1×10^6 cells based on DCs comprising about 80% of the cell population.

2.3.5 Coupling NRAMP1 Peptide to Keyhole Limpet Haemocyanin using Dimethyl Suberimidate

A standard protocol (Van Regenmortal *et al.* 1988) was followed and the Perkin-Elmer web site (Perkin Elmer web site) consulted to determine the appropriate amount of keyhole limpet haemocyanin (KLH) to use. The bisimido ester dimethyl suberimidate (DMS) was used as a coupling agent and the protocol followed gives an estimated 40-70% coupling efficiency.

A forty-fold excess of NRAMP1 peptide (**2.3.1**) over KLH and a 3 DMS:1 peptide molar ratio was required. The commercially available lyophilised KLH contained about 20% of actual KLH, hence, for 2.5mg of KLH (0.5 nanomoles) 12.5mg of the lyophilised powder was used. This was dissolved in 2.5ml of 0.2M triethanolamine-HCl pH8.5 and about 44µl of 1mg/ml peptide in PBS was added. Immediately prior to use 16.4µg of DMS was dissolved in 400µl of ice cold triethanolamine-HCl pH8.5. The DMS solution was quickly transferred, within 30 seconds, to the KLH/peptide and the mixture incubated at 22°C for 3 hours. The reaction solution was loaded into a 0.5-3ml Slide-a-Lyzer cassette (Pierce and Warriner, Chester UK) and dialysed against PBS at 4°C, stirring the PBS gently on a SM1 magnetic stirrer (Stuart Scientific, Staffordshire UK). The PBS was changed three times over 48 hours.

Approximately 3ml of liquid was removed from the cassette, filter sterilised and stored in aliquots at -20°C. Assuming 55% efficiency the solution would contain approximately 0.46µg/µl of coupled protein. The NRAMP1 peptide coupled to KLH is referred to as NRAMP1/KLH conjugate in future text.

2.3.6 Preparation of Peptide in Complete Freund's Adjuvant

0.7ml of NRAMP1 peptide (**2.3.1**) at 1mg/ml in PBS was added to a glass syringe attached to a 3-way valve with the third valve closed. 0.7ml of Complete Freund's Adjuvant (CFA) was added to the glass syringe and the mixture sucked into a second

glass syringe attached to the valve. The CFA and peptide were mixed well by pushing between the two syringes until an emulsion formed.

2.3.7 Preparation of Peptide in Incomplete Freund's Adjuvant

The procedure described above for CFA (**2.3.6**) was followed substituting incomplete Freund's adjuvant (IFA) for CFA.

2.3.8 Immunisations

All animals were kept in conventional animal housing conditions and fed *ad libitum*. For each immunisation procedure animals within groups of two Dutch rabbits or between three and five BALB/c or C57/Black (C57Bl) mice were treated in parallel. Prior to immunisation test bleeds from the ear of the rabbits were collected, allowed to clot overnight at 4°C and repeatedly microcentrifuged, transferring the supernatant to clean 1.5ml tubes until no trace of red blood cells could be seen. The serum was stored in aliquots at -20°C. Rabbits were injected sub cutaneously (s.c.) at four separate sites and test bleeds taken and serum collected as described above at suitable time points. For all steps in the protocols for immunising the mice injections were intra peritoneal (i.p.) except for intra venous (i.v.) injection in the tail of the peptide-pulsed enriched DCs (**2.3.4**). Test bleeds were obtained and pooled from the immunised mice for the separate immunisation protocols except those receiving CFA/IFA-peptide where each animal's response was assayed individually. The serum was collected as above for the rabbit test bleeds. The immunisation protocols followed are described in **5.2.9**.

2.3.9 Fas Ligand Peptide and Anti-Fas Ligand Peptide Polyclonal Sera

A Fas ligand peptide had been synthesised by the Department of Chemistry, University of Edinburgh, in collaboration with Ian Heslop and Professor Robert Rammage, using an Applied Biosynthesis 430A automated peptide synthesiser. This peptide had been used as an immunogen to raise an anti-Fas ligand Ab response in two rabbits and sera was available for characterisation. The Fas ligand peptide had the sequence:

C G H P S P P P E K K E L R K V A H L T G

2.3.10 Sepharose-Protein A Purification of Rabbit Sera

The rabbit sera to be IgG purified were incubated in an equal volume of heat treated normal human serum (NHS) (**Appendix B**) at 4°C overnight or at room temperature for 1 hour to precipitate rabbit anti-human complexes. These complexes were pelleted by microcentrifugation for 10 minutes and the supernatant aspirated off and transferred to a clean tube. A column was prepared by adding Sepharose-protein A beads (Pharmacia Biotech AB, Uppsala Sweden) to a liquid chromatography 0.7 x 10cm column and running 0.2M phosphate buffer pH7.3 (**Appendix B**) through the column several times, ensuring the beads were compacted to about a third of the way up the column. The first serum supernatant sample was run through the column followed by 40-50ml of 0.2M phosphate buffer pH7.3, to remove unbound protein. The column was eluted with 0.1M glycine pH2.5 and one 0.5ml fraction followed by ten 1ml fractions were collected into tubes containing one drop of 0.2M Tris pH10.4. Between purification of subsequent sera supernatants the column was re-equilibrated with 20-30ml of phosphate buffer pH7.3, having ensured the final fractions collected during the glycine elution step were free of protein, as described below, and the phosphate buffer elute was between pH7.2 and pH7.5. Between use the column was stored containing phosphate buffer pH7.3 with 0.02% sodium azide.

5µl samples of the ten 1ml collected fractions were dotted, in order of collection, on to a 2 x 5 grid marked on Hybond-C nitrocellulose (Amersham Pharmacia Biotech, Little Chalfont UK). The samples were allowed to dry completely and stained in Coomasie blue staining mixture (**Appendix B**) for 5 seconds and excess colour removed in destain mixture (**Appendix B**). The filters were dried and protein appeared as a blue stained central spot. The fractions with the most protein were pooled and pH adjusted, if necessary, to between pH6.5 and pH7.5. The protein concentration of the IgG purified sera was estimated by measuring the optical density (OD) at a wavelength (λ) of 280 nanometres (nm) (OD_{280}), using a Philips PU8620 UV/VIS/NIR spectrophotometer (Philip Harris Scientific, Coatbridge UK), and calculating the protein concentration in mg/ml which is equal to $OD_{280}/1.4$.

2.4 WESTERN BLOTTING

2.4.1 Protein Extraction

5 x 10^6 cells were washed twice in ice cold PBS and pelleted by microcentrifgation at 650rpm at 4°C. 333µl of protein lysis buffer (**Appendix B**) was added to the cell pellet, mixed and left on ice for 45 minutes, vortexing intermittently. The cell lysate was microcentrifuged as above for 15 minutes and supernatant transferred to a clean 1.5ml tube.

2.4.2 Lowry Assay to Determine Protein Concentration

Reactions for standards and samples were performed in triplicate. 200µl of BSA standards (200µg/ml, 120µg/ml, 100µg/ml, 80µg/ml, 50µg/ml and 20µg/ml prepared in 0.1M NaOH) and 5µl test sample with 195µl 0.1M NaOH were added to 5ml test tubes. 1ml alkaline carbonate working solution (**Appendix B**) was added to each tube and vortexed, allowed to stand for 10 minutes at room temperature then 100µl Folin-coicalteau reagent (**Appendix B**) added to each tube and left for 30 minutes. 200µl of each sample was transferred to an enzyme linked immunosorbant assay (ELISA) plate (Corning, Newbury UK) and the absorbance at 595nm read on a Dynatech MR5000 plate reader (Dynatech, Guernsey, Channel Islands). Using the Biolinx software (Dynatech, Guernsey, Channel Islands) a standard curve and estimation of the protein concentration of the test samples was obtained

2.4.3 Electrophoresis and Electrophoretic Transfer of Protein Samples

Proteins were analysed by sodium dodecyl sulphate polyacrylamide gel electrophoresis (SDS-PAGE) according to the method of Laemmli (Laemmli 1970). A 12% separating (**Appendix B**) with 4.5% stacking (**Appendix B**) sodium dodecyl sulphate (SDS) polyacrylamide gel, prepared, cast and run using a Bio-Rad Protean II xi Cell system (Bio-Rad, Hemel Hempstead UK) according to the manufacturer's instructions, was found appropriate for resolving proteins in the molecular weight range of the Fas ligand protein (approximately 40kDa) (Takahashi *et al.* 1994). 50µg of protein lysate (**2.4.1-2.4.2**) in an equal volume of sample buffer (**Appendix B**) was boiled for 5 minutes then loaded in the wells of the cast

gel and pre-stained Multimark Multi-colored Standard (Novex, Frankfurt Germany) were electrophoresed in parallel with the protein lysates for reference. The gels were run in 1x running buffer (**Appendix B**) at a constant current of 50mA per gel until the samples had traversed the stacking gel, then continued at 30mA per gel until the 4kDa molecular marker was approaching the bottom of the gel.

The electrophoresis apparatus was disassembled and the plates separated. The stacking gel was removed using a scalpel blade and a corner of the gel marked uniquely for future orientation. A Trans-Blot Electrophoretic Transfer Cell (Bio-Rad, Hemel Hempstead UK) was assembled as described by the manufacturer. The electrophoretic transfer was carried out in transfer buffer (**Appendix B**), to a level 1cm below the electrodes of the transfer tank, at 250mA overnight. The transfer apparatus was dismantled and the plastic holder containing the gel and Hybond-C nitrocellulose (Amersham Pharmacia Biotech, Little Chalfont UK) submerged and opened in TBS Tween (TBST) (**Appendix B**). Excess nitrocellulose around the gel was cut away with a scalpel blade and the nitrocellulose cut into sections containing lanes of appropriate protein samples to be immunoblotted with the sera of choice. The reference molecular weight standards lanes were cut off and retained for analysis after the immunoblotting (**2.4.4**). The gel was removed from the nitrocellulose and the sections clearly marked for future reference and orientation.

2.4.4 Western Blotting and Dot Blots

All incubations and washes were carried out on a Platform Shaker STR6 (Stuart Scientific, Staffordshire UK) at room temperature unless stated otherwise and antisera dilutions were prepared in TBST (**Appendix B**). The nitrocellulose strips for the Western blots to test for an anti-Fas ligand peptide antibody response in the Fas ligand peptide immunised rabbits were obtained as described above (**2.4.3**). Dot blots were used to test sera obtained from mice and rabbits immunised with the NRAMP1 peptide (**2.3.1-2.3.8**). These were prepared by spotting 10µl containing 1µg of the test or control substance on a strip or triangle of nitrocellulose and the dots allowed to dry at room temperature. The substances were NRAMP1 peptide (the

NRAMP1 peptide in PBS) (**2.3.1**), NRAMP1/KLH conjugate (the NRAMP1 peptide conjugated to KLH) (**2.3.5**), KLH (KLH in PBS), BALB/c IgG, BSA and NRS. When only one species of sera was being tested the positive controls for the detection method for the other species were omitted (i.e. positive control when testing rabbit sera: NRS, positive control when testing mouse sera: BALB/c IgG).

The nitrocellulose sections were washed in TBST, blocked in blocking solution (**Appendix B**) for 1 hour, or overnight at 4°C, then washed 3 x 5 minutes in TBST. The sections were incubated for ½-1¾ hours in heat sealed clear plastic "bags" containing 10ml of the appropriate antisera or, for the triangle dot blots, in 2mls of sera in small plastic weighing boats. Sera dilutions are shown in **Table 2.3** and negative controls were incubated in TBST. The sections were washed as above and incubated in the appropriate secondary antisera at 1/1000 for 30 minutes i.e. SAR-BIO (DAKO, Cambridge UK) for testing rabbit sera or RAM-BIO (DAKO, Cambridge UK) for testing mouse sera. The sections were washed as above, incubated in a 1/30 dilution of prepared ABComplex-AP (DAKO, Cambridge UK) for 30 minutes then washed as above. The sections were incubated in nitro blue tetrazolium/5-bromo-4-chloro-3-indoyl phosphate (NBT/BCIP) chromogen substrate (**Appendix B**) in the dark for 5-20 minutes until the blue colour reaction had developed and bands or dots were visible. The sections were washed twice for 1 minute and twice for 5 minutes in dH_2O and the nitrocellulose allowed to dry. The Western blots were aligned against the molecular weight standard strips and the size of immunopositive bands estimated. Anti-CD3 sera was used as a positive control for the Western blotting to check the PBMCs had been stimulated successfully with concanavalin A (**2.18.4**). For the Western blots additional positive controls were included in the form of dot blots of the Fas ligand peptide and pre-immune rabbit sera immunoblotted with the pre-immune serum and serum from the peptide immunised rabbits.

Antiserum	Concentration
Polyclonal anti-CD3 (DAKO, Cambridge UK)	1/500
Pre-immune rabbit serum (for Fas ligand response test)	10μg/ml
Fas ligand peptide immunised rabbit sera	10μg/ml
Pre-immune rabbit serum (for NRAMP1 peptide response test)	1/100
NRAMP1 peptide immunised rabbit sera	1/100
NMS	1/100
NRAMP1 peptide immunised mouse sera	1/100

Table 2.3 Dilutions of sera used for Western blotting to test for a rabbit anti-Fas ligand antibody response, and for dot blots to test for an anti-NRAMP1 peptide antibody response. Immunisation strategies and derivation of sera are described in **2.3** and **5.2.9.5**.

2.5 ENZYME-LINKED IMMUNOSORBENT ASSAY AND CYTOSPINS

2.5.1 To Test Sera for Fas Ligand Peptide Specific Antibody Response

Each test sera dilution and negative control solution was tested in triplicate and the mean absorbance of the three readings calculated. Half the wells of a 96 well ELISA plate were coated with 100μl of Fas ligand peptide solution at 1μg/ml in 0.05M carbonate/bicarbonate buffer pH9.6 and incubated at 4°C overnight. The wells were washed three times with PBS/0.05% Tween 20 (PBST) and 100μl of 1% BSA in PBS was added to each well as blocking agent and incubated at room temperature for 2½-3 hours. The wells were washed as above and 100μl of the appropriate antisera dilutions (**Figure 3.5**) or 1% BSA in PBS added to the appropriate wells such that three peptide coated wells and three uncoated wells received each test dilution and BSA control. The plates were incubated at room temperature for 1½ hours and washed as above. 100μl of SAR-HRP (DAKO, Cambridge UK), diluted 1/1000 in 1% BSA in PBS was added to each well and incubated at room temperature for 1½ hours, then washed as above. 100μl of TMB (tetramethylbenzadine) chromogen substrate (**Appendix B**) was added to each well and left at room temperature for 5-10 minutes, watching for the optimal colour change, at which point the reaction was stopped by the addition of 50μl 3 nolar (N) HCl (Fisher Scientific, Loughborough UK) and the absorbance at 450nm was read on

a Dynatech MR5000 (Dynatech, Guernsey, Channel Islands) plate reader. A graph of anti-sera concentration versus OD_{450} was plotted to compare the specificity of the sera samples tested for the peptide.

2.5.2 To Test Sera for Human NRAMP1 Peptide Specific Antibody Response

A similar protocol to that described in **2.5.1** to test sera for a Fas ligand peptide response was followed with the following alterations. Each combination of sera dilution and NRAMP1 peptide concentration coating the plate was performed in duplicate. NMS at the same concentrations as the test sera were used as controls. The plate was coated with peptide at concentrations of 0μg/ml, 0.5μg/ml, 1.0μg/ml, 2.0μg/ml, 4.0μg/ml and 8.0μg/ml and incubated at 37°C for 1½ hours or at 4°C overnight. The sera were tested at dilutions of 1/50, 1/150, 1/450 and 1/1350 and mouse Ig detected using HRP conjugated rabbit anti-mouse Ig (RAM-HRP) (DAKO, Cambridge UK) at 1/750 dilution. O-phenylenediamine (OPD) chromogen substrate (**Appendix B**) was used to detect a positive reaction, stopping the reaction after about 5 minutes with 25μl of 3N HCl and the OD_{490} read.

2.6 DNA EXTRACTIONS

Extracted genomic DNA was stored at 4°C for short term storage or -20°C for long term storage. Extracted plasmid DNA was stored at -20°C.

2.6.1 DNA Isolation from Blood

DNA extraction was carried out in a BioMAT-1 Class I microbiological safety cabinet (Medical Air Technology, Manchester UK). 100μl EDTA-blood in 800μl Tris-EDTA (TE) (**Appendix B**) was vortexed and microcentrifuged at 13,000rpm for 25 seconds. The supernatant was removed and the cell pellet was washed in 50μl TE, vortexed and microcentrifuged as above and washes repeated until the pellet was creamy white and free from visible red blood cells. 200μl lysis buffer/proteinase K (50mM KCl, 10mM Tris, 2.5mM $MgCl_2$, 10% gelatin, 0.45% NP40, 0.45% Tween 20, 200μg/ml proteinase K) was added and the samples were incubated at 50°C for

20 minutes. Proteinase K was inactivated by boiling for 20 minutes after addition of 100µl distilled H_2O.

2.6.2 DNA Isolation from Paraffin Embedded Tissue

For all the protocols used the following procedures were carried out to avoid contamination from other DNA sources:

Gloves were worn throughout the procedure.

Excess paraffin was removed from the blocks.

Prior to cutting sections the microtome cutting area was cleaned with alcohol and any debris from previous cutting removed.

For each block, and after trimming the block to get a full face, a clean part of the blade was used.

After cutting, the rolled section was transferred from the blade to a sterile 1.5ml tube using a sterile toothpick.

The number and thickness of sections cut depended on the protocol being followed and the size of the block being used. The majority of blocks used were large wedge biopsies of approximately 2cm by 1cm and the quantities for these are given. For smaller blocks the number of sections cut was increased appropriately. For selection of cases see (**2.1.1**).

1) DNA was extracted according to the method of Hubbard and Anderson (Hubbard and Anderson 1993). 15µm sections were boiled for 8 minutes in 100µl lysis buffer (50mM Tris pH 8.4, 1mM EDTA, 0.5% Tween 20) then microcentrifuged briefly to pellet the tissue. Extracted DNA was stored at -20°C. When the DNA solution was being pipetted for PCR analysis (**2.9**) care was taken to avoid transfer of paraffin, which formed an upper phase in the tube. Where necessary this was removed prior to pipetting.

2) 15µm sections were deparaffinised in 600µl xylene (Genta Medical, York UK) at room temperature for 5 minutes and microcentrifuged at 13000rpm for 10

minutes. The supernatant was discarded and the xylene wash was repeated. 600µl absolute ethanol (Hayman Ltd., Witham UK) was added to each tube, incubated at room temperature for 5 minutes then microcentrifuged at 13000rpm for 10 minutes. The supernatant was discarded and the ethanol wash repeated. The tubes were drained on paper towel and air dried for 10 minutes. 200µl lysis buffer (50mM KCl, 10mM Tris, 2.5mM $MgCl_2$, 0.1mg/ml gelatin, 0.45% NP40, 0.45% Tween 20, pH 8.3) containing 200µg/ml proteinase K was added, pipetting gently to mix, and incubated at 50°C for 2 hours, vortexing after 1 hour. The samples were microcentrifuged briefly to pellet the contents of the tubes, boiled for 20 minutes to inactivate proteinase K, then microcentrifuged briefly as before and cooled on ice.

3) DNA was extracted using the Nucleon HT DNA extraction kit (Scotlab, Coatbridge UK) following the protocol for "DNA extraction from Paraffin Sections". 20-30µm sections were covered in xylene (Genta Medical, York UK) and incubated at 37°C for 20 minutes, microcentrifuged at 5000rpm for 5 minutes and the xylene removed. The sections were recovered in xylene, incubated at room temperature for 2 minutes, microcentrifuged at 13000rpm for 5 minutes and the xylene removed. The sections were rehydrated through 100%, 75%, 50% and 25% ethanol (Hayman Ltd., Witham UK) and finally water, incubating for 3 minutes in each alcohol dilution, microcentrifuging at 13000rpm and removing supernatant between the rehydration steps. After pouring off the water. 350µl Reagent B (400mM Tris-HCl, 60mM EDTA, 150mM NaCl, 1% SDS, pH 8.0) and 18µl proteinase K solution (10mg/ml) were added and the tubes incubated at 55°C overnight. The tissue was deproteinised by addition of 100µl sodium percholate and mixed by inverting at least seven times. DNA was extracted by the addition of 600µl chloroform, mixing as above, and 150µl Nucleon resin suspension. Without remixing the phases the tubes were microcentrifuged at 2000rpm for 1 minute and the upper brown phase transferred to a fresh tube. The DNA was precipitated in 2 volumes of cold absolute ethanol at -20°C for 1½ hours. Precipitated DNA was pelleted by microcentrifugation at 13000rpm for 15 minutes, the supernatant was

removed, 1ml cold 70% ethanol added to pellet, inverting several times, and the tube recentrifuged as before. After removal of the ethanol the DNA was air dried for about 10 minutes. 25µl sterile dH_2O was added and the DNA redissolved on a rotary mixer (Stuart Scientific, Staffordshire UK) for several hours.

4) DNA was extracted using the Gentra Systems, Inc. Puregene DNA Isolation Kit (Flowgen, Lichfield UK) following the protocol for "DNA Isolation from Tissue in Paraffin". Reagents were supplied with the kit unless indicated otherwise. 5-10mg of paraffin embedded tissue sections were deparaffinised in 300µl xylene (Genta Medical, York UK) at room temperature, inverting constantly. The tissue was pelleted by microcentrifugation at 9000rpm for 2 minutes and xylene discarded. The xylene wash was repeated twice. 300µl of 100% ethanol (Hayman Ltd., Witham UK) was added and incubated at room temperature for 5 minutes, inverting constantly, then microcentrifuged at 9000rpm for 2 minutes and ethanol discarded. The ethanol wash was repeated once. 300µl Cell Lysis Solution was added, pipetting several times to homogenise the tissue. 3µl proteinase K (10mg/ml) was added to the lysates and the tubes inverted 25 times prior to incubation at 55°C for 1 hour, inverting the tubes periodically. The tubes were cooled to room temperature and 1.5µl of RNase A Solution (4mg/ml) was added to the lysate, mixed by inversion 25 times and incubated at 37°C for 40 minutes then allowed to cool to room temperature. The protein was precipitated by addition of 100µl Protein Precipitation Solution, vortexed for 20 seconds then microcentrifuged at 9000rpm for 3 minutes to pellet the protein. The supernatant was poured off into clean 1.5ml tubes and 300µl isopropanol (Fisher Scientific, Loughborough UK) was added to precipitate the DNA, inverting 50 times, followed by microcentrifugation at 900rpm for 1 minute. The supernatant was discarded and the tubes drained on paper towel. 300µl of 70% ethanol was added to the DNA pellets, inverting to wash the DNA, then microcentrifuged at 9000rpm for 2 minutes. The ethanol was poured off, the tubes were drained on paper towel and allowed to air dry for 15 minutes. The DNA was rehydrated in 10µl DNA Hydration Solution at room temperature overnight.

5) DNA was extracted using the Cleanmix DNA extraction kit (Vh-Bio Ltd., Newcastle-upon Tyne UK) following the protocol for "DNA extraction from paraffin embedded tissues" and "Protocol B". Reagents were supplied with the kit unless indicated otherwise. 20μm sections were deparaffinised by incubation at 65°C for 10 minutes in 1ml octane (Sigma, Poole UK). After microcentrifugation at 13000rpm for 5 minutes the supernatant was discarded and the pellets washed with 1ml absolute ethanol (Hayman Ltd., Witham UK) and microcentrifuged as before. The ethanol wash was repeated and 100μl proteinase K digestion buffer (150mM Tris pH 7.5, 50mM EDTA, 1% Triton X100) and 20μl proteinase K (10mg/ml) were added to the pellets. The tubes were incubated at 50°C for 24 hours. 450μl Cleanmix Binding Solution and 50μl Cleanmix-High Capacity Purification Resin (shaken before addition) were added to each tube and mixed by inversion. The mixture was transferred to 2ml tubes containing a Cleanmix Filter and microcentrifuged at 13000rpm for 30 seconds. The resin with bound DNA should remain on the filter. The filtrate was discarded and 500μl Washing Solution (containing 50% ethanol (Hayman Ltd., Witham UK) was added to the filter, microcentrifuged at 13000rpm for 30 seconds and the filtrate discarded. The wash was repeated using 500μl of 80% ethanol and the filter transferred to a clean tube. DNA was eluted from the filter with 30μl of sterile water pre-warmed to 65°C, allowing the DNA to resuspend for 1 minute before microcentrifuging for 30 seconds.

2.6.3 DNA Isolation from Cells

10^5 viable cells (**2.18.2**) were pelleted in universal tubes (Rosslabs, Cheshire UK) at 1000rpm for 10 minutes and nearly all the supernatant discarded. The cell pellet was resuspended in residual supernatant and transferred to a 1.5ml tube, microcentrifuged at 6000rpm for 6 minutes and the supernatant aspirated off. 250μl lysis buffer (50mM KCl, 10mM Tris, 2.5mM $MgCl_2$, 0.1mg/ml gelatin, 0.45% NP40, 0.45% Tween 20, pH 8.3) and 5μl proteinase K (10mg/ml) were added, pipetting to mix, and incubated at 50°C for 1 hour. Proteinase K was inactivated by boiling for 15 minutes and the samples were cooled on ice.

2.6.4 DNA Isolation from Bacterial Cultures

2.6.4.1 "Quick Mini Preps"

The following protocol was used to extract DNA from mini cultures (**2.16.1**) to determine if cloning and bacterial transfection had been successful by subsequent digestion of DNA with restriction enzymes and analysis of the products. Plasmid DNA from clones with the desired restriction enzyme digestion profile was subsequently isolated for sequencing (**2.15.2**) using QIAprep Spin Plasmid Kit (**2.6.4.2**).

1.5ml of turbid mini culture (**2.16.1**) was poured into a 1.5ml tube and microcentrifuged at 13000rpm for 1 minute. The culture medium was aspirated off and the pellet resuspended in 200µl TEN buffer (0.01mM Tris-HCl pH 8.0, 1mM EDTA, 0.1mM NaCl). 200µl phenol:chloroform:isoamyl alcohol (25:24:1) was added, the samples were shaken quickly and microcentrifuged at 13000rpm for 5 minutes. The aqueous phase was transferred to a clean 1.5ml tube and 400µl of 95% ethanol (Hayman Ltd., Witham UK)/5% 3M NaOAc pH5.0 was added, mixed and microcentrifuged for 10 minutes. The supernatant was removed and the pellet washed in 70% ethanol. The pellet was air dried at 37°C and resuspended in 50µl sterile water. 7µl of extracted DNA was used per restriction enzyme digest (**2.10**), including 1µl of RNase A (10mg/ml), as this protocol does not separate RNA from DNA.

2.6.4.2 QIAprep Spin Plasmid Kit (Mini Preps)

Plasmid DNA for manual sequencing of cloned DNA fragments (**2.15.2**) was isolated using the QIAprep Spin Plasmid Kit (QIAGEN Ltd., Crawley UK) following the "Standard Protocol" as described below. The purification procedure is based on extraction of plasmid DNA from cleared bacterial alkaline SDS lysates, under high salt binding conditions, binding of DNA to a silica-gel membrane, ethanol with high salt washing and elution of DNA. All buffers used were supplied with the kit and their composition is given below where known.

1.5ml of turbid overnight mini culture (**2.16.1**) was poured into a 1.5ml tube and microcentrifuged at 5000rpm for 5 minutes, the supernatant was discarded and a further 1.5ml culture added and pelleted as before. The bacterial pellet was resuspended in 250µl of Buffer P1 (50mM Tris-HCl pH8.0, 10mM EDTA, 100µg/ml RNase A) and 250µl of Buffer P2 (200mM NaOH, 1% SDS) was added mixing by gentle inversion. The mixture was incubated at room temperature for no more than 5 minutes to prevent denaturation of plasmid DNA. Chromosomal DNA and protein was precipitated by addition of 350µl of chilled Buffer N3 (1.32M potassium acetate pH4.8), mixing immediately by gentle inversion of the tube. Following 10 minutes of microcentrifugation at 13000rpm the supernatant was transferred to a QIAprep spin column and placed in a 2ml collection tube. The column was microcentrifuged for about 1 minute at 13000rpm and the flow-through discarded. DNA in the column was washed by the addition of 0.75ml of Buffer PE (200mM NaCl, 20mM Tris-HCl, 5mM EDTA diluted with 95% ethanol (Hayman Ltd., Witham UK) to a final ethanol concentration of 55%) to the column, microcentrifuged for 1 minute, the flow-through discarded and microcentrifuged again as before, to remove residual wash buffer. The column was transferred to a clean 1.5ml tube and the DNA eluted with 50µl of water or TE (**Appendix B**), incubating for 1 minute at room temperature before microcentrifuging at 13000rpm for 1 minute.

2.6.4.3 Plasmid Maxi Kit (Maxi Preps)

The Plasmid Maxi Kit (QIAGEN Ltd., Crawley UK) was used to prepare DNA of quality and quantity suitable for ligation (**2.14**) and transfection (**2.17**). It is based on a modified alkaline lysis procedure, followed by binding of plasmid DNA to QIAGEN anion-exchange resin under low salt and pH conditions. RNA, protein and low molecular weight impurities are removed by a medium salt wash, plasmid DNA is eluted in a high salt buffer followed by concentration and desalting by isopropanol precipitation. All buffers used were supplied with the kit and their composition is given below where known.

Turbid overnight maxi culture (**2.16.1**) was poured into 250ml polypropylene centrifuge bottles (Sorvall, Stevenage UK) and centrifuged at 5000rpm for 15 minutes at 4°C in a Centrikon H-401B centrifuge (Kontron Instruments, UK) using a Sorvall GSA rotor (Sorvall, Stevenage UK) and the supernatant discarded. The bacterial cell pellet was resuspended in 10ml of Buffer P1 (resuspension buffer) (100μg/ml RNase, 50mM Tris-HCl, 10mM EDTA pH8.0). 10ml of Buffer P2 (lysis buffer) (200mM NaOH, 1% SDS) was added and the bottles rolled gently to mix and incubated at room temperature for 5 minutes. 10ml of chilled Buffer P3 (neutralization buffer) (3.0M KOAc pH5.5) was added, the bottles were rolled to mix and incubated on ice for 20 minutes, then centrifuged at 11,500rpm using a Sorvall SS34 rotor (Sorvall, Stevenage UK) for 30 minutes at 4°C and the supernatant was transferred to 50ml centrifuge tubes. A QIAGEN-tip 500 was equilibrated with 10ml Buffer QBT (equilibration buffer) (750mM NaCl, 50mM MOPS pH 7.0, 15% ethanol, 0.15% Triton X-100) and the eluted sample applied to the QIAGEN-tip. The sample was allowed to flow through by gravity and the tip was washed twice with 30ml of Buffer QC (wash buffer) (1.0M NaCl, 50mM MOPS pH7.0, 15% ethanol). The DNA was eluted with 15ml Buffer QF (elution buffer) (1.25M NaCl, 50mM Tris-HCl pH8.5, 15% ethanol) and collected in a 25ml DuPont Instruments Corex tube (Sorvall, Stevenage UK). 10.5ml (0.7 volumes) of room temperature isopropanol (Fisher Scientific, Loughborough UK) was added to precipitate the DNA and the tube centrifuged at 1,500rpm for 30 minutes at 4°C. The supernatant was discarded and the DNA washed with 5ml of chilled 70% ethanol (Hayman Ltd., Witham UK), air dried and resuspended in 500μl TE.

2.6.5 DNA Isolation from Agarose Gels

The QIAEX II Gel Extraction Kit (QIAGEN Ltd., Crawley UK) was used to extract and purify DNA fragments based on solubilisation of agarose and selective, quantitative adsorption of nucleic acids to the QIAEX II silica-gel particles in the presence of high salt. Elution of the DNA is accomplished with a low salt solution. The buffers used were supplied with the kit.

Under UV visualisation using a Herolab UVT-28 MP transilluminator (Scotlab, Coatbridge UK) the appropriate DNA band was excised from agarose gel (**2.11.1**) using a clean scalpel blade and excess agarose removed. The gel slice was weighed in a colourless 1.5ml tube and 3µl of Buffer QX1 for each mg of gel was added. The QIAEX II was resuspended by vortexing for 30 seconds and the appropriate amount added to the tube (10µl for ≤2µg DNA, 30°C for 2-10µg DNA). The tube was incubated at 50°C for 10 minutes to solubilise the agarose and bind the DNA, mixing by vortexing every 2 minutes to keep the QIAEX II in suspension and ensuring the mixture remained yellow. The sample was microcentrifuged for 30 seconds and the supernatant removed with a pipette. The pellet was washed with 500µl Buffer QX1 to remove residual agarose contamination, resuspending by vortexing then microcentrifuged and the supernatant removed as before. The pellet was then washed twice with 500µl Buffer PE, to remove residual salt contamination, and the pellet air dried for 10-15 minutes until it became white. The DNA was eluted by the addition of 20-40µl dH_2O or 10mM Tris-HCl pH8.5 and incubated at room temperature for 5 minutes. The tube was microcentrifuged for 30 seconds and the supernatant containing the DNA was pipetted into a clean tube.

2.7 RNA EXTRACTION AND REVERSE TRANSCRIPTION

2.7.1 RNA Extraction

Total RNA was extracted from cells or frozen tissue using Total RNA Isolation Reagent (Advanced Biotechnologies, Epsom Surrey UK). The method is based on a 14M solution of guanidine salts and urea, which act as a denaturing agent, in conjunction with phenol and detergents, which are very effective for isolation of total RNA. Chloroform extraction of RNA is followed by isopropanol precipitation from the aqueous phase. The labile nature of RNA required all plastic wear, solutions and filter pipette tips to be RNase free and gloves to be worn throughout all procedures involving RNA. All water was pre-treated with 0.1% diethyl pyrocarbonate (DEPC treated dH_2O) (**Appendix B**) overnight in a fume hood (Morgan and Grundy Ltd., Uxbridge, UK) then autoclaved. Following

homogenization of 1) cells or 2) tissue the same protocol 3) was followed, as described below.

1) Homogenization of cells

10^7 viable cells were centrifuged in a universal tube (Rosslabs, Cheshire UK) at 1000rpm for 10 minutes and nearly all the supernatant discarded. The cell pellet was resuspended in the residual supernatant and transferred to an RNase free 1.5ml tube. The cells were not washed prior to RNA extraction as this increases the possibility of mRNA degradation. The cells were lysed by addition of 1ml RNA Reagent, pipetting well to ensure complete homogenization.

2) Homogenization of Frozen Tissue

Tissue destined for RNA extraction was frozen as soon as possible after excision from its source and stored at -70°C. A piece of tissue was cut using a scalpel blade and transferred to an RNase free 1.5ml tube. The weight of tissue was calculated by "weighing by difference". 1ml of RNA Reagent per 10-100mg tissue was added to the tissue and homogenized using a plastic hand homogenizer.

3) The homogenate was kept on ice for 5 minutes to ensure complete dissociation of nucleoprotein complexes. 0.2ml of chloroform per ml of RNA Reagent used was added and the sample shaken vigorously for 15 seconds. After a 5 minute incubation on ice the sample was microcentrifuged at 13000rpm for 15 minutes at 4°C. The upper aqueous phase containing the total RNA was transferred to an RNase free 1.5ml tube leaving the lower organic phase and interface containing the protein and DNA. An equal volume of isopropanol was added to the aqueous phase, mixed by inversion and the RNA allowed to precipitate on ice for about 1 hour. The sample was microcentrifuged at 13000rpm for 10 minutes at 4°C, the supernatant removed and the RNA pellet washed twice with 75% ethanol (Hayman Ltd., Witham UK), vortexing and microcentrifuging the sample at 6500rpm for 5 minutes at 4°C between washes. The pellet was air dried for about

10 minutes and resuspended in 50-100µl DEPC treated dH_2O. The RNA concentration was estimated (**2.7.2**) and the RNA solution stored at -70°C.

2.7.2 Estimation of RNA Concentration

1µl of RNA solution (**2.7.1**) was added to 599µl of DEPC treated dH_2O (**Appendix B**) (**2.7**), previously used as a reference blank, in a quartz cuvette and the absorbance at 260nm (A_{260}) read using a Genequant II RNA/DNA Calculator (Pharmacia Biotech, Cambridge UK). The concentration of RNA was obtained using the Genequant II RNA/DNA calculator, which uses the following equation:

$$A_{260} \times 40 = \mu g/ml \text{ RNA}$$

An indication of the RNA integrity was obtained from the A_{260}/A_{280} ratio where pure RNA has a value of 2.0.

Between samples the cuvette was thoroughly rinsed three times with dH_2O and three times with DEPC dH_2O.

2.7.3 DNase Treatment of Total RNA

Where PCR primers were not able to distinguish between cDNA and possible carry-through-plasmid DNA during the RNA extraction procedure RNA was treated with DNase prior to reverse transcription (**2.7.4**). 1µg of total RNA, 1µl Deoxyribonuclease I, Amplification Grade (Life Technologies, Paisley UK) and 0.909µl 10 x DNaseI reaction buffer (200mM Tris-HCl pH8.4, 20mM $MgCl_2$, 500mM KCl), made up to a final volume of 9.09µl with DEPC treated dH_2O (**Appendix B**), was incubated at room temperature for 15 minutes. 0.91µl 25M EDTA was added and incubated at 65°C for 10 minutes to inactivate the DNase. DNase treated RNA was used immediately as template for reverse transcription (**2.7.4**).

2.7.4 Reverse Transcription

First strand complementary DNA (cDNA) was synthesised from total RNA using RNase H-Moloney Murine Leukaemia Virus reverse transcriptase (RT). Reagents were supplied by Life Technologies, Paisley UK, unless stated otherwise.1μg of DNase treated total RNA (**2.7.3**) or 1μg of total RNA (**2.7.1**), when DNase pre-treatment was not required, was heated at 70°C for 10 minutes with 1μl oligo$(dT)_{18}$ universal primer (500μg/ml) (Advanced Biotechnologies, Epsom UK) in a final volume of 11μl, to allow oligo(dT) primers and mRNA polyA tails to anneal. The mixture was chilled quickly on ice and microcentrifuged briefly. After addition of 4μl of First Strand Buffer (250mM Tris-HCl pH 8.3, 375mM KCl, 15 mM $MgCl_2$), 2μl of 0.1M dithiothreitol (DTT) and 2μl of 20mM DNA polymerisation mix (Advanced Biotechnologies, Epsom UK), the mixture was incubated at 42°C for 2 minutes and 1μl Superscript II was added, mixing gently by pipetting. cDNA was synthesised at 42°C for 50 minutes and the reaction inactivated by heating at 70°C for 15 minutes using a Hybaid Omni Gene thermal heating block (Hybaid, Teddington UK). cDNA was stored at -20°C.

2.8 DESIGN OF PCR PRIMERS AND PCR REACTIONS

All primers were synthesised by Cruachem Ltd., Glasgow UK and were received in a lyophilised state. Primers were rehydrated in sterile dH_2O to give stock solutions of 250μM which were diluted to 25μM working solutions. Lyophilised primers were stored at 4°C and primer solutions were stored at -20°C.

DNA sequence information was obtained from Genbank and the relevant papers as referenced. Primers were designed by determining which region of DNA sequence was required to be amplified and by analysing the intron/exon structure of the genes to ensure cDNA specificity where required. The candidate primer sequences were designed to have an equivalent GC:AT ratio, to show no obvious signs for potential primer-primer interaction and to have equivalent melting temperatures (Tm) of approximately 60°C. This was based on an approximate calculation, summing the primer-template base interactions where every A-T interaction is equivalent to 2°C

and every C-G interaction is equivalent to 4°C. All primers were checked against sequences entered in the Genbank and EMBL databases using BLAST to check for potential cross-reactivity of the primers with other published sequences. When establishing the optimal reaction conditions for the PCRs, an extension time was tried based on allowing approximately 1 minute for a 1 kilobase (kb) PCR product, and annealing temperatures were tested at the approximate Tm calculated as described above and about 5°C lower than the Tm information provided by the primer synthesisers. Reactions were subsequently altered appropriately and $MgCl_2$ concentrations altered if required. The PCRs designed for this project are described below.

2.8.1 NRAMPpol

The NRAMPFpol and NRAMPRpol primers were designed to span the 5' promoter region polymorphic microsatellite repeat region of the *NRAMP1* genomic DNA. A product was required which would generate fragments small enough for a 2bp size difference to be clearly resolved after digestion with restriction enzymes hence, the sequence of the product required suitable restriction enzyme sites to be present which gave products of unique size for all the known alleles. The following primers met these requirements and the sequence of the 194bp amplified product for allele 3 is given in **Figure 2.1** showing the *Rsa1* and *Mnl1* recognition sites used for restriction fragment length polymorphism (RFLP) analysis described in **2.11.2**.

NRAMPFpol **GGACATGAAGACTCGCATTAGG**
(59-70bp Genbank Accession number X82016)

NRAMPRpol **TTAGCTCTGATTTCAGATGCTTCC**
(240-217bp Genbank Accession number X82016)

Mnl I

ggacatgaagactcgcattag|gccaacgaggggtcttggaactccagatcaaagag

cctgtacttctgagcgtaat|ccggttgctccccagaaccttgaggtctagtttctc

Rsa1 *RsaI*

aataagaaagacctgactct**gtgtgtgtgt|acgtgtgtgtgt|acgtgtgtgtgt**

ttattctttctggactgaga**cacacacaca|tgcacacacaca|tgcacacacaca**

Mnl I

gtgtgt|gtggcagaggggggtgtggtcatggggtattgacatgaatacgcaagggg

cacac|acaccgtctccccccacaccagtaccccataactgtacttatgcgttcccc

caggaagcatctgaaatcagagctaa

gtccttcgtagactttagtctcgatt

Figure 2.1 Sequence of the promoter region of the human *NRAMP1* gene (Accession number X82016, 59-240bp) amplified by PCR to genotype the polymorphic microsatellite region shown in bold. The *Rsa1* and *Mnl1* restriction enzyme sites used to digest the amplified DNA are shown. The enzymes recognise the following sites and cut at the position shown by the vertical slash. n represents any base.

Mnl1 |(n)$_6$gagg
|(n)$_7$ctcc

Rsa1 gt|ac
ca|tg

The sequence for allele 3 is used in this figure. Sequences over the polymorphic region of the other alleles identified in this study and those previously published are shown in **Table 4.1**.

The PCR conditions for the NRAMPpol PCR were:

94°C 2½ minutes
(94°C 30 seconds
65°C 15 seconds
72°C 15 seconds) x 35
(94°C 30 seconds
65°C 30 seconds
72°C 10 minutes) x 1

2.8.2 GAPDH

The glyceraldehyde-3-phosphate dehydrogenase (GAPDH) primers were designed to amplify a product specific to the cDNA sequence of GAPDH for use as a control housekeeping gene against which the relative level of expression of the *NRAMP1* and neomycin resistance (*neo*) genes could be determined by a semi-quantitative analysis method. The primers were designed to have a Tm compatible with the NRAMPalu primers (**2.8.3**), so both PCRs could be carried out in a single tube if desired. They were designed to generate a product of approximately the same size as the NRAMPalu product, ensuring the time for amplification of the two products would be comparable and they would run to about the same point when electrophoresed in agarose gel, yet be distinguishable, to enable analysis of the intensity of the bands (**2.11.1**) to be carried out over a similar region of the gel with a homogeneous background. Primer GAPDHF spans sequence in exons 3 and 4 and primer GAPDHR spans sequence in exons 6 and 7 (Ercolani *et al.* 1988). The primers generate a product of 339bp.

GAPDHF **GACCTCAACTACATGGTTTAC**
(190-210bp human GAPDH gene exon sequence Ercolani *et al.* 1988)

GAPDHR **AGGAGGCATTGCTGATGATC**
(529-510bp human GAPDH gene exon sequence Ercolani *et al.* 1988)

The extension time for the reaction varied depending on whether a semi-quantitative analysis was being carried out for the U937 and Mono Mac 6 (MM6) transfectancts (**2.20.1**) comparing NRAMPalu (**2.8.3**), NRpCI (**2.8.4**), neoF1 (**2.8.5**) and neoFexp PCR (**2.8.6**) product yields, in which case 1 minute was necessary due to the larger products of the latter reactions. When the expression in PBC and control liver and the initial analysis of the cell line expression profiles was being determined a 30 second extension time was sufficient. The cycle number for the reaction also varied between 26 and 41 for comparison of the liver expression levels and when the exponential phase of the reaction was being determined. For these variable cycle PCRs the tubes were removed from the Hybaid Omni Gene thermal heating block (Hybaid, Teddington UK) at intervals of a constant number of cycles. For semi-quantitative gene expression analysis of large sample numbers of transfected cells and clones (**2.20.1**) 35 cycles were carried out which lay within the exponential phase of the reaction. The PCR conditions for GAPDH primers were:

94°C 2½ minutes
(94°C 30 seconds or 1 minute
60°C 30 seconds or 1 minute
72°C 15 seconds) x as described above

For semi-quantitative analysis no final extension cycle was performed. However, for reactions to determine if a cDNA had been successfully prepared a final extension cycle was added at the end of the reaction as follows:

(94°C 30 seconds
60°C 30 seconds
72°C 10 minutes) x 1

2.8.3 NRAMPalu

The NRAMPalu primers were designed to be cDNA specific and compatible with the GAPDH primers (**2.8.2**). They were designed to detect both splice variants of the gene reported, one of which includes the *Alu* sequence after the end of exon 4 in the

message encoding the whole protein (Cellier *et al.* 1994), discussed in **1.8.8**. The product including the *Alu* repeat sequence is denoted +alu throughout the text and the product encoding the whole protein -alu and they have the sizes 323bp and 249bp, respectively. NRAMPFalu spans sequence in exons 3 and 4 and NRAMPRalu spans sequence in exons 5 and 6 (Cellier *et al.* 1994).

NRAMPFalu **GCGGGATTCAAACTTCTCTG**
(437-456bp Genbank Accession number D50402)

NRAMPRalu **GAGTGGGATTCGTCCAGCT**
(685-667bp Genbank Accession number D50402)

The reaction conditions and variations for the NRAMPalu PCR are as follows and described for the GAPDH PCR (**2.8.2**), except the variable cycle PCRs were carried out between 32 and 47 cycles for comparison of two liver cDNAs during any one analysis or 41 cycles, which lay within the exponential phase of the reaction, when multiple samples were being analysed semi-quantitatively.

94°C 2½ minutes
(94°C 30 seconds or 1 minute
60°C 30 seconds or 1 minute
72°C 15 seconds) x as described above

These primers were also used to confirm the pCIneo/NRAMP1 plasmid (**5.2.4**) sequence was present in genomic DNA extracted from cells transfected with the plasmid (**2.20.1**) as the cloned *NRAMP1* sequence corresponds to the cDNA sequence. The reaction conditions for this PCR were:

94°C 2½ minutes
(94°C 30 seconds
60°C 1 minute
72°C 1 minute) x 35
(94°C 30 seconds
60°C 2 minutes
72°C 10 minutes) x 1

2.8.4 NRpCI

The NRpCI PCR was designed to discriminate between NRAMP1 sequence expressed from the pCIneo/NRAMP1 plasmid sequence (described in **5.2.4**) and the endogenous gene in cells transfected with the pCIneo/NRAMP1 plasmid (**2.20.1**). The PCR used the NRAMPRalu primer described previously (**2.8.3**) and a forward primer specific for plasmid sequence 5' to the start of the cloned NRAMP1 sequence, which was expressed at the RNA level but was 5' to the translation initiation site. This primer was named pCIneoF and the PCR, and predicted product of 706bp generated by these primers, called NRpCI.

pCIneoF **AGAATTCACGCGTGGTACCT**
(1095-1114bp Promega pCIneo plasmid (pCI-neo Mammalian Expression Vector) sequence data (Promega, Southampton UK))

As described for the GAPDH primers (**2.8.2**) variable cycles were carried out to determine where the exponential phase of the reaction lay and semi-quantitative gene expression analysis was carried out on products generated after 41 cycles, which lay within this phase. The reaction conditions for the NRpCI PCR were:

94°C 2½ minutes
(94°C 30 seconds
60°C 1 minute
72°C 1 minute) x 41

These primers were also used as double confirmation of the presence of the NRAMP1 plasmid sequence in genomic DNA from pCIneo/NRAMP1 plasmid transfected cells, in conjunction with the NRAMPalu primers as described in **2.8.3**, using the same PCR conditions:

94°C 2½ minutes
(94°C 30 seconds
60°C 1 minute
72°C 1 minute) x 35
(94°C 30 seconds
60°C 2 minutes
72°C 10 minutes) x 1

2.8.5 neoF1

Primers specific for the pCIneo plasmid were designed to confirm the pCIneo plasmid sequence was present in genomic DNA from control cells transfected with the pCIneo plasmid and in cells transfected with the pCIneo/NRAMP1 plasmid (**2.20.1**). The primers spanned part of the *neo* gene, generated a product of 729bp and were called neoF1 and neoR. The neoF1 primer sequence was 5' of the transcription initiation site and the neoR primer sequence was within the *neo* coding sequence. These primers were used to analyse genomic DNA and to confirm cDNA prepared from transfected cells did not contain carry-through plasmid DNA (despite DNase treatment (**2.7.3**)) which would be detected if the cDNAs were positive for the neoF1 PCR.

neoF1 **AGCAACCAGGTGTGGAAAGT**
(2162-2181bp Promega pCIneo plasmid sequence data (Promega, Southampton UK))

neoR **TGTTTCGCTTGGTGGTCGAA**
(2880-2861bp Promega pCIneo plasmid sequence data (Promega, Southampton UK))

The reaction conditions for analysing the genomic DNA are as for the NRAMPalu primers used for this purpose (**2.8.3**) and as follows:

94°C 2½ minutes
(94°C 30 seconds
60°C 1 minute
72°C 1 minute) x 35
(94°C 30 seconds
60°C 2 minutes
72°C 10 minutes) x 1

The reaction conditions for analysing the cDNA samples are as for the NRAMPalu primers used for this purpose (**2.8.3**) and as follows:

94°C 2½ minutes
(94°C 30 seconds
60°C 1 minute
72°C 1 minute) x 41

2.8.6 neoFexp

The neoFexp PCR was designed to detect expression of the *neo* gene in G418 sulphate ((Geneticin) referred to throughout this thesis as G418), resistant transfected cells. It used the neoR primer described in **2.8.5** and a forward primer called neoFexp specific for transcribed sequence in the *neo* gene 5' to the neoR primer sequence. The primers generated a 361bp product and were also used as confirmation for plasmid presence in control pCIneo plasmid and pCIneo/NRAMP1 plasmid transfected cells (**2.20.1**).

neoFexp **TATTCGGCTATGACTGGGCA**
(2520-2539bp Promega pCIneo plasmid sequence data (Promega, Southampton UK)

The PCR conditions were as described above for neoF1 (**2.8.5**). To analyse cDNA they were:

94°C 2½ minutes
(94°C 30 seconds
60°C 1 minute
72°C 1 minute) x 41

To analyse genomic DNA they were:

94°C 2½ minutes
(94°C 30 seconds
60°C 1 minute
72°C 1 minute) x 35
(94°C 30 seconds
60°C 2 minutes
72°C 10 minutes) x 1

2.8.7 Fas Ligand

Fas ligand primers were available which had been designed by Dr Graham Cotton, but the reaction conditions had not been determined. The primers were called FasL1 and FasL2 and lay within exons 1 and 4 of the Fas ligand gene, respectively (Takahashi *et al.* 1994). They generated a 319bp product.

FasL1 **TACAGAAGGAGCTGGCAGAA**
(405-424bp Genbank Accession number U624627)

FasL2 **ATGTAGACCTTGTGGCTCAG**
(723-704bp Genbank Accession number U624627)

The reaction conditions used for the Fas ligand PCR were:

94°C 2½ minutes
(94°C 30 seconds
55°C 30 seconds
72°C 30 seconds) x 39
(94°C 30 seconds
55°C 1 minute
72°C 10 minutes) x 1

2.9 POLYMERASE CHAIN REACTION

All necessary precautions were taken to avoid contamination of reactions and stock reagents with PCR products or other sources of DNA. Gloves were worn at all times and water and 0.75ml and 1.5ml tubes were autoclaved prior to use. A set of Gilson pipettes used with filter pipette tips (Anachem, Luton UK) were kept exclusively for RNA and PCR work, prior to addition of template DNA to aliquots of PCR mastermixes. The mastermixes were prepared in a Gelair Flow BSB4A hood (ICN, Buckinghamshire UK) and template DNA added in a Pathfinder hood (Pathfinder, Hampshire UK) in an area spatially isolated from the area where PCR products were handled.

All reactions were carried out in a final volume of 50µl in 0.75ml thin walled tubes (Advanced Biotechnologies, Epsom UK). The following standard reaction conditions were found appropriate: 1x PCR buffer minus $MgCl_2$, 1.5mM $MgCl_2$, 2.5U *Taq* DNA polymerase enzyme (all from Life Technologies, Paisley UK), 0.2mM of each deoxynucleotide triphosphate (dNTP) (dATP, dCTP, dGTP, dTTP) (DNA Polymerisation Mix from Advanced Biotechnologies, Epsom UK), 0.5µM of each primer (**2.8**), autoclaved distilled water as appropriate and 1µl cDNA (**2.7.4**) or 10µl genomic DNA (**2.6**). All reactions were overlayed with two drops of paraffin oil (Fisher Scientific, Loughborough UK) prior to placing on a Hybaid Omni Gene thermal heating block (Hybaid, Teddington UK).

2.10 RESTRICTION ENZYME DIGESTION

All restriction enzyme digestions were carried out according to the manufacturers' instructions with the volume of enzyme never exceeding 1/10th of the final reaction volume. A typical reaction for digestion of PCR products would have a 30µl total volume digesting 10-15µl PCR product (**2.9**) with 2.5U *MnlI* or 5U *RsaI*, 1x reaction buffer and 1x BSA, where required, overnight at 37°C. Digestions of mini or maxi prep DNA typically used 10U of enzyme to digest between 2µl and 7µl of DNA (**2.6.4** and **2.6.5**) in a 10-20µl reaction volume for between 2 and 16 hours, at the appropriate temperature. All enzymes were purchased from Boehringer Mannheim, Lowes UK; Promega, Southampton UK; Life Technologies, Paisley UK; or New England Biolabs, Hitchen UK.

2.11 ELECTROPHORESIS AND DETECTION OF DNA

2.11.1 Horizontal Gel Electrophoresis

Agarose gel electrophoresis was carried out to confirm the size of PCR (**2.9**) or restriction enzyme digestion products (**2.10**), to characterise plasmid DNA (**2.6.4**) or purify restriction fragments (**2.6.5**). Standard agarose gels of between 0.8% and 2% were prepared in 1x Tris-borate EDTA (TBE) buffer (**Appendix B**) by melting the agarose for a couple of minutes in a 1000W microwave (Sambrook *et al.* 1989). The gels were allowed to cool until hand hot when 1µl ethidium bromide (EtBr) (10mg/ml) per 100ml gel was added and mixed well. The gels were cast on a level surface in the casting trays with appropriate combs, allowed to set and either used within a few hours or stored overnight at 4°C wrapped in cling film (Merck, Lutterworth, UK). Gels were submerged in 1x TBE buffer and DNA samples, in 1/3 volume agarose loading dye (**Appendix B**) (typically 15µl final volume), were loaded in the wells. 1µg of 1kb DNA ladder (Life Technologies, Paisley UK), prepared for loading as for DNA samples, was run alongside the DNA and used to estimate the size of the DNA molecules being analysed. The DNA was electrophoresed towards the positive terminus using a current of 30-60mA in an Anachem Origo horizontal electrophoresis tank (Anachem, Luton UK). After the

DNA had been resolved the gels were visualised using a Herolab UVT-28 MP transilluminator and photographs taken as a record or images stored on disk using the Herolab Enhanced Analysis System (EASY) (Scotlab, Coatbridge UK).

2.11.2 Polyacrylamide Gel Electrophoresis and Silver Staining

Standard safety precautions were taken when handling unpolymerised acrylamide and bind silane with procedures being carried out in a safety fume hood (Morgan and Grundy Ltd., Uxbridge, UK). 6% denaturing polyacrylamide gels (**Appendix B**) were prepared using sequencing plates and a 32 square well tooth comb. Both plates were thoroughly cleaned with dH_2O and 70% ethanol (Genta Medical, York UK). The large glass plate was treated with FMC Gel Slick (Flowgen, Lichfield UK) and the small glass plate with 20µl bind silane (γ-methacryloxypropyltrimethoxysilane) in 5ml Ultrapure UV treated dH_2O from a Milli-U10 and Milli-Q_{plus} 185 system (Millipore, Watford UK) (Milli-Q dH_2O) pHed to 3.5, so the gel would remain adhered to the small plate during the silver staining procedure. Excess bind silane was rinsed off by washing twice with 70% ethanol and excess Gel Slick removed with dH_2O. Set gels were stored overnight at room temperature, well wrapped in damp paper towels and cling film (Merck, Lutterworth UK). The gel was warmed by pre-running for an hour at 60 Watts in 0.5x TBE buffer (**Appendix B**). 6µl of digested NRAMPpol PCR product (**2.10**) and 3µl of 3x acrylamide gel loading solution (**Appendix B**) were heat denatured, placed on ice then loaded into the pre-warmed gel and electrophoresed at 60 Watts. *Hinf1* (Life Technologies, Paisley UK) and Marker VIII (Boehringer Mannheim, Lewes UK) molecular weight markers were run in parallel as reference to estimate the size of digested fragments. The resolved fragments were visualised by silver staining the gel adhered to the small glass plate after separating the large plate from the gel.

Milli-Q dH_2O was used throughout the staining procedure. The gel, adhered to the plate, was incubated for 10 minutes in 10% ethanol (Hayman Ltd., Witham UK), for 10 minutes in 1% nitric acid (Fisher Scientific, Loughborough UK), for 5 minutes in Milli-Q dH_2O, for 20 minutes in silver nitrate (2.04g/litre), rinsed briefly in Milli-Q

dH_2O, rinsed briefly in 600ml developer (160g sodium carbonate decahydrate, 1ml formaldehyde in 2 litres), the remaining developer was added and left for about 15 minutes until bands were visible then stopped in 0.1M citric acid and washed in Milli-Q dH_2O. The silver stained gels were photographed on a light box, then the adhered gel scraped off and the plates washed thoroughly.

2.12 ESTIMATION OF DNA CONCENTRATION AND PURITY

The concentration of DNA samples were estimated by 1) spectrophotometry or 2) an ethidium bromide fluorescent quantitation method (Sambrook *et al.* 1989).

1) The OD of 1/100 dilutions of DNA solutions was measured at λ=260nm using a Genequant II RNA/DNA Calculator (Pharmacia Biotech, Cambridge UK): 50μg/ml of double stranded DNA having an A_{260} of 1 and the A_{260} to A_{280} ratio giving a measure of the DNA purity.

2) Equal volumes of a range of serially diluted 1kb DNA ladder (Life Technologies, Paisley UK) and the sample being analysed were spotted on 1% agarose gel containing 5μg/ml EtBr cast in Petri dishes. After allowing the samples to absorb into the agarose the plate was exposed on a Herolab UVT-28 MP transilluminator (Scotlab, Coatbridge UK) and the DNA concentration of the sample estimated by comparison with the fluorescent intensity of the standards.

2.13 DEPHOSPHORYLATION OF THE ENDS OF LINEAR DNA MOLECULES

When a ligation reaction (**2.14**) is set up in the presence of a vector which has compatible or blunt ends background non-recombinant reactions can occur. This occurrence can be considerably reduced by 5' dephosphorylation of the vector fragment, increasing the likelihood of desired recombinant molecules being present in the colonies screened after transformation into *E. coli*. Gel-purified DNA (**2.6.5**) was dephosphorylated using 1 unit of shrimp alkaline phosphatase (SAP) (Amersham Pharmacia Biotech, Little Chalfont UK) in a reaction containing 1x the

appropriate buffer in a typical final volume of 30-35µl. The reaction was incubated at 37°C for one hour and the SAP inactivated by heating at 65°C for 15 minutes.

2.14 T/A CLONING OF PCR PRODUCTS AND DNA LIGATION REACTIONS

Gel-purified PCR products (**2.6.5**) were cloned by ligation into the pCR2.1 vector using the TA Cloning System Version 2.0 Kit (Invitrogen BV, Leek The Netherlands) according to instructions. The linearised pCR2.1 vector has a single 3' deoxythymidine residue which allows efficient ligation of PCR inserts, due to the non-template-dependent addition of a single deoxyadenosine to the 3' end of PCR products by *Taq* polymerase. Ligation reactions were carried out according to the manufacturer's instructions overnight at 15°C and typically contained 4µl gel-purified PCR product (**2.6.5**), 1-4 units T_4 DNA ligase (Promega, Southampton UK), 1x ligation buffer (**Appendix B**), 2µl pCR2.1 (25ng/µl) in a total volume of 10µl. Control reactions omitting the vector were also carried out. Competent cells were transformed with the ligation products as described in **2.17**.

2.15 DNA SEQUENCING

2.15.1 Direct Sequencing of PCR Products

The Sequenase PCR Product Sequencing Kit (Amersham Pharmacia Biotech, Little Chalfont UK) was used according to the recommended protocol. Reagents were supplied with the kit, unless indicated otherwise, and their composition is given in **Appendix B**.

10µl of PCR product (**2.9**), 2µl of Exonuclease I and 2µl of SAP were mixed and incubated at 37°C for 15 minutes to remove residual single stranded PCR primers, any extraneous single-stranded DNA and any remaining dNTPs. The Exonuclease I and SAP were inactivated by heating at 80°C for 15 minutes. 0.5 picomoles (pmol) of treated PCR product DNA (estimated using EtBr plate comparison of standards as described in **2.12**) and 5pmol of PCR primer (**2.8.1**), in a total volume of 10µl, were

denatured for 2-3 minutes at 100°C, cooled on ice for 5 minutes, microcentrifuged briefly then placed back on ice. For some reactions 1µl of DMSO was added with the primers. 2µl of Sequenase Reaction Buffer, 1µl of 0.1M DTT, 2µl of Labelling Mix (diluted 1:4 in dH_2O), 0.5µl of α^{35}SdATP (5µCi) (ICN Biomedicals Inc., Basingstoke UK) and 2µl of Sequenase DNA Polymerase were added to the ice-cold annealed DNA mixture, mixed and incubated at room temperature for 5 minutes. For some reactions 1µl of Mn buffer was added at this point. 3.5µl of the above labelling reaction was added to 2.5µl of the four Termination Mixes (ddG, ddA, ddT and ddC) which had been aliquoted in four separate tubes and pre-warmed to 37°C for 1 minute. The reactions were mixed and incubation at 37°C continued for 5-6 minutes then stopped by the addition of 1µl Stop Solution.

The reactions were heat denatured, loaded into wells created by a shark's tooth comb at the top of a pre-warmed 6% glycerol tolerant polyacrylamide gel (**Appendix B**) or 6% formamide glycerol tolerant polyacrylamide gel (**Appendix B**) and electrophoresed at 75 Watts in 1x glycerol tolerant gel buffer (**Appendix B**) for 1¼-2 hours according to standard protocols using an S2 sequencing apparatus (Life Technologies, Paisley UK). Prior to pouring the gel the small glass sequencing plate was treated with FMC Gel Slick (Flowgen, Lichfield UK) and this plate was removed after the gel had been run. The gel was fixed twice for 5 minutes in 5-10% acetic acid (Fisher Scientific, Loughborough UK)/15-20% methanol (Merck, Lutterworth UK), transferred to 3MM paper, covered in cling film (Merck, Lutterworth UK) and dried *in vacuo* for 2 hours at 80°C, using a model 583 gel dryer and vacuum pump (Bio-Rad, Hemel Hempstead UK). The cling film was removed and the gel exposed to Kodak Biomax MR film in an autoradiography cassette at -70°C for 18-48 hours. The film was processed in a Hyperprocessor (Amersham Pharmacia Biotech, Little Chalfont UK).

2.15.2 Sequencing Cloned PCR Products

The T7 Sequenase Version 2.0 DNA Sequencing Kit (Amersham Pharmacia Biotech, Little Chalfont UK) was used with an amended protocol as described below.

Reagents were supplied with the kit, unless indicated otherwise, and their composition is given in **Appendix B**.

9µl of isolated TA cloned template DNA (**2.14**) and 1µl of -40 M13 primer were heated at 100°C for 4 minutes and snap frozen on dry ice. 2µl of 0.1M DTTl, 2µl T7 Sequenase Reaction Buffer, 0.7µl Labelling Mix (diluted 1:4), 1.5µl of α^{35}SdATP (5µCi) (ICN Biomedicals Inc., Basingstoke UK) and 2.5µl of T7 Sequenase (diluted 1:4 in dH_2O) was added to the thawed template/primer mixture, mixed and incubated at 15-20°C for 4 minutes. After a further 30 seconds 4µl of above mixture was added to 2µl of ddA Termination Mix and at subsequent 30 second intervals an additional 4µl of the above mixture was added to 2µl of ddC, ddG and ddT Termination Mixes. After a further 30 seconds and at subsequent 30 second intervals 4µl of Stop Solution was added sequentially to the ddA, ddC, ddG and ddT reactions.

The reactions were heat denatured, loaded into wells created by a shark's tooth comb at the top of a 6% denaturing polyacrylamide gel (**Appendix B**), and electrophoresed in 1x TBE buffer according to standard protocols at 65 Watts using an S2 sequencing apparatus (Life Technologies, Paisley UK). Prior to pouring the gel the small glass sequencing plate was treated with FMC Gel Slick (Flowgen, Lichfield UK) and this plate was removed after the gel had been run. The gel was fixed in 20% acetic acid (Fisher Scientific, Loughborough UK)/5% methanol (Merck, Lutterworth UK) for 20 minutes, transferred to 3MM paper, covered in cling film (Merck, Lutterworth UK) and dried *in vacuo* for 2 hours at 80°C, using a model 583 gel dryer and vacuum pump (Bio-Rad, Hemel Hempstead UK). The cling film was removed and the gel exposed to Kodak Biomax MR film in an autoradiography cassette for 18-48 hours at -70°C. The film was processed in a Hyperprocessor (Amersham Pharmacia Biotech, Little Chalfont UK).

2.16 BACTERIAL CULTURES AND STORAGE

2.16.1 Mini and Maxi Cultures

Bacteria were cultured to grow single clones, to make cells competent for transformation (**2.17**) or for plasmid DNA isolation (**2.6.4**) from transfected cells. All bacteria were grown in Luria-Bertani broth (L-broth) (**Appendix B**) culture medium. 100μg/ml ampicillin was added for cultures of bacteria transfected with a plasmid containing an ampicillin resistance gene (Amp^R). Single colonies were picked from an L-Broth/agar plate (**2.16.2**) with a sterile pipette tip and dropped into Falcon 2059 tubes (Becton Dickinson UK Ltd., Oxford UK) containing 5ml L-broth (mini cultures) or 1 litre conical flasks containing 100ml L-broth (maxi cultures). Bacteria were cultured overnight for no longer than 16 hours at 37°C in a Sanyo orbital incubator (Fisher Scientific, Loughborough UK) at 220rpm.

2.16.2 L-Broth/Agar Plates

20g agar was added to 1 litre L-broth prior to autoclaving (**Appendix B**). When the medium had cooled to about 40°C antibiotics or chromogens were added when required for selection of transfected bacteria, mixed well and about 25ml poured into sterile 100mm Petri dishes. Bacteria were plated by spreading evenly over the plate with a sterile spreader.

2.16.3 Storage

Mini cultures (**2.16.1**) and L-broth/agar culture plates (**2.16.2**) were kept at 4°C for short term storage. For long term storage bacteria were stored at -80°C in 25% glycerol (Fisher Scientific, Loughborough UK).

2.17 TRANSFORMATION OF BACTERIA

Either 1) XL2 Blue *E. Coli* (Stratagene, Amsterdam The Netherlands) were transformed with plasmid DNA using the calcium chloride heat shock treatment as described by Cohen *et al.* (Cohen *et al.* 1972) or 2) XL1 Blue competent cells (Stratagene, Amsterdam The Netherlands) were transformed following heat shock.

1) 1-2mls of an overnight mini culture (**2.16.1**) was inoculated into 100ml L-broth (**Appendix B**) and cultured at 37°C in an orbital incubator (Fisher Scientific, Loughborough UK) at 220rpm until in the log phase of growth when an OD_{550} of 0.4-0.6 was reached. The culture was transferred to universal tubes (Rosslabs, Cheshire UK), placed on ice for 5 minutes then centrifuged at 3,000rpm for 10 minutes. The cell pellet was resuspended in ice-cold 0.1M $MgCl_2$ and centrifuged as above. The supernatant was discarded and the cell pellet resuspended in 0.5ml ice-cold 0.1M $CaCl_2$ then left on ice for 2 hours to become competent. 100µl of competent cells and 5µl of PCR product cloned into pCR2.1 (**2.14**), 1-10ng plasmid DNA or no DNA were mixed and left on ice for 30 minutes, heat shocked at 42°C for 2 minutes then placed on ice for 15 minutes, before plating out onto L-amp plates (**Appendix B, 2.16.2**). Colonies containing plasmid DNA with an intact Amp^R gene were selected. To select for clones lacking an intact β-D-galactosidase (*lacZ*) gene 80µg/ml 5-bromo-4-chloro-3-indolyl galactopyranoside (X-gal) (Promega, Southampton UK) was included in the L-amp plates. White or light blue colonies indicated the presence of recombinant plasmids containing cloned PCR product or disruption of the *lacZ* α-peptide reading frame by some other mechanism.

2) Commercially available competent XL1 Blue cells (Stratagene, Amsterdam The Netherlands) were defrosted on ice and mixed with 1-10ng of plasmid DNA. The reaction was incubated on ice for 20 minutes then the cells were heat shocked at 42°C for 40 seconds and placed on ice for 2 minutes. 200µl room temperature SOC medium (**Appendix B**) was added and the cells incubated at 37°C for 1 hour in a Sanyo orbital incubator (Fisher Scientific, Loughborough UK) at 220rpm. The cells were plated onto L-amp plates (**Appendix B**) and incubated at 37°C for approximately 15 hours to select for ampicillin resistant colonies containing an intact plasmid Amp^R gene.

2.18 CELL CULTURE

2.18.1 Standard Culture Conditions

Cell lines and isolated cells were cultured in supplemented RPMI-1640 medium (**Appendix B**), unless stated otherwise, in 25cm^2 (small), 80cm^2 (medium) or 175cm^2 (large) tissue culture grade flasks or 6, 24 or 96 well tissue culture plates at 37°C, 5% CO_2 in a Gallenkamp CO_2 incubator (Fisher Scientific, Loughborough UK). Cells were maintained at a density between 10^5 and 10^6 cells/ml and supplemented with fresh medium every 3-4 days, or as required by monitoring the bicarbonate colour indicator in the medium, yellowing indicating supplementation was necessary. Transfected cells were cultured in medium as described in **20.2.3**.

2.18.2 Cell Viability Counts: Trypan Blue Exclusion

To estimate the concentration of viable cells or total cell numbers in cultures 10µl of a well mixed sample of cultured cells and 10µl of 0.4% trypan blue solution were mixed and left at room temperature for a couple of minutes. The cell suspension was transferred to a Neubauer haemocytometer, viewed using an Olympus inverted phase-contrast light microscope and the number of blue (dead) and colourless (live) cells counted within the 4 x 4 square grid. These cell counts were used to estimate the concentration according to the following calculation:

cell count x 2 (dilution factor) x $1x10^4$ (haemocytometer chamber factor) = cells/ml

2.18.3 Isolation of Adherent Peripheral Blood Mononuclear Cells

Adherent peripheral blood mononuclear cells (aPBMC) were isolated from single donor Buffy Coats obtained from the National Scottish Blood Transfusion Service. All donor blood samples were checked for exclusion of HIV, hepatitis B, hepatitis C and syphilis infection by the Transfusion Service prior to collection.

The Buffy Coat was diluted 1:1 with sterile PBS and 25ml of the dilution was carefully layered onto 15ml Lymphoprep (Nycomed Pharma AS, Oslo Norway) in a sterile 50ml centrifuge tube (Becton Dickinson UK Ltd., Oxford UK) and

centrifuged at 2000rpm for 30 minutes with the centrifuge brake switched off. The interface layer of cells was transferred to clean centrifuge tubes, made up to 50ml with PBS and centrifuged at 1700rpm for 15 minutes to wash the cells. The supernatant was removed from the tubes and the cell pellets pooled and resuspended in Iscoves medium supplemented with 100U/ml penicillin, 100µg/ml streptomycin and 2mM L-glutamine (all Life Technologies, Paisley UK) up to a volume of 50ml. Prior to centrifuging the cells at 1200rpm for 10-15 minutes a sample was removed and the cells counted using a Neubauer haemocytometer as described previously but omitting the trypan blue dilution (**2.18.2**). The total number of cells was calculated and the cell pellet resuspended in Iscoves, supplemented as previously, to give approximately 5 x 10^6 cells/ml. The cells were plated out in tissue culture plates as required using 1ml per well of a 24 well plate and 2ml per well of a 6 well plate. The plated cells were incubated at 37°C, 5% CO_2 for 1¼-1½ hours after which time the non adherent cells were aspirated off. The medium was replaced with Iscoves medium supplemented with 100U/ml penicillin, 100µg/ml streptomycin, 2mM L-glutamine and 5% heat treated NHS (**Appendix B**). The cells were cultured overnight at 37°C, 5% CO_2 and the medium aspirated off and replaced with PBS while the removed medium was centrifuged at 1000rpm for 10 minutes. The PBS was removed and replaced with the conditioned medium, without the pelleted non adherent cells, and the cells cultured as previously for 3-7 days until required.

2.18.4 Isolation of Peripheral Blood Mononuclear Cells and Stimulation with Concanavalin A

50ml of blood was collected by venous puncture from a healthy volunteer and added to 500µl of heparin, mixed well, placed on ice and diluted with an equal volume of ice cold sterile PBS. 10ml aliquots of the dilution were carefully overlayed onto 10ml of Lymphoprep (Nycomed Pharma AS, Oslo Norway) in universal tubes (Rosslabs, Cheshire UK) and centrifuged at 18000rpm for 15 minutes at 8°C. The interface cells were transferred to clean universal tubes, washed with excess PBS and centrifuged at 1000rpm for 10 minutes at 8°C. The cell pellets were resuspended and pooled in 3-4ml of PBS. A 1/20 dilution of the cell suspension was made in crystal

violet (**Appendix B**) and the cells with deep violet-black stained nuclei in the 4 x 4 grid of a Neubauer haemocytometer counted, from which an estimate of the cell concentration was calculated as follows:

cell count x 20 (dilution factor) x $1x10^4$ (haemocytometer chamber factor) = cells/ml

The cells were cultured at a density of $1x10^6$ cells/ml in standard supplemented RPMI 1640 culture medium, as described in **2.18.1**, or the same medium containing 1μg/ml concanavalin A. After 72 hours the cells were pelleted by centrifugation at 1000rpm for 10 minutes and the cell viability estimated (**2.18.2**). 5 x 10^6 cell aliquots were taken for protein extraction (**2.4.1**) and 2 x 10^6 cell aliquots were taken for RNA extraction (**2.7.1**).

2.19 TRANSFECTION OF aPBMCs

A number of methods, described below, were used in an attempt to transfect aPBMCs with a β-gal plasmid (pSV-β-galactosidase Control Vector: Promega, Southampton UK) containing the *lacZ* gene encoding β-D-galactosidase. Having determined a successful procedure it was intended to use this to transfect aPBMCs with the pCIneo/NRAMP1 plasmid described in **5.2.4**. The aPBMCs were isolated and plated out (**2.18.3**) approximately 4 days before transfection.

2.19.1 Lipofectin Reagent

Lipofectin Reagent (Life Technologies, Paisley UK) is a 1:1 (w/w) liposome formulation of the cationic lipid N-[1-(2-3-dioleyloxy)propyl]-n,n,n-trimethylammonium chloride (DOTMA) and the neutral lipid dioleoyl phosphotidylethanolamine (DOPE) in membrane filtered water which interacts spontaneously with DNA to form a lipid-DNA complex. The complex fuses with tissue culture cells resulting in uptake and expression of the DNA.

Unless otherwise stated the medium used during transfection and for all dilutions was Iscoves medium (Life Technologies, Paisley UK) containing 2mM L-glutamine (no antibiotics or serum). A range of DNA:Lipofectin Reagent ratios were tested for

transfection of aPBMCs plated in 6 well plates (**2.18.3**). DNA was diluted to give concentrations of 0.5μg/100μl, 0.75μg/100μl, 1.0μg/100μl and 1.5μg/100μl. Lipofectin Reagent was diluted appropriately to give final concentrations of 4μg/ml, 5μg/ml, 6μg/ml, 7μg/ml, 9μg/ml and 11μg/ml when added to the cells after subsequent dilution. The DNA and Lipofectin Reagent dilutions were incubated at room temperature for 45 minutes then 100μl DNA and 100μl Lipofectin Reagent of each dilution mixed gently to give 24 DNA/Lipofectin Reagent combinations. The DNA/Lipofectin Reagent mixtures were incubated at room temperature for about 15 minutes and then 200μl of each mixture added to 800μl Iscoves medium, mixing gently by pipetting. The plated cells were washed with Iscoves medium and the diluted DNA/Lipofectin mixtures added to the washed cells which were incubated at 37°C, 5% CO_2 for 6 hours. The DNA/Lipofectin mixtures were removed, being retained for further analysis on some occasions, and replaced with 2ml Iscoves medium supplemented with 100U/ml penicillin, 100μg/ml streptomycin, 2mM L-glutamine and 5% heat treated NHS (**Appendix B**) and incubated at 37°C, 5% CO_2 for 64 hours before assaying for β-gal expression (**2.20.2.1**).

2.19.2 Lipofectamine Reagent

Lipofectamine Reagent (Life Technologies, Paisley UK) is a 3:1 (w/w) liposome formulation of the polycationic lipid 2,3-dioleyloxy-N-[2(sperminecarboxamido)ethyl]-N,N-dimethyl-1-propanaminium trifluoroacetate (DOSPA) and DOPE in membrane filtered water.

Unless otherwise stated the medium used during transfection and for all dilutions was Iscoves medium (Life Technologies, Paisley UK) containing 2mM L-glutamine (no antibiotics or serum). A range of DNA:Lipofectamine Reagent ratios were tested for transfection of aPBMCs plated in 24 well plates (**2.18.3**). DNA was diluted to give concentrations of 1.0μg/100μl and 1.5μg/100μl. Lipofectamine Reagent was diluted appropriately to give final concentrations of 8μg/300μl, 10μg/300μl, 12μg/300μl, 14μg/300μl, 18μg/300μl and 22μg/300μl when added to the cells after subsequent dilution. 100μl DNA and 100μl Lipofectamine Reagent of each dilution

was mixed gently to give 12 DNA/Lipofectamine Reagent combinations and incubated at room temperature for 45 minutes to allow DNA-liposome complexes to form. 100µl of Iscoves medium was added and mixed gently and the diluted complex solution added to the plated cells, which had been washed with Iscoves medium. The plates were incubated at 37°C, 5% CO_2 for 6 hours at which point the transfection medium was removed, retained for analysis, and replaced with 1ml Iscoves medium supplemented with 100U/ml penicillin, 100µg/ml streptomycin, 2mM L-glutamine and 5% heat treated NHS (**Appendix B**) and the plates incubated at 37°C, 5% CO_2 for 48 hours before assaying for β-gal expression (**2.20.2.1**).

2.19.3 DOSPER Liposomal Transfection Reagent

DOSPER Liposomal Transfection Reagent (Boehringer Mannheim, Lowes UK) is a polycationic liposomal reagent consisting of a spermine head group and fatty acid tails, 1,3-di-oleoyloxy-2-(6-carboxy-spermyl)-propylamide. The positively charged spermine head group binds negatively charged DNA molecules forming polycationic complexes which are non-specifically adsorbed to the overall negatively charged surface of cells which take the DNA up.

aPBMCs plated in 24 well plates were used for transfection (**2.18.3**). DNA and DOSPER were diluted in HEPES-buffered saline (HBS) (20mM HEPES (Life Technologies, Paisley UK), 150mM NaCl pH7.4). All Iscoves medium used was supplemented with 100U/ml penicillin, 100µg/ml streptomycin, 2mM L-glutamine and 5% heat treated NHS (**Appendix B**). DNA was diluted appropriately to give 0.5µg, 1.0µg, 1.5µg or 3.0µg per transfection. DOSPER was diluted appropriately to give 3µg, 4.5µg, 6µg, 9µg, 12µg or 15µg per transfection. 50µl of each DNA dilution and 50µl of each DOSPER dilution were mixed gently to give 24 DNA/DOSPER combinations which were incubated at room temperature for 15 minutes. Shortly before transfection the culture medium in the wells was replaced with 0.5ml fresh supplemented Iscoves medium. 60µl of the DNA/DOSPER complexes were added dropwise to the appropriate wells, rocking the plate gently to mix. The plates were incubated at 37°C, 5% CO_2 for 6 hours at which point an

additional 0.5ml supplemented Iscoves medium was added to each well and the plates incubated, as before, for a further 26 hours. The medium was removed from the wells and retained for analysis replacing it with 0.5ml supplemented Iscoves medium. The plates were incubated as before and assayed for β-gal activity 48 hours after the start of transfection (**2.20.2.1**).

2.19.4 SuperFect Transfection Reagent

SuperFect Transfection Reagent (QIAGEN Ltd., Crawley UK) is a polycation of defined shape and diameter. It possesses a spherical architecture, with branches radiating from a central core, terminating at charged amino groups. SuperFect assembles DNA into compact structures with a net positive charge allowing them to bind to negatively charged receptors (e.g. sialylated glycoproteins) on the surface of eukaryotic cells. Inside the cell SuperFect Reagent buffers the lysosome after fusion with endosomes leading to pH inhibition of lysosomal nucleases ensuring stability of the complexes and transport of intact DNA to the nucleus.

aPBMCs plated in 24 well plates were used for transfection (**2.18.3**). DNA dilutions were prepared in Iscoves medium containing 2mM L-glutamine (both Life Technologies, Paisley UK) (no antibiotics or serum). DNA was diluted appropriately to give 0.5μg, 1.0μg, 1.5μg or 2.5μg per transfection. To 60μl of each DNA dilution 9μg, 15μg, 21μg, 27μg, 36μg or 45μg SuperFect Reagent was added to give 24 DNA/SuperFect combinations, mixing gently by pipetting. The mixtures were incubated for 10-20 minutes at room temperature to allow complex formation. The culture medium was removed from the wells of the aPBMCs, which were washed in pre-warmed PBS. 350μl of supplemented Iscoves medium containing 100U/ml penicillin, 100μg/ml streptomycin, 2mM L-glutamine and 5% heat treated NHS (**Appendix B**) was added to each DNA/SuperFect combination, mixed gently by pipetting and added to the washed wells. The plates were incubated at 37°C, 5% CO_2 for 2-3 hours at which point the medium was removed and replaced with 1ml supplemented Iscoves medium (containing the antibiotics and serum), after the wells

had been washed with pre-warmed PBS. The plates were incubated at 37°C, 5% CO_2 and assayed for β-gal activity 45 hours after the start of transfection (**2.20.2.1**).

2.19.5 Diethylaminoethyl (DEAE)-Dextran

aPBMCs plated in 24 well plates were used for transfection (**2.18.3**). The cells were cultured overnight prior to transfection in supplemented Iscoves medium (with 100U/ml penicillin, 100μg/ml streptomycin, 2mM L-glutamine (all Life Technologies, Paisley UK)) containing 20%, 5% or 2% heat treated NHS (**Appendix B**). The wells pre-incubated in 20% serum were either transfected in medium containing 5% heat treated NHS, 2% heat treated NHS or in serum free medium. The wells pre-incubated in 5% serum were transfected only in medium containing 5% heat treated NHS and the wells pre-incubated in 2% serum were transfected only in medium containing 2% heat treated NHS. DEAE-dextran (Amersham Pharmacia Biotech, Little Chalfont UK) was used at a final concentration of 250μg/ml in 50mM Tris pH7.4. DNA was used at concentrations of 2μg, 5μg, 8μg, 10μg, 15μg and 20μg per transfection. The wells were washed twice with pre-warmed Hanks' balanced salt solution (HBSS) (Life Technologies, Paisley UK) and 500μl of the appropriate combination of DEAE-dextran/Tris, DNA, serum and supplemented Iscoves medium was added to the wells. The plates were incubated at 37°C, 5% CO_2 for 4 hours at which point the transfection medium was removed from wells which were to receive DMSO osmotic shock or glycerol shock. To the wells for DMSO shock, 1ml HBSS with 10% DMSO was added for 2 minutes, removed and the wells washed twice with cold HBSS. The wells for glycerol shock were washed with PBS and 1.5ml 15% glycerol in HBS added and removed after 30 seconds. The wells were then washed twice with HBSS. The transfection medium was removed from the remaining wells, which were washed twice with cold HBSS, and all wells received 1ml supplemented Iscoves medium containing either 2% or 5% heat treated NHS. The plates were incubated as before for 50 hours then assayed for β-gal activity (**2.20.2.1**).

2.20 ELECTROPORATION OF CELL LINES AND REPORTER GENE ASSAYS

2.20.1 Electroporation of U937 and MM6 Cell Lines

5 x 10^6 MM6 or U937 cells were pelleted at 1000rpm and resuspended in 0.25ml RPMI-1640 with 20% FCS (both Life Technologies, Paisley UK) (no antibiotics or L-glutamine), transferred to a 0.4cm electrode Bio-Rad Gene Pulser Cuvette (Bio-Rad, Hemel Hempstead UK) and placed on ice for 10 minutes. 10μg of plasmid DNA was added, mixed gently and the cells were electroporated, using a Bio-Rad Gene Pulser with Capacitance Extender (250mV, 960μF) (Bio-Rad, Hemel Hempstead UK). Time constants varied between 48 and 55 milliseconds. The cells were placed on ice for 10 minutes after electroporation then made up to 12ml with supplemented RPMI-1640 medium (**Appendix B**) and plated in 6 well plates. The cells were cultured at 37°C, 5% CO_2 for about 24 hours, at which point 1ml medium was removed from each well and replaced with medium containing G418 (Life Technologies, Paisley UK) to give an appropriate final concentration to select stable transfectants on the basis of expression of the plasmid *neo* gene (**2.20.3**).

2.20.2 Detection of β-D-Galactosidase Expression

The β-D-galactosidase gene (*lacZ*) was used as a reporter gene to determine whether cells transfected with a β-gal plasmid (pSV-β-galactosidase Control Vector: Promega, Southampton UK) containing the *lacZ* gene successfully expressed the gene and protein. Expression can be assayed by the activity of the *lacZ* gene product, β-D-galactosidase (β-gal). Two protocols were followed to determine the efficiency of various transfection methods of aPBMCs and cell lines (**2.19-2.20.1**). The first (**2.20.2.1**) uses cleavage of X-gal by β-gal to liberate an intensely blue halogenated indoxyl derivative, which can be visually identified in transformed cells by examination under light microscopy. The second (**2.20.2.2**) involves liberation of a bright green fluorescent product, which can be detected by flow cytometry. The fluorogenic substrate in this DetectaGene Green *lacZ* Gene Expression Kit (Cambridge Bioscience, Cambridge UK) is 5-chloromethylfluorescein di-β-D-

galacto-pyranoside (CMFDG) which reacts with intracellular glutathione through a glutathione S-transferase-mediated reaction. In *lacZ* positive cells the CMFDG-glutathione adduct is converted to a bright green fluorescent product which, being a peptide, does not readily cross cellular membranes hence the fluorescent product is well retained in the cell.

2.20.2.1 X-gal Cleavage by β-gal

This method was used to detect expression of β-gal in transfected aPBMCs in 6 well or 24 well plates (**2.19**). The volumes stated here refer to 24 well plates and were increased appropriately for the 6 well plates. The plates were centrifuged briefly at 1000rpm after incubation for the appropriate period following transfection. The wells were washed with PBS and the cells fixed for 5 minutes in 0.05% glutaraldehyde (TAAB Laboratories Equipment Ltd, Aldermaston UK) prepared in PBS. The wells were washed once quickly with PBS then washed in PBS for 10 minutes. 250µl of X-gal stain (**Appendix B**) was added to the washed wells and the plates were incubated in a sealed humidified container at 37°C for approximately 24 hours. The plates were viewed under an inverted phase contrast light microscope for visible signs of blue cells, replacing the X-gal stain with PBS when the incubation period in the stain was deemed sufficient.

2.20.2.2 CMFDG

Reagents were provided in the DetectaGene Green *lacZ* Gene Expression Kit (Cambridge Bioscience, Cambridge UK), unless indicated otherwise, and their composition is given in **Appendix B**. This method was used to detect expression of β-gal in cell lines which grow in suspension. After an appropriate incubation period following transfection by electroporation (**2.20.1**) the cells were counted by trypan blue exclusion (**2.18.2**) and a cell suspension containing 2.5 x 10^5 live cells was pelleted at 1000rpm. The pellet was resuspended in 100µl of pre-warmed supplemented RPMI-1640 medium (**Appendix B**) containing 10mM HEPES (Life Technologies, Paisley UK) and 50µM DetectaGene Green Substrate Reagent. The cells were plated in wells of a 96 well plate and incubated at 37°C, 5% CO_2 for 40 minutes then transferred to 200µl of ice cold PBS. 6µl of propidium iodide was

added and the cell suspension diluted in PBS as appropriate for immediate analysis by flow cytometry. A Coulter EPICS XL Flow cytometer (Coulter, Bedfordshire UK) with an air cooled, software controlled, 15mW argon ion laser operating at 488nm was set up and calibrated to detect fluorescein, propidium iodide and forward scatter according to standard procedures. To compensate for the background autofluorescence of the cells the voltage of the flow cytometer was adjusted appropriately.

2.20.3 Selection of G418 Resistant Transfectants

G418 sulphate (G418) is an amino glycoside antibiotic that induces cytotoxicity by blocking translation. Neomycin phosphotransferase, encoded by the *neo* gene, inactivates G418 through phosphorylation blocking the antibiotic's toxic effects. The lethal concentration of G418 (Life Technologies, Paisley UK) for the U937 and MM6 cell lines was determined by generating a "G418 death curve" for the two cell lines. The percentage of viable cells for each concentration of G418 which the cells were cultured in was monitored and recorded graphically over a 2-3 week period to determine the lethal dose of G418 for the cell lines. This was repeated for a second batch of G418 because the specific activity of preparations is known to vary. The concentrations of G418 to kill 100% of the cells were 300mg/ml for U937 cells for the first batch of G418 and 500mg/ml for U937 and 400mg/ml for MM6 cells for the second batch of G418. The cytotoxic effect of the G418 was apparent by day 13 of culture in the antibiotic. Cells were selected for the presence and expression of the *neo* gene in the appropriate G418 concentration for several weeks after control plates of cells, which had been electroporated in the absence of DNA (**2.20.1**) or not electroporated, showed 100% cell death. The transfected cells were subsequently maintained at half the selection concentration of G418 to ensure the plasmid DNA was retained in the transfectants.

2.20.4 Single Cell Cloning by Limiting Dilution

The concentration of viable cells in the population from which single clones were being derived was determined from an average of at least two cell viability counts by trypan blue exclusion (**2.18.2**). The cells were gently drawn up and down the bore of

a 19G needle (Becton Dickinson UK Ltd., Oxford UK), to ensure a suspension of single cells existed. Cells were sequentially diluted to give no more than 485 cells in 97ml of supplemented RPMI-1640 medium (**Appendix B**) containing G418 (Life Technologies, Paisley UK) at the appropriate concentration (**2.20.3**). 200µl aliquots of the diluted cell suspension were plated into the wells of five 96 well plates which should, theoretically, result in one cell per well.

2.21 ANALYSIS OF CELLULAR METAL CONTENT

In peripheral blood 1µg/litre of Mn can be detected using inductively coupled plasma mass spectophotometry (ICPMS). The normal white blood cell count is approximately 10^{10}/litre (Department of Haematology 1997). An estimation of the number of cultured cells necessary to enable accurate analysis of the metal content is, therefore, of the order of 10^6-10^7 cells.

2.21.1 Cell Culture and Pelleting Cells for Analysis of Cellular Metal Content

Cells were typically cultured at an initial concentration of 3 x 10^5 cells/ml in large flasks for 2-3 days prior to checking for their viability (**2.18.2**) before pelleting as follows. All cells analysed in parallel were cultured in the same batch of supplemented RPMI-1640 medium (**Appendix B**) with the exception of comparison of transfectants and parent cell lines. Transfectants had G418 (Life Technologies, Paisley UK) at 150µg/ml added to the medium which the parent cell line received. Samples of the medium used to culture the cells were taken for analysis when the cultures were set up to ensure the media had uniform concentrations of the metals analysed.

The cell suspensions were transferred to sterile universal tubes (Rosslabs, Cheshire UK), pelleted at 1000rpm for 10 minutes and the pellets washed in PBS. The washed pellets were centrifuged as before and the pellets resuspended in PBS, pooling the pellets into a single universal tube for each sample. The cell suspensions were counted for viability (**2.18.2**) and the total cell number calculated. The cell pellets were carefully transferred to 1.5ml tubes, ensuring maximum transfer, and

microcentrifuged at 2000rpm for 5 minutes and the supernatant carefully aspirated off.

The cell pellets were frozen at -20°C to rupture the cell walls and a known volume of Milli-Q dH_2O added to the ruptured cells. The lysed cells were pipetted to ensure the cells were completely fragmented and then microcentrifuged at 13000rpm for 10 minutes. The supernatants were transferred to fresh tubes and the cell extracts were analysed by ICPMS (**2.21.2**).

2.21.2 Inductively Coupled Plasma Mass Spectophotometry Analysis

Determination of Mn, Cu, Zn and Fe concentrations were carried out simultaneously by ICPMS using a VG Elemental Plasmaquad 3 (VG Elemental, Winsford UK) at the Department of Chemistry, University of Edinburgh in collaboration with Dr Marina Patriarca and Professor Peter Sadler. Samples of the cell extracts (**2.21.1**) were diluted 1 in 10 with a solution containing 0.2% HNO_3 and 10μg/litre rhodium as internal standards. Calibration was obtained for each experiment using aqueous standard solutions prepared from appropriate dilution of a certified multi element standard solution for ICP analysis (10580 ICP Multi Element Standard VI, Lot No. 70240283, Merck, Leicester UK). All intensities were corrected for drift using the internal standard. Calibration curves and concentrations of the samples were calculated using the Plasmavision instrument software (VG Elemental, Winsford UK). The analysis of a certified reference material (SRM 2670 'Toxic Metals in Urine', National Institute of Standards and Technology, Gaithersburg, Maryland, USA) containing 0.13 ± 0.02mg/litre of Cu with an indicative value of 0.03mg/litre for Mn yielded average values of 0.141 ± 0.007mg/litre (4.6%) for Cu, 0.031 ± 0.001mg/litre (3.6%) for Mn, 1.61 ± 0.047mg/litre (2.9%) for Zn and 0.874 ± 0.041mg/litre (4.7%) for Fe (mean ± standard deviation (relative standard deviation)) when analysed with batches of cell samples on six different occasions. Information on the content of Fe and Zn in this material was not available. Precision was assessed by replicate analysis of the same cell extracts.

3 IMMUNOHISTOCHEMISTRY OF PBC LIVER SECTIONS FOR MARKERS OF APOPTOSIS, PROLIFERATION AND THE PRESENCE OF MACROPHAGES

3.1 Introduction

There is no doubt that PBC sufferers have a marked paucity of BECs, a situation that increases as disease progresses. However, the manner in which these cells are lost is uncertain. It is possible, and evidence exists suggesting, the cells may die by apoptosis (Nakanuma *et al.* 1983; Kuroki *et al.* 1996; Koga *et al.* 1997.). However, the transient nature of this cellular phenomenon makes histological observation of apoptotic BECs in sections from small liver biopsies a challenging task. Such sections from PBC patients contain ever decreasing numbers of the cells of interest and as execution of the apoptotic pathway itself may take only a couple of hours (Howie *et al.* 1994) the likelihood of catching the "process in action" in a liver section of area 3-4mm^2 is optimistic.

Rather than try to identify apoptotic cells morphologically the following study attempted to examine, immunohistochemically, the cellular expression pattern of proteins which participate in regulating the apoptotic pathway. In this way an indication of the potential for these cells to undergo apoptosis, and whether they possess a different profile from normal BECs, might be determined. The aim was to determine if the PBC BECs express the pro-apoptotic bax, bcl-x (reviewed in Adams and Cory 1998) and p53 (reviewed in Evan and Littlewood 1998) proteins and the anti-apoptotic bcl-2 protein (reviewed in Adams and Cory 1998). I was also interested in identifying whether these cells express the Fas/CD95 antigen, whose presence and ligation provides a possible stimulus to initiate apoptotic death (Ashkenazi and Dixit 1998) and to identify which cells may be expressing the Fas ligand antigen and, as such, potential initiators of cell death. As any net loss of tissue may have a component due to a lack of cell proliferation and tissue regeneration, I also examined the proliferative status of the BECs by analysing the expression profile of the Ki-67 antigen, a marker of cell proliferation (Gerdes *et al.* 1991).

In addition to determining the expression pattern of the above proteins, I was interested in observing the well documented presence of Mϕs in PBC liver and the extent of granuloma formation in sections from early and late stage biopsies, on the basis that the presence and activity of these cells may be significantly important in the initiation and/or maintenance of PBC. The PG-M1 monoclonal antibody was chosen to identify Mϕs. PG-M1 detects the CD68 antigen which belongs to a family of highly glycosylated lysosomal/plasma membrane shuttling proteins known as the LAMP1 group. The antibody does not react with granulocytes or their precursors, which are also known to express CD68.

For all the antigens except Fas ligand commercially available antisera were available for the study. For Fas ligand, antisera which had been raised against a synthetic Fas ligand peptide was available which required characterisation to determine its reactivity against the peptide and Fas ligand protein.

3.2 Results

3.2.1 Immunohistochemical Analysis of Bax, Bcl-x, Bcl-2, CD95/Fas and Ki-67 Expression in Liver Sections

3.2.1.1 Analysis of Results

The intensity of immunostaining for bcl-2, bax, bcl-x and Fas/CD95 was homogeneous with little variation between cells within a single duct or between ducts. For this reason biopsies were scored as follows; strong (that is, clearly visible granular stain at low power examination (x400)); moderate (definite but weak immunopositivity visible at low power but needing confirmation by high power microscopic examination (x200)); weak/negative (equivocal staining, not consistently greater than in negative control section where primary antibody was omitted). When Ki-67 or p53 were present they produced clear, discrete, nuclear staining. Cases were scored positive if the nucleus of one or more BEC was stained and negative if no positive cells were seen. Thereafter, an estimate was made of the proportion of individual biliary epithelial cells stained. Bile ducts were classified as

small (<75mm) or large (>75mm) by measurement using the Highly Optimised Microscope Environment (HOME) semi-automated computer system (Carl Zeiss, Welvyn Garden City UK).

PG-M1 positive cells were clearly visible as intensely stained cells.

3.2.1.2 Normal Liver: Bax, Bcl-x, Bcl-2, CD95/Fas and Ki-67 Expression

Bax (**Figure 3.1a**) and bcl-x (**Figure 3.2b**) were expressed uniformly in both hepatocytes and bile ducts but were not detected in Kupffer cells or endothelial cells. Moderate bax expression was seen in bile ducts <75mm in 11/15 sections (**Table 3.1**) and moderate bcl-x expression in 8/15 sections (**Table 3.2**). Only 3/15 cases expressed detectable bcl-2 in biliary epithelium. Bcl-2 was not detected in hepatocytes. Eight of fifteen cases showed moderate staining of biliary epithelium with the anti-Fas/CD95 antibody. In all cases hepatocytes were positive with the anti-Fas/CD95 antibody, the staining pattern being granular as previously reported in paraffin embedded tissue (Mochizuki *et al.* 1996). p53 was not detected and BECs did not express Ki-67. A lack of immunohistochemical reactivity of the anti-Fas ligand peptide sera prevented determination of the expression pattern of Fas ligand (see **3.2.2.3**).

	bax (<75μm)				bax (>75μm)			
	strong	moderate	weak/ negative	n	strong	moderate	weak/ negative	n
Normal	0	11	4	15	0	10	2	12
Early	14	1	0	15	12	0	0	12
Late	6	4	4	14	8	3	3	14

Table 3.1 Results of bax immunocytochemistry in bile ducts <75mm and >75mm of histologically normal and early and late stage PBC liver biopsy material. The figures are the number of sections with detectable strong, moderate and weak/negative expression scored as described in **3.2.1.1**. Expression when detected was homogeneous and uniform. **n**: total number of sections.

	bcl-x (<75μm)				bcl-x (>75μm)			
	strong	moderate	weak/ negative	n	strong	moderate	weak/ negative	n
Normal	0	8	7	15	0	8	4	12
Early	14	0	1	15	11	0	1	12
Late	13	1	0	14	13	1	0	14

Table 3.2 Results of bcl-x immunocytochemistry in bile ducts <75mm and >75mm of histologically normal and early and late stage PBC liver biopsy material. The figures are the number of sections with detectable strong, moderate and weak/negative expression scored as described in **3.2.1.1**. Expression when detected was homogeneous and uniform. **n**: total number of sections.

3.2.1.3 PBC Liver: Bax, Bcl-x, Bcl-2, CD95/Fas and Ki-67 Expression

Residual bile ducts showed strong staining of bax (**Table 3.1, Figure 3.1c**) and bcl-x (**Table 3.2, Figure 3.2a**) which appeared more intense than in normal liver. Bax and bcl-x were expressed strongly in "metaplastic" biliary ductules (**Figure 3.1c and Figure 3.2a**). Lymphocytes showed intense expression of bcl-2 (**Figure 3.3**). Bcl-2 expression seen in surviving BECs was weak and inconsistent, similar to normal liver (**3.2.1.2**). No change in Fas/CD95 staining was noted compared with the normal sections (**3.2.1.2**). p53 expression was not detected. In PBC cases up to 8% of BECs in large ducts and in residual small ducts expressed Ki-67 (**Figure 3.4**). The number of positive nuclei seen was greatest in ducts >75mm in sections showing histological early stage PBC. Areas of ductal "metaplasia" remained Ki-67 negative. A lack of immunohistochemical reactivity of the anti-Fas ligand peptide sera prevented determination of the expression pattern of Fas ligand (see **3.3.2.3**).

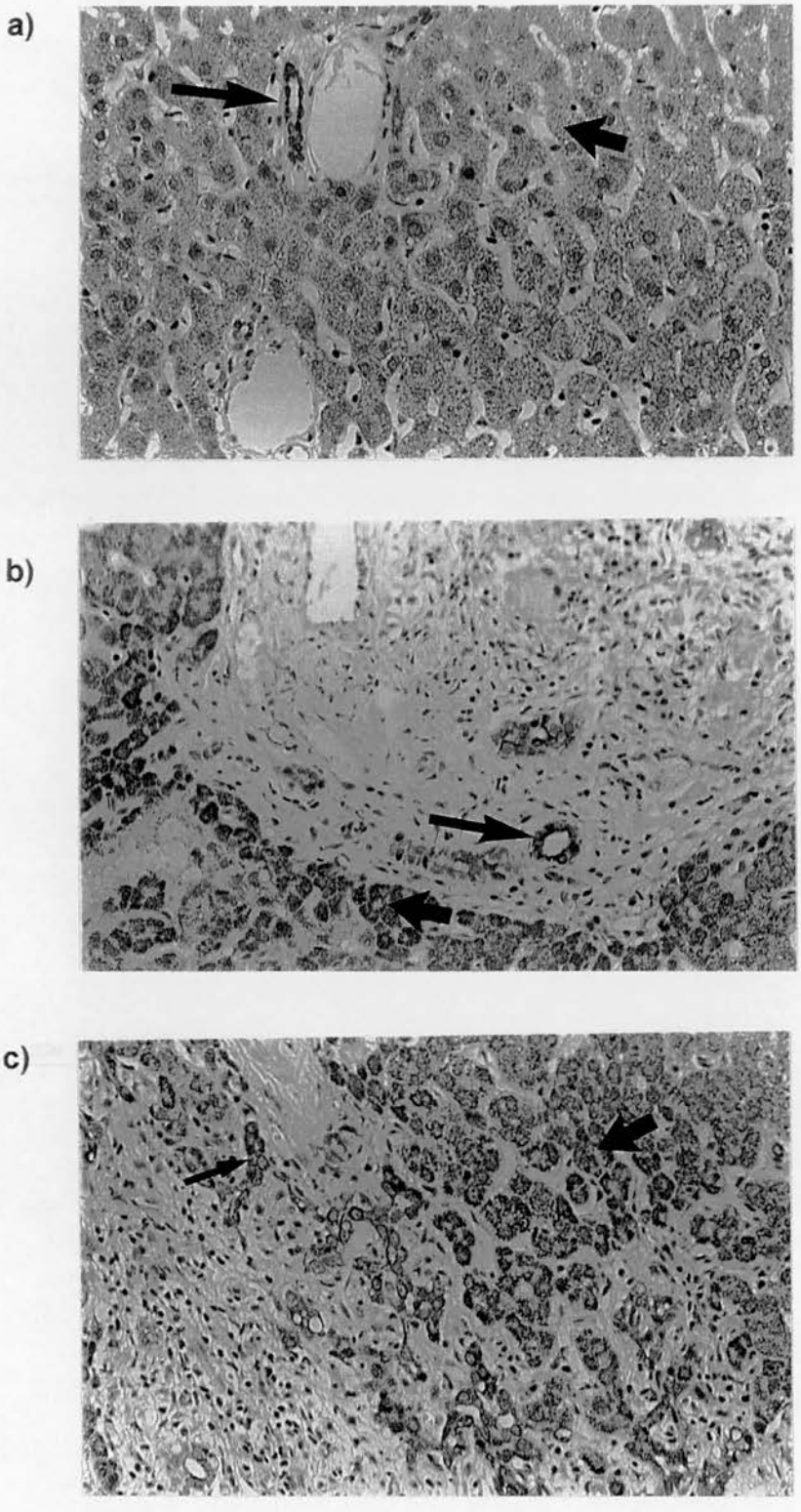

Figure 3.1 Immunohistochemical detection of expression of bax in **a)** normal bile ducts (➡) and hepatocytes (⬅); **b)** PBC stage I liver showing strong expression in bile ducts (➡) and upregulation of bax in hepatocytes (⬅); **c)** PBC stage II liver showing upregulation of bax in "metaplastic ductules" (➡) and hepatocytes (⬅). Original magnification x200. Immunohistochemistry protocols are described in **2.2**.

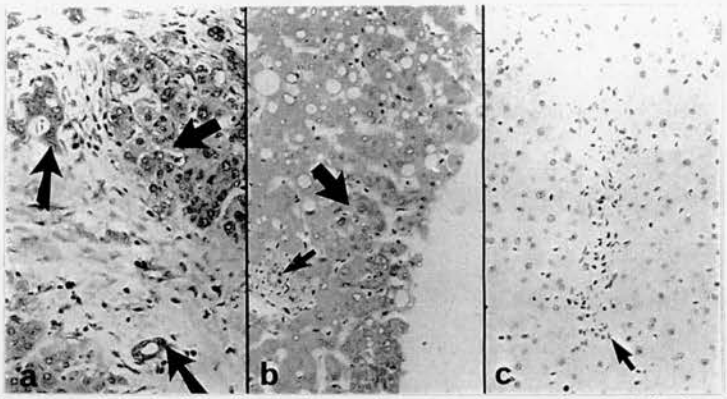

Figure 3.2 Immunohistochemical detection of expression of bcl-x in **a)** PBC stage IV liver hepatocytes ( ) and "metaplastic ductules" ( ) which show upregulation compared with **b)** histologically normal liver showing only mild steatosis; hepatocytes ( ) and bile duct ( ). **c)** Negative control omitting primary antibody on histologically normal liver section, bile duct ( ). Original magnification x200. Immunohistochemistry protocols are described in **2.2**.

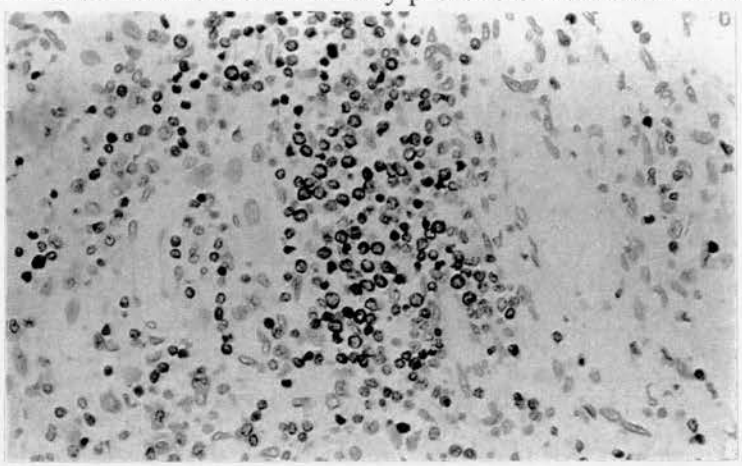

Figure 3.3 Immunohistochemical detection of expression of bcl-2 in infiltrating lymphocytes in PBC stage IV liver showing strong expression in lymphocytes. Original magnification x200. Immunohistochemistry protocols are described in **2.2**.

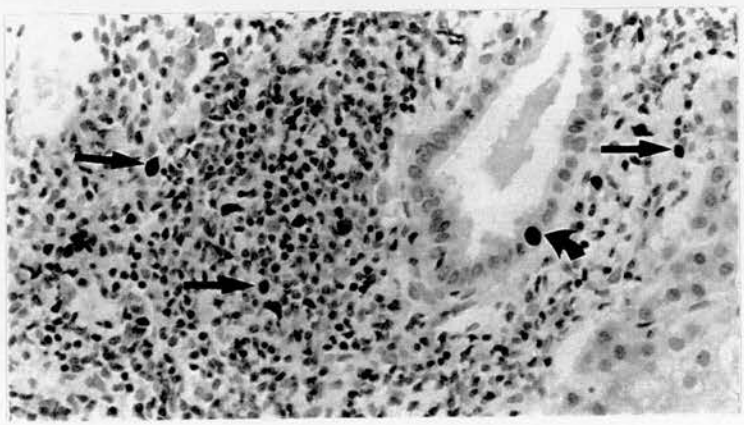

Figure 3.4 Immunohistochemical detection of expression of Ki-67 in a proliferating biliary epithelial cell ( ) and infiltrating cells ( ) in PBC stage I liver. Original magnification x200. Immunohistochemistry protocols are described in **2.2**.

3.2.2 Characterisation of Rabbit Polyclonal Anti-Fas Ligand Peptide Serum

No commercial anti-Fas ligand antisera were available while this study was in progress which would ideally have been used to investigate the Fas ligand expression pattern in conjunction with the monoclonal anti-Fas antibodies. However, rabbit sera from two animals immunised with a Fas ligand peptide, synthesised by Ian Heslop at the Department of Chemistry, were available (**2.3.9**). The reactivity and specificity of the sera were not known, requiring their characterisation before any potential use.

3.2.2.1 ELISA

Using an ELISA to test the pre-immune sera and sera from the immunised rabbits before and after IgG purification with protein A, reactivity against the peptide immunogen was detected in the immunised sera from both animals which was not seen in the pre-immune sera (**Figure 3.5**).

3.2.2.2 RT-PCR and Western Blotting

RNA and protein extracted from PBMCs which had been stimulated with concanavalin A (**2.18.4**), known to upregulate Fas ligand expression, showed detectable upregulation of Fas ligand expression at the gene and protein level assayed by RT-PCR and Western blotting, respectively. The upregulation of Fas ligand mRNA expression confirmed successful stimulation of the cells (**Figure 3.6a**). Western blotting using a mixture of equal protein concentrations of the IgG purified immunised rabbit sera showed obvious upregulation of an immunoreactive product of approximately 40kDa, consistent with the estimated size of the Fas ligand protein (**Figure 3.6b**) (Takahashi *et al.* 1994). This was not observed in the blot using the pre-immune rabbit sera suggesting an anti-Fas ligand antibody response had been raised successfully in the immunised rabbits (**Figure 3.6b**). The positive control blots showed upregulation of CD3 after stimulation with concanavalin A and negative control blots, omitting the primary sera, showed lack of specific immunoreactivity (**Figure 3.6b**). Control dot blots for the chromogen detection

a)

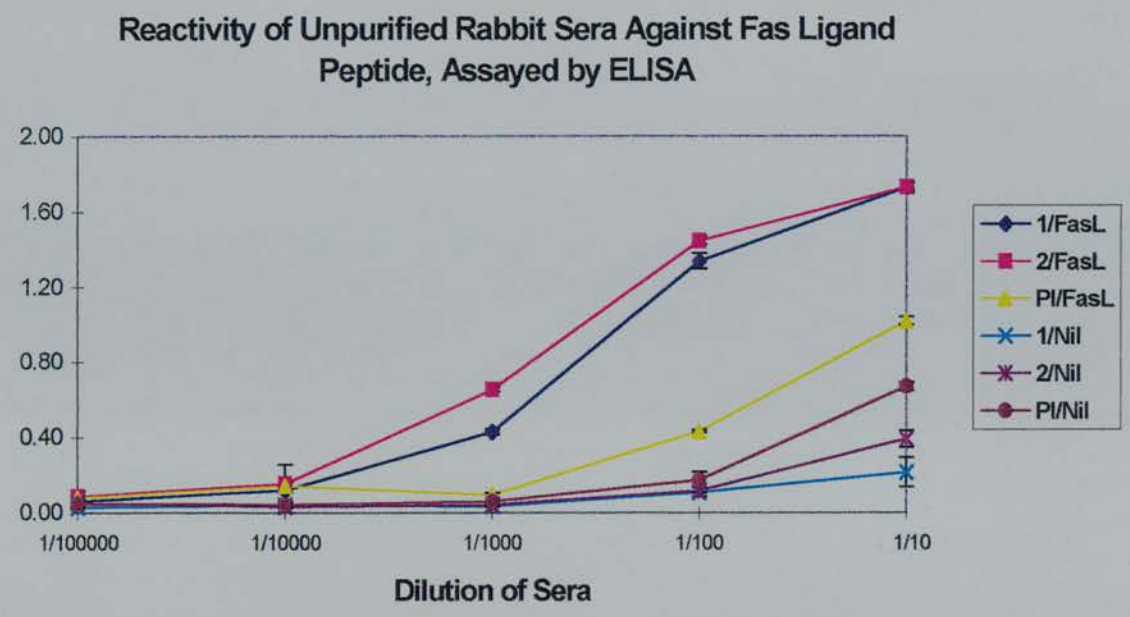

b)

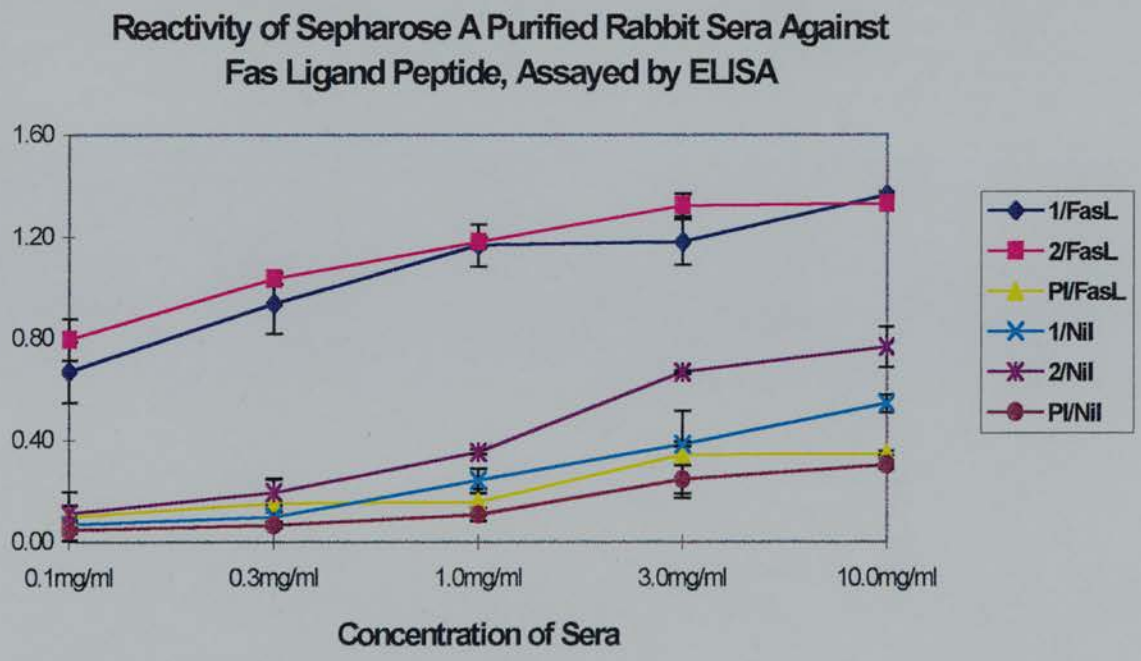

Figure 3.5 showing reactivity of **a**) unpurified rabbit sera and **b**) sepharose A purified rabbit sera against a Fas ligand peptide assayed by ELISA, as described in **2.5.1**. **1** and **2** refer to two rabbits immunised with the Fas ligand peptide and **PI** to the sera from the rabbits prior to immunisation. **FasL** and **Nil** denote the ELISAs where the plate was coated with the Fas ligand peptide or control blocking agent, respectively. The error bars show the standard deviation from triplicate results.

method were positive and dot blots of the Fas ligand peptide showed a positive reaction with the immunised sera but not with the pre-immune serum.

3.2.2.3 Immunohistochemistry

When the pre-immune serum and sera from the rabbits immunised with the Fas ligand peptide were used for immunohistochemistry on paraffin embedded tonsil sections, using the standard ABC-HRP-DAB detection method and humidified chambers (**2.2**), no specific staining pattern was seen with the immunised sera. This lack of specificity was present on all sections regardless of the antigen retrieval pre-treatment they had received (i.e. microwave in citrate buffer, trypsin digestion or no pre-treatment) but the sections which had been microwaved in citrate buffer showed the strongest staining. Both the pre-immune and immunised sera showed high levels of non-specific background staining. To try to overcome this problem the sera were incubated overnight at 4°C with NHS, to complex rabbit anti-human epitope responses contributing to the background staining, and the complexes removed after centrifugation. The sera were subsequently IgG purified by running them through a sepharose-protein A column. The IgG purified sera was tested on tonsil sections as before using a sheep fragment antigen binding ($F(ab')_2$) anti-rabbit Ig secondary antisera (diluted 1/1000) to reduce the background staining. No specific staining was seen with any of the pre-treatments of the tonsil sections at any of the sera concentrations tested. This suggests the immunised sera does not recognise an epitope present in the native protein, or the epitope was not successfully unmasked after paraffin embedding by the antigen retrieval methods tried or the epitope is sterically inaccessible due to the membrane location of the Fas ligand protein. The anti-Fas ligand sera were, therefore, unsuitable for immunohistochemical analysis of Fas ligand expression in the PBC cases analysed for markers of apoptosis and proliferation (**3.2.1**).

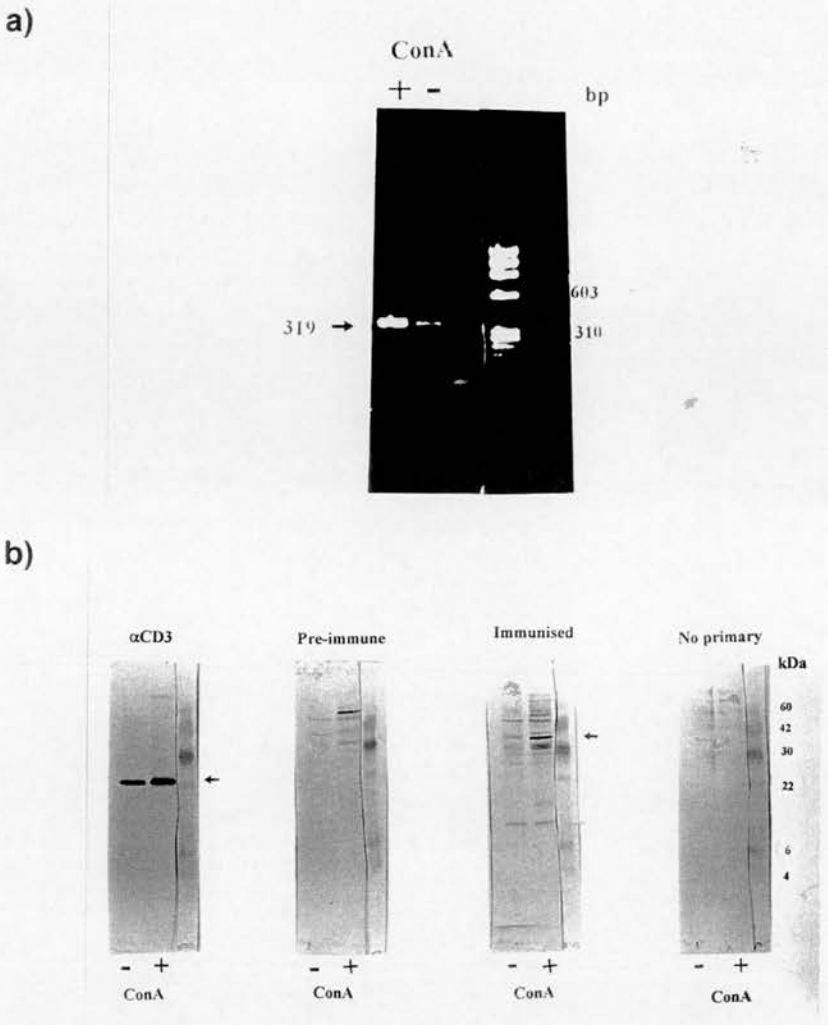

Figure 3.6 showing upregulation of Fas ligand **a)** mRNA by RT-PCR and **b)** protein by Western blotting (**Immunised** blot) in PBMCs after stimulation with concanavalin A (+ **ConA** lanes) compared to unstimulated PBMCs (- **ConA** lanes). In **a)** the arrow points to the 319bp Fas ligand product. Molecular weight marker, with sizes shown in bp, was run in the right hand lane adjacent to the negative control lane. In **b)** positive control blot (**αCD3** blot) incubated in anti-CD3 polyclonal rabbit sera shows upregulation of CD3 protein expression in ConA treated cells indicated by the arrow. The pre-immune rabbit sera (**Pre-immune** blot) and negative control (**No primary** blot) blots do not show the specific reactivity (arrow) with ConA stimulated PBMCs seen with the Fas ligand peptide immunised rabbit sera (**Immunised** blot). Molecular weight marker is shown to the right of each blot with the kDa sizes shown at the far right. RT-PCR and Western Blotting are described in **2.7**, **2.8.7**, **2.9** and **2.4.4**.

3.2.3 PG-M1 Immunohistochemistry

All liver biopsy sections showed discrete positive staining of cells distributed throughout the parenchyma. These cells had a spindly, elongated appearance and their parenchymal location suggests they may be resident KCs (**Figure 3.7**). The number of these cells was noticeably increased in the PBC sections compared with the normal sections. As disease progressed and fibrosis became apparent these positive cells concentrated in the areas of remaining non-fibrotic tissue. In addition to cells situated in the parenchyma, positive cells were also seen in the leucocyte infiltrates of the disease sections. These had a different morphology being rounder and bearing more resemblance to blood monocytes (**Figure 3.7b** and **c**). The most significant observation in the PBC sections was the areas where many positive cells were congregated together, forming regions of extensive positivity (**Figure 3.7b**). These regions were obvious granulomas and their development from the initial formation to extensive immune foci could be seen in the different sections analysed. In some sections the granulomas appeared focused around or in close proximity to damaged bile ducts, but they were also seen in the parenchyma. From the two-dimensional view of the sections the latter did not appear to be in close proximity to bile ducts. Granulomas were seen in sections representing all histological stages of PBC progression.

3.3 Discussion

The results of this immunohistochemistry study (Graham *et al.* 1998) show that bile ducts constitutively express pro-apoptotic proteins, particularly bax, and the apoptotic regulator bcl-x. In contrast the anti-apoptotic protein bcl-2 is barely expressed and thus appears to play little part in regulating apoptosis in BECs in the cases studied. In addition to exhibiting a phenotype permissive for apoptosis, there is evidence that BECs retain the ability to proliferate based on the positive Ki-67 staining seen in PBC liver sections. This supports the observation of Nakanuma and Harada who showed increased proliferative activity of epithelial cells in affected ducts in PBC liver (Nakanuma and Harada 1993).

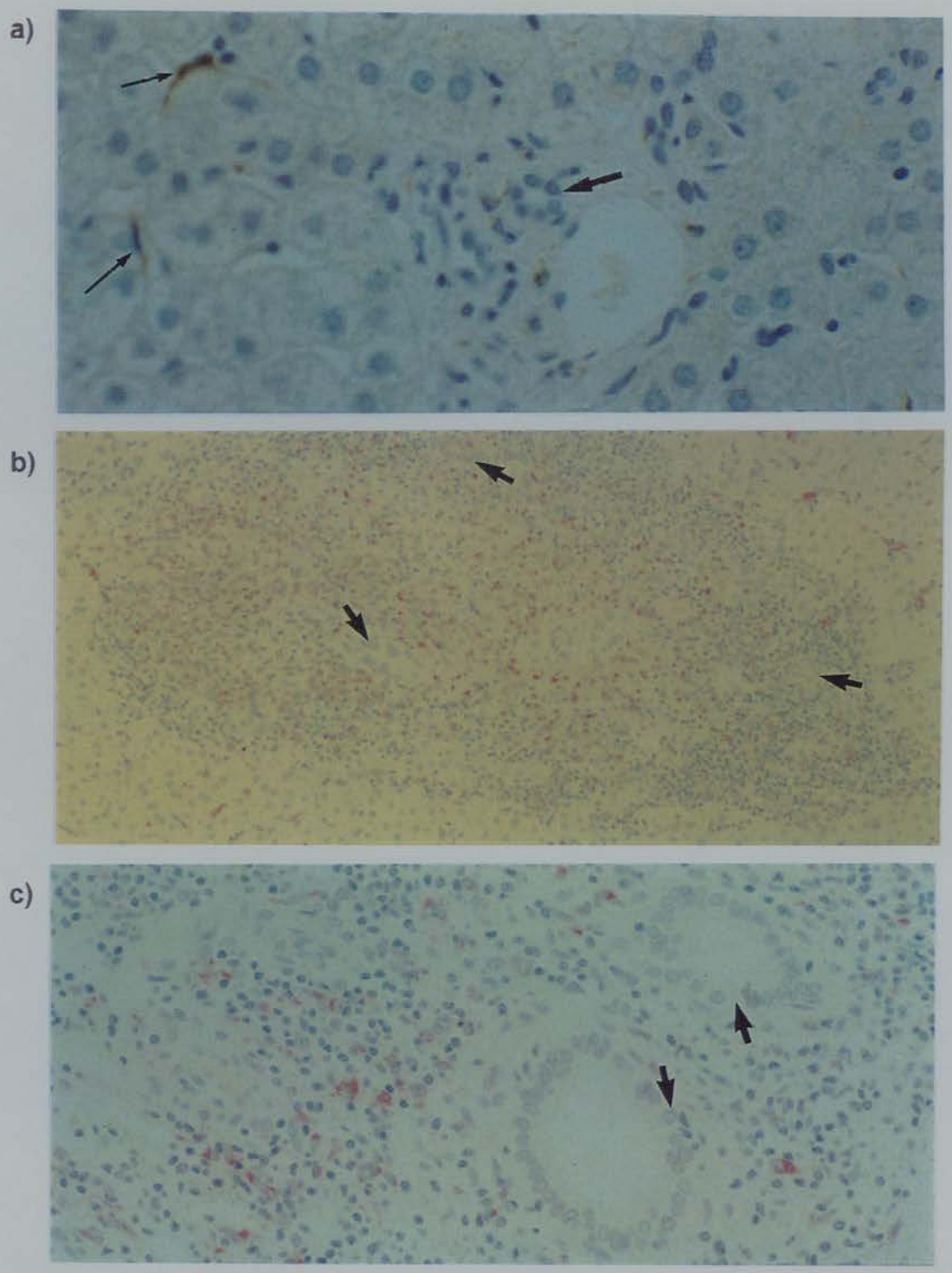

Figure 3.7 Immunohistochemical staining (described in **2.2**) with the PG-M1 monoclonal antibody to stain CD68 positive cells in **a**) normal liver and **b**) and **c**) PBC stage II liver sections. In **a**) Kupffer cells, stained brown with DAB, can be seen in the parenchyma (→) and an undamaged bile duct is marked (←). In **b**) pink (Fast Red) stained granulomas are visible around damaged bile ducts (→) within a region of extensive leukocyte infiltration. In **c**) two bile ducts showing signs of damage (→) are visible surrounded by inflammatory cells including pink (Fast Red) stained CD68 positive cells. Original magnification **a**) x400, **b**) x100 and **c**) x200.

Charlotte *et al.* have reported that normal bile ductules and small bile duct epithelium, but not large bile duct epithelium or hepatocytes, show weak expression of bcl-2 as detected immunohistochemically (Charlotte *et al.* 1994). However, Kuroki *et al.* found no bcl-2 expression in biliary epithelium of normal or PBC livers (Kuroki *et al.* 1996). The weak/equivocal bcl-2 staining pattern I observed in both histologically normal and PBC sections appears consistent with these previous reports with bcl-2 likely to be expressed at levels bordering on the undetectable by immunohistochemistry. Other studies have shown more prominent bcl-2 staining in ductules at the borders of cirrhotic nodules relative to normal liver (Koukoulis *et al.* 1995). However, I did not notice a similar consistent pattern in the cases examined. This suggests a potential "life-saving" mechanism for BECs in the presence of a pro-cirrhotic environment may be lacking in PBC liver and contributing to the destruction of these cells. The absence of bcl-2 expression I observed in hepatocytes is consistent with previous observations (Charlotte et al. 1994; Krajewski *et al.* 1994). Parenchymal damage in PBC is generally accepted as being, primarily, the result of secondary responses in the liver with the resulting fibrosis and cirrhosis apparent in the later stages of disease. On the basis of this immunohistochemistry study bcl-2 does not appear to be exerting protection against hepatocyte cell death. The intense bcl-2 staining of infiltrating lymphocytes and those around bile ducts under destruction is consistent with previous reports (Deguchi *et al.* 1998). Though I did not seek to identify whether these bcl-2 positive cells were CD4+ or CD8+ T lymphocytes these authors report the same distribution of bcl-2 positive and CD4 positive cells in the PBC biopsies they immunostained and propose CD4/bcl-2 double positive cells have a pathological role in PBC. Autoreactive T lymphocytes expressing bcl-2 may escape apoptosis leaving them free to accentuate tissue destruction and cause autoimmune disease.

I observed weak expression of Fas/CD95 in bile ducts in normal and PBC liver sections which supports the findings of Kuroki *et al.* (Kuroki *et al.* 1996) and, as previously reported, I am able to confirm its presence in hepatocytes (Hiramatsu *et al.* 1994; Galle *et al.* 1995; Okazaki *et al.* 1995; Mochizuki *et al.* 1996; Harada *et al.*

1997b; reviewed in Faubion and Gores 1999). It is worth noting that my findings and those of others (Kuroki *et al.* 1996) differ from those of Harada and colleagues who failed to identify Fas/CD95 expression in BECs of the normal liver sections used in their study. They did, however, observe various intensities of cytoplasmic staining of the antigen in bile ducts of PBC, chronic hepatitis and extrahepatic biliary obstruction sections with the PBC cases showing the strongest staining (Harada *et al.* 1997b). The discrepancies between my findings and these results may reflect the different antisera used in the two studies or the nature of the normal control tissue used. Though biopsy reports state a tissue may appear histologically normal with respect to malignant growth it is possible that the tissue exhibits other pathological phenomena which may or may not be apparent from microscopic examination. In at least one of the normal cases used in my study a degree of infiltration of inflammatory cells was observed which suggests this biopsy was obtained from liver undergoing some reaction not expected of ideal control tissue. Finding a source of true "normal" control liver material for these studies is always a problematic issue.

As previously mentioned the monoclonal Ab I used against Fas/CD95 did not detect increased levels of the antigen in the PBC livers. TNFα and IFNγ expression in PBC liver has been reported (Tovey *et al.*1991, Martinez *et al.* 1995, Shindo *et al.* 1996), which might suggest an accompanying elevation in Fas expression. However, many of the experiments which have shown increased Fas expression induced by TNFα and IFNγ were *in vitro* studies using high doses of cytokine (Maciejewski *et al.* 1995; Panayiotidis *et al.* 1995). In contrast, PBC is a chronic disease and levels of these cytokines present in the liver have not been quantified. In addition most reports for cytokine expression patterns in liver of PBC patients rely on mRNA analysis, the results of which can not always be transposed to the protein expression pattern. It is possible that any changes in Fas expression which may be induced by the presence of these cytokines are not of sufficient magnitude for detection by immunohistochemistry with the antisera I used. Alternatively, these pleiotropic cytokines may be exerting other effects on the disease state in PBC independent of Fas.

I had hoped to study the expression pattern of Fas ligand in conjunction with that of Fas/CD95. However, at the time of this study no commercially available antiserum against Fas ligand was available and I found the rabbit sera raised in our laboratory against a synthetic Fas ligand peptide was unreactive on paraffin embedded tissue. As all the material used for this study was archival paraffin embedded tissue and I had access to only two frozen PBC liver biopsies, attempts to determine whether the antisera was reactive with frozen sections were not pursued. The lack of reactivity of the antisera for immunohistochemical use was unfortunate, particularly in the light of its reactivity against the denatured protein, which I identified by Western blotting using protein from concanavalin A stimulated PBMCs. The fact that increased Fas ligand expression was detected by RT-PCR as well as Western blotting in the concanavalin A treated PBMCs, and the reactive band on the Western blot which showed this increase was of the appropriate size for Fas ligand (Takahashi *et al.* 1994), strongly suggests the sera was reactive against denatured Fas ligand protein. The use of synthetic peptides as an immunogen to raise specific antisera can be highly successful. However, there are a number of problems that may be encountered. The peptides used need to contain both a T cell and B cell epitope to induce an effective antibody response. As linear peptides represent a tiny fraction of the whole amino acid sequence of the native protein, potential secondary structure, which this region of the molecule may naturally adopt, is unlikely to form. As a T cell epitope this is not an issue but recognition of the native protein by Abs may require retention of this structure. In the case of the anti-Fas ligand sera it may be that the amino acids of the synthetic peptide adopt a particular structure in the native protein which Abs raised against the peptide fail to recognise. It is also possible that the Abs raised against the peptide recognise part of the molecule that is sterically hindered and inaccessible when the protein is expressed at the cell surface.

Expression of Fas ligand has subsequently been detected by others using immunohistochemistry. It was reported to be expressed occasionally by infiltrating mononuclear cells within the portal tracts, and at a significantly higher level in PBC liver around injured bile ducts. The expression in the PBC liver was greater than in

normal, chronic hepatitis and extrahepatic biliary obstruction liver (Harada *et al.* 1997b). This study also identified expression of perforin and granzyme B in infiltrating mononuclear cells and BECs. Granzyme B was expressed at a higher level in PBC liver than the control livers while perforin expression was higher in the three groups of liver disease compared with the normal tissue. These findings may support the reports of apoptosis of biliary epithelial cells in PBC (Bernuau *et al.* 1981; Nakanuma *et al.* 1983; Harada *et al.* 1997b; Koga *et al.* 1997) and be associated with the presence of cytotoxic CD8+ T cells (Si *et al.* 1984; Krams *et al.* 1990; Hashimoto *et al.* 1993). Analysis of Fas ligand expressing cells in PBC has shown CD4+, CD8+ and CD3- cells to express the antigen, but only the former two cell types were closely localised around the bile ducts (Koga *et al.* 1998). These authors suggest both CD4+ and CD8+ T cells may be involved in inducing apoptosis of BECs. However, my findings of the low level of Fas/CD95 expression in PBC BECs suggest a Fas/CD95-mediated mechanism is unlikely. Such mechanisms have been invoked in a number of inflammatory diseases of the liver, especially viral hepatitis (Hiramatsu *et al.* 1994; Galle *et al.* 1995; Okazaki *et al.* 1995; Mochizuki *et al.* 1996) and ligation of constitutively expressed Fas/CD95 on hepatocytes by antibodies results in rapid hepatocyte apoptosis (Trauth *et al.* 1989; Yonehara *et al.* 1989; Ogasawara *et al.* 1993). CD8+ T cells are able to induce apoptosis in target cells via Fas independent mechanisms, such as perforin or cytokine mediated cell death (reviewed in Griffiths 1995; reviewed in Kägi *et al.* 1996), and a perforin/granzye B mediated induction of cell death remains a possibility, particularly in the light of the perforin and granzyme B expression in PBC liver mentioned above (Harada *et al.* 1997b).

Both bax and bcl-x proteins appeared to be upregulated in biliary epithelium in the PBC cases I studied. These results are based on staining intensities for the two antigens observed by eye under light microscopy and such conclusions must be considered with caution. Immunohistochemistry is not an ideal technique for quantitating levels of expression of antigens because of possible inter-section variations throughout the course of the procedure. The DAKO Techmate™ 500

automated immunocytochemistry stainer was used for this study to enable large numbers of sections to be stained in a single run with all the sections being incubated for the same time under the same conditions throughout the protocol. Using bench top staining techniques there is an increased chance of introducing inter-section variability when staining large numbers of sections at one time. In addition to potential variations during the staining procedure, the fixation process the biopsy material undergoes may introduce variation out with the control of the immunostainer. Bearing in mind these potential problems the staining intensity observed in the majority of disease sections examined was stronger when compared with the control sections, suggesting an increased level of protein expression which may be indicative of an increased potential to undergo bax-mediated apoptosis. The expression of bax is induced by p53 (Miyashita *et al.* 1994; Selvakumaran *et al.* 1994) and the protein heterodimerises with bcl-2, inhibiting the anti-apoptotic effect of bcl-2 (Oltvai *et al.* 1993). I did not see upregulation of p53 suggesting p53-independent induction of bax and bcl-x may be occurring, as has been reported by others (Hung and Chuang 1996). The bcl-x gene codes for two splice variants, full length bcl-x_l protein and a smaller bcl-x_s (Boise *et al.* 1993). Bcl-x_l protects cells from apoptosis and bcl-x_s blocks the protective effect of bcl-2 and bcl-x_l, acting as an "anti-anti-apoptosis" protein. It is the relative ratio of homo- and hetero-dimeric forms of these interactive proteins which affects the apoptotic pathway. At the time of this study no antibody specific for the short or long form of bcl-x was commercially available so the polyclonal serum I used does not discriminate between bcl-x_l and bcl-x_s. Because of this I am unable to draw any conclusions as to their relative ratios and role in regulating cell death in PBC BECs. One could hypothesise a pro-apoptotic agonistic effect accentuating the elevated bax expression or, alternatively, an antagonistic effect.

My findings of bax and bcl-x expression in BECs of normal and PBC liver are supported by Dr Matthias Dollinger who carried out a similar immunohistochemistry study phenotyping liver biopsy sections from cases of acute and chronic rejection following orthotopic liver transplantation. He identified particularly strong

expression in BECs during acute rejection and, in biopsies with identifiable bile ducts, during chronic rejection (personal communication).

It is of significant interest to note that at least a proportion of BECs in the PBC liver sections were capable of proliferation. Though the level of proliferating cells may appear relatively low (less than 8% of cells in any duct) it is feasible that, as for the analogous situation where a low level of apoptosis over a long period of time results in a significant, accumulative net loss of tissue, a low level of proliferation may be capable of regenerating a significant amount of tissue. However, one must also consider the differential time length of the two processes with apoptosis proceeding in a fraction of the time taken to complete the cell cycle (Alberts *et al.* 1989; Yonehara *et al.* 1989; Howie *et al.* 1994). Ki-67 positive BECs were more prevalent in the sections showing histological early stage disease, which may reflect a state throughout the liver because studies analysing the proliferative status of hepatocytes in PBC have shown increased proliferation of these cells, which was particularly apparent in the early stages of disease (Rudi *et al.* 1995). There is mounting evidence that intrahepatic bile ducts develop from primitive hepatocytes around branches of the portal vein. A ring of primitive hepatocytes closest to the portal vein branches transforms into bile duct type cells, followed by a second layer forming a double-walled cylinder with a slit like lumen, called the ductal plate. The ductal plate is gradually remodelled, forming a system of anastomising bile ducts. The pattern of expression of a subset of cytokeratins (CK) appears to be specific for this developmental process (Van Eyken *et al.* 1988). Hepatocytes and BECs both express CK8 and CK18, but as the primitive hepatocytes differentiate into BECs they begin to express CK19 followed by CK7. In the adult, liver hepatocytes appear to retain the capacity to acquire these latter "bile duct type" CKs, transforming into bile duct type cells. This has been observed in cases of chronic choleostasis, hepatocellular carcinomas and a case of focal nodular hyperplasia. It is interesting to consider whether the ductular hyperplasia seen in PBC liver sections is an attempt to regenerate the lost BECs via a process analogous to the initial development of the liver during ontogeny. If this is indeed taking place then a better understanding of the

developmental processes resulting in bile duct formation might enable appropriate intervention to enhance this process and regenerate functional bile ducts. However, such a proposition requires elucidation and prevention of the processes causing destruction of BECs to prevent new or regenerated cells succumbing to the same fate.

These results have not, nor did they attempt to, elucidate the actual mechanism by which BECs are destroyed during the course of PBC. We still remain at a loss in understanding how the initial destruction takes place. There is the possibly over pessimistic view that even once we have grasped this knowledge the chronicity of this disease will hamper successful intervention. Patients frequently do not present at clinics until they experience symptoms due to significant and extensive tissue damage, by which time secondary responses probably predominate and prevention of the initial destructive mechanism is likely to be of little therapeutic benefit. In one of the animal models, using a murine graft-versus-host reaction to attempt to induce PBC-like hepatic lesions, administration of monoclonal antibody against LFA-1, but not ICAM-1, was found to inhibit the lesions (Kimura *et al.* 1996). However, the Abs had to be administered prior to cell transfer for this effect to be seen necessitating foresight of the impending tissue destruction, which in the case of PBC is presently unavailable. Does this suggest we should be putting more resources into identifying those most likely to succumb to disease for potential therapies to be successful? If we are able to identify genetic factors that appear to predispose an individual to PBC, when should preventative intervention of the future be initiated? At present there is a relatively wide age range over which patients present but the actual time of disease initiation may be even more variable. PBC is likely to be the result of a multitude of genetic and environmental factors, which will make accurate identification of those unfortunate to suffer the disease a daunting process.

As expected cells of Mϕ/monocyte lineage expressing the CD68 antigen were seen in all liver sections stained with PG-M1. KCs represent 30% of the non-parenchymal sinusoidal cells in the liver (reviewed in te Velde 1994) and were obviously visible

in tissue sections distributed throughout the parenchyma, bearing an elongated, spindly morphology. As there is no antibody which specifically recognises KCs it is not possible to say definitively whether these cells I observed are KCs, though their morphology and situation is strongly suggestive of this. It is interesting to note that the density of these cells was increased in the PBC liver sections. Whether this represents an influx of blood monocytes developing *in situ* into KCs or proliferation of existing KCs is not known. It is also not known whether these cells are contributing directly to the pathogenesis of PBC or merely represent a visible marker of a generally pro-inflammatory, immuno-stimulating environment within the diseased liver. More of these cells were seen in sections showing histological late stage disease suggesting their accumulation may be a secondary effect. If they are involved in BEC destruction one would expect them to be focused around the damaged ducts, however, such PG-M1 positive cells were generally rounder and larger with increased cytoplasmic staining. This morphology is suggestive of activated and stimulated Mϕs. Many reports have highlighted the presence of extensive epithelioid granulomas in PBC liver (Nakanuma and Ohta 1983; Takezawa and Yamada 1984; Yunoue *et al.* 1984; Nakanuma *et al.* 1997) and this study has confirmed their presence in both early and late stage tissue, but not normal liver. Though it has been suggested that granulomas are particularly apparent in early stage disease, I also saw extensive granulomas in late stage disease. One problem with allocating a stage to a particular section is the continuity of this disease. In any section, particularly from larger wedge biopsies, from which late stage sections were frequently derived, there may be tissue destruction representative of several stages of the disease. One duct may be undergoing what histologically appears to represent early stage destruction while other ducts may be completely destroyed. Thus, in such a section allocated histologically late stage, features of early stage disease are also likely to be present. Analysing a single section from a needle biopsy also only gives a two-dimensional view of a tiny section of a vast organ. Though granulomas were often centred around bile ducts, both those apparently intact as well as those undergoing destruction, I frequently observed granulomas in the parenchyma, as others have (Yunoue *et al.* 1984). A three-dimensional image might actually show

these latter granulomas to be focusing around ducts out of the plane of the section. Serial sections would need to be analysed to determine whether this may be the case, but the scarcity of PBC liver biopsy material thwarts such extensive studies.

Granulomas are often seen in diseases such as tuberculosis, leprosy and sarcoidosis where Mϕs centre around indigestible or poorly degradable, persistent substances. It is interesting to speculate whether such material is present in PBC liver stimulating the granulomatous response and what the origin of such material might be. As mentioned in **1.1.4** a variety of infectious agents (*M. gordonae, enterobacteriacae, Salmonella* and *E. coli*) have been advocated to play a role in the aetiology of PBC. Such agents could act as a persistent trigger for an immune response and, if they infected primarily BECs, could explain the focused attack on the ducts. It is also possible that the BECs concentrate some granuloma-inducing material because the cells act as a passage for excretion into the bile ducts and the liver, being a major organ for detoxification, would be a prime site for extraction of such material from the circulation. This localised concentration of such a trigger may explain the initial focused destruction.

Though the actual function of the Mϕ in PBC has not been addressed this analysis of the presence and distribution of PG-M1 positive cells of Mϕ/monocyte lineage supports a role of these cells in the pathogenesis of PBC. Their large numbers, the focused, localised situation of positive cells with increased cytoplasm and extensive epithelioid granulomas suggests they are playing a greater role than merely the result of secondary stimulation accompanying inflammation of the liver.

3.4 Conclusion

To conclude I have shown the presence of proteins involved in executing apoptosis in BECs in PBC consistent with previous reports of apoptosis of these cells (Nakanuma *et al.* 1983; Kuroki *et al.* 1996; Harada *et al.* 1997b; Koga *et al.* 1997). It is still not known what causes this apoptosis but I have also shown at least a subset of BECs is capable of regeneration. It may be that a change in the balance between

apoptosis and regeneration of biliary epithelial cells during the course of disease contributes to the ultimate loss of bile ducts in PBC. However, because of the prolonged time course of this chronic disease and the secondary effects and immune response resulting from bile duct loss intervention of apoptosis is unlikely to be a therapeutic target in the treatment of PBC. I have also confirmed the reports of others showing cells of Mϕ/monocyte lineage contribute to the immune response in PBC. Their presence is increased in diseased liver sections and significant, extensive granulomas exist in tissue of all histological stages.

4 GENOTYPIC ANALYSIS OF THE 5' POLYMORPHIC MICROSATELLITE REGION IN HUMAN *NRAMP1* IN PATIENTS WITH LIVER DISEASE AND EXAMINATION OF *NRAMP1* EXPRESSION

4.1 INTRODUCTION

4.1.1 Analysis of the 5' Promoter Microsatellite Polymorphic Region in the Human *NRAMP1* Gene.

The identification of *nramp1* as a pivotal factor in determining murine susceptibility to a variety of intracellular pathogens was a revelation (Vidal *et al.* 1995a and 1995b). By understanding the mode of action of the gene it was hoped light would be cast upon natural resistance mechanisms against such pathogens, not only in mice but also in the human race where affliction with diseases such as TB and leprosy remain an ever increasing clinical problem. As yet a human equivalent of the murine G>D mutation at residue 169 of the murine protein has not been identified but the human gene has been shown to have at least ten polymorphic sites (Blackwell *et al.* 1995; Buu *et al.* 1995; Liu *et al.* 1995). To date the most interesting of these sites, situated in the 5' untranslated promoter region of the gene, has been associated with susceptibility to RA (Shaw *et al.* 1996 and 1997), TB (Bellamy and Hill 1998; Bellamy *et al.* 1998) and leprosy (Bellamy and Hill 1998). This polymorphic site was reported to have four alleles differing by the number of gt dinucleotide repeats at a putative Z-DNA forming microsatellite repeat. The identified alleles affect *NRAMP1* mRNA expression with allele 3 driving the highest level of expression (Searle and Blackwell 1999). Genotypic-phenotypic analysis has shown an association of this allele with RA (Shaw *et al.* 1996 and 1997) and it has been proposed that under situations where *NRAMP1* is overexpressed hyperstimulated Mϕs could initiate and perpetuate tissue damage, chronic pathology and autoimmune disease. Conversely, in situations where insufficient *NRAMP1* is expressed understimulated Mϕs may fail to overcome and contain pathogens, such as *M. tuberculosis* or *M. leprae*, resulting in increased susceptibility to disease or an inability to fight these infections: an

hypothesis which appears to hold credibility with the reported association between allele 2 and susceptibility to TB (Bellamy and Hill 1998; Bellamy *et al.* 1998). Reporter gene studies have shown allele 3 drives up to ten fold higher levels of expression than alleles 1, 2 or 4. After exogenous stimulation with IFNγ, reporter gene expression increased for all the constructs. However, after addition of LPS, as a second exogenous signal, a further two fold enhancement of expression was seen with allele 3, expression driven by alleles 1 and 4 remained unchanged and there was a significant decrease in allele 2 driven expression (Searle and Blackwell 1999).

It is the possible association of autoimmune disease and the polymorphic microsatellite repeat region that interested me with respect to susceptibility to PBC. As for RA (reviewed in Kingsley and Panayi 1997) mycobacterial or bacterial infection has been proposed as a contributory factor in initiation of PBC. In both diseases Mϕs appear to play an important role, being particularly obvious histologically in granulomas in PBC liver. In both RA and PBC high levels of AAbs are present, though it has yet to be proved whether these are pathogenic. For instance, rheumatoid factor, an Ab directed against the Fc portion of Ig, is found in the majority of RA patients, though it is not specific for RA and is often undetectable in early disease. I wished to genotype PBC patients by RFLP analysis for the 5' microsatellite repeat polymorphism to identify if these patients resemble RA patients in showing a similar increased frequency of allele 3, which may be indicative of Mϕ induced pathology mediated in part via the *NRAMP1* gene. As control populations hepatitis C sufferers were chosen to represent individuals with cirrhosis resulting from infection with a Mϕ-tropic virus, individuals with alcoholic liver disease (ALD) to represent a chemical induced form of cirrhosis and normal non-cirrhotic blood donors. There is no evidence that *NRAMP1* affects the outcome of viral infections and none of the control populations were expected to be associated with a particular *NRAMP1* genotype.

4.1.2 Analysis of *NRAMP1* Expression by Semi-Quantitative RT-PCR

The focus of this project centres around the genotypic and phenotypic effect of *NRAMP1*, in particular with respect to PBC and disease. It was, therefore, natural to investigate the expression of *NRAMP1* in PBC patients at the site of tissue damage, namely the liver. Working on the principle that *NRAMP1* overexpression might be a contributory factor in the pathogenesis of such diseases through its effect on Mϕ activation and function, I wished to analyse the expression profile of the gene in liver biopsy material from PBC patients compared to control tissue. I was interested to determine whether *NRAMP1* was expressed and if a difference in the relative expression levels of the two splice variants of the *NRAMP1* mRNA (Cellier *et al.* 1994) existed in the disease sufferers. The significance of the two identified splice variants of *NRAMP1* is not known but their differential expression represents a possible mode of regulating the amount of functional NRAMP1 protein synthesised. The +alu variant introduces a premature stop codon, which would be expected to result in either a truncated protein or degradation of the partial protein. The analysis was approached by extracting RNA from frozen liver material and developing a semi-quantitative RT-PCR assay to determine the ratio of the two mRNA species expressed using the intensity of the resolved PCR products measured under UV radiation with the Herolab EASY store software. The primers NRAMPFalu and NRAMPRalu (**2.8.3**) were cDNA specific and generated products of different sizes depending on whether the *Alu* insert was present in the template cDNA. The expression levels of the splice variants were compared to those of the housekeeping gene GAPDH, which acted as an internal control. Normal tonsil material was also analysed, representing a tissue with a Mϕ population which could be compared with the liver tissue.

4.2 RESULTS

4.2.1 Genotypic Analysis of the 5' Polymorphic Microsatellite Region in Human *NRAMP1*

4.2.1.1 Development of Genotyping Strategy

Using the primers NRAMPFpol and NRAMPRpol the optimal annealing temperature and cycle number of 65°C and 35, respectively, were determined to give a specific product of approximately 194bp at a point during the exponential phase of the PCR reaction (**Figure 4.1**). It was important that a point during the exponential phase of the reaction was chosen if PCR products were to be analysed on a non-denaturing gel to exclude heteroduplex formation of single stranded DNA sequences of the different alleles in heterozygotic cases. Attempts to resolve the PCR products in 4.5% MetaPhor agarose gel (Flowgen, Lichfield UK) and subsequent staining with EtBr failed to discriminate between the 2bp size differences in PCR products of approximately 194bp, despite manufacturer's claims. This had been anticipated, hence, the *Rsa1* and *Mnl1* digestion strategy, discussed in **2.8.1**, had been designed and was used for all subsequent analyses. Recommended instructions using a rapid horizontal 5% MetaPhor agarose gel procedure to resolve the digested PCR products were followed, but proved problematic due to overheating of the gel (despite running it at 4°C) and the inconvenience of handling the high concentration gel mixture. Lower MetaPhor agarose concentrations were unable to resolve the fragments with sufficient clarity for genotyping.

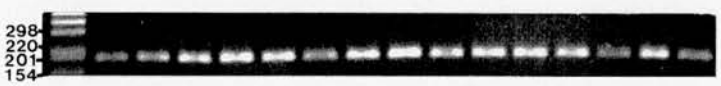

Figure 4.1 NRAMPpol PCR products amplified from genomic DNA of patients with liver disease, prior to restriction enzyme digestion for RFLP analysis to genotype the polymorphic microsatellite repeat region in the promoter of the *NRAMP1* gene. Molecular weight marker, with sizes shown in bp, was run in the left hand lane.

As polyacrylamide gels have better resolution capacity than agarose and its equivalents, MDE gels (Flowgen, Lichfield UK) and 6% and 12% denaturing polyacrylamide gels were tried, with subsequent silver staining of the digested PCR products. Silver staining has a much higher sensitivity as a DNA stain than intercalation of EtBr and UV visualisation. The 6% denaturing polyacrylamide gels gave clear, distinct bands enabling accurate genotyping and were used to genotype all the DNA samples analysed. By using a denaturing gel any possible problem of heteroduplexes arising during late stages of the PCR reaction were eliminated and a double band was observed for each of the denatured fragments.

4.2.1.2 Identification of Novel Polymorphisms

The system of allele identification was designed to identify individual alleles on the basis of differential mobility by gel electrophoresis according to the length of the digested fragments (**Figures 4.2a** and **4.2b**). As predicted I found the band patterns expected for the previously published alleles 1, 2 and 3 whose sequence is shown in **Table 4.1**, but have not identified a pattern representing any of the sequences published as allele 4 in any of the 246 cases I analysed. The sequence of the microsatellite repeat region of allele 2 and allele 3 were initially confirmed by sequencing undigested PCR products. PCR products from individuals homozygous for allele 3 (according to the RFLP analysis results) gave a clear, distinct sequence with nine (gt) repeats for the terminal repeat (**Figure 4.3**). At the time of sequencing the PCR products no individuals homozygous for allele 2 had been identified by RFLP analysis so PCR products from an allele 2/allele 3 heterozygote were sequenced. As expected clear, distinct sequence was obtained until the ninth (gt) repeat of the terminal repeat, after which point the sequences of allele 2 and allele 3 became superimposed. Though this technique proved capable of generating sequence data over the microsatellite repeat region for the two alleles it was insufficient for obtaining sequence data across the whole length of the PCR products, despite exhaustive attempts altering the protocol by adding DMSO and/or manganese, substituting 7-deaza-dNTPs for the dNTPs, altering the primer concentrations and including formamide in the sequencing gel. Therefore, the alleles

were subsequently sequenced completely after cloning the PCR products in the pCR2.1 vector (**Figure 4.4**).

In addition to the expected alleles described above, I found two unexpected banding patterns showing variation in size of the *Rsa1* and *Mnl1* bands, predicted to be of constant size 84bp and 77bp respectively. These were investigated further and named allele 5 and allele 6, respectively. Identification of these allele patterns were consistent when analysis was repeated several times from DNA extracted at different times from the same blood sample, from separate blood samples from the same individual, and from DNA extracted from blood and paraffin embedded material from the same individual. Alleles 5 and 6 were only seen in the heterozygous state. The banding patterns corresponding to alleles 2, 3, 5 and 6 are shown in **Figures 4.2c** and **4.2d**.

Allele	Sequence
Allele 1*$#	$t(gt)_5ac(gt)_5ac(gt)_{11}ggcaga(g)_6$
Allele 2*$#	$t(gt)_5ac(gt)_5ac(gt)_{10}ggcaga(g)_6$
Allele 3*$#	$t(gt)_5ac(gt)_5ac(gt)_9ggcaga(g)_6$
Allele 4*	$t(gt)_5ac(gt)_{10}ggcaga(g)_6$
Allele 4$	$t(gt)_5ac(gt)_5ac(gt)_4ggcaga(g)_6$
Allele 4#	$t(gt)_5ac(gt)_9ggcaga(g)_6$
Allele 5	$t(gt)_4ac(gt)_5ac(gt)_{10}ggcaga(g)_6$
Allele 6	$t(gt)_5ac(gt)_5ac(gt)_4at(gt)_4ggcaga(g)_7$

Table 4.1 Summary of alleles of human *NRAMP1* 5' promoter polymorphic site showing the sequence of the alleles identified in previous studies (alleles 1-4) (* Blackwell 1996; Shaw *et al.* 1996 and 1997: $ Blackwell *et al.* 1995: # Searle and Blackwell 1999) and in this study (alleles 1, 2, 3, 5 and 6).

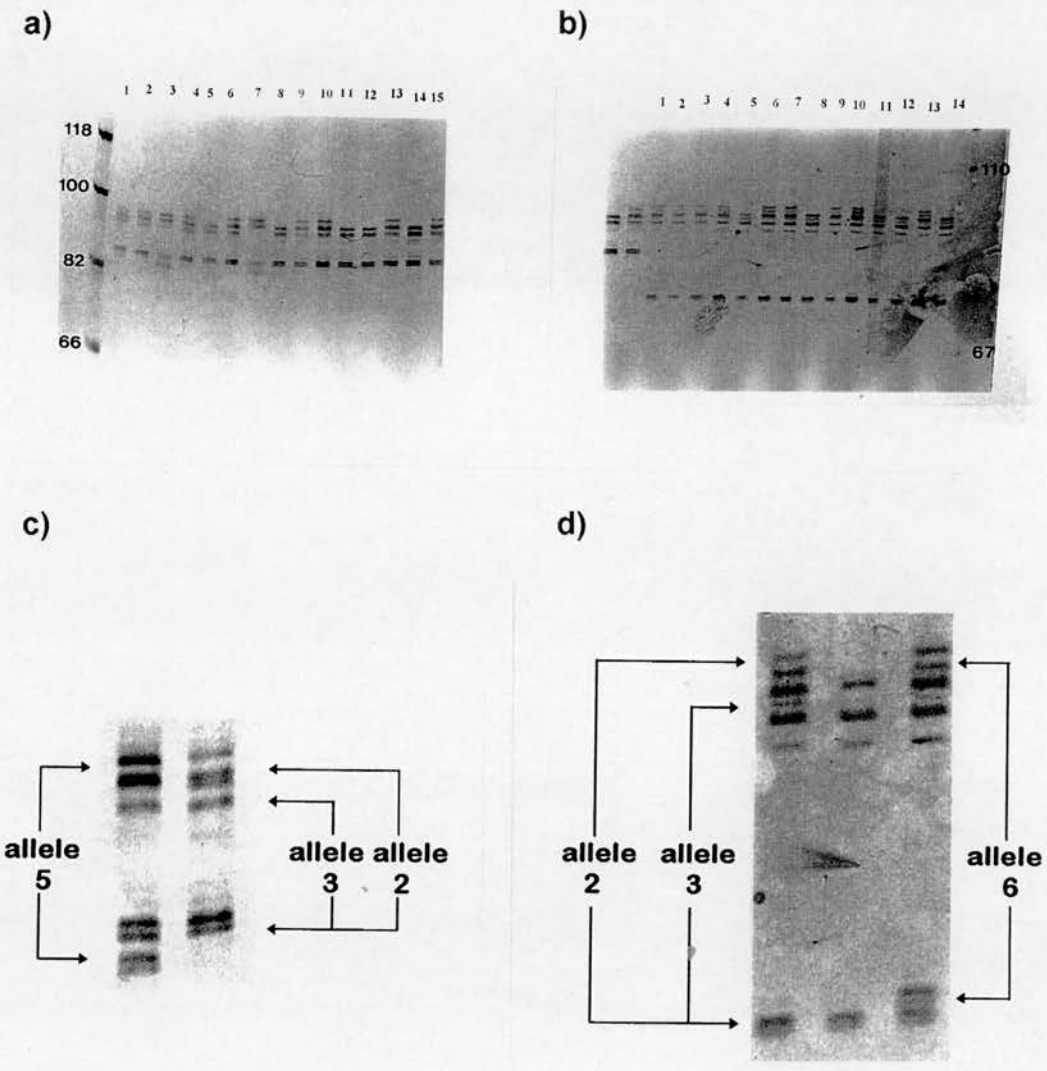

Figure 4.2 showing the type of RFLP gel for **a)** *RsaI* and **b)** *MnlI* restriction enzyme digestion of NRAMPpol PCR products amplified from genomic DNA from patients with liver disease (**1-15**) from which genotypes were deduced. Patients **3** and **7** show the allele 5 banding pattern. Precise identification of allele 5 and allele 6 can be seen in close up in **c**) depicting the *RsaI* digestion products for **alleles 2**, **3** and **5** and **d**) depicting the *MnlI* digestion products for **alleles 2**, **3** and **6**. Molecular weight marker with sizes in bp is shown in the left hand lane in **a)** and the right hand lane in **b)**.

4.2.1.3 Characterisation of Allele 5

In cases showing the banding pattern associated with allele 5 the *Mnl1* digestion repeatedly resulted in a variable fragment consistent with allele 2 ($t(gt)_5ac(gt)_5ac(gt)_{10}g$) but a product 2bp less than the predicted 84bp "constant" fragment (**Figure 4.2c**). This predicted a 2bp deletion in the region of the amplified sequence 5' to the first *Rsa1* site and, based on the *Mnl1* digestion results, 3' to the first *Mnl1* site (**Figure 4.5**). This region includes the initial $(gt)_5$ of the microsatellite region. The *Mnl1* digestion gave a fragment encompassing this region predictive of allele 3 ($t(gt)_5ac(gt)_5ac(gt)_9g$), 2bp less than allele 2 (not shown). To confirm this hypothesis and identify the site of the predicted deletion I cloned undigested PCR products from DNA known to contain allele 5, genotyped the cloned DNA and sequenced the insert of clones giving a pattern representing allele 5. This showed allele 5 to have the sequence $t(gt)_4ac(gt)_5ac(gt)_{10}g$, with a gt deletion in the first $(gt)_5$ dinucleotide repeat identified in the other alleles (**Figure 4.6**).

4.2.1.4 Characterisation of Allele 6

In the case showing the banding pattern associated with allele 6 the *Rsa1* digestion gave a product of size intermediate to that predicted for alleles 2 and 3 (not shown). The *Mnl1* digestion produced a variable fragment predictive of allele 3 and a product estimated to be 1bp larger than the "constant" 77bp fragment (**Figure 4.2d**). These findings were consistent with a 1bp insertion 3' to the second *Mnl1* site downstream of the polymorphic microsatellite repeat region (**Figure 4.5**). To confirm this hypothesis and identify the site of the predicted insertion I cloned undigested PCR products from DNA known to contain allele 6, genotyped the cloned DNA and sequenced clones giving a pattern representing allele 6. This showed insertion of an extra dGTP in a hexanucleotide g repeat seven base pairs 3' of the final gt of the polymorphic site. In addition sequencing of this allele showed the final polymorphic gt repeat was interrupted and the region had the sequence $t(gt)_5ac(gt)_5ac(gt)_4at(gt)_4g$ (**Figure 4.7**).

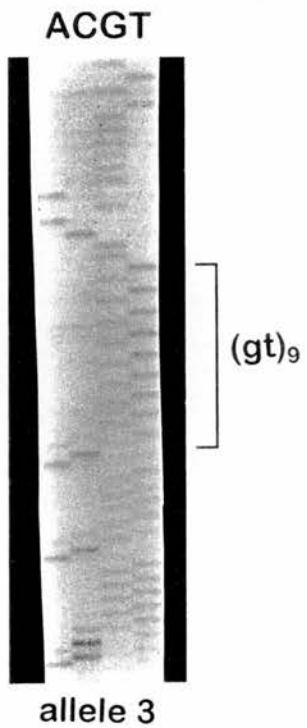

Figure 4.3 Sequence of **allele 3** of the polymorphic microsatellite region in the *NRAMP1* promoter, sequenced from NRAMPpol PCR products (as described in **2.8.1** and **2.15.1**). **A**: adenine, **C**: cytosine, **G/g**: guanine, **T/t**: thymine.

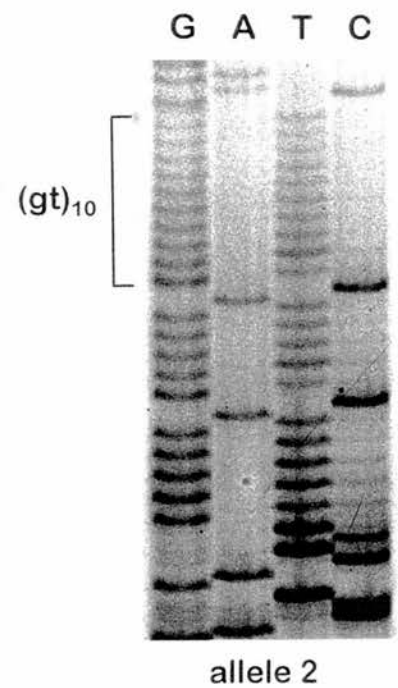

Figure 4.4 Sequence of **allele 2** of the polymorphic microsatellite region in the *NRAMP1* promoter, sequenced from cloned NRAMPpol PCR products (as described in **2.8.1** and **2.15.2**). **G/g**: guanine, **A**: adenine, **T/t**: thymine, **C**: cytosine.

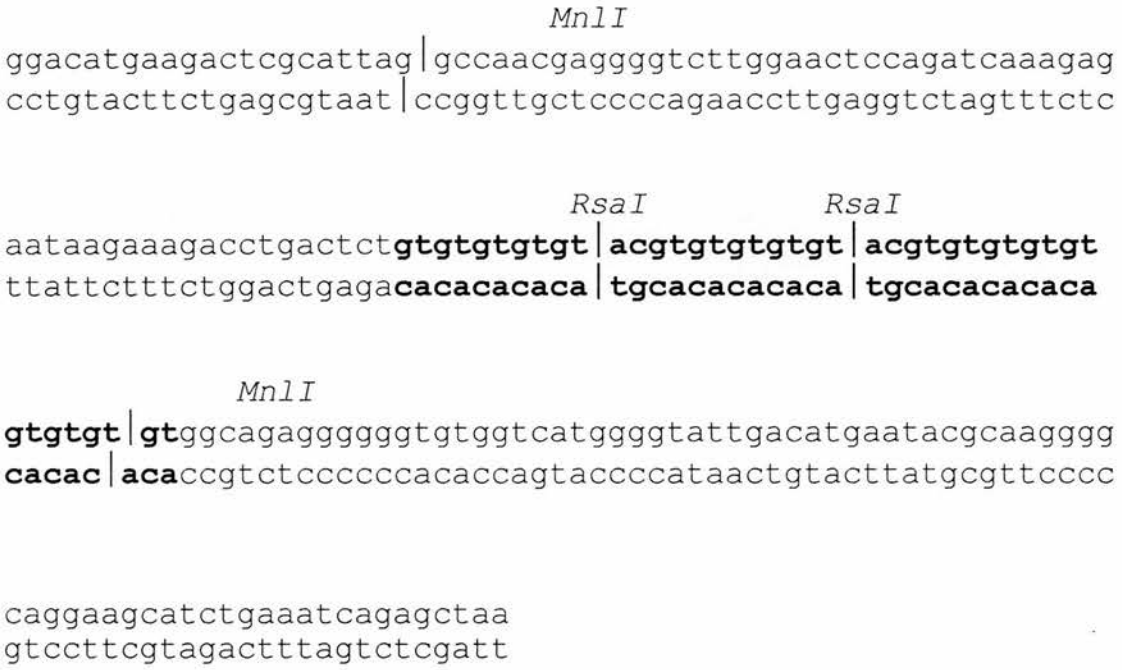

Figure 4.5 Sequence of part of the promoter region of the human *NRAMP1* gene (Accession number X82016, 59-240bp) amplified by PCR using NRAMPpol primers to genotype the polymorphic microsatellite region, shown in bold. The *RsaI* and *MnlI* restriction enzyme sites used to digest the amplified DNA are shown. The enzymes recognise the following sites and cut at the position shown by the vertical slash; n represents any base.

MnlI | $(n)_6$gagg
| $(n)_7$ctcc

RsaI gt|ac
ca|tg

The sequence for allele 3 is used in this figure. Sequences over the polymorphic region of the other alleles identified in this study and those previously published are shown in **Table 4.1**.

4.2.1.5 Frequency of Alleles Identified in the Groups Studied.

The sequence of the five alleles I detected (alleles 1, 2, 3, 5 & 6) and allele 4 reported by Blackwell *et al.*, as three different sequences, are shown in **Table 4.1**. **Table 4.2** shows the frequency of alleles in the normal group I analysed and those reported in previous studies. The frequencies of the five alleles identified in the four groups I genotyped: normal controls, PBC, ALD and hepatitis C patients are shown in **Table 4.3**. In the PBC population genotyped allele 5 was significantly more common, though still rare, than in the other groups studied ($p<0.024$ compared with normal controls; $p<0.012$ compared with ALD or hepatitis C; Fisher Exact Test).

	Allele					
	1	**2**	**3**	**4**	**5**	**6**
Present study n=78	<0.01	0.27	0.70	0.00	0.02	0.00
***Brazilian n=72**	0.02	0.33	0.64	<0.01	0.00	0.00
#Caucasian n=120	0.02	0.25	0.73	0.00	0.00	0.00
#Asian n=40	0.05	0.10	0.85	0.00	0.00	0.00

Table 4.2 Frequencies of alleles at the 5' *NRAMP1* microsatellite repeat polymorphic site identified in the normal control group in this study (**Present study**) compared to the frequencies of alleles in normal **Brazilian**, **Caucasian** and **Asian** control groups published previously (* Blackwell *et al.* 1995: # Liu *et al.* 1995). The sequences of the six alleles are given in **Table 4.1**.

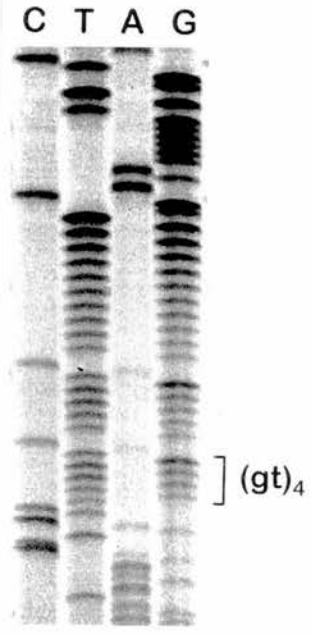

Figure 4.6 Sequence of **allele 5** of the polymorphic microsatellite region in the *NRAMP1* promoter, sequenced from cloned NRAMPpol PCR products (as described in **2.8.1** and **2.15.2**). **C**: cytosine, **T/t**: thymine, **A**: adenine, **G/g**: guanine.

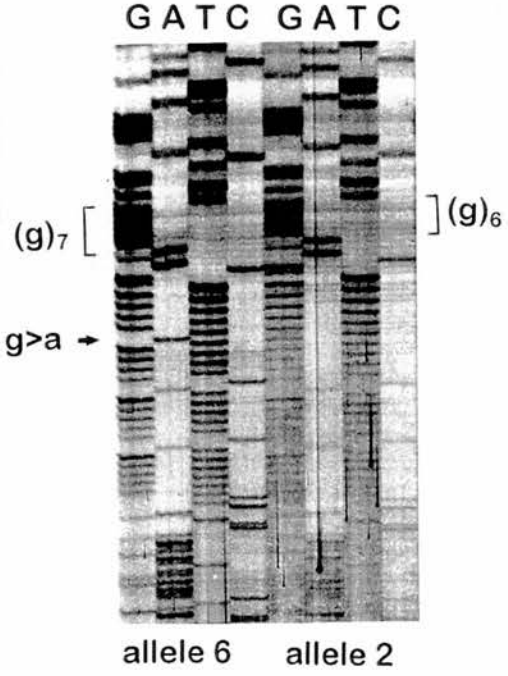

Figure 4.7 Sequence of **allele 6** and **allele 2** of the polymorphic microsatellite region in the *NRAMP1* promoter, sequenced from cloned NRAMPpol PCR products (as described in **2.8.1** and **2.15.1**). **G/g**: guanine, **A**: adenine, **T/t**: thymine, **C**: cytosine.

	Allele					
	1	**2**	**3**	**4**	**5**	**6**
Normal n=78	1 (<0.01)	42 (0.27)	110 (0.70)	0 (0.00)	3 (0.02)	0 (0.00)
ALD n=76	0 (0.00)	40 (0.26)	109 (0.71)	0 (0.00)	2 (0.01)	1 (<0.01)
PBC n=53	0 (0.00)	28 (0.26)	70 (0.66)	0 (0.00)	^8 (0.08)	0 (0.00)
Hepatitis C n=39	0 (0.00)	22 (0.28)	56 (0.72)	0 (0.00)	0 (0.00)	0 (0.00)

^p<0.024 compared to normal control.

Table 4.3 Numbers and frequencies, in brackets, of the alleles at the 5' *NRAMP1* microsatellite repeat polymorphic site identified in the four groups, **Normal** controls, alcoholic liver disease (**ALD**), primary biliary cirrhosis (**PBC**) and **Hepatitis C**, analysed in this study. The sequences of the alleles are given in **Table 4.1**. Statistical analysis of frequencies was carried out using the Fisher Exact Test.

4.2.2 Analysis of *NRAMP1* Expression by Semi-Quantitative RT-PCR

4.2.2.1 Developing Semi-Quantitative RT-PCR Assay

The housekeeping gene encoding the GAPDH protein was chosen as a standard control against which expression of *NRAMP1* could be compared. Only a ratio of the two *NRAMP1* splice variants relative to each other and to GAPDH was sought, not absolute amounts of message of the three species. Titrations of RNA, cDNA and Mg^{2+} in the reactions determined the optimal conditions to be a fixed amount of 1μg RNA as template for the RT reaction and a fixed amount of 1μl template cDNA and 1.5mM Mg^{2+} in the PCR. Comparison of the intensity of the different species was made over the exponential phase of the reactions, determined by comparing the intensity of the products, resolved by 2% agarose gel electrophoresis, at different cycle numbers using the Herolab EASY store software. **Figure 4.8** shows a typical graphical representation showing the exponential phase for amplification of GAPDH. The +alu (containing the *Alu* sequence insert) and -alu (encoding the full length message) products, generated using the NRAMPalu primers, were amplified at equal efficiency over the cycle numbers analysed (**Figure 4.9**), which is necessary for such comparisons. As the GAPDH and NRAMPalu primers had been

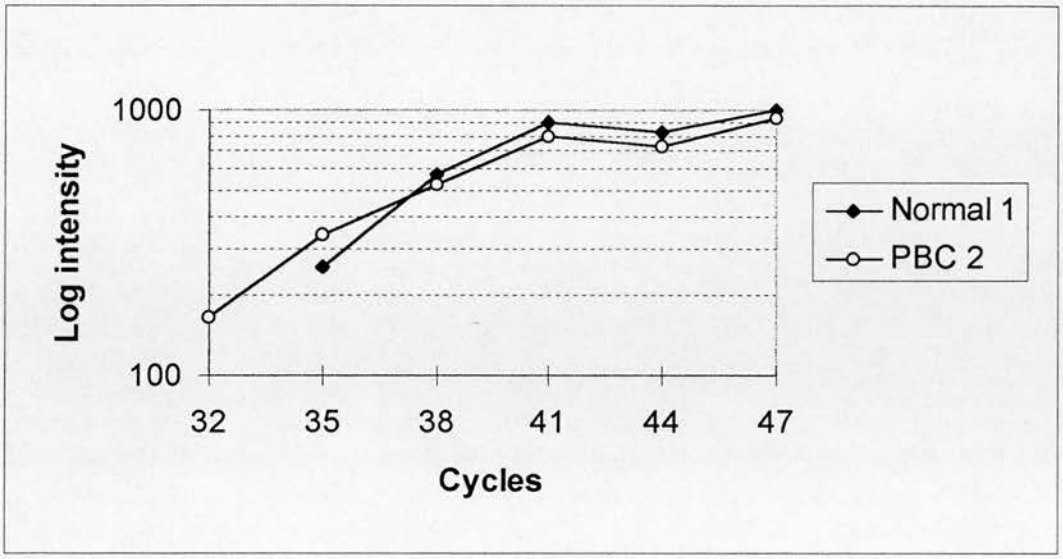

Figure 4.8 Log intensity values for GAPDH RT-PCR products removed after variable numbers of cycles during the PCR reaction to determine where the exponential phase of the reaction occurs. The RNA was extracted from normal and PBC liver tissue; the patient numbers correspond to those used in **Figures 4.12** and **4.13**.

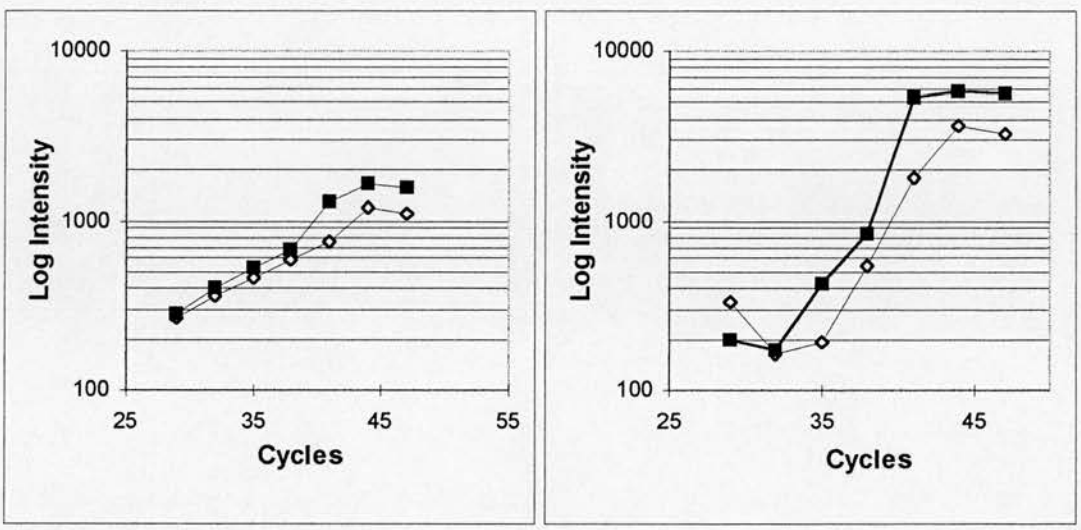

Figure 4.9 Log intensity values for two normal liver samples of the +alu (open diamonds) and -alu (closed squares) RT-PCR products removed after variable numbers of cycles during the PCR reaction to determine where the exponential phase of the reaction occurs and confirm the two splice variant products are amplified with equal efficiency. The NRAMPalu primers used are described in **2.8.3**.

designed with each primer spanning an intron-exon boundary all products resulted from amplification of mature spliced message. The primers were designed to work at the same annealing temperature and extension time so all three species could theoretically be amplified in one reaction to reduce pipetting errors. However, after checking for cross-primer interference by adding primers specific for genomic DNA (NRAMPFpol and NRAMPRpol described in **2.8.1**) to PCRs for amplification of GAPDH cDNA there was an obvious decrease in the yield of the GAPDH product when the second pair of primers was present. This interference, solely due to the presence of the second set of primers which were not generating any PCR product, suggested results obtained from a PCR containing both the GAPDH and NRAMPalu primers would be unrepresentative of the real message status of the samples. Hence, all analyses were carried out with separate reaction tubes for the GAPDH and NRAMPalu PCRs using the same PCR thermal heating block to eliminate inter-block temperature variations.

4.2.3 mRNA Expression in Human Tissue

GAPDH mRNA expression was detected by RT-PCR in all the human tissues tested (**Figure 4.10**) which acted as a positive control for successful RNA extraction and cDNA synthesis. In normal tonsil expression of the +alu splice variant was seldom detected by RT-PCR and on the one occasion when it was found it was at a low level (**Figure 4.11**).

Both -alu and +alu splice variants were consistently detected by RT-PCR in normal (**Figure 4.11**) and PBC liver material. However, due to the scarcity of frozen PBC and normal liver material only limited analysis and comparison of the expression pattern of *NRAMP1* in these samples could be carried out. **Figure 4.12** shows the ratios of the intensities of the -alu/+alu message and the -alu and +alu product intensities relative to the GAPDH product intensities for the analyses carried out with three PBC and two normal liver samples. When cDNAs prepared from the three PBC livers and two normal livers were compared two of the patients had a higher

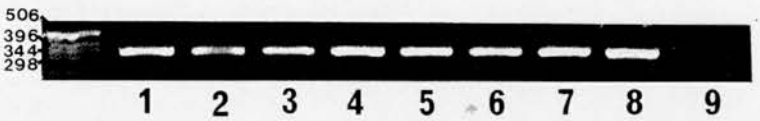

Figure 4.10 GAPDH RT-PCR products showing expression of *GAPDH* mRNA in normal liver (lanes **1-3** and **5-7**) and normal tonsil (lanes **4** and **8**). Lane **9** shows the negative control reaction and a molecular weight marker, with sizes shown in bp, was run in the left hand lane. For details of GAPDH primers see **2.8.2**.

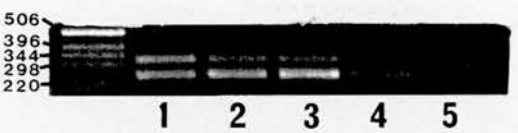

Figure 4.11 NRAMPalu RT-PCR products showing expression of *NRAMP1* mRNA in normal liver (lanes **1-3**) and normal tonsil (lane **4**). The higher molecular weight band represents the +alu product and the lower molecular weight band represents the -alu product. Lane **5** shows the negative control reaction and a molecular weight marker, with sizes shown in bp, was run in the left hand lane. For details of NRAMPalu primers see **2.8.3**.

ratio of the intensity of the –alu:+slu message compared to the control liver analysed in parallel. In the third paired analysis the reverse was found with the normal liver having a higher -alu:+alu message ratio (**Figures 4.12** and **4.13**). As such, no conclusion could be drawn as to the relative levels of expression of the two splice variants of the *NRAMP1* mRNA in the disease liver samples compared to the normal liver samples. In the two samples where the PBC liver showed a higher -alu:+alu message ratio over the normal liver samples the same normal liver material was being used as the control. In all liver samples analysed more -alu message was present, i.e. the message encoding the full length protein.

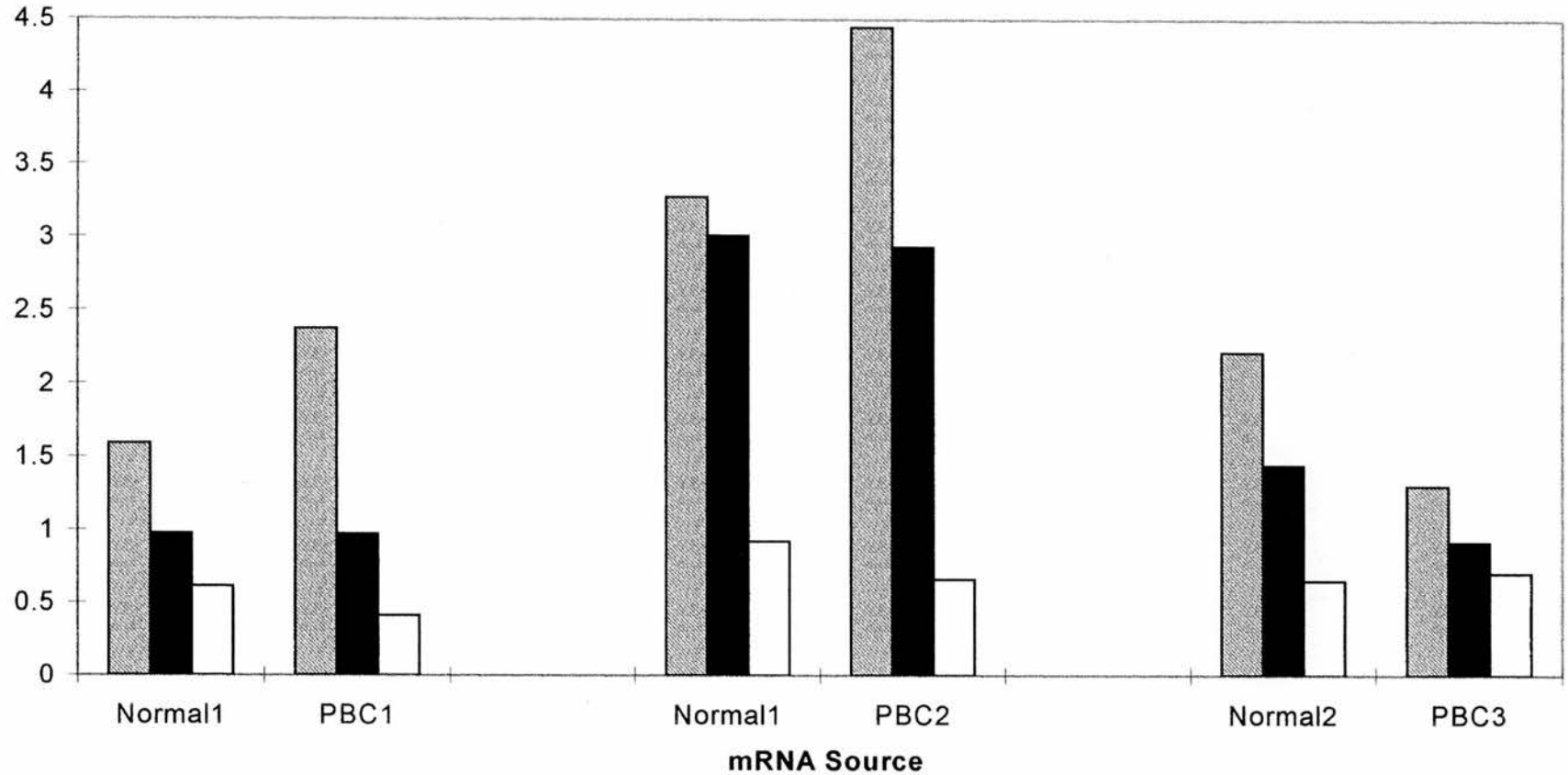

Figure 4.12 Ratio of the intensities of **-alu/+alu** (shaded), **-alu/GAPDH** (black) and **+alu/GAPDH** (white) RT-PCR products for two normal (**Normal1** and **2**) and three PBC (**PBC1**, **2** and **3**) liver samples. The patient numbers correspond to those used in **Figure 4.8**. Details of the assay design and PCR primers are described in **2.8.2** and **2.8.3.**

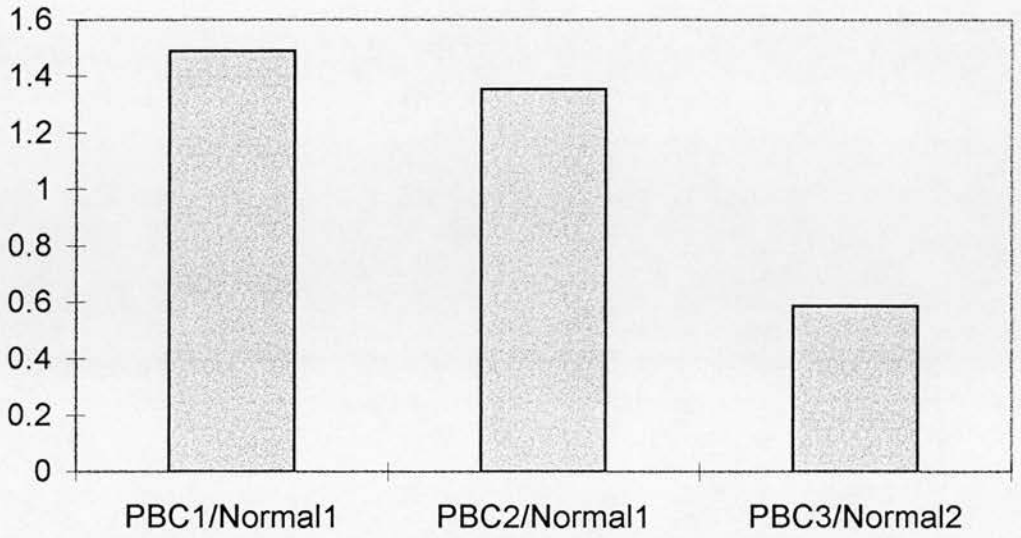

Figure 4.13 Bar chart showing the ratio of PBC liver -alu/+alu RT-PCR products relative to normal liver -alu/+alu RT-PCR products for tissue from two PBC and two normal cases. The NRAMPalu primers and RT-PCR design are described in **2.8.3**.

Attempts to determine relative levels of expression of the *NRAMP1* splice variants in liver tissue from hepatitis C sufferers were unsuccessful. These samples were chosen to represent a cirrhosis disease mediated by a viral infection for comparison with the PBC cases. In none of the six cDNAs used as template DNA was +alu message detected. In two of the cases a barely detectable -alu species was identified. Re-amplification of PCR products from the initial amplification rounds still failed to generate detectable *NRAMP1* message in the majority of the samples, only increasing the level of product of the -alu species in cases where a very low level of product had been detectable after the first PCR amplification round. GAPDH message was successfully amplified from all cDNAs from the hepatitis C cases.

4.3 DISCUSSION

This study identified two novel alleles (Graham *et al.* in press) at the previously identified polymorphic microsatellite repeat sequence in the promoter of the human *NRAMP1* gene (Blackwell *et al.* 1995). One of these, allele 5, is significantly more frequent, but still uncommon, in the PBC population studied (8/53) compared to the

normal controls (3/78) ($p<0.024$), ALD (2/76) ($p<0.012$) or hepatitis C patients (0/39) ($p<0.012$) (Fisher Exact Test). The repetitive nature of the sequence analysed required a stringent, sensitive and reproducible detection method, due to the possibility of slippage or infidelity of the *Taq* polymerase enzyme during PCR amplification. The method I adopted gave consistent results when DNA was extracted from the same blood sample at different times, when DNA was extracted from blood taken from the same individual at different times and when DNA was extracted from blood and paraffin embedded material from the same individual.

A number of alleles at this site have previously been reported by sizing this polymorphic region as a single fragment (Blackwell *et al.* 1995; Liu *et al.* 1995). However, my strategy used restriction enzyme digests designed to size both the whole polymorphic site as a single fragment (*Mnl1*), and the size of fragments containing the 5' dinucleotide and 3' dinucleotide repeats of the region as distinct entities (*Rsa1*) (**Figure 4.5**). It was the combined results of these digests which allowed detection of allele 5 and allele 6 and confirmation of the previously reported alleles 1, 2 and 3 (reviewed in Blackwell 1996; Shaw *et al.* 1996 and 1997).

Allele 5, has a gt deletion in the first, normally $(gt)_5$, repeat region of the microsatellite repeat of allele 2. I am confident that this is a genuine allele and not an artefact or the result of infidelity of the *Taq* polymerase enzyme used. The allele was identified consistently and repeatedly when samples were reanalysed. Allele 5 was only found in the heterozygous state with no bias to inheritance with allele 2 or 3. I do not know what effect, if any, this allele has on the levels of *NRAMP1* expression but it is feasible that its position within this Z-DNA forming sequence may influence expression, as the previously described alleles have been reported to do (Searle and Blackwell 1999). When *NRAMP1* expression levels have been compared for the previously reported alleles 1, 2, 3 and 4, allele 3 was shown to drive the highest levels of expression of a reporter gene under unstimulated conditions. Stimulation with IFNγ and LPS differentially affected expression from the alleles with allele 1 showing a significant increase on addition of IFNγ and a further increase when LPS

was added. Allele 2 responded to IFNγ stimulation by increasing reporter gene expression, however, subsequent LPS addition resulted in decreased expression. The other two alleles were unresponsive to LPS addition but showed increased expression in response to IFNγ (Searle and Blackwell 1999). Reporter gene expression studies, similar to those described, would be required to investigate the effect of allele 5 on mRNA expression compared to the other identified alleles, but in the light of the above report it is highly likely that this allele will have a functional effect on expression. Whether this has a significant impact physiologically, particularly in the subset of PBC patients carrying allele 5, to influence the course of disease or infection remains an area for further research. None of the individuals who carried allele 5 were homozygotes and, therefore, for the allele to have a significant phenotypic effect one would expect it would need to act in a dominant fashion. However, the overall levels of expression will reflect the message potentially derived from both alleles, so an individual carrying one allele which drives either a very high or a very low level of expression, or an allele which responds optimally or is unresponsive to immune stimulants, could display a phenotypic effect despite carrying a second "normal" allele which lacks such extreme characteristics. It is possible that the increased frequency of allele 5 in the PBC population reflects inheritance of another susceptibility locus or functional *NRAMP1* polymorphism, in partial linkage disequilibrium with allele 5, which contributes to initiation or maintenance of the disease.

It is important to note that had I been relying solely on results from a single analysis of the size of the microsatellite repeat as a whole, then allele 5 would have been mistaken for allele 3, the allele which is at highest frequency in all previously published reports, as both alleles are the same length. Previous reports have been sizing the whole microsatellite repeat region within PCR fragments of 108-122bp (Blackwell *et al.* 1995) or 286-290bp (Liu *et al.* 1995; Abel *et al.* 1998) and individuals actually carrying allele 5 may have been mistakenly identified as allele 3 bearers. As allele 5 is at a much lower frequency than allele 3, sequencing random

cases genotyped to have an allele the size of allele 3 in these studies would be unlikely to include a case with allele 5, hence, these might go undetected.

I failed to find evidence for any of the alleles 4 previously published in the 246 cases I genotyped. However, allele 4 was only found at a frequency of <0.01 when 72 Brazilians were genotyped for this polymorphic site (Blackwell *et al.* 1995). Publication of the sequence allele 4 represents has been inconsistent with three sequences published to date (Blackwell *et al.* 1995; reviewed in Blackwell 1996; Shaw *et al.* 1996 and 1997; Searle and Blackwell 1999). In the most recent publication the authors say the initial sequence published (Blackwell *et al.* 1995) was an error but publish a third sequence in this paper (Searle and Blackwell 1999). It is presently not known whether this is the genuine sequence or a further error.

Allele 6 is unlikely to be present in the general population at a significant level and it was only found in one ALD patient. This individual had altered sequence in both the final dinucleotide repeat and in a single nucleotide repeat region, in close vicinity to the microsatellite repeat under investigation, which may reflect the instability of such repetitive DNA sequence. As my procedure for allele designation is reliant on differences in the size of digested fragments of DNA it can not be ruled out that other individuals may have interrupted repeats or altered sequence at sites other than the *Mnl1* or *Rsa1* restriction enzyme recognition sites, which could only be determined by sequencing every individual for both alleles.

It is perhaps surprising that greater variation at this polymorphic site has not been reported by others or identified in this study. Such dinucleotide repeats are inherently unstable and subject to expansion or retraction during DNA replication. It appears that this stability also extends to sequence further upstream of the site I analysed because a study of the region from -3434 to -594, upstream of the transcription start site at position zero, has identified eleven *Alu* element-related sequences and one *Mer* family element (Roger *et al.* 1998). Over 500,000 *Alu* repeated sequences exist interspersed throughout the haploid genome with an average spacing of 4kb. The 11

Alu elements in this 3kb region flanking *NRAMP1* is, therefore, unusual particularly with the additional presence of a relatively rare *Mer* element. This high density of different DNA repeats and recombination hot spots would lead one to believe the region would be a focus of genomic instability, genetic recombination and/or sequence variability. However, this does not appear to be the case and the region has been well conserved since the divergence of humans and great apes. The oldest *Alu* elements of the five *Alu* subfamilies present in the region, *Alu J*, is estimated to have transposed 80 million years ago, providing ample opportunity for variation. It is also interesting to point out that *Alu* insertions are not restricted to the flanking region of *NRAMP1* as the mRNA splice variant, discussed below and in **1.8.8.1**, results from alternative splicing of an *Alu* sequence element.

A familial predisposition to PBC has been reported (Bach and Schaffner 1994) and, as discussed in **1.1.4**, studies to investigate association between PBC and polymorphisms at a number of genetic loci, including HLA (Ercilla *et al.* 1979; Santrach *et al.* 1990; Fugger *et al.* 1991; Morling *et al.* 1992; Underhill *et al.* 1992 and 1995; Gregory *et al.* 1993; Seki *et al.* 1993; Onishi *et al.* 1994; Zhang *et al.* 1994a; Mella *et al.* 1995), TNFα (Fugger *et al.*1989; Spengler *et al.* 1990; Messer *et al.* 1991; Gordon *et al.* 1996; Watt *et al.* 1997), TAP1 and 2 (Gregory *et al.* 1994), GSTM1 (Davies *et al.* 1993) and interleukin-10 (Zappala *et al.* 1998) have been carried out. However, to date only weak associations with C4B2 (Briggs *et al.* 1987) and TNFα have been reported and HLA Class II associations remain controversial. The idea that overexpression of *NRAMP1*, due to inheritance of allele 3, in combination with additional genetic, infectious and environmental factors is an attractive proposition in the initiation of chronic pathology or autoimmune disease such as RA. However, I did not find a similar association in the PBC population I studied: in fact the frequency of allele 3 was lowest in the PBC group of the 4 groups tested, the decreased incidence being accounted for in the increased frequency of allele 5. Susceptibility to PBC, and the other diseases which *NRAMP1* polymorphisms have been reported to associate with (Shaw *et al.* 1996 and 1997; Hofmeister *et al.* 1997; Neibergs *et al.* 1997; Abel *et al.* 1998; Bellamy *et al.* 1998),

are complex diseases and likely to result from a combination of interacting factors, which may include *NRAMP1* genotype. The low, but significantly increased frequency of allele 5 I have found in PBC patients, compared to control groups, may affect the activity or function of these individuals' macrophages. However, its presence in only 15% of the cases I studied suggests it is unlikely to play a significant role in the aetiology of PBC.

Using RT-PCR analysis to characterise the expression profile of the *NRAMP1* gene in human tissue I have successfully shown expression of the -alu mRNA splice variant in normal tonsil, but little or no expression of the +alu variant. The tonsil RNA was extracted from pieces of stored frozen material, but it is not known if these originated from one or more than one individual. If they were from a single donor then the repeated lack of detection of the +alu message may be of little significance. If, however, the results are representative of a larger number of paediatric tonsillitis sufferers, the lack of +alu message may reflect the state of activation of Mϕs partaking in the inflammatory immune response present in this peripheral lymphoid organ. As the tonsil material available was derived from sufferers with severe tonsillitis one would expect influx into the tissue of a large number of activated Mϕs. It is interesting to consider what the expression status of *NRAMP1* in an uninflamed, resting tonsil might be and whether the relative levels of the splice variants may alter, suggesting a potential regulatory role of the +alu species.

My RT-PCR results, analysing a limited supply of normal and PBC liver, confirmed previous reports of *NRAMP1* expression in this tissue (Cellier *et al.* 1994). The aim of analysing the relative levels of expression of the +alu and -alu splice variants and their comparison with *GAPDH* expression was hampered by the lack of frozen liver tissue for RNA extraction. Therefore, comparative results of only three paired analyses are available and two of these include the same normal liver sample. As such it is not possible to conclude whether the expression pattern varies in the disease liver, though the presence of large numbers of Mϕs in a histologically activated state in PBC liver biopsy material suggests this is a likely possibility. Had

further liver samples been available one would have hoped to determine if these preliminary results represent natural widespread variations between liver expression profiles or an isolated occurrence in one of the two normal liver samples analysed, with the disease and normal livers showing genuine differences.

It was unfortunate that results were unavailable to compare the third, hepatitis C, population's *NRAMP1* expression profile with the PBC and normal cases. It is not known whether the lack of *NRAMP1* RT-PCR products detected in these cases is indicative of expression of the relevant mRNAs below a threshold for detection by the procedure adopted or a genuine lack of expression in the liver of these hepatitis C patients. I am in no doubt of the quality of the RNA the cDNA was derived from as it was kindly provided by an experienced and professional colleague, Mrs Frances Rae, who had utilised a similar practice and technique to myself when undertaking the extraction.

Semi-quantitative RT-PCR analyses have been frequently criticised and it is important to take into account the potential pitfalls and limitations of this technique. The exponential amplification nature of PCR means small errors can be greatly amplified. Throughout the experiments great care was taken to standardise the procedure and tissue samples were taken through the whole analysis study in parallel. Though potential inter-tube variations can not be eliminated by this approach, external variations between separate experiments, such as ambient temperature, stock reagents etc., can be excluded. When extracting the RNA the appropriate weight of tissue to RNA Reagent ratio was used, and the sample weights were kept as similar as possible. After the RNA had been extracted its concentration was estimated by spectrophotometry and cDNA synthesised from 1μg of total RNA in a fixed volume so the cDNA reflected the messages present in this fixed amount of RNA. The PCRs used 1μl of the cDNA solution and all reactions and pipetting were performed as scrupulously as possible to avoid incorporating inter-tube variations. When semi-quantitatively comparing PCR products it is essential that the species in question are amplified equivalently and this was confirmed by analysing

the intensity of the product band, after agarose gel electrophoresis, of samples removed from the PCR thermal heating block after successive cycles of the reaction. A point during the exponential phase of the amplification reaction must be used for analysis before the reaction plateaus off due to exhaustion of the enzyme or reagents in the tube. My analyses consistently found the range of the exponential phase to be over the same cycle numbers and they also showed the +alu and -alu species were amplified at the same rate, enabling a genuine comparison to be made between the initial levels of the mRNAs. By comparing the levels of GAPDH products I was able to confirm the starting levels of RNA were equivalent in the samples supporting the fidelity of the technique. When analysing the PCR products great care was taken to load the agarose gels with an equal volume of the amplified DNA. The intensity reading of the bands varies depending on the integration at which the detector is set, the thickness of the agarose gel and the amount of EtBr incorporated in the gel. Therefore, samples to be compared were always loaded as close to each other on the gel as possible, which reduced variation in the background reading of the gel against which the bands' intensities were measured. I designed the PCR primers so that they would amplify products of approximately similar sizes but which were still easily resolvable. This was because the intensity of the detected product band is proportional to the amount of EtBr incorporated by the DNA, which is dependent on the size of the DNA fragment, and I did not want large variations in the intensity of the bands to reflect excessive variations in product size. Such variations might have introduced problems when comparing the band intensities if different integration settings were required to avoid saturation of the detector with very bright bands and to allow detection of weaker bands. These principles proved effective in generating consistent patterns in the relative levels of expression of the products of interest. However, it is important to stress that only relative levels were being sought and I would not advocate this approach for absolute quantitative analysis.

4.4 CONCLUSION

NRAMP1 expression has been successfully detected by RT-PCR in the liver of normal and PBC patients. A scarcity of frozen PBC and normal liver material has

meant attempts to determine the relative levels of expression of the +alu and -alu mRNA splice variants in these populations remain inconclusive, though all cases expressed higher levels of the -alu message encoding the full length protein. In the tonsil material analysed the +alu message was seldom detected though the -alu message was present. A study to genotype cirrhotic and normal individuals for the functional 5' promoter region microsatellite polymorphism has identified two novel alleles (allele 5 and allele 6) at this site and confirmed the existence of three previously published alleles (allele 1, allele 2 and allele 3). Allele 5 was found at a significantly higher frequency in the PBC population studied; though it was still uncommon. Whether its presence in 15% of the PBC population has a functional effect in this sub group remains unresolved and the effect of this allele on regulating *NRAMP1* expression warrants further investigation.

5 GENERATION OF A MAMMALIAN EXPRESSION VECTOR CONTAINING *NRAMP1* cDNA FOR TRANSFECTION STUDIES AND DETECTION OF *NRAMP1* OVEREXPRESSION

5.1 INTRODUCTION

Evidence is mounting to support the theory that the level of *NRAMP1* expression, and polymorphic variants regulating its expression, play a significant role in determining the susceptibility of individuals to autoimmune or infectious disease (reviewed in Blackwell and Searle 1999). Certain infectious diseases such as tuberculosis and leprosy appear to be influenced by *NRAMP1* genotype with increased susceptibility being associated with allele 2 at the 5' promoter polymorphic microsatellite repeat region. Reporter gene studies have identified this allele to respond to IFNγ stimulation by increasing transcription of *NRAMP1*, but subsequent LPS stimulation resulted in decreased expression (Searle and Blackwell 1999). Such a scenario can be envisaged to have a major impact on the ability of Mϕs to control infection and it is, therefore, not surprising that allele 2 adversely influences the outcome of an individual faced with microbial pathogens. Conversely, allele 3 has been identified as driving the highest levels of *NRAMP1* expression under non-stimulatory conditions and when stimulated with IFNγ or IFNγ and LPS. High levels of *NRAMP1* expression are likely to partake in Mϕ activation enabling them to deal effectively with pathogens. However, should this activation state continue once an infection has been eliminated, or under situations where stimulated Mϕs are not required, self-tissue destruction and an uncurtailed immune response is a probable outcome. It is this idea of overexpression of *NRAMP1* contributing to autoimmune disease initiation and/or maintenance in which I was particularly interested. I wished to investigate what effect such expression has on cells of Mϕ origin and determine whether physiological functions or effects of *NRAMP1* overexpression could be identified which would increase the likelihood of autoimmunity.

To this end, I aimed to construct a plasmid containing the human *NRAMP1* cDNA which would result in high levels of *NRAMP1* expression when transfected into human cells. I wished to use cells of Mϕ origin for my transfection studies because I believed that the effect of NRAMP1 might be inextricably linked to Mϕ function as a whole and their defence mechanisms. The broad spectrum of effects of the gene on Mϕs which have been reported (reviewed in Blackwell 1996) are suggestive of a necessity for an intact biological system which centred on the inherent characteristics of the Mϕ. The most physiological system was sought, which appeared to be transient transfection of human aPBMCs isolated from Buffy Coats. These cells are derived from blood monocytes but develop the characteristics of Mϕs as they are cultured *in vitro*. After transient transfection of the cells I wished to assay the physiological effect of overexpression of the gene after verifying *NRAMP1* was being overexpressed at the RNA level, by RT-PCR analysis, and at the protein level, using antisera raised against an NRAMP1 peptide.

The aim, therefore, was to construct a mammalian expression vector containing the intact *NRAMP1* cDNA and transfect aPBMCs with the plasmid. It is a generally accepted fact that such cells are inherently difficult to transfect so it was necessary to seek a transfection method resulting in successful expression of transfected genes. To try to find such a technique a plasmid containing the easily assayed reporter gene encoding β-D-galactosidase (*lacZ*) was used; successful expression of which indicated a transfection procedure that might be appropriate for use with the plasmid containing the *NRAMP1* cDNA.

To assay for the presence and expression of the plasmid containing the *NRAMP1* cDNA I aimed to design suitable PCR and RT-PCR protocols and to generate NRAMP1 specific antisera, as no commercially available antisera exist.

5.2 RESULTS

5.2.1 Information known about the *NRAMP1* cDNAs used for Construction of pCIneo/NRAMP1 Plasmid

Three cloned *NRAMP1* cDNAs were the kind gift of Fumio Kishi. These cDNAs had been named phNRAMP1 (D38171), 5'NRAMP8 (D50402) and 5'NRAMP37 (D50402) and the following information was available.

5.2.1.1 phNRAMP1 (D38171)

phNRAMP1 (D38171) was cloned in the pUC12 vector and contained 2245bp of *NRAMP1* cDNA sequence, which was provided by Kishi with the cDNA (**Appendix C**). Analysis of this cloned *NRAMP1* sequence compared with the cDNA sequence published by Cellier and colleagues (Cellier *et al.* 1994) showed phNRAMP1 lacked 5' sequence data. This missing sequence data included an ATG initiation codon encoding the first methionine residue resulting in the translated cDNA sequence of phNRAMP1 lacking 52 N terminal amino acid residues. Compared with the full length sequence (Cellier *et al.* 1994) phNRAMP1 lacked 230bp of 5' sequence.

5.2.1.2 5'NRAMP8 (D50402)

This was the cDNA clone that had been requested from Kishi after analysing the Genbank entries of *NRAMP1* cDNA sequences registered by his group. D50402 was entered as the 'human mRNA for NRAMP' and was 2573bp long. However, the "5'NRAMP8" name of the plasmid I received suggested this may not be the case and the cloned sequence might not be the full 2573bp entered in Genbank. Additional diagrammatic information accompanying the three cDNA clones showed the 5'-RACE strategy used by Kishi to identify the extreme 5' end of *NRAMP1* cDNA and indicated 5'NRAMP8 and 5'NRAMP37 represented a relatively short length of sequence with 5'NRAMP8 extending further into the 5' promoter region of *NRAMP1* than 5'NRAMP37. This was consistent with the Genbank D50402 entry which contained an extra 89bp at the 5' end of the sequence over that of the D50403 entry. However, no information accompanied 5'NRAMP8 about the vector or the

plasmid size, except for the diagram depicting the insert as much smaller than, and spanning, the 5' end of the phNRAMP1 insert.

5.2.1.3 5'NRAMP37 (D50403)

The D50403 Genbank entry was registered as 2484bp of 'human mRNA for NRAMP'. However, the information accompanying the 5'NRAMP37 clone showed it to represent 718bp of sequence cloned in the vector pCRII (**Appendix C**). As mentioned in **5.2.1.2**, the accompanying diagram of the 5'-RACE strategy was consistent with an insert much smaller than that of the phNRAMP1 plasmid and more concordant with a size of 718bp. This suggested that the cloned sequence included 5' sequence of phNRAMP1 and additional sequence 5' to this, which was present in the Genbank D50403 entry. A similar situation was likely to exist for the 5'NRAMP8 plasmid (**5.2.1.2**).

This fragmented and partially circumspective information about the three cDNAs clones required their analysis by restriction enzyme digestion to try to determine which components of the *NRAMP1* cDNA sequences entered in the Genbank database by Kishi they represented, and the orientation of the DNA inserts in the plasmids. To obtain sufficient plasmid DNA for this analysis XL1 Blue cells were transformed with the three plasmids (**2.17**) and maxi preps carried out (**2.6.4.3**).

5.2.2 Characterisation of *NRAMP1* cDNAs

The insert sequence of phNRAMP1 and 5'NRAMP37 provided, the Genbank sequences D38171, D50402 and D50403 and the sequence for the vectors pUC12 and pCRII were used with the Vector NTI software (Informax Inc., Maryland USA) package to identify suitable restriction enzymes to characterise the cDNA clones.

In order to design the restriction enzyme digestions to characterise the plasmids, initial postulations had to be made on the possible cloning strategies which had been adopted by Kishi. Therefore, I started by assuming that the cDNA inserts had been cloned using the vectors' *EcoRI* sites in the polylinkers, as this is common practice, particularly when TA cloning methods are used. As no information was available

regarding the vector which 5'NRAMP8 had been cloned into it was hypothesised that either pCRII or pUC12 had been used, and most likely pCRII, because of the similarity of 5'NRAMP8 in name and diagrammatic representation to 5'NRAMP37.

5.2.2.1 phNRAMP1

Two double digests of phNRAMP1 were carried out:

***NheI* and *XbaI*:** *NheI* was expected to cut once in the *NRAMP1* insert after base 273 of the accompanying phNRAMP1 sequence (**Appendix C**). *XbaI* was expected to cut once in the pUC12 polylinker at position 255 of the vector sequence. As expected two fragments were obtained from the plasmid. The small fragment was estimated to be in the region of 300bp consistent with an expected size of about 297bp. It was not possible to accurately determine the size of the large fragment due to its high molecular weight. Based on sequence information of the pUC12 vector being 2680bp and the insert being 2245bp this fragment should have been of the order of 4.6kb.

NheI* and *HindIII: *NheI* was expected to cut once in the *NRAMP1* insert and *HindIII* was expected to cut once in the vector polylinker at position 276 and also 161bp downstream of the *NheI* site in the *NRAMP1* insert. Three fragments were released, as expected. The largest fragment was slightly smaller than the equivalent fragment generated from the *NheI* and *XbaI* digestion. The smallest fragment was estimated to be smaller than the 220bp molecular weight standard and the third fragment smaller than the 364bp molecular weight standard. These latter two fragments were predicted to be 161bp and 318bp, respectively.

These results showed the insert had been cloned in a reverse orientation as the *NheI* site was proximal to the *XbaI* site and, in conjunction with available sequence data, aspects of the plasmid which could be determined are depicted below in **Figure 5.1**.

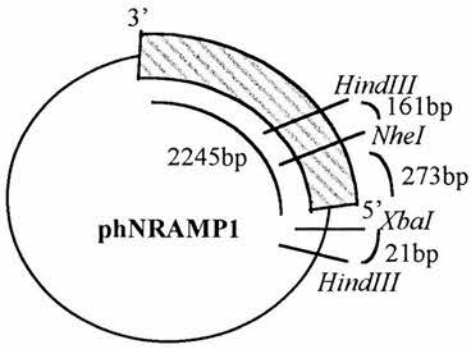

Figure 5.1 Diagram showing the sizes in bp of fragments of the phNRAMP1 plasmid determined from restriction enzyme digestion and known sequence data. The *HindIII, NheI* and *XbaI* sites are shown and the *NRAMP1* cDNA insert, with its 5' and 3' ends denoted, is shaded.

5.2.2.2 5'NRAMP8

A double digest with *NheI* and *XbaI*, and single digests with *EcoRI* and *NsiI* were carried out:

NheI* and *XbaI

Two fragments were generated when 5'NRAMP8 was digested with *NheI* and *XbaI*. The smaller fragment ran between the 5117bp and 1018bp molecular weight standards and was estimated to be approximately 600-700bp. The larger fragment could not be sized accurately but was smaller than the high molecular weight fragments generated from the digestions of phNRAMP1, described above.

EcoRI

Two fragments were detected when 5'NRAMP8 was digested with *EcoRI*. No *EcoRI* sites are present in the published *NRAMP1* sequence so the sites had to be present within the vector sequence. pCRII is used as a TA cloning vehicle. When inserted in this way the cloned DNA is flanked on both sides by *EcoRI* sites with 15bp of vector DNA in addition to the cloned DNA between the two sites. It was highly probable that this was the situation for 5'NRAMP8. Alternatively, the insert could have been cloned directly using the *EcoRI* sites in the polylinker, in which case the 11bp of intervening vector sequence would be absent from the plasmid. The smaller of the two released fragments ran with a slightly higher molecular weight than the smaller

fragment generated from the *NheI* and *XbaI* digestion and was estimated to be 700-800bp. The larger fragment ran with a slightly lower molecular weight than the larger fragment from the *NheI* and *XbaI* digestion.

Taken in conjunction with the likely situation that 5'NRAMP8 consisted of the 5' region of the D50402 Genbank entry and the results of the 5'NRAMP37 digests (**5.2.2.3**), I was able to conclude that the cloned sequence had 5' *NRAMP1* sequence of phNRAMP1 which extended at least as far as the *NheI* site. The whole insert was slightly larger than 712bp (the expected size of the equivalent region of the 5'NRAMP37 insert) and the similar size of the smaller fragments released from the two digests of 5'NRAMP8 implied the insert had been cloned in the reverse orientation because the *NheI* site was distal to the *XbaI* site.

However, these results did not determine which vector 5'NRAMP8 was cloned in as pCRII and pUC12, the likely candidates, both have an *EcoRI* cloning site and neither has an *NheI* site. There was also the possibility that another common vector, pCR2.1, may have been used to clone 5'NRAMP8 and 5'NRAMP37 because the hand written-pencilled vector name on the sequence accompanying the latter was rather indistinct and ambiguous. As pCRII and pCR2.1 can be distinguished by digestion with *NsiI* this digestion was carried out to resolve the issue. pCRII has two *NsiI* sites flanking the TA cloning site in the vector whereas pCR2.1 only has one site. No *NsiI* site exists in the *NRAMP1* sequence or pUC12.

NsiI

When 5'NRAMP8 and 5'NRAMP37 were digested with *NsiI* two fragments were released from each plasmid, providing evidence that pCRII was the plasmid in which both cDNAs had been cloned.

A diagrammatic representation of the structure of 5'NRAMP8 is shown in **Figure 5.2**.

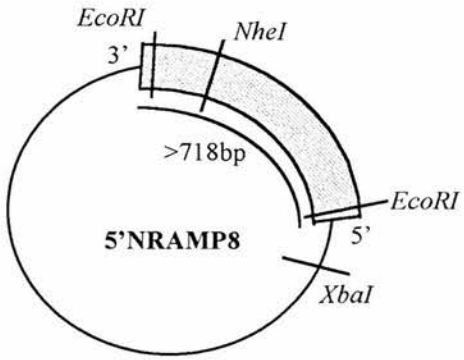

Figure 5.2 Diagram showing the approximate size of the *NRAMP1* cDNA insert in the 5'NRAMP8 plasmid and the position of the *EcoRI*, *NheI* and *XbaI* restriction sites. The *NRAMP1* cDNA insert, with its 5' and 3' ends denoted, is shaded.

5.2.2.3 5'NRAMP37

As described above for 5'NRAMP8 (**5.2.2.2**) a double digest with *NheI* and *XbaI*, and single digests with *EcoRI* and *NsiI* were carried out:

NheI* and *XbaI

Two fragments were generated when 5'NRAMP8 was digested with *NheI* and *XbaI*. The smaller fragment ran between the 5117bp and 1018bp molecular weight standards with a lower molecular weight than the equivalent 5'NRAMP8 fragment (**5.2.2.2**) and was estimated to be approximately 600bp. This was consistent with a calculated size of 615bp, based on the sequence data available. The larger fragment could not be sized accurately but was expected to be 4015bp. It was of a similar size to the larger fragment generated from the *NheI* and *XbaI* digestion of 5'NRAMP8 giving an indication of the size of the latter.

EcoRI

Two fragments were detected when 5'NRAMP37 was digested with *EcoRI*. As discussed in **5.2.2.2** no *EcoRI* sites are present in the published *NRAMP1* sequence, hence, the sites had to be present in the vector. The expected size of the fragments generated from the *EcoRI* digestion were based on the assumption that a TA cloning strategy had been employed, as discussed previously (**5.2.2.2**). The smaller of the two released fragments ran with a slightly higher molecular weight than the smaller

fragment generated from the *NheI* and *XbaI* digestion and was estimated to be between 700bp and 800bp, consistent with a calculated size of 712bp. The larger fragment ran with a slightly lower molecular weight than the larger fragment from the *NheI* and *XbaI* digestion. It appeared very similar to the equivalent 5'NRAMP8 fragment and was calculated to be 3918bp.

As for 5'NRAMP8 the similar size of the smaller fragments released from the *NheI* and *XbaI* double digest and *EcoRI* single digest showed the insert had been cloned in the reverse orientation, as the *NheI* site was distal to the *XbaI* site.

NsiI

As discussed above, when 5'NRAMP37 was digested with *NsiI* two fragments were released confirming pCRII was the plasmid used to clone the cDNA (**5.2.2.2**).

A diagrammatic representation of the structure of 5'NRAMP37 is shown in **Figure 5.3**.

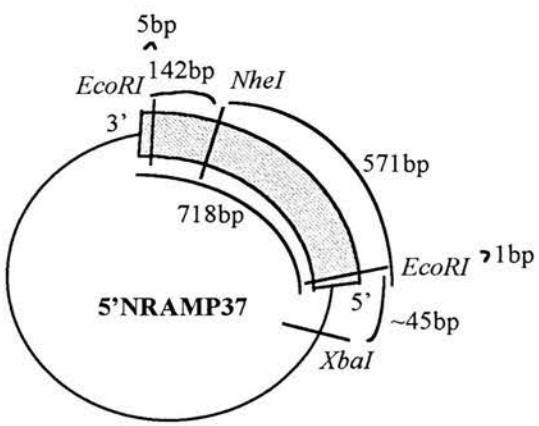

Figure 5.3 Diagram showing the sizes in bp of fragments of the 5'NRAMP37 plasmid determined from restriction enzyme digestion and known sequence data. The *EcoRI*, *NheI* and *XbaI* sites are shown and the *NRAMP1* cDNA insert, with its 5' and 3' ends denoted, is shaded.

5.2.3 Construction of the Whole *NRAMP1* cDNA in pUC12

The phNRAMP1 plasmid was chosen as the vector in which the entire NRAMP1 cDNA would be constructed with the majority of the cDNA being derived from this plasmid. 5'NRAMP8 was chosen as the source of 5' sequence to complete the cDNA because the restriction enzyme characterisation supported this cDNA to have more 5' *NRAMP1* sequence than 5'NRAMP37. It is desirable to have the maximum upstream regulatory elements of genes when attempting to express them in transfected cells.

To construct the whole cDNA, phNRAMP1 and 5'NRAMP8 were digested with *NheI* and *XbaI*. The smaller 5'NRAMP8 fragment of approximately 700bp contained the 273bp of sequence excised from phNRAMP1 5' to the *NheI* site, present in both plasmids, plus the additional *NRAMP1* sequence lacking in phNRAMP1. This fragment was ligated into the larger fragment generated from digestion of phNRAMP1 of approximately 4900bp (4902bp) as depicted in **Figure 5.4**. After transforming competent XL1 Blue cells with the ligated plasmid DNA, colonies were analysed for correct orientation and insertion of the DNA fragment and two were found to be suitable. *NheI* and *XbaI* are isoschizomers though religation of *NheI* and *XbaI* digested DNA ends can not be redigested with the enzymes enabling appropriately ligated plasmids to be identified. Clones 1 and 10 released the appropriate 5'NRAMP8 derived fragment of approximately 700bp and phNRAMP1 derived fragment of approximately 4900bp when digested with *NheI* and *XbaI*.

5.2.4 Cloning *NRAMP1* cDNA in pCIneo

The pCI-neo mammalian expression vector (Promega, Southampton UK), referred to as pCIneo plasmid, was chosen as a suitable vehicle for overexpression studies in mammalian cells. The vector carries the human cytomegalovirus (CMV) immediate-early enhancer/promoter region, to promote constitutive expression of cloned DNA inserts in mammalian cells, and the neomycin phosphotransferase (*neo*) gene from Tn5, under control of the SV40 enhancer and early promoter region, enabling selection of stable transfectants in the antibiotic G418.

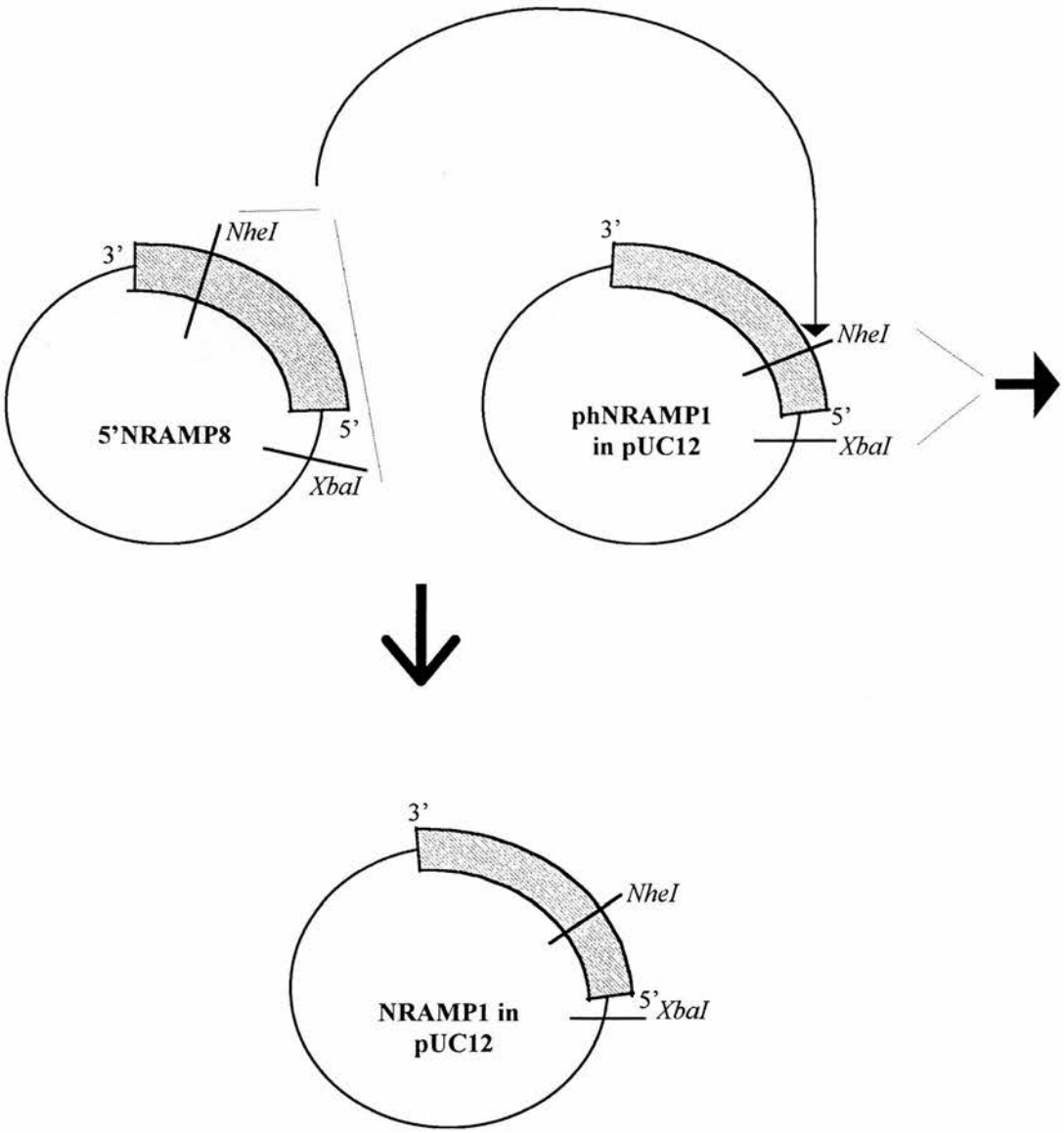

Figure 5.4 Diagram showing how the whole *NRAMP1* cDNA sequence was constructed in the pUC12 vector. ➡ shows the section of phNRAMP1 which was discarded. The *NheI* and *XbaI* sites used are shown. The *NRAMP1* sequence was subsequently cloned into the pCIneo mammalian expression vector as described in **5.2.4**.

The *NRAMP1* cDNA sequence in pUC12 was excised using *MscI* and *XbaI*. *XbaI* cuts in the vector polylinker proximal to the 5' end of the cDNA insert. The *MscI* site was present at the 3' end of the phNRAMP1 sequence 629bp downstream of the termination codon: thus, all the coding sequence was present in the excised fragment.

An attempt was made to identify the *NRAMP1* polyadenylation signal so that it could be included in the excised DNA. However, no single site was found with several possible regions of consensus. As the pCIneo vector contains the SV40 late polyadenylation signal downstream of the multiple cloning site it was not imperative for the cloned DNA to have its own polyadenylation site, though it may further enhance the stability of RNA transcribed from the plasmid.

The pCI-neo plasmid was digested with *XbaI* and *SmaI* to linearise it prior to insertion of the *NRAMP1* cDNA. The *XbaI* site was proximal to the CMV immediate-early enhancer/promoter and the *SmaI* site was proximal to the SV40 late polyadenylation signal. Ligation of the *XbaI* generated end of the plasmid with that of the cDNA sequence and ligation of the blunt *SmaI* generated end of the plasmid with the blunt *MscI* generated end of the cDNA resulted in the correct orientation of the insert in the vector. Successful ligations were confirmed by digesting plasmid DNA from XL1 Blue transformed colonies singly with *KpnI* and *NheI*. Seven clones were isolated which generated fragments of the appropriate size, approximately 3.4kb and 4.5kb, when digested with *KpnI*. This showed the plasmids contained a cDNA insert of the expected size. Two of these seven clones were taken for further analysis and by digesting them with *NheI* they were shown to contain the insert in the correct orientation. The *NheI* digestion was expected to generate fragments of 774bp and 7187bp. The successfully cloned whole *NRAMP1* cDNA in the pCIneo plasmid was named pCIneo/NRAMP1 and is referred to in this way throughout the text.

5.2.5 Transfection of Adherent Peripheral Blood Mononuclear Cells

Having constructed the pCIneo/NRAMP1 plasmid (**5.2.4**) a suitable method for transfecting primary aPBMCs was sought. As described in (**5.2.5.2**) a variety of

protocols were attempted using *lacZ*, encoding β-D-galactosidase (β-gal), as a reporter gene.

5.2.5.1 Isolation of Adherent Peripheral Blood Mononuclear Cells (aPBMC)

Adherent peripheral blood mononuclear cells (aPBMC) were successfully isolated from Buffy Coats and cultured *in vitro*. The cells had the characteristics and morphology of Mϕs and survived in culture for approximately 7-10 days.

5.2.5.2 Transfection with β-D-Galactosidase Plasmid

Several attempts were made to transfect the aPBMCs with a plasmid containing the β-D-galactosidase (β–gal) encoding gene (Promega, Southampton UK) to determine if an efficient transfection procedure could be established and adopted for use with the pCIneo/NRAMP1 plasmid. aPBMCs were chosen because I wished to study the effect of overexpression of the *NRAMP1* gene in cells which have the phenotype and capacity to exhibit the characteristics and effects which *NRAMP1* overexpression may result in, and which may be required for the full effect of the gene's activity to be realised. Expression of the *lacZ* gene was chosen as a reporter gene for successful transfection and expression because it is easily assayed using X-gal substrate and detection of a blue colour in β-gal expressing cells (**2.20.2.1**).

Lipofectin Reagent

When aPMMCs were treated with twenty four combinations of concentrations of Lipofectin (4μg, 5μg, 6μg, 7μg, 9μg and 11μg) and β-gal plasmid (0.5μg, 0.75μg, 1.0μg and 1.5μg) and stained for expression of β-gal only a very faint blue colour was seen in a minority of the cells. The observed faint blue colour was equivocal and may not have been genuine staining but was more apparent in the wells transfected with the higher DNA concentrations. There was a dramatic reduction in the number of adherent cells remaining in the wells of the tissue culture plates after the transfection and staining procedure. When this transfection and staining for β-gal expression procedure was repeated negligible blue staining was observed again but the obvious reduction in confluency of the cells was seen, which had reduced to about one eighth of that at the start of the transfection.

Lipofectin/Lipofectamine Reagent Comparison

When aPBMCs were transfected with Lipofectin Reagent, as just described, or Lipofectamine Reagent (8μg 12μg, 14μg, 18μg and 22μg) with 1.0 or 1.5μg of β-gal plasmid no blue stained cells were observed in the Lipofectin Reagent transfected cells. During the washing stages after the transfection and during the staining procedure any de-adhered cells were collected to determine if these cells had been successfully transfected. None of the de-adhered cells showed a blue colour after staining for β-gal expression. After transfection with Lipofectamine Reagent the cell confluency and morphology was similar to that at the start of the experiment. No bright blue cells were visible after staining for β-gal expression though the wells containing cells transfected with 12μg/ml and 14μg/ml Lipofectamine Reagent contained a low level of very pale blue cells, visible when the objective lens control of the microscope was racked up and down. It is not known if this represented genuine weak expression of β-gal or was an artefact.

DOSPER Liposomal Transfection Reagent

When aPMMCs were treated with twenty four combinations of DOSPER (3μg, 4.5μg, 6μg, 9μg, 12μg and 15μg) and β-gal plasmid (0.5μg, 0.75μg, 1.0μg and 1.5μg) and stained for expression of β-gal no blue cells were visible. The majority of cells remained adherent throughout the procedure and the few cells which had de-adhered and been collected were also negative for β-gal expression.

SuperFect Transfection Reagent

When aPMMCs were treated with twenty four combinations of SuperFect Reagent (9μg, 15μg, 21μg, 27μg, 36μg and 45μg) and β-gal plasmid (0.5, 0.75, 1.0 and 1.5μg) and stained for expression of β-gal no blue cells were seen. The cells had an unhealthy appearance and looked smaller and "caving in".

Diethylaminoethyl dextran (DEAE Dextran)

It has been reported that higher transfection efficiencies of murine peritoneal Mϕs were obtained using a diethylaminoethyl dextran (DEAE dextran) approach

compared with Lipofectin Reagent or calcium-phosphate protocols (Rupprecht and Coleman 1991) so this method was tried on the human aPBMCs. Cells were transfected with 5μg, 10μg, 15μg or 20μg β-gal plasmid DNA after pre-incubation in 20% or 5% heat treated NHS, with and without osmotic shock with 10% DMSO or glycerol shock after transfection. Transfection of the cells pre-incubated in 20% serum was carried out in the presence or absence of heat treated NHS while cells incubated in 5% serum were only transfected in 5% serum. In three of the twenty-four wells representing the different combinations of conditions a few strongly blue stained cells were seen after assaying for β-gal expression. Of the cells pre-incubated with 20% NHS, transfected in the presence of 5% NHS with 5μg DNA, without any shock treatment, at least one strongly and two weakly stained cells were seen. A weakly stained cell was seen in the well receiving the above treatment but transfected with 10μg DNA. Several strongly stained cells were seen in the cells which were pre-treated with 5% NHS and transfected with 20μg of DNA without DMSO osmotic shock. All the remaining wells showed no sign of successful transfection.

Though transfection of aPBMCs using DEAE-dextran showed a few cells expressing β-gal the level of transfection was far too low to be used successfully to study the effect of *NRAMP1* overexpression in these cells. I, therefore, decided to try to transfect the MM6 and U937 cell lines.

5.2.6 Transient Transfection of the U937 Cell Line

The level of efficiency of transfection using any of the methods attempted (**5.2.5.2**) was insufficient for analysing the effect of expression of any gene of interest in primary cultures of aPBMCs. As an alternative transfection of cell lines of monocyte/Mϕ lineage was attempted. Though less physiological than primary cultures of aPBMCs the U937 and MM6 cell lines represent cells whose phenotype of monocyte/Mϕ related activities could be compared with their pCIneo/NRAMP1 transfected counterparts. MM6 is a monocytic cell line which was established from peripheral blood of a 64 year old male patient with monoblastic leukaemia. The cell

line exhibits phenotypic and functional features of mature monocytes (Ziegler-Heitbrock *et al.* 1988; Cytokines Online Pathfinder Encyclopaedia web site). U937 is a cell line established from a diffuse histiocytic lymphoma of a 37 year old male patient and displays many monocytic characteristics (Cytokines Online Pathfinder Encyclopaedia web site).

Successful transfection by electroporation of U937 cells has been reported (Hewison *et al.* 1994; Zhang *et al.* 1994b; Dobrescu *et al.* 1995; Rhoades *et al.* 1995) and a similar protocol was followed, electroporating the cells with equal quantities of circular or linearised β-gal plasmid, to determine if the circular DNA was more resistant to endogenous exonucleases within the cells. Personal communication with fellow colleagues highlighted the difficulties that may be encountered when attempting to transfect monocyte/Mϕ cell lines. It is possible that the low efficiency of such transfections results from the cells' innate degradative activity of phagocytosed and internalised material. I successfully electroporated U937 cells with circular β-gal plasmid DNA, assayed by DetectaGene Green CMFDG using a flow cytometry read out (**2.20.2**). The events were gated to exclude dead cells on the basis of forward and side scatter and propidium iodide positivity. A significant shift in the fluorescein peak (β-gal expressing cells) was observed in cells electroporated with the circular plasmid (**Figure 5.5**). 95.5% of the gated viable cell population showed a positive fluorescein signal with a mean fluorescence signal of 2.4. Of the cells electroporated with the linearised DNA a much smaller shift in the mean fluorescence intensity to 0.7 was seen. Compared to the controls, where cells were electroporated in the absence of DNA (mean fluorescence intensity of 0.6) or were not electroporated (mean fluorescence intensity of 0.5), the increase in the fluorescein signal of the cells electroporated with the linearised plasmid was not significant. Events gated for propidium iodide positivity showed a significant increase in positive cells in the electroporated samples. Cells electroporated with circular plasmid, with linearised plasmid and in the absence of DNA showed 21.5%, 19.7% and 17.2% propidium iodide positive cells, respectively, contrasting with 3.1% for the cells which were not electroporated. These results suggested that the

efficiency of transfection of cell lines of monocyte/Mϕ lineage by electroporation is dramatically increased when the plasmid DNA is not linearised prior to transfection. The act of electroporation induces a significant amount of cell death regardless of the presence or absence of DNA.

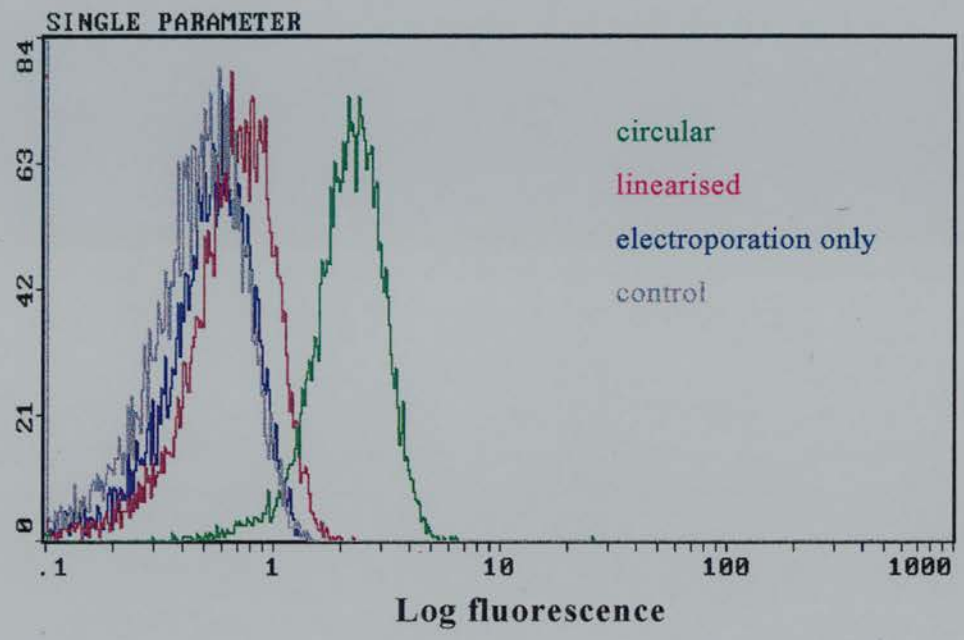

Figure 5.5 showing the shift in the fluorescence intensity for events, gated to exclude propidium iodide positivity, for cells electroporated with circular (green) or linearised (red) β-gal plasmid DNA, cells electroporated in the absence of DNA (blue) and cells not electroporated (grey), assayed by DetectaGene Green CMFDG and flow cytometry as described in **2.20.1** and **2.20.2.2**.

5.2.7 Stable Transfection of MM6 and U937 Cell Lines with the pCIneo/NRAMP1 Plasmid and Generation of Clones

5.2.7.1 Stable Transfection of MM6 and U937 Cell Lines with the pCIneo/NRAMP1 Plasmid

All transfections of the MM6 and U937 cell lines were carried out using circular plasmid DNA based on results of the transient transfection with the β-gal plasmid (**5.2.6**). Each cell line was electroporated with the pCIneo/NRAMP1 plasmid and the control pCIneo vector lacking the *NRAMP1* cDNA. Due to the lack of success in generating specific anti-NRAMP1 sera (**5.2.9**) successful transfection was

determined by analysing genomic DNA by PCR for the presence of the plasmid DNA in question and expression of the plasmid sequence was analysed by semi-quantative RT-PCR. Single cell clones of stable transfectants were sought to give a homogeneous population of long lasting cells that could be used for functional studies.

5.2.7.2 Generation of Clones of MM6 and U937 Transfectants by Limiting Dilution

By limiting dilution of cells into 96 well plates (**2.20.4**) the probability (P) of 1 cell per well is:

$$P = \frac{m^x e^{-m}}{x!}$$

where m is the average number of cells per well and x is the occupancy number of a well (Wardlaw 1992).

Ideally, if time had allowed, the limiting dilution and clonal selection would have been repeated at least once more to increase the likelihood of cells selected from a single well being truly clonal. Cell populations which had been assayed by PCR (**5.2.8.1**) and RT-PCR (**5.2.8.2**) and determined to contain cells successfully transfected with and expressing the plasmid DNA were used as the source of cells from which clones were derived. "Clones" were selected from wells which showed signs of cell proliferation. Wells were carefully selected, avoiding any which showed evidence of poor cell proliferation or in which the cells' distribution suggested they may have originated from more than one region within the well. The cells were chosen from wells which were showing yellowing of the culture medium, indicating active cellular metabolism, and in which the clonal proliferation appeared to originate from one region at the outer edge of the well. Of these clones, genomic analysis for the presence of the plasmid of interest (**5.2.8.1**) and appropriate gene expression (**5.2.8.2**) was carried out.

For the MM6 cells electroporated with the pCIneo/NRAMP1 plasmid, five 96 well plates were prepared for each of five mixed cell populations from five wells of cells

cultured in a six well plate. Seventeen of these clones were selected, as described above, and sequentially transferred to 24 well plates, 6 well plates, small and then medium tissue culture flasks. Clones were discarded which failed to proliferate or which failed the genomic DNA and RT-PCR analysis for presence and expression of the plasmid, leaving four clones for analysis of the effect of *NRAMP1* overexpression. These clones were identified as D12, B4, B6 and F12 (**Appendix D**).

A similar selection process for cloning the MM6 cells electroporated with the control pCIneo plasmid involved plating five 96 well plates for the limiting dilution for each of five mixed cell populations from five wells of a six well plate. Twenty-four clones were selected and transferred to 24 well plates of which cells from nine wells were cultured on to small flasks and eight on to medium flasks. Six of these clones showed the presence of the plasmid DNA at the genomic level by PCR and expression of the *neo* gene by RT-PCR and were selected as suitable control transfectants. These clones were identified as M/pB2, M/pB10, M/pC6, M/pF2, M/p F7, and M/pG3 (**Appendix D**).

For the U937 cells electroporated with the pCIneo/NRAMP1 plasmid five 96 well plates were prepared by limiting dilution for each of four mixed cell populations from four wells of cells cultured in a six well plate. Forty-seven clones were transferred to 24 well plates and cells from twenty-three of these to six well plates. PCR analysis identified thirteen of these clones to be positive for PCRs showing presence of the plasmid and five of these were selected as suitable for *NRAMP1* overexpression studies on the basis of their gene expression profiles determined by RT-PCR. These clones were identified as 2, 4, 5, 18 and 27 (**Appendix D**).

For the U937 control cells, electroporated with the pCIneo plasmid, clones were selected by limiting dilution from five 96 well plates prepared from a single mixed cell population. Seventeen clones were transferred to 24 well plates, cells from

eleven of these wells were transferred to small flasks and PCR analysis showed ten of them to contain the plasmid sequence. One of these was selected as a control clone which showed the appropriate gene expression profile and was identified as 39 (**Appendix D**).

5.2.8 Characterisation of MM6 and U937 Cells Transfected with the pCIneo/NRAMP1 and pCIneo Plasmids

5.2.8.1 Detection of Plasmid DNA in G418 Resistant Cells

All DNA extracted from transfected cells was positive for the NRAMPpol PCR used for the *NRAMP1* 5' promoter region polymorphism analysis described in **2.8.1** and **4.2.1** (**Figure 5.6a**). This PCR acted as a positive control to show genomic DNA had been successfully extracted. NRAMPalu PCRs were positive for genomic template DNA from cells successfully transfected with the pCIneo/NRAMP1 plasmid (**Figure 5.6b** and **Figure 5.7b**). As these primers were designed for detection of expression of the mature spliced *NRAMP1* mRNA message by RT-PCR they were suitable for detection of the presence of the pCIneo/NRAMP1 plasmid which contained the *NRAMP1* cDNA sequence. Successful transfectants also gave a positive reaction with the NRAMPRalu and pCIneoF primers, referred to as NRpCI and described in **2.8.4** (**Figure 5.7a**). The latter primer was designed to discriminate between expression from the endogenous *NRAMP1* gene and the plasmid sequence, but acted as additional evidence for presence of the pCIneo/NRAMP1 plasmid in transfectants and showed the 5' region of the sequence was intact. In addition to detection of the *NRAMP1* cDNA sequence in successful transfectants the presence of the plasmid *neo* gene sequence was demonstrated by two PCRs referred to as neoF1 (**Figure 5.8a**) and neoFexp (**Figure 5.8b**). All successful transfectants gave products of the appropriate size for these PCRs. The design of these primers is detailed in **2.8.5** and **2.8.6**

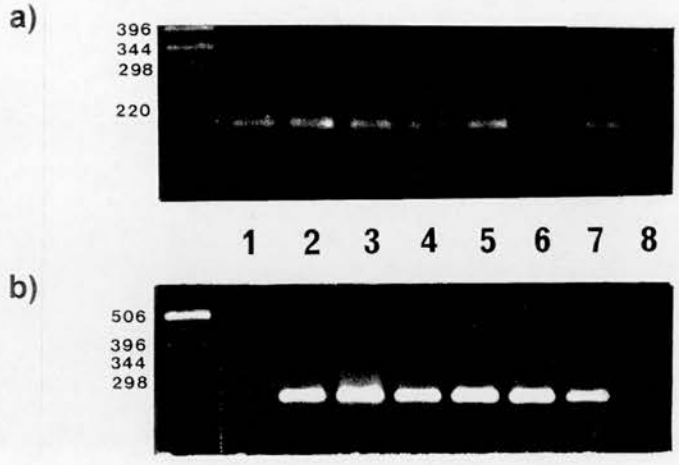

Figure 5.6 a) NRAMPpol and **b)** NRAMPalu PCR products amplified from genomic DNA extracted from the parent cell line (lane **1**) and cells transfected with the pCIneo/NRAMP1 plasmid (lanes **1-6**). Lanes **7** and **8** show positive and negative control reactions, respectively. Molecular weight marker, with sizes shown in bp, was run in the left hand lanes. For details of NRAMPpol and NRAMPalu primers and transfectants see **2.8.1**, **2.8.3**, **5.2.7** and **5.2.8**.

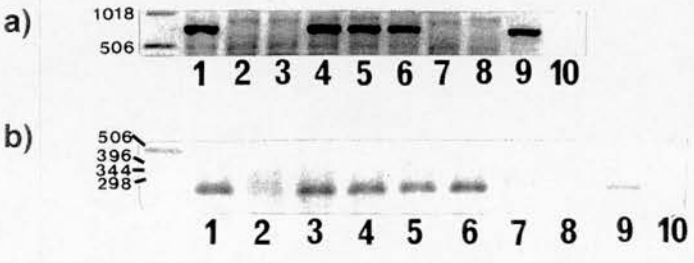

Figure 5.7 a) NRpCI and **b)** NRAMPalu PCR products amplified from genomic DNA extracted from cells transfected with the pCIneo/NRAMP1 plasmid (lanes **1-6**), the parent cell line (lane **7**) and control cells transfected the pCIneo vector (lane **8**). Lanes **9** and **10** show positive and negative control reactions, respectively. Molecular weight marker, with sizes shown in bp, was run in the left hand lanes. For details of NRpCI and NRAMPalu primers and transfectants see **2.8.4**, **2.8.3**, **5.2.7** and **5.2.8**.

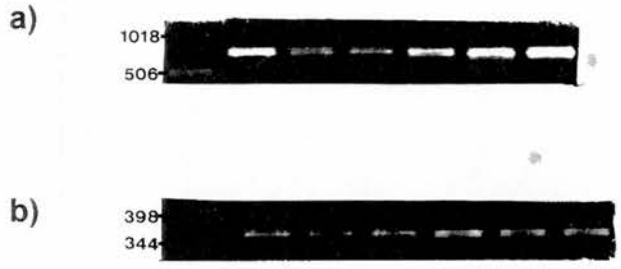

Figure 5.8 a) neoF1 and **b)** neoFexp PCR products amplified from genomic DNA extracted from cells transfected with the pCIneo/NRAMP1 plasmid or pCIneo vector. Molecular weight maker, with sizes shown in bp, was run in the left hand lane. For details of neoF1 and neoFexp primers and transfectants see **2.8.5**, **2.8.6**, **5.2.7** and **5.2.8**.

5.2.8.2 Detection of Expression of Plasmid Derived *NRAMP1* Sequence

Analysis of the expression of endogenous and plasmid derived DNA sequences, assayed by RT-PCR, showed a positive result for the GAPDH PCR for all clones. This PCR acted as a positive control for successful generation of cDNA. Though all RNA samples were DNase treated prior to the RT reaction, samples were checked to ensure no contaminating genomic or plasmid DNA was present in the cDNAs. Any samples that gave a positive result with the neoF1 PCRs, designed to detect untranscribed plasmid sequence (described in **2.8.5**), were repeated and eliminated where necessary. NRAMPalu, NRpCI and neoFexp PCRs were positive in clones of successful pCIneo/NRAMP1 transfectants and NRAMPalu and neoFexp PCRs were positive in the vector transfected control clones. Clones successfully transfected with the pCIneo/NRAMP1 plasmid and pCIneo plasmid had the profile shown in **Table 5.1**.

	NRAMPpol	GAPDH	NRAMPalu	NRpCI	neoF1	neoFexp
pCI/NRAMP1 transfectant gDNA	+	-	+	+	+	+
pCI/NRAMP1 transfectant cDNA	-	+	+	+	-	+
pCIneo transfectant gDNA	+	-	-	-	+	+
pCIneo transfectant cDNA	-	+	+	-	-	+

Table 5.1 The profile of cells successfully transfected with the pCIneo/NRAMP1 plasmid (**pCI/NRAMP1 transfectant**) and pCIneo plasmid (**pCIneo transfectant**) for PCR analysis of genomic DNA (**gDNA**) and RT-PCR analysis of **cDNA**. Design of the primers and PCRs (NRAMPpol, GAPDH, NRAMPalu, NRpCI, neoF1 and neoFexp) is described in **2.8**. + denotes a positive PCR/RT-PCR result. - denotes a negative PCR/RT-PCR result.

5.2.8.3 Semi-Quantitative Analysis of *NRAMP1* Expression

For semi-quantitative gene expression analysis of the transfected clones by RT-PCR the samples being analysed were taken through the whole procedure in parallel to eliminate as many potential inter-sample variations as possible. The GAPDH PCR was used as a standard housekeeping gene whose level of expression was compared with that of the PCR product in question by measuring the intensity of the signal of the PCR products by densitometry. As the products for the complete RT-PCR analysis from only three or four cDNA samples could be loaded on any one row of the agarose gels a comparison of every sample's GAPDH level with that of all the other samples could not be carried out. To obtain some level of inter-sample GAPDH expression comparison a ratio of the intensities of the GAPDH products for the samples run on the same row of each gel was calculated. Clones of successful pCIneo/NRAMP1 transfectants showed a variation in the level of plasmid encoded *NRAMP1* and *neo* expression. When repeated analyses of the clones of interest were carried out, particular clones consistently showed the highest levels of expression. An example of a gel from which the intensity of the RT-PCR products of interest (namely NRAMPalu, NRpCI and neoFexp) relative to GAPDH was determined is shown in **Figure 5.9**, with the results depicted graphically in **Figure 5.10**.

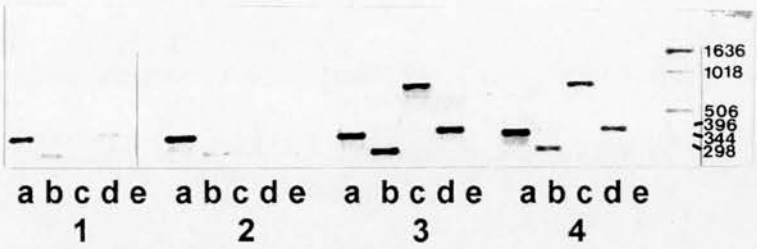

Figure 5.9 RT-PCR mRNA expression analysis of parent cell line MM6 and transfected clones. Lanes **1a-1e**: pCIneo vector transfected clone; lanes **2a-2e**: parent MM6 cells; lanes **3a-3e**: pCIneo/NRAMP1 plasmid transfected clone F12; lanes **4a-4e**: pCIneo/NRAMP1 plasmid transfected clone B4. **a**: GAPDH, **b**: NRAMPalu, **c**: NRpCI, **d**: neoFexp, **e**: neoF1 RT-PCR products. Molecular weight marker, with sizes shown in bp, was run in the right hand lane. For details of PCR primers and transfected clones see **2.8**, **5.2.7** and **5.2.8**.

The MM6 derived pCIneo/NRAMP1 plasmid transfected clone named D12 consistently showed the highest level of expression of plasmid encoded *NRAMP1* sequence as shown by the high NRpCI to GAPDH product ratio (**Figure 5.10**). The F12, B4 and B6 clones also showed expression but at a lower level. The relative NRAMPalu product intensity was also increased in these clones when compared with that of the parent cell line. D12 was the pCIneo/NRAMP1 transfected clone of particular interest during investigation of the possible effects of *NRAMP1* overexpression.

Of the U937 transfectants at least fifteen clones were identified which exhibited plasmid derived *NRAMP1* expression. Nine of these were considered to show high levels of expression but unfortunately, for some of these clones, on one out of the several repeated RT-PCR assays the DNase treated cDNA gave a product with the neoF1 PCR. This suggested carry through plasmid DNA was present in the cDNA. In these cases it was not possible to determine how much of the NRpCI signal was due to expression of the plasmid sequence and how much due to plasmid DNA carry through. These clones require further analysis to determine whether they are genuinely expressing high levels of pCIneo/NRAMP1 encoded *NRAMP1*. At present at least three clones appear to be doing so, identified as clones 2, 5 and 18 and a further two clones are showing expression at a lower level.

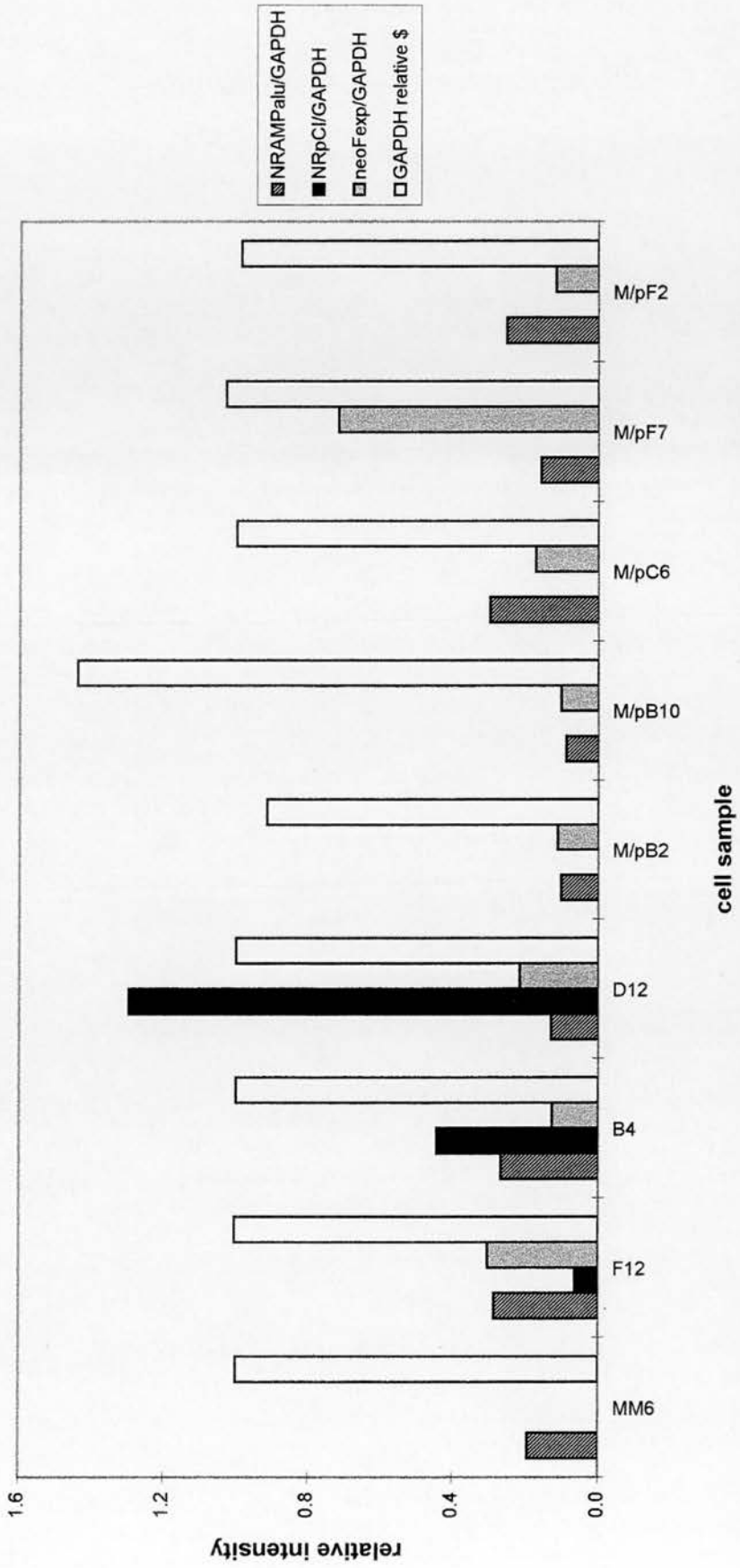

Figure 5.10 The intensities of NRAMPalu, NRpCI and neoFexp RT-PCR products relative to the GAPDH intensity for the parent cell line (**MM6**) and a selection of pCIneo/NRAMP1 plasmid transfected clones (**F12**, **B4** and **D12**) and pCIneo plasmid transfected clones (**M/pB2**, **M/pB10**, **M/pC6**, **M/pF7** and **M/pF2**). **$ GAPDH relative**: GAPDH values relative to those of the other samples on the same row of the analysis gel. Design of the primers used is described in **2.8.2-2.8.4** and **2.8.6**, and the semi-quantitative RT-PCR analysis is described in **5.2.8.3**.

For both the MM6 and U937 cells transfected with the control pCIneo plasmid many clones were successfully isolated and analysed as described in **5.2.7.2**. As mentioned previously, the levels of the *neo* sequence expressed in the pCIneo/NRAMP1 plasmid transfected clones varied and the significance or impact this heterogeneity may have on the cells is not known. There did not appear to be consistent high expression of *neo* accompanying high expression of *NRAMP1* in pCIneo/NRAMP1 transfectants, but for experiments looking at functional or phenotypic effects of *NRAMP1* overexpression control pCIneo plasmid transfectants were chosen which expressed similar levels of *neo* to the pCIneo/NRAMP1 transfectants being analysed.

5.2.8.4 Morphology of Transfected Cells

Examination of pCIneo/NRAMP1 transfectants under light microscopy and monitoring cell proliferation showed no obvious detrimental effect to survival of the cells. The MM6 parent cell line shows significant polyploidy, anuploidy and often multinuclear cells that were much larger than mononuclear cells. These characteristics were also apparent in cultures of the MM6 derived transfectants but the frequency of massive cells with more than one nucleus appeared greater when the D12 clone was examined in close detail. It is not known if this was an effect of the electroporation procedure, the presence and expression of plasmid DNA or the rate of growth of the cells. It is possible these large multinuclear cells are the result of multiple rounds of proliferation and mitosis and as the cells age mitosis proceeds with defective cytokinesis. The D12 cells may have been cycling at an increased rate when analysed.

5.2.8.5 Immunocytochemistry using Sera from Rabbits Immunised with an NRAMP1 Peptide

Despite evidence at the genomic and cDNA level of the presence and expression of pCIneo/NRAMP1 plasmid encoded sequence, I had no way of showing NRAMP1 overexpression at the protein level in the transfected clones. Though attempts to show NRAMP1 peptide specificity of sera from rabbits immunised with an NRAMP1 peptide were unsuccessful (**5.2.9**), the sera were tested on cytospins

prepared from MM6 cells, U937 cells, two MM6 and three U937 derived clones transfected with the pCIneo/NRAMP1 plasmid and one MM6 and one U937 derived clone transfected with the control pCIneo plasmid. A membrane-staining pattern was observed in a subset of cells of the cytospins. However, this pattern was also seen in cells treated with the pre-immmune rabbit sera and was, therefore, not specific for NRAMP1. The antigen(s) the sera reacted with is not known but could potentially be an Fc receptor interaction, with differential expression of these receptors accounting for only a subset of cells exhibiting the membrane-staining pattern.

5.2.9 Generation and Testing of Serum from Animals Immunised with an NRAMP1 Peptide

No antiserum to human or murine NRAMP1 was commercially available, so attempts were made to generate Abs specific for human NRAMP1. Previous attempts in the laboratory raising Abs against low molecular weight synthetic peptides had been successful so a similar approach was followed. Each immunisation procedure adopted will be described and their results presented in turn, though some were carried out simultaneously or were dependent on material or results from another procedure. The methods for the peptide preparations are described in **2.3.1-2.3.7**.

5.2.9.1 Immunisation of BALB/c Mice using Imject Alum as Adjuvant

Five female BALB/C mice, over 10 weeks of age, were immunised (**2.3.8**) as outlined below and generation of an anti-NRAMP1 peptide Ab response was tested by ELISA.

Day 0	10μg peptide i.p. in Imject Alum (**2.3.2**)
Day 3	10μg peptide i.p. in PBS (**2.3.1**)
Day 7	10μg peptide i.p. in PBS (**2.3.1**)
Day 22	7.5μg peptide i.p. in Imject Alum (**2.3.2**)
Day 37	ELISA to test first test bleed (**2.5.2**)
Day 38	10μg peptide i.p. with nitrocellulose (**2.3.3**)
Day 51	ELISA to test second test bleed (**2.5.2**)

Day 37 ELISA (First bleed test)

There was little evidence of an anti-NRAMP1 peptide Ab response in the immunised mice compared to the NMS control when the sera were tested by ELISA. At 1/50 and 1/150 dilutions of sera from the immunised mice in wells coated with 4.0μg/ml and 8.0μg/ml peptide there was a slight, approximately 1.5 to 2 fold, increase in the absorbance measured. However, this finding did not extend to the wells coated with lower peptide concentrations or the more dilute sera samples tested. The absorbance readings of the wells that had not been coated with peptide were similar to, or in some instances greater than, those of wells coated with peptide, which showed this negative control was not working appropriately.

Due to the low or negligible response mounted in the immunised mice, they were immunised with a peptide/nitrocellulose mixture 38 days after the initial immunisation, in the hope that the nitrocellulose would act as a more effective adjuvant.

Day 51 ELISA (Second bleed test)

A similar result to the Day 37 ELISA was obtained with the lowest sera dilutions and highest peptide coating concentrations giving the highest absorbance readings. However, these were still only approximately 1.5 to 2 fold greater than the NMS controls. The wells that had not been coated with peptide still showed absorbencies of a similar order of magnitude to those coated with peptide. This may have been due to the carbonate/bicarbonate buffer added at the peptide coating stage, which was used to dilute the peptide and increase the adherence of the peptide to the plate. When the mouse sera was subsequently added to the wells, the effect of the carbonate/bicarbonate buffer might be increasing non-specific adherence of the sera. Because the wells which were not coated with peptide were proving unsuitable as a negative control and no positive control anti-NRAMP1 sera was available, it was decided that future sera samples would be tested using dot blots.

Dot Blots

When the second bleed serum was tested alongside subsequent sera samples, to be described in **5.2.9.2** and **5.2.9.3**, there was no difference in the reactivity of this serum to any of the test substances on the dot blots when compared to the reactivity of the NMS (**Figure 5.11**).

5.2.9.2 Immunisation of BALB/c Mice with NRAMP1 Peptide-Pulsed Dendritic Cells

As the DC is the most potent and efficient APC I attempted to isolate DCs from the spleens of the BALB/c mice immunised with NRAMP1 peptide, described in **5.2.9.1**. These cells were subsequently pulsed with the peptide *in vitro* and injected i.v. (**2.3.8**) into four female BALB/c mice, over 10 weeks of age. By loading the DCs with the peptide prior to injection it was hoped they would act as efficient APCs *in vivo*, presenting the NRAMP1 peptide to T cells which would initiate an effective anti-peptide response and provide T cell help for a B cell anti-peptide Ab response.

Day 0	4.35×10^5 peptide-pulsed DCs injected i.v. (**2.3.4**)
Day 13	10μg peptide i.p. in Imject Alum (**2.3.2**)
Day 28	10μg peptide i.p. in PBS (**2.3.1**)
Day 60	10μg peptide i.p. in PBS (**2.3.1**)
Day 69	Dot blots to test first test bleed (sera at 1:100) (**2.4.4**)
Day 96	10μg NRAMP1/KLH conjugate in PBS (**2.3.5**)
Day 107	Dot blots to test second test bleed (sera at 1:100) (**2.4.4**)

Day 69 Dot Blots (First Bleed Test)

Dot blots were performed using pooled sera from the NRAMP1 peptide-pulsed DC immunised mice, NMS and omitting mouse sera to test for reactivity against the NRAMP1 peptide, NRAMP1/KLH conjugate, KLH, BALB/c IgG, BSA and NRS.

No Ab response against the NRAMP1 peptide was seen in the developed dot blots testing the sera from mice immunised with the NRAMP1 peptide-pulsed DCs or

NMS (**Figure 5.11**). This implied the immunised animals had failed to mount an appropriate B cell response against the peptide. A weak positive reaction against the KLH dot and a very weak positive reaction against the NRAMP1/KLH conjugate was seen with the immunised sera and the NMS which was likely to be due to the presence of pre-existing Abs cross reactive with epitopes of the KLH molecule (**Figure 5.11**). A strong blue dot was seen for the BALB/c IgG positive control dot for all the mouse sera tested and the negative control incubated without mouse serum demonstrating the anti-mouse Ig detection method had been carried out successfully (**Figure 5.11**). The negative control strip was negative for all the other dots except for a virtually negligible response against the KLH dot, which may be due to the presence of pre-existing Abs in the secondary, rabbit anti-mouse sera, cross reactive with KLH epitopes (**Figure 5.11**). The NRS dot was negative in all the blots as expected (**Figure 5.11**). Interestingly a response was observed against the BSA dot when the immunised sera were tested which was absent in the control dot blot tested with NMS (**Figure 5.11**). This response must have been mounted against residual FCS, containing BSA, in the DC preparation after the *in vitro* culture and showed that these mice were capable of mounting an Ab response.

As all the mice to date had failed to mount an appropriate response against the NRAMP1 peptide when it was given with Imject Alum or nitrocellulose adjuvant and boosted in PBS, or when the mice were immunised with DCs which had been pulsed with the peptide, an attempt was made to conjugate the peptide to KLH. KLH acts as a carrier protein for peptides and stimulates an immune response against KLH which can spread to and enhance a response against small, attached peptides which on their own are non-immunogenic. Peptides are most easily and efficiently conjugated by terminal cysteine residues but the NRAMP1 peptide did not have such a residue. Instead the peptide was conjugated to KLH via NH_2 amino groups using DMS (**2.3.5**). The five BALB/c mice, previously unresponsive to the peptide-pulsed DCs were immunised with the KLH conjugated peptide in PBS and a second bleed was tested by dot blotting.

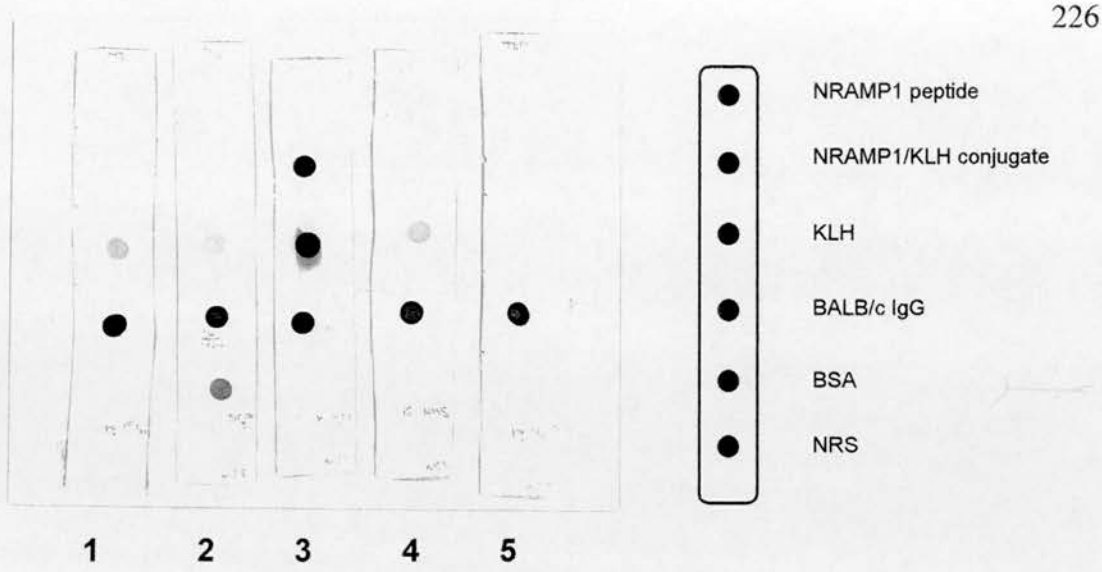

Figure 5.11 Dot blots to test reactivity of mouse sera. Blots were incubated with **1** sera from mice immunised with the NRAMP1 peptide with Imject Alum and nitrcellulose as adjuvant, **2** sera from mice immunised with NRAMP1 peptide-pulsed DCs, **3** sera from mice immunised with the NRAMP1/KLH conjugate, **4** NMS, **5** no primary sera. A diagram showing the position of the dots of test substances on the strips is shown to the right hand side. KLH: Keyhole limpet haemocyanin, BALB/c IgG: control IgG from BALB/c mice, BSA: bovine serum albumin, NRS: normal rabbit sera. Immunisation protocols are described in **5.2.9.1-5.2.9.3**.

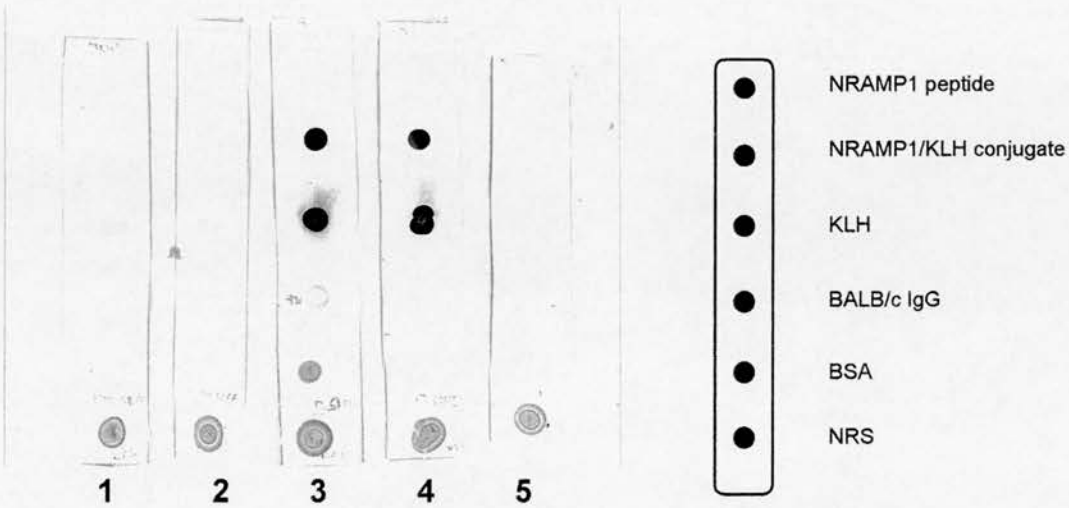

Figure 5.12 Dot blots to test reactivity of rabbit sera. Blots were incubated with pre-immune sera from rabbits **1** 51FF and **2** 62FF, sera from rabbits **3** 51FF and **4** 62FF after immunisation with NRAMP1 peptide/KLH conjugate or **5** no primary sera. A diagram showing the position of dots of test substances on the strips is shown to the right hand side KLH: Keyhole limpet haemocyanin, BALB/c IgG: control IgG from BALB/c mice, BSA: bovine serum albumin, NRS: normal rabbit sera. The immunisation protocol is described in **5.2.9.5**.

Day 107 Dot Blots (Second Bleed Test)

Blots were performed to test the pooled sera from mice immunised with the NRAMP1 peptide-pulsed DCs followed by the NRAMP1/KLH conjugate, NMS or omitting mouse sera.

No Ab response against the NRAMP1 peptide was seen in the developed dot blots testing the sera from any of the groups. The results of the NMS were as for the Day 69 dot blot (**Figure 5.11**) with the exception that a faint blue colour was seen over the NRS dot. This was also seen with the sera from mice immunised with the NRAMP1 peptide-pulsed DCs followed by the NRAMP1/KLH conjugate, and is likely to be due to the presence of mouse anti-rabbit Abs which became detectable when the blots were developed for slightly longer than in the previous analysis. The results of the rest of the blot for the immunised sera were also as for the Day 69 blot (**Figure 5.11**), except for an increase in the response against dots containing KLH. This showed the mice had successfully mounted an Ab response against the KLH component of the conjugate with which they had been immunised. The results for the negative control strip incubated without mouse sera were as for the Day 69 dot blot (**Figure 5.11**).

5.2.9.3 Immunisation of BALB/c Mice with the NRAMP1 peptide/KLH Conjugate

The NRAMP1 peptide/KLH conjugate previously discussed (**5.2.9.2**) was used as an immunogen with Imject Alum as an adjuvant to immunise five 8 week old, female, BALB/c mice according to the following protocol.

Day 0	8-9μg NRAMP1/KLH conjugate in Imject Alum i.p. (**2.3.5**)
Day 28	10μg NRAMP1/KLH conjugate in Imject Alum i.p. (**2.3.5** and **2.3.1**)
Day 40	Dot blots to test first test bleed (sera at 1:100) (**2.4.4**)

Day 67	10μg NRAMP1/KLH conjugate and 10μg peptide in PBS i.p. (**2.3.5** and **2.3.1**)
Day 78	Dot blots to test second test bleed (sera at 1:100) (**2.4.4**)

Day 40 Dot Blots (First Bleed Test)

The pooled sera from the first test bleeds from the mice immunised with the NRAMP1/KLH conjugate were tested alongside the Day 69 dot blots described in **5.2.9.2**, therefore, the NMS and negative control results have been outlined. The sera from the NRAMP1/KLH conjugate immunised mice failed to show any Ab response against the NRAMP1 peptide dot but a strong reaction against the KLH and NRAMP1 peptide/KLH dots was seen (**Figure 5.11**). This implied a successful Ab response had been mounted by the mice against the KLH molecule but a response against the NRAMP1 peptide component of the conjugate could not be detected. There was no detectable response against the BSA or NRS dots (**Figure 5.11**). The positive control BALB/c IgG dot was strongly positive confirming the successful detection method for the murine Igs (**Figure 5.11**).

The mice had already received two immunisations with the NRAMP1/KLH conjugate in Imject Alum so, despite none of the animals showing any adverse effects of the immunisations, the final immunisation was carried out without the adjuvant. Because the mice had mounted such a strong response against the KLH component of the conjugate the final immunisation of this group of mice consisted of a mixture of the conjugate, to increase the immunogenicity of the peptide, and the NRAMP1 peptide alone, to increase the relative concentration of the component against which a response was desired.

Day 78 Dot Blots (Second Bleed Test)

The results of the dot blots to test the second test bleed for the pooled sera from mice immunised with the NRAMP1/KLH conjugate were similar to those of the first test bleed for this group of mice. The only difference was a slight increase in the relative intensity of the response to the dots with a KLH component compared to the BALB/c

IgG dot, as might be expected after the booster immunisation. A very weak colour was seen over the NRS dot implying the presence of anti-rabbit Abs in the mouse sera tested. This was also seen in the other groups of murine sera tested and was not a result of the immunisation procedures. No detectable Ab response was seen against the NRAMP1 peptide or the BSA dot in any of the groups of mice tested. The negative control blot incubated without mouse sera showed a positive result for the BALB/c IgG dot, confirming the anti-mouse Ig detection method had been successful, and a very weak blue colour over the dots with a KLH component, suggesting the presence of Abs in the secondary rabbit anti-mouse Ig which cross react with KLH epitopes.

5.2.9.4 Immunisation of BALB/c and C57/Bl Mice using Freund's Adjuvant

All previous immunisation strategies and adjuvants had failed to generate a detectable anti-NRAMP1 peptide Ab response so it was decided to try an immunisation protocol using the more potent Freund's adjuvant. Freund's complete adjuvant (CFA) and Freund's incomplete adjuvant (IFA) have proved highly effective in stimulating Ab responses against molecules which are non-immunogenic when given alone. The amount of peptide given to each mouse was also increased to determine if this might enhance the response.

All the previous immunisations had been carried out on BALB/c mice because established techniques exist for raising monoclonal Abs from lymphocytes derived from these mice. However, BALB/c mice carry the susceptibility allele of the murine *nramp1* gene and, hence, may have a genetic trait that affects their capacity to respond to an NRAMP1 peptide. Therefore, I wished to immunise a group of C3H mice, which carry the resistance *nramp1* allele, in parallel with a group of BALB/c mice, to try to eliminate this as a possible reason preventing the desired response. However, due to shortages in the animal house C3H mice were unavailable so C57/Bl mice were used instead. These mice also carry the susceptibility *nramp1* allele though they have a different H2 haplotype from the BALB/c mice. Three mice of each strain were immunised as outlined below.

Day 0	50μg peptide in CFA (1:1) i.p. (**2.3.6**)
Day 14	50μg peptide in IFA (1:1) i.p. (**2.3.7**)
Day 25	Dot blots to test first test bleed (sera 1:100) (**2.4.4**)
Day 32	50μg peptide in IFA (1:1) i.p. (**2.3.7**)
Day 55	Dot blots to test second test bleed (sera 1:100) (**2.4.4**)

Day 25 Dot Blots (First Bleed Test)

Triangular dot blots were performed with test dots of the NRAMP1 peptide, BSA and BALB/c IgG. The serum samples from each of the six immunised mice and NMS were tested separately and a negative control blot, incubated without mouse serum, was included. On all the blots no detectable Ab response was seen against the NRAMP1 peptide. The BSA dots were all negative except for a very faint reaction with the serum from one of the C57/Bl mice. All the dot blots showed a strong positive blue colour over the BALB/c IgG dot confirming the anti-mouse Ig detection method had worked successfully.

As no detectable Ab response was detected against the peptide, the mice were immunised again with the peptide in IFA and a second test bleed taken.

Day 55 Dot Blots (Second Bleed Test)

As for the first bleed dot blots no Ab response was detected on any of the dot blots. All of the serum samples tested, but not the negative control blot, showed a weak response to the BSA dot, which may reflect a longer development period in the NBT/BCIP substrate rather than any increased Ab response in the immunised animals. This is supported by the NMS blot's BSA dot also being weakly positive, which was not seen when the same serum sample was used as a control when the first bleeds were tested. The BALB/c IgG dot was positive on all the dot blots, confirming the anti-mouse Ig detection method had worked successfully.

5.2.9.5 Immunisation of Rabbits with the NRAMP1//KLH Conjugate

As attempts to raise NRAMP1 peptide-specific Abs in mice had failed, immunisation of two rabbits with the NRAMP1/KLH conjugate was tried. The rabbit *nramp1* gene or protein sequence was not available so the degree of conservation between the peptide sequence and the equivalent region of the rabbit protein was not known. Rabbits have previously been immunised successfully with substances that have been non-immunogenic in mice and they have the advantage that a larger amount of serum can be obtained from each animal. However, established methods to raise monoclonals from rabbits are not available. The rabbits were immunised sub cutaneously (s.c.) at four sites with the NRAMP1/KLH conjugate in the Imject Alum adjuvant to increase the immunogenicity of the NRAMP1 component. The rabbits were identified as 62FF and 51FF and a pre-immune serum sample was collected from each animal prior to immunisation as outlined below.

Day 0	100μg NRAMP1/KLH conjugate in Imject Alum at 4 sites s.c. (**2.3.5** and **2.3.2**)
Day 28	100μg NRAMP1/KLH conjugate in Imject Alum at 4 sites s.c. (**2.3.5** and **2.3.2**)
Day 40	Dot blots to test first test bleed (sera at 1:100) (**2.4.4**)
Day 67	100μg NRAMP1/KLH conjugate and 100μg peptide in PBS at 4 sites s.c. (**2.3.5** and **2.3.1**)
Day 78	Dot blots to test second test bleed (sera at 1:100) (**2.4.4**)

Day 40 Dot Blots (First Bleed Test)

Dot blots for the pre-immune and first bleed sera were performed and a negative control dot blot, incubated without any rabbit serum, was included. None of the blots showed any detectable Ab response against the NRAMP1 peptide dot. Both of the pre-immune serum samples showed a weak response against the KLH dot and an even weaker response against the NRAMP1/KLH conjugate dot. A similar intensity of blue colour was seen in the dot blot incubated without any rabbit serum, suggesting this reaction was the result of Abs present in the secondary swine anti-

rabbit Ig which were cross reactive with KLH epitopes. The intensity of these responses was greatly increased in the serum samples from the two immunised rabbits, which showed a successful response had been mounted by both animals to the KLH component of the immunogen. A response was also seen against the BSA dot and a weaker response against the BALB/c IgG dot in the serum from immunised rabbit 51FF. The response of serum from immunised rabbit 62FF against the BALB/c IgG dot was negligible and against the BSA dot was undetectable. The dot blots for the pre-immune serum from both animals and the negative control blot were all negative for the BALB/c IgG and BSA dots. All the dot blots gave a positive reaction for the NRS dot confirming the anti-rabbit Ig detection method had been successful (**Figure 5.12**).

The rabbits' Ab response against the KLH component of the conjugate showed they were capable of mounting Ab responses. In an attempt to extend this response to the NRAMP1 component of the conjugate, the animals were immunised with a mixture of the conjugate and the unconjugated peptide. By increasing the concentration of the peptide in the innoculum, I hoped the desired response against the peptide might occur.

Day 78 Dot Blots (Second Bleed Test)

The results for all the dots on all of the blots were as described for the Day 40 dot blots, described above. Where very weak dots had been seen previously these were stronger because the blots had been developed for a longer time in the NBT/BCIP chromogen, but no positive reaction against any of the dots previously negative was seen.

5.2.9.6 Immunocytochemistry on *NRAMP1* Transfected Cell Lines

Sera from the rabbits immunised with the NRAMP1 peptide (**5.2.9.5**) showed no evidence of specific anti-NRAMP1 reactivity when tested on clones of MM6 and U937 cells which had been transfected with the pCIneo/NRAMP1 plasmid and shown to express the plasmid *NRAMP1* sequence at the RNA level (**5.2.7-5.2.8**).

5.3 DISCUSSION

A mammalian expression vector containing the whole *NRAMP1* cDNA (pCIneo/NRAMP1) was successfully constructed from partial *NRAMP1* cDNAs in the pCIneo plasmid. The initial intention to use this as a vehicle for overexpression of *NRAMP1* in primary cultures of aPBMCs was hampered by the failure to find a means of efficient transfection of these cells. In order to carry out experiments to assay a physiological effect of *NRAMP1* overexpression a reproducible, efficient transfection procedure was necessary. The liposome based methods I attempted (Lipofectin Reagent, Lipofectamine Reagent, DOSPER Liposomal Transfection Reagent and SuperFect Reagent) have been documented by the respective suppliers for use with many cell lines from a variety of species. However, the data on successful transfection of primary cell lines is sparser. Such reported successes have generally used primary fibroblasts, hepatocytes, endothelial cells or smooth muscle cells and none of the suppliers were able to confirm success using their product for transfection of primary aPBMCs. Personal communication with other scientists attempting similar transfections revealed comparable problems were being encountered. It is interesting to note that these workers also found the most promising, though still inefficient, results with DEAE-dextran transfection. For successful transfection genes must be delivered intracellularly, ultimately to the nucleus, in functional form and retained and expressed therein. Electron microscopy studies of cationic liposomes alone or complexed with DNA and/or gold particles have tracked their transit in cultured cells, including a variety of cell lines and primary human peripheral blood monocytes, primary rat alveolar type II cells and primary rat alveolar Mϕs (Friend *et al.* 1996). The results suggest the DNA-cationic liposome complexes enter the cell in a manner resembling receptor mediated endocytosis in clathrin coated pits. The complexes were seen in early endosomes, late endosomes and lysosomes. Some cells showed evidence of gold particles dispersed through the cytoplasm and a membrane system resembling the ER developed in the nucleus of some CV-1 (African green monkey kidney) and U937 cells. The authors suggest the DNA complexes are released from the endosomal compartment and are transferred through the cytoplasm to the nucleus, though, in

some instances the cationic lipid may react with the nuclear envelope. I have not tracked the passage and fate of the liposome-DNA complexes used when trying to transfect my primary aPBMCs and can not confirm or quantitate successful entry of DNA into the nucleus. The nature of these cells, which are highly efficient at degrading foreign internalised material, suggests problems in the delivery of intact DNA are likely. The reported study was looking at transit of the complexes and did not determine whether the cells successfully expressed the transfected DNA. It appears that in primary Mϕs there are additional problems getting the cells to express exogenous DNA. Despite evidence of transfected DNA being present in the nucleus it is common for the DNA to remain unexpressed (personal communication). Whether this is the result of an inherent aversion to expression of foreign DNA by cells designed to eradicate pathogens, such as viral particles, is not known but emphasises the complexity of the problems to be considered. All my attempts at transfection were carried out with non-linearised plasmid DNA which I found to be expressed successfully in comparison to linearised DNA when U937 cells were electroporated and, hence, the DNA should have been more resistant to exonuclease digestion.

Primary cultures of murine peritoneal Mϕs have been transfected more successfully with DEAE-dextran, followed by osmotic shock with DMSO, than by a variety of other protocols, including calcium-phosphate precipitation or lipofection (Rupprecht and Coleman 1991). Despite finding a few cells which showed expression of the reporter gene encoding β-gal when I tried to transfect primary aPBMCs under various DEAE-dextran conditions, the efficiency was still exceedingly low and of no use for the studies with which I hoped to continue. As my results also showed greater transfection success using DEAE-dextran rather than lipofection, as this report found, it appeared unlikely calcium phosphate precipitation would be any more successful in my system. The decision was, therefore, taken to try to transfect cell lines with the pCIneo/NRAMP1 plasmid, rather than persevere further with primary cultures. It is possible, however, that I might have had more success with particle bombardment techniques (Burkholder *et al.* 1993) but in the light of the lack of anti-

NRAMP1 antisera which would be necessary for rapid detection of NRAMP1 overexpression to identify successful pCIneo/NRAMP1 transient transfectants, stable transfection seemed more appropriate.

Both MM6 and U937 cell lines were successfully transfected on the basis of the presence of plasmid DNA in transfected cells, assayed by PCR, and plasmid encoded expression, assayed by RT-PCR, of *NRAMP1* and *neo*, or *neo* alone, in the pCIneo/NRAMP1 and pCIneo plasmid transfected cells, respectively. Despite exhaustive attempts to raise Abs against NRAMP1 in mice and rabbits, I failed to detect any sera specific for the peptide that was used as an immunogen, and hence was unable to confirm translation of the *NRAMP1* mRNA. It is well documented that nramp1 family members are highly conserved across species (Cellier *et al.* 1995) and this may be the reason for the lack of response encountered in the immunised animals. Where highly homologous proteins exist, tolerance induction to the endogenous protein of one species may extend to proteins of another species. Though the sequence of the peptide used as an immunogen was from the region of greatest divergence between the murine and human proteins significant conservation still existed. To raise an Ab response both a T cell and B cell epitope are required and there may have been a shortfall on this account with the NRAMP1 peptide used. It is not known whether the alternative peptide sequence I considered as an immunogen, at the N terminus of NRAMP1, may have proved more successful in generating anti-NRAMP1 Abs. The C terminal peptide was chosen in preference for two reasons. Firstly, it is not known whether the +alu *NRAMP1* splice variant is translated to protein, but if it is, the resultant protein would not be detected by Abs raised against the C terminal peptide. In contrast, Abs raised against the N terminal peptide considered could theoretically react with both truncated and full length protein and, hence, would be uninformative with respect to the levels of full length functional NRAMP1 protein known to be functional. Secondly, the generation of polyclonal rabbit sera has been reported which was against a very similar NRAMP1 peptide, conjugated to KLH (Kishi and Nobumoto 1995; Kishi *et al.* 1996a). However, in the light of more recent information about the expression pattern,

localisation and molecular weight of NRAMP1 and nramp1 (Atkinson *et al.* 1997; Gruenheid *et al.* 1997) the specificity of this sera is now in question.

Both strains of mice used for the immunisations with the NRAMP1 peptide, BALB/c and C57Bl, carry the *nramp1* susceptibility allele. As this allele is a null allele and nramp1 protein is undetectable in these mice, the question of tolerance induction against nramp1 is an interesting consideration. In the absence of nramp1 protein one could hypothesise that these animals should not have specific nramp1 tolerance and would, therefore, be an ideal strain in which to raise such a response. However, it is also possible that there is a level of translation of the mutant mRNA to protein which is then subsequently degraded due to potential misfolding and recognition by the cells' protein degradative machinery. In this case one could envisage a system flooded with nramp1 peptides to which the mice could become tolerant. These potential peptides might encompass the C terminal peptide I used as an immunogen and, as such, explain the failure to mount an Ab response. Had mice carrying the resistance allele been available for immunisation, it would have been interesting to see if these mice were any more responsive to the peptide, though these strains would be expected to have unequivocal nramp1 tolerance. The BALB/c and C57Bl mice carry different H2 haplotypes, but these differences did not appear to influence the lack of an Ab response against the NRAMP1 peptide. Whether exhaustive attempts of immunising mice carrying other H2 haplotypes would have been met with more success remains unclear, though the general lack of success in all the animals immunised suggests not. Rabbits have been found to be more responsive to certain antigens which appear non-immunogenic in mice, though in the case of the NRAMP1 peptide this was not so. It is relevant to point out that Professor Jenefer Blackwell, the eminent scientist working in the nramp1 field in this country, has also been unsuccessful in raising antisera against human NRAMP1 despite having antisera reactive against the murine protein (personal communication).

Analysis of the pCIneo/NRAMP1 and pCIneo plasmid transfected cell lines was, therefore, totally reliant on DNA and mRNA analysis. A methodical procedure was

exercised to identify G418 resistant mixed cell populations which contained the relevant plasmid DNA, assayed by PCR. Southern blots were considered as an alternative assay but were rejected in favour of the PCR strategy for a number of reasons. The plasmids were transfected in a circular form and as such no control was had over where the DNA would linearise prior to integration into the genomic DNA. Choosing a region of the plasmid which would be suitable as a probe for all the clones was, therefore, a problem in case the chosen fragment spanned the point of linearisation. The NRAMPalu PCR primers I used were conveniently available, having been designed to detect RNA expression. They were cDNA specific and would not cross react with the endogenous *NRAMP1* gene sequence. Cross-hybridisation of a probe with the endogenous gene or other homologous *NRAMP1* family members was a potential issue if Southern hybridisation had been performed. Perfecting the stringency to detect only the plasmid DNA might have been problematic. As I was dealing with large numbers of clones which I wished to screen rapidly, whose RNA expression profile also needed extensive analysis, PCR was considered a relatively quick and straightforward procedure in comparison to Southern blotting. In addition because I designed a variety of primers I had four reactions for the pCIneo/NRAMP1 transfectants and two reactions for the pCIneo transfectants to confirm presence of the plasmid DNA and, hence, quadruplicate or duplicate proof.

From the mixed cell populations showing the appropriate PCR and RT-PCR profiles, single clones were derived on the basis of limiting dilution. Due to time constraints this process was carried out once for each of the mixed cell populations selected. Ideally, limiting dilution of the clones derived from the first round would have been repeated at least twice more to increase the probability of obtaining a genuine clone. Taking this into consideration the cell samples I have considered as single clones may actually be derived from more than one founder cell.

The semi-quantitative RT-PCR assay successfully and consistently identified certain clones as expressing higher or lower levels of the plasmid DNA. The clone

expressing the highest level of *NRAMP1* was D12, derived from the MM6 parent cell line. Inclusion of RT-PCR reactions with primers specific for untranscribed plasmid DNA enabled me to ensure only cDNA sequence, and not carry through plasmid DNA which had been incompletely DNase-treated, was amplified. Semi-quantitative RT-PCR approaches have been criticised as being unreliable and open to the "quirks" of PCR. I did not find this to be a problem because I was not looking for an absolute quantitative result, which appears a challenging task using a PCR approach, but only a measure of the relative amount of message of the genes of interest with respect to the housekeeping GAPDH gene. By measuring the intensity of the product bands by UV densitometry a relatively simple and reproducible result could be obtained. Though the ratios for a single clone analysed repeatedly were not identical the hierarchy of ratios for the different clones consistently identified the same clones to be expressing the greatest or least amounts of plasmid message. There are several stages involved in the analysis from extraction of RNA from the cell lines through to the final analysis of the electrophoresed RT-PCR products, and hence multiple opportunities for incorporating error in the samples. However, it is unlikely that the same clone would be subjected to the same error during every analysis I undertook, hence, I believe my results are genuine. As mentioned previously I do lack evidence of translation of the plasmid *NRAMP1* mRNA to protein and I have no information with respect to the cellular localisation of such protein in the transfectants. In interpreting any results of experiments investigating the effect of *NRAMP1* overexpression it is important to acknowledge this short fall. Increased levels of plasmid-originating NRAMP1 protein directed to the plasma membrane, for instance, may well cause a measurable physiological effect. However, if the endogenous protein is targeted to late endosomes/lysosomes (Gruenheid *et al.* 1997) the results may be very misleading. Taking this into consideration the tools were now available to further investigate the effect of overexpression of plasmid derived *NRAMP1* mRNA in clones derived from the MM6 parent cell line.

5.4 CONCLUSION

I have successfully constructed a mammalian expression vector (pCIneo/NRAMP1) for overexpression of the human *NRAMP1* gene and have transfected the MM6 and U937 cell lines with this plasmid and the control pCIneo plasmid. I have shown the presence of plasmid sequence by PCR in G418 resistant transfectants, which were cloned by limiting dilution, and plasmid encoded mRNA expression by RT-PCR. Attempts to raise Abs against NRAMP1 were unsuccessful and I found no evidence of an anti-NRAMP1 peptide Ab response in any of the mice or rabbits which had been immunised with the NRAMP1 peptide using a variety of adjuvants (Imject Alum, nitrocellulose, CFA, IFA), as peptide alone, conjugated to KLH or given i.v. in the form of peptide-pulsed DCs. The lack of antisera specific for NRAMP1 meant I was unable to identify NRAMP1 protein expression patterns or profiles in the parent and pCIneo/NRAMP1 transfected cells. Therefore, all expression data for the *NRAMP1* gene was dependent on analysis of mRNA expression by semi-quantitative RT-PCR which identified the clone expressing the highest levels of *NRAMP1* to be D12, a MM6 derived transfectant.

6 FUNCTION OF NRAMP1

6.1 INTRODUCTION

Since the initial identification and cloning of the murine *nramp1* gene (Vidal *et al.* 1993) significant light has been shed on the physiological function of the encoded protein. The majority of information suggesting the protein acts as a divalent cation transporter was primarily gleaned indirectly from comparison of the function of homologous proteins from other species including the *Drosophila mvl* (Orgad *et al.* 1998), *S. cerevisiae SMF1* and *SMF2* (Supek *et al.* 1996 and 1997), *O. sativa Osnramp* (Belouchi *et al.* 1997) and, more recently, the *nramp2* (Fleming *et al.* 1996 and 1997; Nussberger *et al.* 1997) gene product homologues. Murine and rat nramp2 proteins encode transporter proteins with a broad substrate range for a number of divalent cations, though they have highest affinity for Fe^{2+} ions. Mutations in these genes are responsible for the *mk* mouse (Fleming *et al.* 1997) and Belgrade rat (Fleming *et al.* 1998) phenotypes which result from defects in iron uptake and transport. Nramp1 and nramp2 proteins are 63% identical (Gruenheid *et al.* 1995) and though it is possible, and has been shown to be the case (Atkinson and Barton 1998 and 1999), that the former may also act as an iron transporter there is sufficient divergence between the proteins to suggest nramp1 could have a higher affinity for another metal ion. Recent reports have focused on the ability of nramp1 to transport iron (Atkinson and Barton 1998 and 1999), but its affinity for Fe^{2+} has been shown to be much lower than that of the rat nramp2 protein (Gunshin *et al.* 1997) which may be indicative of a function distinct from that of nramp2.

Comparatively little is known about transport mechanisms of manganese in cells compared with a variety of other metal ions. The suggestion that the *mvl* gene product might play an important role in this process (Supek *et al.* 1996 and 1997) prompted me to investigate whether NRAMP1 functions as a manganese transporter protein. I wished to determine whether the cells which I had transfected with the pCIneo/NRAMP1 plasmid (**5.2.7** and **5.2.8**), designed to overexpress *NRAMP1*, behaved differently, compared to their parent cell line, with respect to their cellular

content of manganese under standard culture conditions or when cultured in increased Mn^{2+} concentrations. I addressed this problem by utilising the highly sensitive inductively coupled plasma mass spectophotometry (ICPMS) system to measure the levels of a variety of metal isotopes (Mn^{55}, Cu^{65}, Zn^{66} and Fe^{57}) in extracts obtained from lysed cells after *in vitro* culture.

Initial analysis of cells cultured in parallel under standard culture conditions were performed to determine if the base levels of the metals of interest differed between the parent cell line and pCIneo/NRAMP1 plasmid transfectants. The MM6 parent cell line and the D12 transfected cell clone, which had been shown by RT-PCR to express high levels of the plasmid derived *NRAMP1* (**5.2.8.3**), were then analysed after culture in standard culture medium or medium containing 1μM or 10μM $MnCl_2$.

6.2 RESULTS

6.2.1 Analysis of Cellular Metal Content

The sensitivity of ICPMS necessitated rigorous care being adopted to ensure all flasks of cells were cultured under the same conditions with media containing the same content of the metals of interest. Samples of prepared culture media were routinely analysed to exclude variations in media components contributing to potential differences in cellular metal content. These checks showed the metal content of the various media samples to be equivalent and, hence, not a source of variation in results between the different cell samples.

Extracts from cells, which had been cultured and treated in parallel, were analysed and the results obtained displayed graphically for comparison. This method of illustrating the results showed a general trend between samples, which was reproducible when extracts were reanalysed, though the absolute concentrations may have varied between separate analyses. For this reason absolute concentrations are not being quoted in the text and the graphical results represent one of the sets of results where the same cell extract sample was analysed more than once.

6.2.2 Metal Content of Cells Cultured under Standard Culture Conditions

6.2.2.1 MM6 and U937 Parent Cell Lines

When the MM6 and U937 parent cell lines were cultured under standard conditions (**2.18.1**) and their Mn, Cu and Zn cellular content measured, a marked difference was seen in the levels of Mn and Cu between the two cell lines. The MM6 cells had a higher cellular content of Mn and Cu (**Figures 6.1a** and **6.1b**) but there was no marked difference in the Zn levels of the two cell lines (**Figure 6.1c**).

6.2.2.2 MM6, B6, D12 and F12 Cell Lines

When the MM6 parent cell line was compared with the D12 clone, cultured under standard conditions (**2.18.1**), it was noted that the absolute concentrations of the three metals measured varied between separate samples from the same cell line/clone which were analysed at the same time. The overall pattern did not show a conclusive elevated level of Mn, Cu or Zn in extracts from either the MM6 or D12 cells (**Figures 6.2a**, **6.2c** and **6.2e**). In some of the analyses the D12 cells appeared to have a slightly elevated Mn content, but this was not seen consistently (**Figure 6.2a**).

A similar situation existed for the B6 and F12 clones, with cell extracts from neither clone showing a marked difference in the levels of the metals analysed (**Figures 6.2b**, **6.2d** and **6.2f**). The comparison of Cu levels for these cells is shown for completion. However, one of these readings for the B6 cells appears to be extraneous and may be the result of an experimental error or Cu contamination at some point in the procedure (**Figure 6.2d**).

The MM6 and D12 cells were cultured and analysed in parallel, as were the B6 and F12 cells. Though I have found it inappropriate to compare absolute values of the

a)

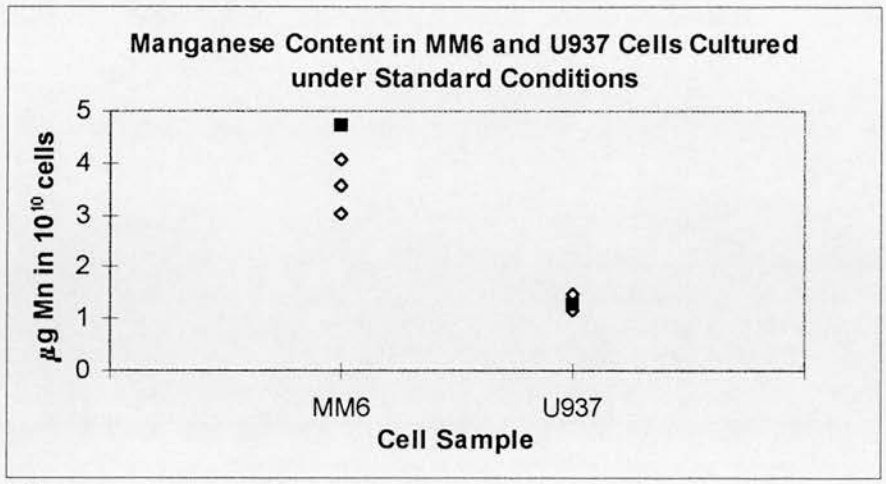

b)

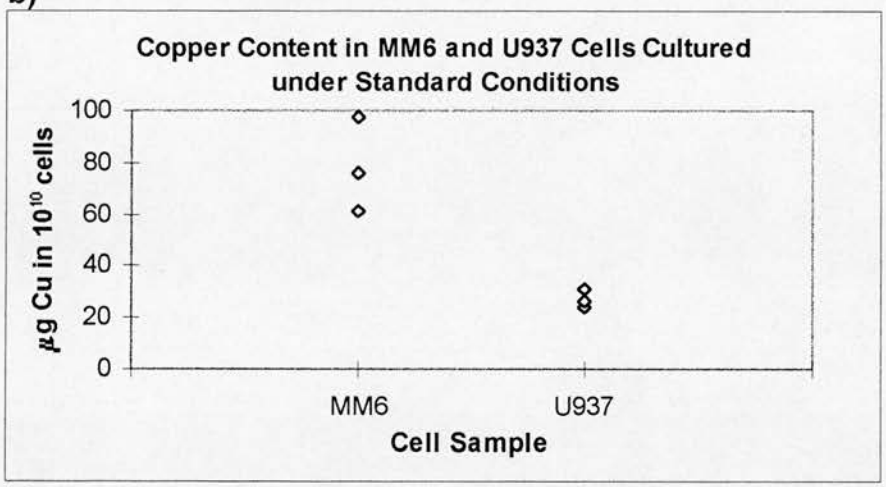

c)

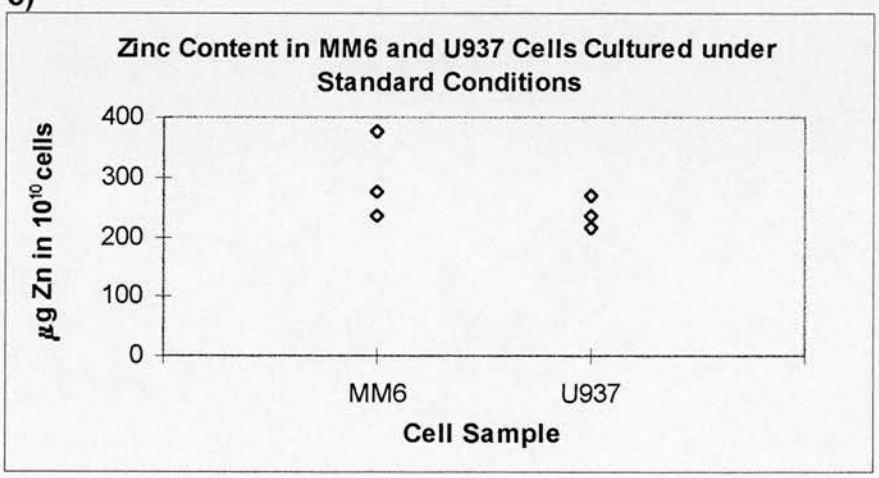

Figure 6.1 Comparison of the **a)** Mn, **b)** Cu and **c)** Zn content in extracts from MM6 and U937 cells cultured under standard conditions. The symbols (open diamonds and solid squares) represent two separate analyses where samples were analysed in parallel. Extracts from U937 cells have a lower Mn (**a**) and Cu (**b**) content compared to the MM6 cell extracts. The ICPMS analysis method used is described in **2.21**.

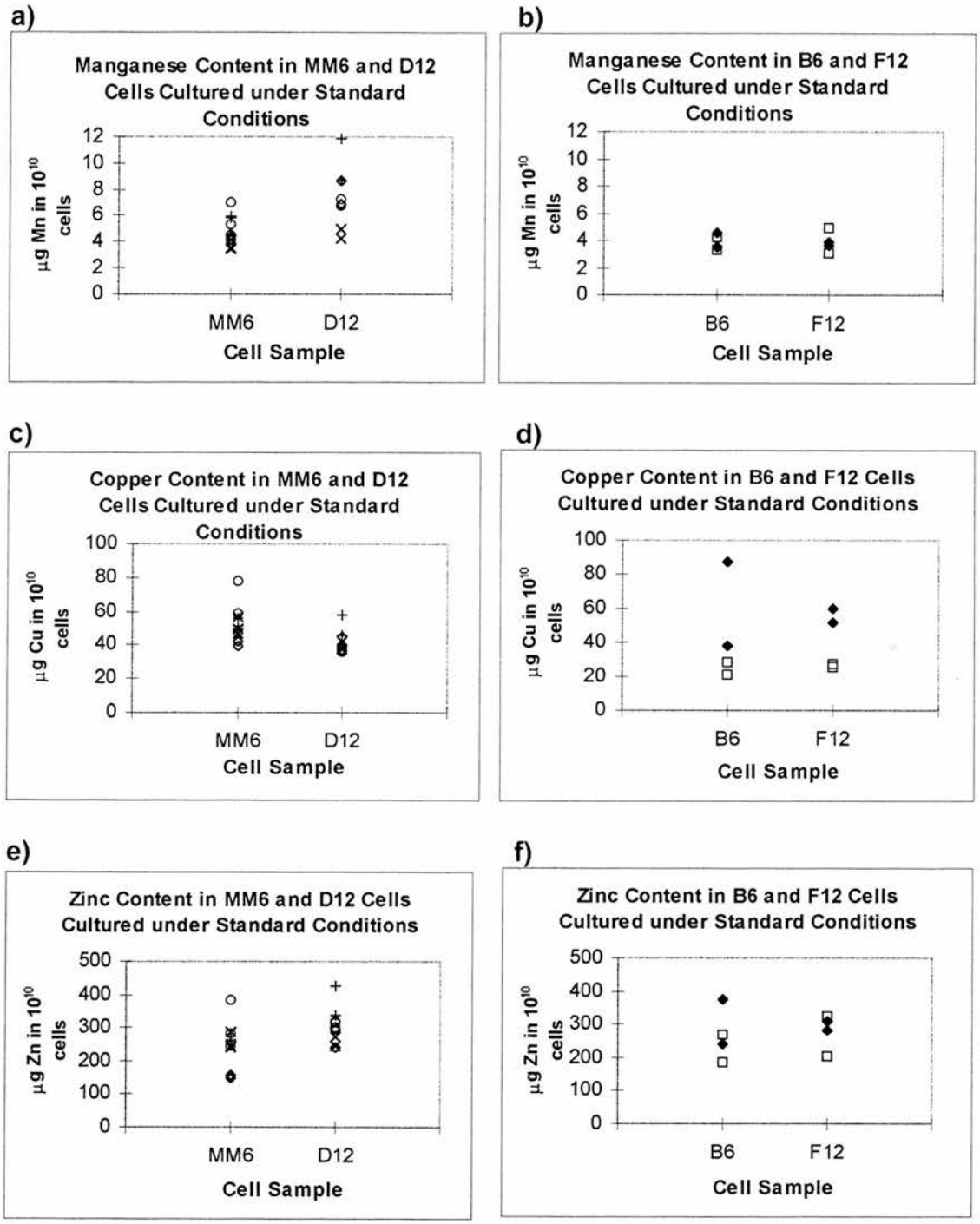

Figure 6.2 Comparison of the Mn (**a** and **b**), Cu (**c** and **d**) and Zn (**e** and **f**) content in extracts from MM6 and D12 cells (**a**, **c** and **e**) and B6 and F12 cells (**b**, **d** and **f**) cultured under standard conditions. The symbols represent separate analyses where samples were analysed in parallel. There is no significant difference in levels of the metals in the MM6 parent cell line and the D12, B6 and F12 clones of pCIneo/NRAMP1 transfected cells (described in **5.2.7** and **5.2.8**). The ICPMS analysis method used is described in **2.21**.

metal concentrations between cells cultured and analysed at different times the values obtained for B6 and F12 cells appear to be of the same order of magnitude as those for the parent MM6 cell line, suggesting there are no obvious variations between the parent cell line and any of the transfectants analysed (**Figure 6.2**).

In conclusion, it appears that under standard culture conditions in resting MM6 and cells transfected with the pCIneo/NRAMP1 plasmid there is no significant difference between the Mn, Cu or Zn cellular content of the cells analysed. This suggests that if active NRAMP1 protein is being expressed in the transfectants, under standard culture conditions no effect on transport of these metals is detectable when measured by the procedure I adopted. Therefore, I wished to investigate if the transfectants behaved differently when cultured under conditions of increased Mn concentrations, which may reflect a physiological function for the protein as a putative Mn transporter protein.

6.2.3 Metal Content of Cells Cultured in Manganese Chloride

Duplicate flasks of MM6 and D12 cells were cultured under standard culture conditions (**2.18.1**) or in medium which had been supplemented with 1μM or 10μM manganese chloride ($MnCl_2$). Prior to setting up these flasks the potential toxicity of these increased $MnCl_2$ concentrations was checked by comparing the viability of cells cultured in a range of $MnCl_2$ concentrations with that of cells cultured in standard medium. No difference in viability was apparent over the range of $MnCl_2$ concentrations tested and it was assumed that at the levels of $MnCl_2$ to be used for the subsequent experiment there would be no detrimental effect to the health of the cells. The results of this single experiment were illustrated graphically and will be discussed in detail in **6.2.3.1-6.2.3.4**. The samples were analysed twice and both analyses gave a similar pattern, though absolute concentrations varied slightly. The average values of the duplicate samples for each cell line were used when comparing the concentration change of the metals, and the percentage change of the metal content of the cells cultured in the different $MnCl_2$ concentrations.

6.2.3.1 Copper Content

As for the previous analyses of the MM6 and D12 cells cultured in standard medium (**6.2.2.2**) both groups of cells had a similar cellular Cu content when the samples from cells which had been cultured without additional $MnCl_2$ were compared (**Figure 6.3a**). When cultured in 1μM $MnCl_2$ both MM6 and D12 cells showed a similar pattern of a slight, but insignificant, increase in cellular Cu content (**Figures 6.3a-c**) compared to the standard culture condition values. However, when the cells were cultured in 10μM $MnCl_2$ the Cu level in the MM6 cells remained approximately the same as when they were cultured without or with 1μM $MnCl_2$ supplementation, while the level in the D12 cells dropped below that of the cells cultured without $MnCl_2$ (**Figures 6.3b** and **6.3c**). This could be the result of competition of Mn^{2+} ions at the elevated $MnCl_2$ concentration for Cu^{2+} sites in a transporter molecule which is either NRAMP1 itself, or physiologically affected by transfection of the cells with the pCIneo/NRAMP1 plasmid. Elevated levels of NRAMP1 protein in the D12 cells could be transporting both Cu and Mn but the Mn ions compete at the expense of the Cu ions when the cells are cultured in 10μM $MnCl_2$. This effect might only be observable when both the NRAMP1 protein and one or other of the relevant metal ions are present at non-physiological levels, hence, the MM6 cells remaining unaffected.

It is also possible that the NRAMP1 protein may be responsible, directly or indirectly, for the export of Cu from the cells.

6.2.3.2 Zinc Content

Comparison of the effects of culturing MM6 and D12 cells in the different $MnCl_2$ concentrations on cellular Zn levels showed a remarkably similar picture to that described in **6.2.3.1** for the cellular Cu content of the cells. Both groups of cells showed a slight increase in Zn content when cultured in medium with 1μM $MnCl_2$ compared to cultures with no added $MnCl_2$ (**Figure 6.4a**). The average percentage increase in zinc content of extracts from MM6 and D12 cells from cultures supplemented with 1μM $MnCl_2$ compared to those without supplementation was

Figure 6.3a

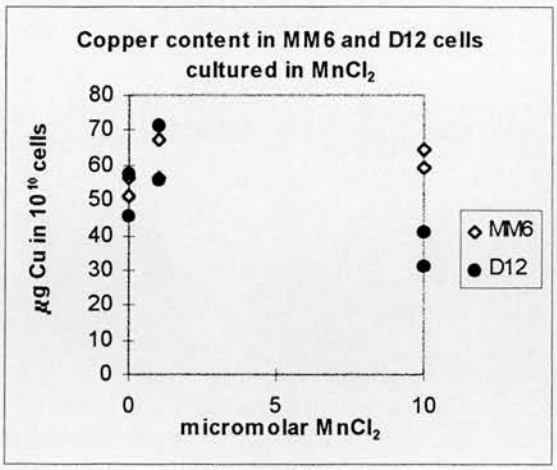

Figure 6.4a

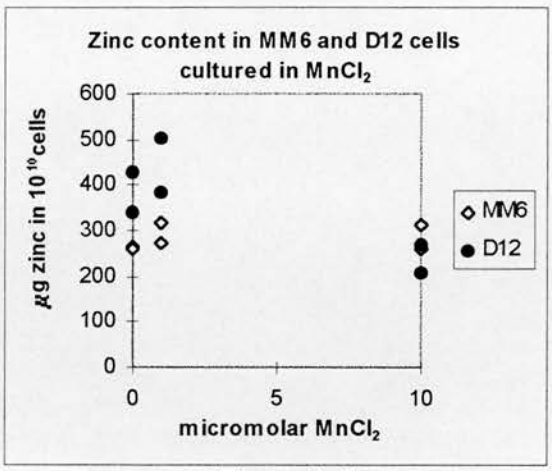

Figure 6.3b

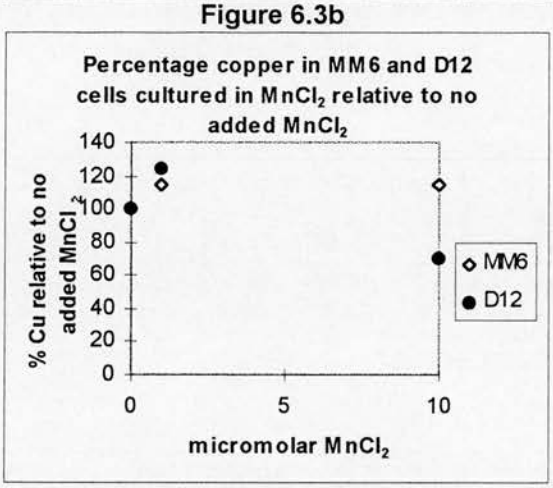

Figure 6.4b

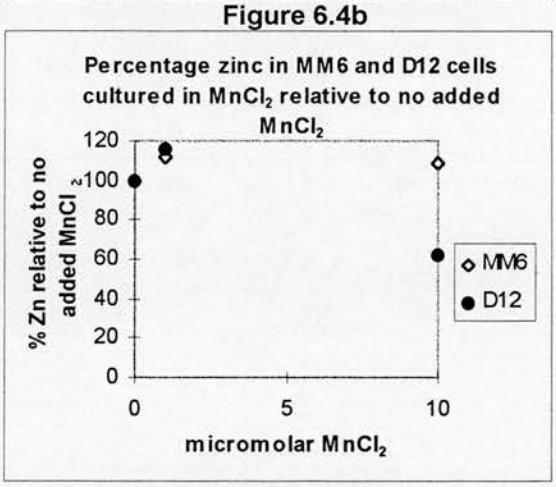

Figure 6.3c

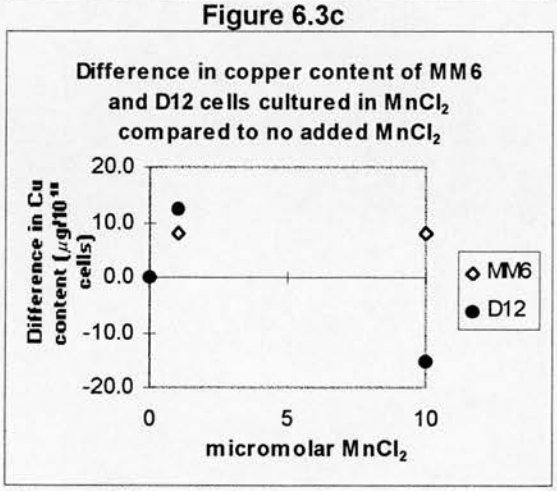

Figure 6.4c

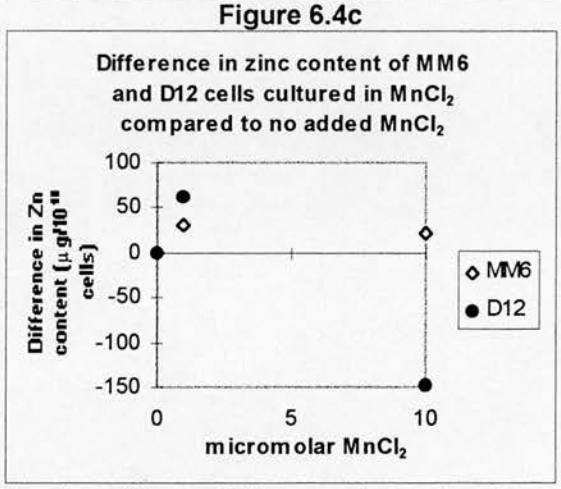

Figures 6.3 and **6.4** The effect on Cu (**Figure 6.3**) and Zn (**Figure 6.4**) content in MM6 and D12 cells cultured in medium supplemented with **0µM**, **1µM** and **10µM** $MnCl_2$. **a)** shows the metal content of extracts from triplicate cultures of the two cell lines. **b)** shows the percentage of the average metal content of the triplicate samples relative to those of the cells cultured without added $MnCl_2$. **c)** shows the difference between the average metal content of the triplicate samples and the cultures without added $MnCl_2$. Extracts from D12 cells cultured with 10µM $MnCl_2$ supplementation show a decrease in Cu and Zn levels compared to the extracts from the cells cultured in the lower $MnCl_2$ concentrations. This effect is not seen in the equivalent MM6 extracts. The ICPMS analysis method used is described in **2.21** and the D12 pCIneo/NRAMP1 transfected clone is described in **5.2.7** and **5.2.8**.

approximately the same (**Figure 6.4b**). When samples of the cells cultured in 10μM $MnCl_2$ were compared, the Zn level in the MM6 cells was similar to that of the cells cultured in 1μM $MnCl_2$, however, the D12 samples showed a decrease in Zn content compared to samples from D12 cells cultured without $MnCl_2$ supplementation (**Figures 6.4a-c**). This pattern of alteration in cellular Zn content of the cell lines cultured at the different $MnCl_2$ concentrations could be postulated to be the result of similar mechanisms as mentioned above for the effect of the culture conditions on the cellular Cu content of the D12 cells (**6.2.3.1**).

6.2.3.3 Manganese Content

The level of Mn in the cells cultured without additional $MnCl_2$ was similar to the results obtained from previous analyses of the two cell lines (**6.2.2.2**, **Figures 6.2a** and **6.5a**). The D12 samples had a slightly higher content than the MM6 samples, a difference that became accentuated when extracts from cells cultured in 1μM $MnCl_2$ were compared (**Figures 6.5a** and **6.5c**). Though the difference between the Mn content of the cells cultured without and with 1μM $MnCl_2$ supplementation was greater in the D12 cells (**Figure 6.5c**), the percentage increase in Mn content in the 1μM cultured cells relative to those without added $MnCl_2$ was similar in the MM6 and D12 extracts, with extracts from both cell lines showing an approximate two fold increase (**Figure 6.5b**).

There was little further increase in Mn content of the extracts from D12 cells cultured in 10μM $MnCl_2$ compared to the samples from D12 cells cultured in 1μM $MnCl_2$. This suggested that these cells experienced a maximal physiological effect in the presence of the lower, 1μM $MnCl_2$ concentration. However, the MM6 cells cultured in 10μM $MnCl_2$ showed a further increase in cellular Mn content over the 1μM levels. These cells reached approximately the same Mn level which the D12 cells reached when cultured in 1μM and 10μM $MnCl_2$ (**Figure 6.5a**). The difference in Mn content of the samples from the two cell lines cultured in medium supplemented with 10μM $MnCl_2$ compared to the cells cultured without additional $MnCl_2$ was the same (**Figure 6.5c**). This suggested that a maximal Mn cellular

Figure 6.5a

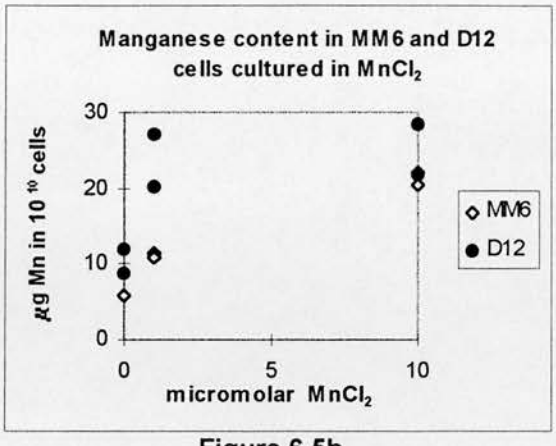

Figure 6.6a

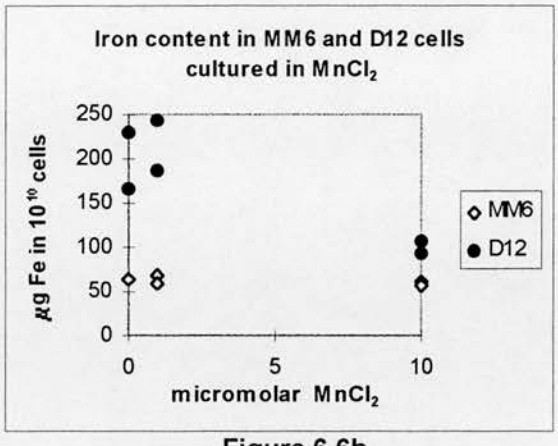

Figure 6.5b

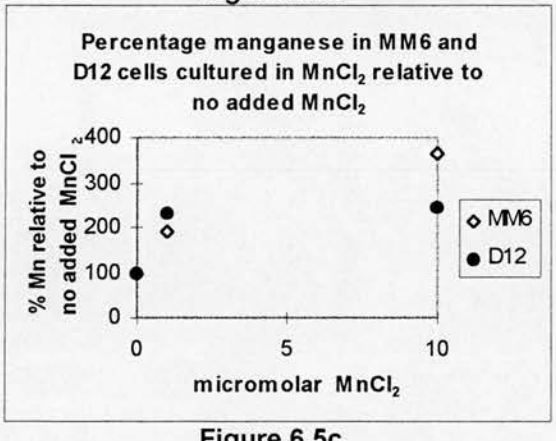

Figure 6.6b

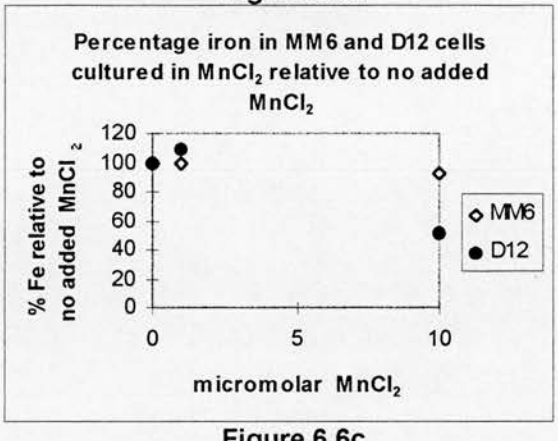

Figure 6.5c

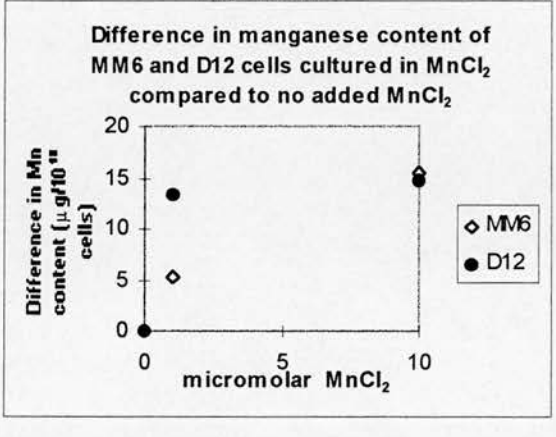

Figure 6.6c

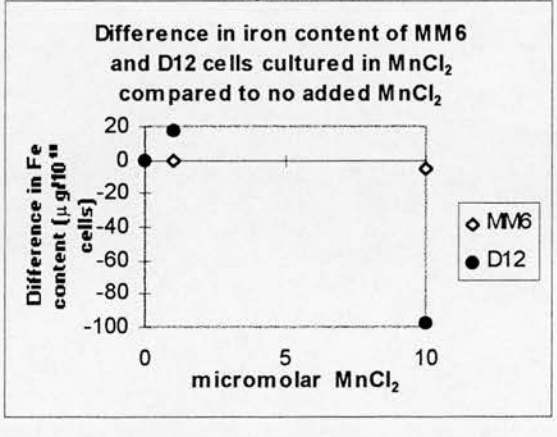

Figures 6.5 and **6.6** The effect on Mn (**Figure 6.5**) and Fe (**Figure 6.6**) content in MM6 and D12 cells cultured in medium supplemented with **0µM**, **1µM** and **10µM** $MnCl_2$. **a)** shows the metal content of extracts from triplicate cultures of the two cell lines. **b)** shows the percentage of the average metal content of the triplicate samples relative to those of the cells cultured without added $MnCl_2$. **c)** shows the difference between the average metal content of the triplicate samples and the cultures without added $MnCl_2$. D12 cells show a maximal Mn content when supplemented with 1µM $MnCl_2$, whereas MM6 cultures require supplementation with 10µM $MnCl_2$ to reach this level. D12 cells show a higher Fe content than MM6 cells when supplemented with 0µM and 1µM $MnCl_2$ but this level falls to approach that of the MM6 cells under supplementation with 10µM $MnCl_2$. The ICPMS analysis method used is described in **2.21** and the D12 pCIneo/NRAMP1 transfected clone is described in **5.2.7** and **5.2.8**.

content was reached by both cell lines, but the D12 cells reached this level when cultured in a ten fold lower concentration of $MnCl_2$ than the MM6 cells.

6.2.3.4 Iron Content

When samples from MM6 and D12 cells cultured without $MnCl_2$ supplementation were analysed for their cellular iron content the D12 samples were found to have a higher level than the MM6 samples (**Figure 6.6a**). The isotope of iron chosen to be measured by ICPMS was Fe^{57}. Fe^{57} is a rare isotope, present naturally at only 2.19% of the total iron. As such one must take into account potential problems with the sensitivity of detection of this ion and the amplification of small errors when low levels of Fe^{57} are being compared. It was not possible to measure the levels of Fe^{56}, the most abundant Fe isotope and isotope of first choice which is present at 91.66%, because of the presence of argon oxide generated in the plasma core of the ICPMS, which has the same molecular weight as Fe^{56}. Taking the potential problems into consideration, when D12 cells were cultured without or with 1μM $MnCl_2$ supplementation the Fe levels in the samples were higher than in the equivalent MM6 samples (**Figure 6.6a**). A slight increase in iron content was seen in samples from the D12 cells cultured with 1μM $MnCl_2$ supplementation compared to those cultured without additional $MnCl_2$ (**Figures 6.6b** and **6.6c**). An equivalent increase was not seen in the MM6 samples (**Figures 6.6b** and **6.6c**). However, when samples from D12 cells cultured in 10μM $MnCl_2$ were analysed there was a dramatic decrease in Fe content to a level approaching the MM6 samples (**Figures 6.6a** and **6.6c**). Under all $MnCl_2$ culture conditions the iron content of the MM6 cells remained approximately the same (**Figures 6.6a-c**). These results suggest that elevated NRAMP1 expression in the D12 cells affects the intracellular iron content of these cells, resulting in increased uptake or retention of the metal. When cultured in elevated levels of Mn this effect is reversed, possibly due to competition of Mn for Fe sites in the transporter protein.

6.3 DISCUSSION

Results measuring the levels of Mn, Cu and Zn in extracts from the MM6 parent cell line and pCIneo/NRAMP1 plasmid transfected clones, cultured under standard

conditions, did not show a consistent or significant difference in the content of these metals in the samples analysed. These results suggest that, provided functional NRAMP1 protein is being over expressed in the transfectants, there is no observable effect of high levels of NRAMP1 on the cellular content of Mn, Cu or Zn when assayed by ICPMS. It was unfortunate that data for the iron content of these cell extracts was not available, considering the present interest in nramp family members functioning as iron transporter proteins (Fleming *et al.* 1997 and 1998; Atkinson and Barton 1998 and 1999). Measuring iron levels using ICPMS is a difficult task because it is not possible to measure levels of the most abundant iron isotope (Fe^{56}) due to the generation of species within the plasma core, i.e. argon oxide, which have the same molecular mass as this iron isotope. Therefore, less abundant iron isotopes are the only measurable form of iron, by ICPMS, which means very low levels of the measurable species are present in normal samples. At the time of analysis of the samples cultured under standard conditions results for the Fe^{57} isotope levels were not available. Had further investigation of the iron levels in the cells been warranted it might have been possible to supplement the growth medium of the cells with Fe^{57} in place of the more abundant Fe^{56} isotope, which would then be assimilated in the same way as the Fe^{56} isotope. Alternatively, electron paramagnetic resonance (EPR) spectroscopy analysis (Farcasanu *et al.* 1996), chemical assays such as the ferrozine method (Carter 1971) or radioactive detection methods after incubation with radioisotopes of iron could have been tried. However, one of the reasons the ICPMS system was adopted was to determine if the technique was a suitable alternative to the use of radioisotopes for measuring the cellular content of a variety of metals using a single detection procedure.

It is interesting to note that a significant difference was seen in the Mn and Cu content, and to a lesser extent the Zn content, of the cell extracts from the MM6 and U937 cell lines. It is not known whether the increase in cellular content of these metals in the MM6 cells is associated with their more mature phenotype and function of the MM6 cells or a reflection of their size. This observation is, however,

a useful control showing that the ICPMS system was capable of detecting differences at the concentrations of cell extracts being analysed.

The results obtained for the MM6 and pCIneo/NRAMP1 plasmid transfected clone, D12, cells cultured under various concentrations of $MnCl_2$ are interesting. Though they represent a single experiment, albeit analysed more than once, further investigation to confirm these initial findings could substantiate whether the differences I have observed are reproducible. The experiment was designed to determine if increasing the Mn concentration in the culture medium affected the Mn content of *in vitro* cultured cells and whether the level of *NRAMP1* expression was influential. My preliminary results suggest that the cells overexpressing *NRAMP1* respond to lower levels of increased Mn by accumulating higher levels of the metal. When cultured with 1μM $MnCl_2$ supplementation the D12 cells reached a level of Mn content which remained largely unaltered when compared to extracts from cells cultured with 10μM $MnCl_2$ supplementation. On the other hand the MM6 cells showed an increase in cellular Mn content when cultured in 1μM $MnCl_2$ supplementation and a further increase when cultured in 10μM $MnCl_2$ supplemented medium. The MM6 cells only approached the absolute Mn concentration which the D12 cells had reached in 1μM $MnCl_2$ when the MM6 cells were cultured in 10μM $MnCl_2$. These findings suggest that the NRAMP1 protein may be affecting the Mn content of the cells, such that a greater concentration of the protein results in more ready uptake of Mn in the D12 cells, possibly due to the affinity of the protein for the metal. When lower levels of the protein are present, in the untransfected MM6 cells, a higher concentration of extracellular Mn appears to be required for the cells to reach their saturation level of intracellular manganese.

One major problem in interpreting these results is the lack of information regarding the cellular localisation of any overexpressed NRAMP1 protein in the transfectants. Recent immunolocalisation studies suggest murine nramp1 exists primarily in lysosomes and it has been challenged whether an effect of alterations in the extracellular ligand concentration could, therefore, be observed (Gruenheid *et al.*

1999). It is possible that my transfectants display mistargeting of the overexpressed protein such that an increased level of NRAMP1 is expressed at the plasma membrane. This could be due to the form the gene exists as in the plasmid, or a failure of the normal cellular regulation of NRAMP1 localisation when faced with an excess of the protein. If a parallel can be drawn between the proposed post-translational control of SMF1 then one could hypothesise that there is insufficient of a human bsd2 homologue to control all the NRAMP1 protein in the D12 cells (Liu and Culotta 1999a). In *S. cerevisiae* the bsd2 protein targets SMF1 to the vacuole for degradation. When cells are depleted of Mn, SMF1 is targeted to the plasma membrane in a bsd2 independent fashion and rescued from degradation. Re-supplementation with Mn results in a bsd2 dependent return to the situation of SMF1 being targeted to the vacuole for degradation. It has been proposed that synthesised SMF1 bound to the metal ion is recognised by bsd2 and targeted to the vacuole for degradation. However, apo SMF1, which is not metal bound e.g. under metal depleted conditions, is not recognised by bsd2 and, hence, traffics to the plasma membrane. It is conceivable that in the D12 transfectants there is an excess of NRAMP1 protein to the extent that a bsd2-homologue regulatory protein is in short supply. Though most reports favour a lysosomal localisation for nramp1 it is possible that under this artificial situation of transfection, NRAMP1 may be expressed at the plasma membrane.

An alternative proposition exists where NRAMP1 remains located in intracellular vacuoles and Mn enters the cell by NRAMP1-independent transport systems, for instance Tf/Tf-receptor mediated endocytosis. The increased uptake of the metal ions by both MM6 and D12 cells would be equivalent in the elevated Mn^{2+} concentrations, and the ions could pass through the vesicular pathway to NRAMP1-located compartments. Here, in the D12 cells, expressing elevated NRAMP1 levels, the accumulating Mn^{2+} ions could be transported out into the cytoplasm increasing the cytoplasmic Mn concentration. However, in the MM6 cells bearing normal NRAMP1 levels, or decreased levels due to potential down regulation of the endogenous protein under elevated Mn conditions, the rate of export of the

accumulating ions into the cytoplasm may be insufficient, resulting in a percentage of the ions being recycled to the cell surface and exported into the extracellular medium.

Mn is an essential trace element and a component of a number of enzyme systems including mitochondrial Mn-SOD, the astrocyte specific glutamine synthase in the CNS, concanavalin A, galactosyl transferase, pyruvate carboxylase and chloroplast photosystem II, to name a few (reviewed in Fraústo da Silva and Williams 1991). It is especially critical during development and is essential for growth and development of the CNS (Aschner and Aschner 1990). In mammals the majority of research into Mn uptake has been carried out on cells and cell lines of CNS origin due to the known toxicity of excess Mn which include "manganese madness", bradykinesia and a Parkinson-like rigidity (reviewed in Suarez *et al.* 1995). Though not conclusive, the neurotoxicity effects appear to be mediated by Mn^{3+}, not Mn^{2+}, and have been proposed to be at least partly due to effects on mitochondrial function. Mn toxicity may be mediated through its accumulation in mitochondria and interference with oxidative phosphorylation, most likely due to binding the F_1ATPase (Gavin *et al.* 1992). The mitochondrial electron transport system is one of the few known significant sources of superoxide, which may initiate the oxidation of Mn^{2+}. An important factor in the potential toxicity of Mn within mitochondria is the apparent imbalance of influx and efflux mechanisms, with the latter occurring at an extremely slow rate. Gavin *et al.* have also shown Mn^{2+} to inhibit Na^+-dependent Ca^{2+} efflux and enhance Ca^{2+} influx, which they propose may increase mitochondrial Ca^{2+} sufficiently to create significant oxidative stress and decrease mitochondrial GSH (Gavin *et al.* 1990). It has been suggested that Mn may inhibit dopamine production or storage and/or reduce the number of neurones in the substantia nigra. This has been hypothesised to be mediated by Mn-dopamine complexes being transported into neurones via the Na^+- and Cl^--dependent dopamine reuptake carrier (DAT) and Mn may compete with Na^+ for co-transport with dopamine (reviewed in Aposhian *et al.* 1999).

Mn can also act as a mutagenic agent at high concentrations, which is a serious threat to eukaryotic DNA, but not such a problem for prokaryotes as mutation leads to variation in the species. It is generally accepted that mitochondria and chloroplasts are derived from prokaryotic cells, all of which accumulate Mn to a greater degree than eukaryotic cytoplasm. Eukaryotic cells appear to transport Mn into any vesicular partition (e.g. lysosomes, chloroplasts, mitochondria, Golgi apparatus, thylakoids, vacuoles) rather than leave it in the cytoplasm (reviewed in Fraústo da Silva and Williams 1991).

Mn accumulates in many tissues to several times the blood plasma concentration of 0.05-0.1μM. The liver is one of the major sites of Mn accumulation, the majority being contained in the mitochondria, and it is also the major secretory organ with bile containing several fold increased Mn concentrations compared to those of plasma (Galeotti *et al.* 1995). It is apparent that homeostasis of this metal is critical for normal physiology and, therefore, transport mechanisms for Mn are of significant interest.

Manganese can assume eleven different oxidation states but in living tissues is found in the +2, +3, and +4 oxidation states. Due to its formation of very tight complexes with other substances the free plasma and tissue concentrations of manganese tend to be very low (reviewed in Aschner 1999). Manganese appears to be taken up by cells via at least three mechanisms. Transport across the blood brain barrier includes facilitated diffusion, active transport and Tf dependent transport (reviewed in Aschner 1999); three apparently saturable uptake systems exist in liver (Aschner and Gannon 1994; Galeotti *et al.* 1995); and rabbit erythroid cells possess three saturable manganese transport systems (Chua *et al.* 1996). Though Mn enters the brain more readily when non-protein-bound than when Tf bound (reviewed in Aschner 1999) the Tf-Fe^{3+}/TfR mediated uptake mechanism can be utilised to take up Mn^{3+} (Ashner and Ashner 1990; Suarez *et al.* 1995). Tf molecules have two binding sites for their substrate ions and under normal plasma concentrations of iron (0.9-2.8μg/ml) and Tf (3mg/ml), 30% of Tf molecules are occupied by Fe^{3+}, leaving 50μmol of unoccupied

potential Mn^{3+} binding sites available per litre (Ashner and Ashner 1990). A bicarbonate-binding site is activated for each bound manganese ion, which requires carbonic anhydrase. Once internalised via the metal ion-Tf/TfR complex, acidification in endosomes results in release of the metal ion, which is reduced to Mn^{2+}, and the TfR recycles to the surface. One of the Mn uptake systems identified in rabbit erythroid cells involves Mn-Tf uptake and the similarities in the characteristics of the three identified Mn uptake mechanisms in these cells with those of Fe suggest both metals may be transported by the same mechanisms (Chua *et al.* 1996). It is of interest to note that the Tf-mediated Mn uptake ceases as reticulocytes mature to erythrocytes, due to loss of TfR expression, highlighting a maturation state-dependency in Mn uptake. Ontogenic studies in rats also suggest there is an age-related uptake, retention and distribution of Mn in the brain (reviewed in Aschner and Gannon 1994; Takeda *et al.* 1999) and the TfR expression status of sub classes of brain cells, such as oligodendrocytes, varies with maturity, adding to the complexity of this system (reviewed in Malecki *et al.* 1999). The Tf mediated uptake system has a relatively extensive substrate range and, likewise, it is not surprising that the divalent transporter proteins of the nramp family may similarly be capable of transporting, amongst other metal ions, both Fe^{2+} and Mn^{2+}. It is feasible that some of the Mn^{2+} ions used in my culture experiments may have been oxidised to Mn^{3+} ions and Tf mediated uptake of Mn may contribute to the observed results. However, it is unlikely that oxidation would have been extensive over the course of the experiment and this mechanism appears unable to explain the difference observed between the MM6 and D12 cells.

Though the MM6 and D12 cells appeared to respond differently when cultured in the $MnCl_2$ concentrations I used, it can not be ruled out that this effect was mediated via one of the other Mn uptake mechanisms which exist in cells, and not that mediated by NRAMP1. The existence of several transport systems makes it difficult to interpret my results, particularly in the light that these systems are likely to be affected differently in the presence of elevated or decreased concentrations of other ions. For instance, increased Zn^{2+} and Cu^{2+} levels have been shown to increase Mn^{2+}

accumulation in astyrocytes whereas Ca^{2+} competitively inhibited Mn^{2+} uptake by these cells and mitochondrial Mn^{2+} uptake (reviewed in Aschner 1999). The *ALR1* and *ALR2* genes of *S. cerevisiae* encode Mg^{2+} transporters but, like similar systems throughout biology, the transporters are capable of transporting other ions including Mn^{2+}, Zn^{2+}, Cu^{2+}, Ni^{2+}, Ca^{2+}, Co^{2+} and La^{2+} (MacDiarmid and Gardner 1998). The true physiological implications of this broad spectrum of substrates is not known. However, it may be that the comparatively high K_m values for these secondary substrates mean they are unlikely to contribute to the accumulation of such cations at physiologically significant concentrations and this must be acknowledged when interpreting observations made from systems where substrates or relevant genes are present at abnormal levels, such as my own. Whether the ability of Mn^{2+} to substitute for Ca^{2+} in the Na^{+}/Ca^{2+}-exchange transport of red blood cells, or for Ca^{2+} in receptor-operated channels of hepatocytes (reviewed in Galeotti *et al.* 1995) occurs physiologically is open to question. In rat brain mitochondria Mn^{2+} does not exchange with Na^{+} across the inner membrane in place of Ca^{2+}, yet its presence enhances Ca^{2+} uptake by these organelles (Gavin *et al.* 1990). It has also been proposed that the low affinity Mn uptake system in rabbit reticulocytes and erythrocytes may be mediated by a Na^{+}/Mg^{2+} antiport (Chua *et al.* 1996). The high affinity transport system observed in rabbit reticulocytes is inhibited by Fe^{2+}, Zn^{2+}, Ni^{2+} and Co^{2+} as well as NaCl and a number of metabolic inhibitors, while it is stimulated by valinomycin and SITS (4-acetamido-4'-isothyocyanatostibene-2,2'-disulphonic acid). These findings suggest changes in transmembrane potential difference and changes in membrane surface potential may be involved in a transport system for this range of substrates. Not all transition metal transporter systems and the relevant metals, however, seem to be inter-dependent and capable of affecting the expression of the transporters or concentration of metal ions. Though the SMF proteins may be able to transport iron, their expression was unaltered, and their deletion had no effect, on *S. cerevisiae* with a deletion of the surface ferroxidase (*FET3*) which is involved in high affinity iron transport (Li and Kaplan 1998). This serves to illustrate a partial interconnection of this complex homeostatic regulatory system in which a functional capacity measured under certain conditions may not

transpose to a similar activity under physiological or different conditions, and only a subset of those genes or proteins potentially responding or being affected by a change in the status quo actually being so.

The influence of one particular metal ion on the uptake and physiological effect of another does not always appear to be explained as simply as competition for a common transport mechanism. *S. cerevisiae* displays reduced Mn^{2+} uptake and can be protected from Mn^{2+} toxicity following pre-incubation with Mg^{2+}. The resistant Mg^{2+}-loaded cells did not need to be present in Mg-enriched medium when the high levels of Mn^{2+} were added (Blackwell *et al.* 1997). Al^{3+} toxicity in *S. cerevisiae* appears to be the manifestation of reduced Mg^{2+} influx, and the resulting intracellular deficiency of this essential element, rather than a direct effect of increased intracellular aluminium (MacDiarmid and Gardner 1998). In addition, *in vivo* incubation of rat oligodendrocytes with Al-Tf down regulated surface expression of TfRs, and limited Fe and Mn uptake via the Tf/TfR system (Golub *et al.* 1996).

It is often possible to glean some insight into mammalian systems from studying those of lower organisms. Mn^{2+} is essential for the glucan-associated adhesion of some mutans group streptococcal species and for pneumococcal transformation, necessitating uptake mechanisms for this ion. The *Streptococci gordonii scaCBA* operon, which encodes genes also found in *S. parasanguis* and *S. pneumoniae*, is necessary for the activity of a high affinity Mn^{2+} uptake system (reviewed in Kolenbrander *et al.* 1998). This system is inhibited by Zn^{2+} but not Mg^{2+}, Ca^{2+}, Hg^{2+}, Cu^{2+} or Fe^{2+}. The operon encodes an abc transport system, which is of interest in the light of the presence of the conserved transport motif in a number of bacterial abc transporter proteins and nramp family members. *S. gordonii* also contains one or more lower affinity Mn^{2+} uptake systems which allow growth under Mn^{2+}-replete conditions. The lower affinity system was proton motive dependent and not significantly inhibited by Zn^{2+}. In addition an Adc Zn^{2+} transporter has been proposed to be capable of transporting Mn^{2+}. The *S. pneumoniae psa* locus encodes

an abc-type Mn permease complex hypothesised to be part of a signalling pathway indirectly affecting adhesion, lysis, transformation and virulence, though Mn transport only partially contributes to this signalling (Novak *et al.* 1998). Thus, even in these organisms Mn^{2+} transport is a complex multi-system process.

Insight into the regulation of the *S. cerevisiae* SMF proteins via the bsd2 protein and Mn levels prompts consideration that a similar system may exist in mammals regulating nramp protein levels and its cellular localisation (Liu and Carlotta 1999a). As discussed previously, the finding that physiological Mn^{2+} concentrations result in SMF1 targeting for vacuolar degradation introduces the possibility that overexpressed NRAMP1 protein in the D12 cells may be destined for a similar fate, mediated via a mammalian bsd2 homologue. Particularly noteworthy is the observation that in Mn^{2+}-starved cells SMF1 was redirected to the cell surface in a bsd2 independent way, saving SMF1 from degradation. When re-supplemented with Mn^{2+} the SMF protein was again targeted for degradation in a bsd2 dependent way. It is possible, therefore, that a proportion of overexpressed NRAMP1 protein in my system escapes the degradation pathway due to a comparative shortage of the hypothesised bsd2 homologue, and the effects observed in my functional studies do reflect the presence of increased NRAMP1 protein levels. This vacuolar-targeting pathway is consistent with the immunolocalisation studies of the murine nramp1 protein (Gruenheid *et al.* 1997) to vacuolar compartments, such as lysosomes, and may help explain the failure to identify significant levels of the protein at the plasma membrane.

Gruenheid *et al.* report unpublished results of a failure to demonstrate nramp1-mediated transport of ^{54}Mn or ^{55}Fe in RAW cells transfected and overexpressing nramp1 protein. They suggest this might be due to the non-overlapping distribution of the nramp1 and nramp2 proteins. Despite both proteins being capable of transporting the ions, the lysosomal localisation of nramp1 may preclude its transport of extracellular ligand, which plasma membrane located nramp2 could perform. The

authors suggest an observable effect of overexpression of nramp1 would require the presence of its ligand in the phagolysosomal space (Gruenheid *et al.* 1999).

The main variation I observed in the behaviour of the MM6 and D12 cells with respect to their Cu and Zn content was seen when the cells were cultured in medium supplemented with 10μM $MnCl_2$. In extracts from D12 cells the absolute concentration of both metals decreased below the levels of samples from these cells cultured without or with 1μM $MnCl_2$ supplementation. In contrast, the MM6 cells behaved in a similar manner when cultured in both 1μM and 10μM $MnCl_2$, deviating only slightly from the control culture conditions. Assuming the overexpressed NRAMP1 protein was functional in the D12 cells the slight increase in the cellular content of the two metals when supplemented with 1μM $MnCl_2$ could be the result of increased uptake via NRAMP1. Alternatively, because the MM6 cells varied in a similar way, showing an approximately equivalent percentage increase relative to the control cell samples cultured without additional $MnCl_2$, this observation may be NRAMP1 independent and the result of other transport mechanisms or experimental variation. The decrease in Cu and Zn content in the D12 cells cultured under the highest $MnCl_2$ concentration suggests a competitive effect of Mn at the expense of transport of these metals. As the decrease was only seen in the D12 cells it is tempting to speculate that it is a direct or indirect effect of NRAMP1 overexpression. It is possible that the physiological effect of NRAMP1 overexpression down regulates transport systems that would otherwise transport Cu and Zn. If it was the case that the relative affinities of the three metals in question were such that at 10μM $MnCl_2$ Cu and Zn could not compete for uptake by NRAMP1 in the D12 cells, and Mn was transported at the expense of the other metals, one might expect to see a decrease in the Cu and Zn concentrations in the MM6 cells as well due to the effect on transport by the endogenous NRAMP1 protein. This was not seen, suggesting a more complex interaction of metal ions, transport systems and their regulation may be operating. It is possible, however, that the effect of elevated levels of NRAMP1 on Cu and Zn transport is only seen at 10μM $MnCl_2$ culture conditions in the D12 cells and the other slight variations seen in the remaining samples are coincidental

and independent of NRAMP1. The competitive effect of Mn for transport at the expense of Cu or Zn might only be seen when both the NRAMP1 protein and one of the relevant metal ions is present at extreme non-physiological levels, hence the MM6 cells being unaffected. Though there is no evidence as far as I am aware it is also possible that NRAMP1 may be capable of exporting Cu and Zn in a Mn dependent way.

Taking into consideration the drawbacks in analysing iron concentrations by measuring the level of the low abundance Fe^{57} isotope the results are worthy of discussion. Under normal culture conditions and supplementation with 1μM $MnCl_2$, extracts from D12 cells had a markedly elevated Fe content compared to the equivalent MM6 samples. This suggests that overexpression of NRAMP1 may be increasing transport of Fe into the D12 cells; or from the cytoplasm into intracellular vacuoles; or from intracellular vacuoles into the cytoplasm, depending on the direction of transport of the metal, to an extent that a continuous uptake of Fe from the extracellular medium continues to replenish the Fe depleted compartment(s). In the MM6 cell samples with normal NRAMP1 levels this increase in Fe content is not seen under any of the culture conditions analysed. However, in the D12 extracts from cultures supplemented with 10μM $MnCl_2$ the level of Fe in the cells approached that of the untransfected cells, suggesting that Mn at this high concentration is sufficient to compete with Fe and inhibit the effect of NRAMP1 overexpression on Fe transport, which was seen at the lower extracellular Mn concentrations. If this is the case one would expect the difference in Mn levels of extracts from D12 cells cultured in 1μM and 10μM $MnCl_2$ to be significant. However, this was not seen, introducing the possibility of another Mn export system operating which prevents intracellular Mn accumulating above a certain level. This might also explain the plateau effect of the maximum Mn concentrations observed in both MM6 and D12 cells. One could envisage a continuous import followed by export cycle of Mn, at the expense of Fe, when the D12 cells were cultured in 10μM $MnCl_2$ due to Mn competing for Fe transport.

These preliminary results suggest NRAMP1 may be partaking in the regulation of intracellular Fe levels which supports previous studies (Atkinson and Barton 1998 and 1999). However, the physiological effect of this regulation remains unresolved with a variety of suggestions being propounded (reviewed in Blackwell and Searle 1999). NRAMP1 may be involved in transporting iron out of the endosome/lysosome following release of the metal from internalised Tf/TfR complexes. This would be in keeping with the requirement of low pH for iron dissociation and fusion of early lysosomes with nramp1-positive late endosomes/lysosomes for its transport. Nramp1 has also been postulated to be involved in scavenging Fe from phagocytosed senescent red blood cells, by transporting it into the cytoplasm from whence it can be returned to the blood stream. One effect of this efflux of Fe from phagolysosomes would be to starve pathogenic bacteria of this vital nutrient, which could account for the phenotypic difference observed in *nramp1* mutant mice following infection with certain microorganisms. However, not all observations are consistent with these ideas and Zwilling *et al.* have hypothesised that nramp1 may be transporting Fe into phagosomes, where the low pH environment would favour the generation of toxic free radicals, via the Fenton reaction, to kill invading microorganisms (Zwilling *et al.* 1999). These workers found that the growth inhibitory effect on *M. avium* of Mϕs from resistant mice was stimulated by the addition of iron. Inhibitors of hydroxyl radical generation prevented this effect and the group suggest $^{\cdot}OH$, generated from H_2O_2 via the Fe^{2+} catalysed Fenton reaction, was mediating the antimicrobial effect, with nramp1 regulating the Fe^{2+} transport. In contrast to Mϕs from resistant mice they found that addition of iron to susceptible Mϕs stimulated the growth of *M. avium*. Splenic adherent cells from resistant mice show superior $^{\cdot}OH$ production on infection with BCG compared to their susceptible counterparts, which is consistent with this hypothesis (Denis *et al.* 1988). IFNγ treatment was shown to decrease the levels of intracellular iron in resistant Mϕs, but not susceptible Mϕs, an effect speculated to be mediated by NO (Zwilling *et al.* 1999). NO induces the loss of iron, in part, by attacking iron-sulphur centres with associated inhibition of cell metabolism and growth. The increased NO production by resistant Mϕs (Barton *et al.* 1995) may be responsible for the loss of intracellular iron following IFNγ treatment.

The role of NO in *nramp1*-mediated growth inhibition of the relevant pathogens remains controversial (reviewed in Blackwell *et al.* 1991; Brown *et al.* 1995) but this idea suggests an indirect role of the free radicals affecting the cells' iron status, with potential knock on effects. Further work is obviously required to clarify the situation regarding the direction of transport of nramp1's substrate(s). The two schools of thought remain open with Zwilling feeling a scavenger function, removing effete iron, too passive a role of nramp1. The proponents of this hypothesis challenge Zwilling's theory, questioning such a unique role of nramp1 in enhancing antimicrobial activity, which poses problems reconciling the pleiotropic effects of nramp1 in regulating many cellular functions. The latter problem may be accounted for in the regulatory effect of iron on mRNA stability (reviewed in Zwilling *et al.* 1999).

It is interesting to consider what effect an alteration in localised concentrations of divalent cations may have on signalling pathways and cell activation. Mn^{2+} has been shown to modulate integrin function, altering the ligand binding affinity and specificity of VLA-3 (Elices *et al.* 1991), VLA-5 (Gailit and Ruoslahti 1988), GPIIb/IIIa (Kirchhofer *et al.* 1990), vitronectin receptor (Conforti *et al.* 1990), VLA-4 and VLA-6 (Sonnenberg *et al.* 1988). It appears to directly alter the conformation of LFA-1 in a manner that favours LFA-1/ICAM-1 binding, an effect only seen with Mg^{2+} when Ca^{2+} is removed by chelation with EGTA (Dransfield *et al.* 1992). ICAM-3 is also dependent on the presence of Mn^{2+} or Mg^{2+} for binding to LFA-1 (Woska Jr *et al.* 1998). This modulatory effect of divalent cations on ligand/receptor interactions involved in signal transduction may be a wide spread phenomenon affecting a variety of integrins. It is worth considering whether nramp1 partakes in regulating cell function in this way through its effect on divalent cation transport and cellular localisation.

Whether Fe^{2+} and/or Mn^{2+} is the physiological substrate for nramp1 it is likely that the protein plays a critical regulatory role within phagocytes with respect to the cells' redox balance. The effect of altering the redox balance could modulate the effect of

other genes and ultimately affect bacterial killing, as well as altering the function of enzymes and the environment within which the pathogen resides.

It is clear that further investigation is needed to address the transport of Mn in its different oxidation states as well as different exposure routes at physiologically relevant concentrations of Mn in the blood.

6.4 CONCLUSION

Overexpression of NRAMP1 in the MM6 derived pCIneo/NRAMP1 transfected clone, D12, does not appear to affect the cellular content of Mn, Cu or Zn under standard culture conditions when compared to the parent cell line. However, when cultured in increased levels of $MnCl_2$, D12 and MM6 cells show differential effects with respect to their Fe, Mn, Cu and Zn levels. The effect on Cu and Zn levels were similar with D12 cells showing a decrease in cellular content of these metals when the cells were cultured in the highest (10μM) $MnCl_2$ concentration. This decrease was not seen in the MM6 cells. The Mn levels in both D12 and MM6 cells increased when cultured in 1μM $MnCl_2$, with the D12 cells reaching a maximal plateau level which did not increase further when the cells were cultured in 10μM $MnCl_2$. In contrast, the Mn level of MM6 cells cultured in 10μM $MnCl_2$ increased above its level in 1μM $MnCl_2$ approaching the plateau level observed in the D12 cells cultured in 1μM $MnCl_2$. The Fe levels were greater in D12 cells than in MM6 cells when the cells were cultured under conditions without and with supplementation of 1μM $MnCl_2$. When cultured in 10μM $MnCl_2$ the Fe level in D12 cells decreased significantly, approaching that of the MM6 cells, whose Fe content remained approximately the same under all $MnCl_2$ culture conditions. These findings suggest NRAMP1 transfection of the MM6 cell line influences the homeostasis of a number of divalent cations when the cells are cultured under increased concentrations of Mn^{2+}. How the protein is controlling and affecting the transport and cellular localisation of these metals remains an area for further investigation, as does elucidation of NRAMP1's physiological substrate(s).

7 FINAL DISCUSSION

As the project to sequence the human genome races to completion the science world will be faced with an ever increasing pool of genes influencing health and disease. Dissecting the extent to which these impact on our daily well being and constitution, and their complex interaction is likely to be a major challenge. The genes responsible for many of the genetic diseases caused by mutations in a single gene have now been identified, but we face the problem of the more common multi-gene/multi-factorial ailments. It is likely that numerous genes, each carrying a small weight, contribute in an additive way in combination with particular environmental and life style factors, culminating in these ailments. *NRAMP1* is one such candidate gene and its influence on Mϕ function, in the context of other contributory factors, could have subtle or significant effects. It is interesting to consider the interaction of Mϕs and the genes expressed by these cells with the *NRAMP1* profile of those with human primary immunodeficiencies with a Mϕ involvement (e.g. CVID, CHS, WAS); parasitic, viral and bacterial infections; and autoimmune diseases, as summarised in **1.6**. These conditions and their outcome are not accountable to a simple or single cause and the complex immune system interactions involved result from additive cellular, genetic, molecular and environmental inter-dependent factors. The effect of APCs, such as Mϕs, in initiating and skewing these responses can not be underestimated. Though this project has not shown a strong association of PBC, a typical example of one such complex disease, with the *NRAMP1* polymorphic site affecting expression levels of the gene which I investigated, an influence of *NRAMP1* can not be ruled out entirely. Further expression studies and more extensive genetic analysis of this gene and the potential factors regulating expression and function of the protein, such as bsd2 homologues (Liu and Culotta 1999b), is warranted in PBC patients. In addition, it is tempting to hypothesise that the novel allele, allele 5, which I have identified at an increased frequency in the PBC population I genotyped, may be contributing to pathology in this subset of patients by influencing expression levels of *NRAMP1* and hence, Mϕ function. Reporter studies will shed light on this proposal.

The *nramp1* genotype has a significant effect on induction of murine Mϕ apoptosis induced by *M. tuberculosis*, which is dependent on the production of elevated NO by resistant Mϕs (Rojas *et al.* 1998). It is probable that *NRAMP1*, likewise, influences the antimycobacterial/antibacterial activity of human Mϕs and their apoptosis. Whether this extends to induction of apoptosis in non-Mϕ cells is an interesting point to consider. The potential role of mycobacterial and bacterial infection in induction of autoimmune conditions such as PBC, which is characterised by the presence of extensive granulomas in the diseased liver, harkens to Mϕs playing a significant role in the pathogenesis. It is tempting to extend this possibility to include the status of Mϕs with respect to the pleiotropic effects of *NRAMP1* on the activity of these cells. This may parallel those of RA sufferers' Mϕs whose *NRAMP1* genotype appears significant in influencing disease susceptibility (Shaw *et al.* 1996 and 1997). However, my study does not provide evidence for an analogous increased frequency of the RA associated *NRAMP1* allele 3 at the 5' promoter region polymorphic site, but it is notable that if allele 5 carriers were present in the RA populations studied, they may have been inadvertently classified as allele 3 carriers. This suggests reanalysis of the RA populations should be considered. It is worth contemplating whether *NRAMP1* may influence the severity of PBC after its initiation rather than actually determining susceptibility to the disease. There are two sides to this coin. Individuals with an *NRAMP1* genotype resulting in hyperstimulated Mϕs might face a worse prognosis due to an accentuated and extended destructive immune response, as proposed in the case of RA patients (reviewed in Blackwell 1996). On the other hand, if PBC really is triggered by an as yet unidentified infection, effective control of this pathogen in the early stages may limit or reduce the extent of the potential subsequent pathological immune responses of the autoimmune syndrome.

Elucidation of the significance of expression of the two *NRAMP1* splice variants I have shown in PBC and normal liver might shed light on potential post-transcriptional regulation of *NRAMP1* and, hence, the level of functional protein expressed. Exactly how NRAMP1 exerts its pleiotropic effects on Mϕ function and activity is a fascinating area of research. At first sight a divalent cation transporter

seems an unlikely candidate for such a regulator. My preliminary studies, using cells transfected to overexpress *NRAMP1* cultured in increased concentrations of $MnCl_2$, support previous reports that NRAMP1 alters transport of such cations, in particular iron and manganese. Further investigation and clarification of the direction of transport and intracellular location of the overexpressed protein need elucidation before meaningful interpretation of these results can be made.

With respect to the mechanism of BEC destruction in PBC I have identified further evidence that apoptosis may be the mechanism by which these cells die on the basis of their expression of the pro-apoptotic bax and bcl-x proteins. The stimulus or trigger for this fate is still under investigation but a number of potential candidates exist, including NO which is produced at high levels by Mϕs. Serum NO levels are increased in PBC patients (Notas *et al.* 1999) and decrease as disease progresses (Battista *et al.* 1997). NO production by DCs from PBC patients has been shown to be greatly enhanced in *in vitro* allogeneic MLR when compared with that of chronic hepatitis sufferers or normal controls, and DCs from PBC patients are defective in their stimulatory capacity (Yamamoto *et al.* 1998a and 1998b). It is worth noting that NO induced apoptosis can be independent of p53 (Messmer and Brüne 1995), the stabilisation of which I failed to observe in the PBC liver sections I immunostained. A number of observations support a role of free radicals in association with a decrease in antioxidant levels in the pathogenesis of PBC (Gibbons *et al.* 1999), oxidative stress being a significant feature of early stage PBC (Aboutwerat *et al.* 1999). The NRAMP1 protein acts as a divalent cation transporter and its proposed substrates, including Fe^{2+} and Mn^{2+}, have the potential to partake in redox regulation. It is worth considering whether NRAMP1 is a factor contributing to the oxidative imbalance in PBC. Though the observations mentioned above do not prove a direct role of NO and APCs, a potential NO source, in the pathogenesis of PBC they are suggestive that PBC is the result of more complex abnormalities than mere T lymphocyte or AAb mediated destruction. These non-antigen-specific components of the immune system may prove to be of major significance as we glean a greater understanding of the true events initiating and perpetuating this perplexing disease.

Another possible initiator of apoptosis of BECs in PBC is TNFα which is widely recognised for its role in triggering cell death (Cytokines Online Pathfinder Encyclopaedia web site). TNFα expression by BECs in PBC liver sections has been reported and the accompanying upregulated expression of TNFαR by these cells presents potential for an autocrine destruction method (Yasoshima *et al.* 1998). As well as exerting receptor-mediated effects TNFα can act indirectly, inducing mediators such as IL-1 and NO. TNFα can disturb the barrier function of bile ducts, which may lead to leakage of toxic bile substances and initiation of local inflammatory processes. It is interesting to note that UDCA, the most widely used therapy for PBC pre-transplantation, has the effect of decreasing serum TNFα levels (Angulo *et al.* 1999) and iNOS mRNA and protein expression (Hattori *et al.* 1996; Invernizzi *et al.* 1997). Thus, decreasing levels of these mediators may be one of the therapeutic benefits of UDCA, amongst other reported immunomodulatory and cell membrane effects. The beneficial effect of this drug has also been suggested to involve decreased apoptosis. Glycoursodeoxycholic acid reduces caspase-3 like activity; mitochondrial cytochrome c release; and apoptosis in BECs induced to undergo apoptosis (Que *et al.* 1999). The drug has also been proposed to exert beneficial effects by acting as an antioxidant, blocking the peroxidative effect of hydrophobic bile acids, such as deoxycholic acid, and suppressing KC activation (Ljubuncic *et al.* 1996). It remains to be seen whether these observations identify significant players in pathology specific to PBC and how they could be manipulated to delay or halt disease progression. I have shown that BECs in PBC patients are capable of proliferation, which offers some hope that increasing this innate capacity might be possible, in conjunction with decreasing BEC destruction. The increased IL-6 production by BECs of PBC patients may be inducing this proliferation in an autocrine manner (Yasoshima *et al.* 1998) and directed, controlled IL-6 therapy may be one future option.

Though this project has centred on the Mϕ as playing an important role in the pathogenesis of PBC, and in investigating the fascinating *NRAMP1* gene and NRAMP1 function it is important to emphasise that multicellular organisms exist as

holistic entities. Mϕs interact with, influence and are influenced by a host of other cells, chemicals and mediators and though we would be lost without them, and medicine has a lot to learn and appreciate about their functions, Sir Ralph Bloomfield Bonington in Bernard Shaw's The Doctor's Dilemma was possibly granting them slightly more omnipotence than they merit when he claimed "*There is at bottom only one genuinely scientific treatment for all diseases, and that is to stimulate the phagocytes*" (Shaw 1947).

8 Bibliography

Abbas, A.K., Lichtman, A.H., and Pober, J.S. (1994). *Cellular and Molecular Immunology.* Second Edition. W.B. Saunders Company, Philadelphia. p21-23.

Abedi, M.R., Hammarström, L., Broomé, U., Angelin, B., Edvard Smith, C.I., and Christensson, B. (1996). Reduction in serum levels of antimitochondrial (M2) antibodies following immunoglobulin therapy in severe combined immunodeficient (SCID) mice reconstituted with lymphocytes from patients with primary biliary cirrhosis (PBC). *Clin. Exp. Immunol.* **105**, 266-273.

Abel, L., Sánchez, F.O., Oberti, J., Thuc, N.V., Van Hoa, L., Lap, V.D., Skamene, E., Lagrange, P.H., and Schurr, E. (1998). Susceptibility to leprosy is linked to the human NRAMP1 gene. *J. Infect. Dis.* **177**, 133-145.

Aboutwerat, A., Pemberton, P., Smith, A., Jain, S.K., and Warnes, T.W. (1999). Evidence of oxidative stress in early stage primary biliary cirrhosis. *Gut* **Vol. 44**, Supp. 1, pA60, W238.

Adams, J.M., and Cory, S. (1998). The bcl-2 protein family: arbiters of cell survival. *Science* **281**, 1322-1326.

Adams, D.O., and Hamilton, T.A. (1989). The activated macrophage and granulomatous inflammation in Cell kinetics of the inflammatory reaction. *Curr. Top. Pathol.* **79**, Chpt. VII.

Agarwal, K., Grove, J., Pearce, S., Daly, A., Jones, D.E.J., and Bassendine, M.F. (1998). CTLA-4 gene polymorphism associated with primary biliary cirrhosis (PBC). Abstract *Hepatology* **Vol. 28**, No. 4, Part 2, p404A, 965.

Akisawa, N., Maeda, T., Iwasaki, S., and Onishi, S. (1997). Identification of an autoantibody against alpha-enolase in primary biliary cirrhosis. *J. Hepatol.* **26**, 845-851.

Alberts, B., Bray, D., Lewis, J., Raff, M., Roberts, K., and Watson, J.D. (1989). *Molecular Biology of the Cell.* Second Edition. Garland Publishing Inc., New York. **Chapter 13**.

Aliprantis, A.O., Diez-Roux, G., Mulder, L.C.F., Zychlinsky, A., and Lang, R.A. (1996). Do macrophages kill through apoptosis? *Immunol. Today* **17**, 573-576.

Angulo, P., Uae, M.N., Neuman, M.G., Jorgensen, R.A., Shear, N.H., Malkiewicz, I., Dickson, E.R., and Lindor, K.D. (1999). Serum cytokines in patients with primary biliary cirrhosis: effect of treatment with ursodeoxycholic acid. Abstract *Gastroenterology* **Vol. 116**, No. 4, Part 2, pA1239, L259.

Aposhian, H.V., Ingersoll, R.T., and Mongomery Jr, E.B. (1999). Transport and control of manganese ions in the central nervous system. *Environ. Res.* **80**, 96-98.

Arala-Chaves, M.P., Korn, J.H., Galbraith, G.M.P., Porto, M.T., Smith, C.L. and Fudenberg, H.H. (1982). Effects of thymosin and evidence of monocyte suppression of both T- and B-cell functions in two cases of 'common variable immunodeficiency'. *Scand. J. Immunol.* **15**, 97-104.

Ashkenazi, A., and Dixit, V.M. (1998). Death receptors: signaling and modulation. *Science* **281**, 1305-1308.

Aschner, M., and Aschner, J.L. (1990). Manganese transport across the blood-brain barrier: relationship to iron homeostasis. *Brain Res. Bull.* **24**, 857-860.

Aschner, M., and Gannon, M. (1994). Manganese (Mn) transport across the rat blood-brain barrier: saturable and transferrin-dependent transport mechanisms. *Brain Res. Bull.* **33**, 345-349.

Aschner, M. (1999). Manganese homeostasis in the CNS. *Environ. Res.* **80**, 105-109.

Aterman, K. (1992). The stem cells of the liver - a selective review. *J. Cancer Res. Clin. Oncol.* **118**, 87-115.

Atkinson, P.G.P., Blackwell, J.M., and Barton, C.H. (1997). Nramp1 locus encodes a 65 kDa interferon-γ-inducible protein in murine macrophages. *Biochem. J.* **325**, 779-786.

Atkinson, P.G.P., and Barton, C.H. (1998). Ectopic expression of Nramp1 in COS-1 cells modulates iron accumulation. *F.E.B.S. Lett.* **425**, 239-242.

Atkinson, P.G.P., and Barton, C.H. (1999). High level expression of nramp1^{G169} in RAW264.7 cell transfectants: analysis of intracellular iron transport. *Immunology* **96**, 656-662.

Auger, M.J., and Ross, J.A. (1992). The biology of the macrophage in *The Macrophage: The Natural Immune System.* Edited by Lewis, C.E., and McGee, J.O.D.. Oxford University Press, New York. Chpt. 1.

Bach, N., and Schaffner, F. (1994). Familial primary biliary cirrhosis. *J. Hepatol.* **20**, 698-701.

Ballardini, G., Bianchi, F.B., Doniach, D., Mirakian, R., Pisi, E., and Bottazzo, G.F. (1984). Aberrant expression of HLA-DR antigens on bileduct epithelium in primary biliary cirrhosis: relevance to pathogenesis. *Lancet* **2**, 1009-1013.

Ballardini, G., Ghetti, S., Lari, F., Descovich, C., Grassi, A., Zauli, D., and Bianchi, F.B. (1998). Apoptosis is not a frequent cholangiocyte pattern of death in primary biliary cirrhosis (PBC). Abstract *Hepatology* **Vol. 28**, No. 4, Part 2, p626A, 1855.

Barrera, L.F., Kramnik, I., Skamene, E., and Radzioch, D. (1997). I-Aβ gene expression regulation in macrophages derived from mice susceptible or resistant to infection with M. bovis bcg. *Mol. Immunol.* **34**, 343-355.

Barton, C.H., White, J.K., Roach, T.I.A., and Blackwell,. J.M. (1994). NH_2-terminal sequence of macrophage-expressed natural resistance-associated macrophage protein (nramp) encodes a proline/serine-rich putative src homology 3-binding domain. *J. Exp. Med.* **179**, 1683-1687.

Barton, C.H., Whitehead, S.H., and Blackwell, J.M. (1995). Nramp transfection transfers Ity/Lsh/Bcg-related pleiotropic effects on macrophage activation: influence on oxidative burst and nitric oxide pathways. *Mol. Med.* **1**, 267-279.

Battista, S., Mengozzi, G., Zoia, I., Bar, F., Martinotti, R., Bauducci, M., Poli, G., Rosina, F., and Molino, G. (1997). Nitric oxide levels decline with the progression of primary biliary cirrhosis. Abstract *Gastroenterology* **Vol. 112**, No. 4, pA1222.

Bauer, J., Ruuls, S.R., Huitinga, I., and Dijkstra, C.D. (1996). The role of macrophage subpopulations in autoimmune disease of the central nervous system. *Histochem. J.* **28**, 83-97.

Baum, H., and Staines, N.A. (1997). MHC-derived peptides and the $CD4^+$ T-cell repertoire: implications for autoimmune disease. *Cytokines Cell. Mol. Ther.* **3**, 1-11.

Bellamy, R.J., and Hill, A.V.S. (1998). Host genetic susceptibility to human tuberculosis in *Genetics and Tuberculosis.* Edited by Chadwick, D.J., and Cardew, G.. Wiley, Chichester. Novartis Foundation Symposium Vol. 217, p3-23.

Bellamy, R., Ruwende, C., Corrah, T., McAdam, K.P.W.J., Whittle, H.C., and Hill, A.V.S. (1998). Variations in the NRAMP1 gene and susceptibilty to tuberculosis in West Africans. *N. Eng. J. Med.* **338**, 640-644.

Belouchi, A., Cellier, M., Kwan, T., Saini, H.S., Leroux, G., and Gros P. (1995). The macrophage-specific membrane protein nramp controlling natural resistance to infections in mice has homologues expressed in the root system of plants. *Plant Mol. Biol.* **29**, 1181-1196.

Belouchi, A., Kwan, T., and Gros, P. (1997). Cloning and characterization of the OsNramp family from Oryza sativa, a new family of membrane proteins possibly implicated in the transport of metal ions. *Plant Mol. Biol.* **33**, 1085-1092.

Berg, P.A., Klein, R., and Röcken, M. (1997). Cytokines in primary biliary cirrhosis. *Semin. Liver Dis.* **17**, 115-123.

Bernuau, D., Feldmann, G., Degott, C., and Gisselbrecht, C. (1981). Ultrastructural lesions of bile ducts in primary biliary cirrhosis. *Hum. Path.* **12**, 782-793.

Björkland, A., Festin, R., Mendel-Hartvig, I., Nyberg, A., Lööf, L. and Tötterman, T.H. (1991). Blood and liver-infiltrating lymphocytes in primary biliary cirrhosis: increase in activated T and natural killer cells and recruitment of primed memory T cells. *Hepatology* **13**, 1106-1111.

Blackwell, J.M., Roach, T.I.A., Atkinson, S.E., Ajioka, J.W., Barton, C.H., and Shaw, M.A. (1991). Genetic regulation of macrophage priming/activation: the Lsh gene story. *Immunol. Lett.* **30**, 241-248.

Blackwell, J.M., Barton, C.H., White, J.K., Searle, S., Baker, A.M., Williams, H., and Shaw, M.A. (1995). Genomic organization and sequence of the human NRAMP gene: identification and mapping of a promoter region polymorphism. *Mol. Med.* **1**, 194-205.

Blackwell, J.M. (1996). Structure and function of the natural-resistance-associated macrophage protein (nramp1), a candidate protein for infectious and autoimmune disease susceptibility. *Mol. Med. Today* **2**, 205-211.

Blackwell, K.J., Tobin, J.M., and Avery, S.V. (1997). Manganese uptake and toxicity in magnesium-supplemented and unsupplemented Saccharomyces cerevisiae. *Appl. Microbiol. Biotechnol.* **47**, 180-184.

Blackwell, J.M. (1998). Genetics of host resistance and susceptibility to intramacrophage pathogens: a study of multicase families of tuberculosis, leprosy and leishmaniasis in north-eastern Brazil. *Int. J. Parasitol.* **28**, 21-28.

Blackwell, J.M. and Searle, S. (1999). Genetic regulation of macrophage activation: understanding the function of NRAMP1 (=Ity/Lsh/Bcg). *Immunol. Lett.* **65**, 73-80.

Boise, L.H., González-García, M., Postema, C.E., Ding, L., Lindsten, T., Turka, L.A., Mao, X., Nuñez, G., and Thompson, C.B. (1993). Bcl-x, a bcl-2-related gene that functions as a dominant regulator of apoptotic cell death. *Cell* **74**, 597-608.

Borum, M.L. (1998). Hepatobiliary diseases in woman. *Med. Clin. N. Amer.* **82**, 51-75.

Bradley, D.J. (1974). Genetic control of natural resistance to Leishmania donovani. *Nature* **250**, 353.

Briggs, D.C., Donaldson, P.T., Hayes, P., Welsh, K.I., Williams, R., and Neuberger, J.M. (1987). A major histocompatibility complex class III allotype (C4B2) associated with primary biliary cirrhosis (PBC). *Tissue Antigens* **29**, 141-145.

Broomé, U., Eriksson, L.S., Sundin, U., and Sundqvist, K.G. (1992). Decreased in vitro production of tumor necrosis factor in primary biliary cirrhosis patients. *Scand. J. Gastroenterol.* **27**, 124-128.

Broomé, U., Hauzenberger, D., and Klominek, J. (1996). Adhesion molecules in primary biliary cirrhosis and primary sclerosing cholangitis. *Hepato-Gastroenterology* **43**, 1109-1112.

Brown, D.H., LaFuse, W., and Zwilling, B.S. (1995). Cytokine-mediated activation of macrophages from Mycobacterium bovis bcg-resistant and -susceptible mice: differential effects of corticosterone on antimycobacterial activity and expression of the Bcg gene (candidate nramp). *Infect. Immun.* **63**, 2983-2988.

Brown, D.H., LaFuse, W.P., and Zwilling, B.S. (1997). Stabilized expression of mRNA is associated with mycobacterial resistance controlled by nramp1. *Infect. Immun.* 65, 597-603.

Buettner, G.R. (1993). The pecking order of free radicals and antioxidants: lipid peroxidation, α-tocopherol, and ascorbate. *Arch. Biochem. Biophys.* **300**, 535-543.

Burkholder, J.K., Decker, J., and Yang, N.S. (1993). Rapid transgene expression in lymphocyte and macrophage primary cultures after particle bombardment-mediated gene transfer. *J. Immunol. Methods* **165**, 149-156.

Burroughs, A.K., Rosenstein, I.J., Epstein, O., Hamilton-Miller, J.M.T., Brumfitt, W., and Sherlock, S. (1984). Bacteriuria and primary biliary cirrhosis. *Gut* **25**, 133-137.

Burroughs, A.K., Butler, P., Sternberg, M.J.E., and Baum, H. (1992). Molecular mimicry in liver disease. *Nature* **358**, 377-378.

Bussmann, V., Lantier, I., Pitel, F., Patri, S., Nau, F., Gros, P., Elsen, J.M., and Lantier, F. (1998). cDNA cloning, structural organization, and expression of the sheep nramp1 gene. *Mamm. Genome* **9**, 1027-1031.

Buu, N.T., Cellier, M., Gros, P., and Schurr, E. (1995). Identification of a highly polymorphic length variant in the 3' UTR of NRAMP1. *Immunogenetics* **42**, 428-429.

Calafat, J., Kuijpers, T.W., Janssen, H., Borregaard, N., Verhoeven, A.J., and Roos, D. (1993). Evidence for small intracellular vesicles in human blood phagocytes containing cytochrome b_{558} and the adhesion molecule CD11b/CD18. *Blood* **81**, 3122-3129.

Cantlay, A.M., Smith, C.A.D., Wallace, W,A., Yap, P.L., Lamb, D., and Harrison, D.J. (1994). Heterogeneous expression and polymorphic genotype of glutathione S- transferases in human lung. *Thorax* **49**, 1010-1014.

Carter, P. (1971). Spectrophotometric determination of serum iron at the submicrogram level with a new reagent (ferrozine). *Anal. Biochem.* **40**, 450-458.

Cellier, M., Govoni, G., Vidal, S., Kwan, T., Groulx, N., Liu, J., Sanchez, F., Skamene, E., Schurr, E., and Gros, P. (1994). Human natural resistance-associated macrophage protein: cDNA cloning, chromosomal mapping, genomic organization, and tissue specific expression. *J. Exp. Med.* **180**, 1741-1752.

Cellier, M., Privé, G., Belouchi, A., Kwan, T., Rodrigues, V., Chia, W., and Gros, P. (1995). Nramp defines a family of membrane proteins. *Proc. Natl. Acad. Sci. USA* **92**, 10089-10093.

Cellier, M., Belouchi, A., and Gros, P. (1996). Resistance to intracellular infections: comparative genomic analysis of nramp. *T.I.G.* **12**, 201-204.

Cellier, M., Shustik, C., Dalton, W., Rich, E., Hu, J., Malo, D., Schurr, E., and Gros, P. (1997). Expression of the human NRAMP1 gene in professional primary phagocytes: studies in blood cells and in HL-60 promyelocytic leukemia. *J. Leukoc. Biol.* **61**, 96-105.

Cha, S., Leung, P.S.C., Van de Water, J., Tsuneyama, K., Joplin, R.E., Ansari, A.A., Nakanuma, Y., Schatz, P.J., Cwirla, S., Fabris, L.E., Neuberger, J.M., Gershwin, M.E., and Coppel, R.L. (1996). Random phage mimotopes recognized by monoclonal antibodies against the pyruvate dehydrogenase complex-E2 (PDC-E2). *Proc. Natl. Acad. Sci. USA* **93**, 10949-10954.

Charlotte, F., L'Hermine, A., Martin, N., Geleyn, Y., Nollet, M., Gaulard, P., and Zafrani, E.S. (1994). Immunohistochemical detection of bcl-2 protein in normal and pathological human liver. *Am. J. Pathol.* **144**, 460-465.

Chedid, A., Spellberg, M.A., and DeBeer, R.A. (1974). Ultrastructural aspects of primary biliary cirrhosis and other types of cholestatic liver disease. *Gastroenterology* **67**, 858-869.

Chilosi, M., Menestrina, F., Capelli, P., Montagna, L., Lestani, M., Pizzolo, G., Cipriani, A., Agostini, C., Trentin, L., Zambello, R., and Semenzato, G. (1988). Immunohistochemical analysis of sarcoid granulomas. Evaluation of $Ki67^+$ and $interleukin\text{-}1^+$ cells. *Am. J. Path.* **131**, 191-198.

Chiricolo, M., Lenzi, M., Bianchi, F., Franceschi, C., Bartolini, G., Orlandi, M., Tomasi, V., and Licastro, F. (1989). Immune dysfunction in primary biliary cirrhosis. *Scand. J. Immunol.* **30**, 363-367.

Chua, A.C.G., Stonell, L.M., Savigni, D.L., and Morgan, E.H. (1996). Mechanisms of manganese transport in rabbit erythroid cells. *J. Physiol.* **493.1**, 99-112.

Clemente, M.G., Frau, F., Farci, G., Ponti, M.L., Pilleri, G.P., Sole, G., Congia, M., and De Virgiliis, S. (1998). Primary biliary cirrhosis is associated to the HLA DRB1*0301-DQA1*0501-DQB1*0201 haplotype in Sardinians. Abstract *Hepatology* **Vol. 28**, No. 4, Part 2, p649A, 1948.

Cohen, S.N., Chang, A.C.Y. and Hsu, L. (1972). Nonchromosomal antibiotic resitance in bacteria: genetic transformation of *Escherichia coli* by R-factor DNA. *Proc. Natl. Acad. Sci. USA*. **69**, 2110-2114.

Coligan, J.E., Kruisbeek, A.M., Margulies, D.H., Shevach, E.M., and Strober, W (Editors) (1995). Enrichment of dendritic cells by plastic adherence in *Current Protocols in Immunology*. Third Edition. John Wiley & Sons, Inc., USA.. **Vol. 1**, 3.7.1-3.7.11.

Conforti, G., Zanetti, A., Pasquali-Ronchetti, I., Quaglino Jr, D., Neyroz, P., and Dejana, E. (1990). Modulation of vitronectin receptor binding by membrane lipid composition. *J. Biol. Chem.* **265**, 4011-4019.

Curry, M.P., Smith, F., Norris, S., Doherty, D., Golden-Mason, L., McEntee, G., Traynor, O., Nolan, N., Hegarty, J.E., and O Farrelly, C. (1998). Intrahepatic γδT lymphocytes are proportionately reduced in advanced primary biliary cirrhosis. Abstract *Hepatology* **Vol. 28**, No. 4, Part 2, p545A, 1532.

Cytokines Online Pathfinder Encyclopaedia web site: http://www.copewithcytokines.de/

Czaja, A.J. (1994). Chronic graft-versus-host disease and primary biliary cirrhosis: sorting the puzzle pieces. *Lab. Invest.* **70**, 589-592.

Czaja, A.J., Santrach, P.J., and Moore, S.B. (1998). Autoimmune cholangitis: a distinct entity in the spectrum of autoimmune liver disease? Abstract *Hepatology* **Vol. 28**, No. 4, Part 2, p547A, 1540.

Davies, M.H., Elias, E., Acharya, S., Cotton, W., Faulder, G.C., Fryer, A.A., and Strange, R.C. (1993). GSTM1 null polymorphism at the glutathione S-transferase M1 locus: phenotype and genotype studies in patients with primary biliary cirrhosis. *Gut* **34**, 549-553.

Deguchi, A., Arima, K., Yachida, M., Watanabe, S., and Nishioka, M. (1998). Enhanced expression of bcl-2 on infiltrating T cells in the liver in patients with primary biliary cirrhosis. Abstract *Hepatology* **Vol. 28**, No. 4, Part 2, p189A, 108.

Demetris, A.J., Sever, C., Kakizoe, S., Oguma, S., Starzl, T.E., and Jaffe, R. (1989). S100 protein positive dendritic cells in primary biliary cirrhosis and other chronic inflammatory liver diseases. *Am. J. Path.* **134**, 741-747.

Denis, M., Forget, A., Pelletier, M., and Skamene, E. (1988). Pleiotropic effects of the Bcg gene: III. Respiratory burst in Bcg-congenic macrophages. *Clin. Exp. Immunol.* **73**, 370-375.

Department of Haematology (1997). *Laboratory Handbook*. The Royal Infirmary of Edinburgh, NHS Trust, Lauriston Place, Edinburgh. p10

Dobrescu, D., Ursea, B., Pope, M., Asch, A.S., and Posnett, D.N. (1995). Enhanced HIV-1 replication in Vβ12 T cells due to human cytomegalovirus in monocytes: evidence for a putative herpesvirus superantigen. *Cell* **82**, 753-763.

Doherty, T.M., and Sher, A. (1997). Defects in cell-mediated immunity affect chronic, but not innate, resistance of mice to Mycobacterium avium infection. *J. Immunol.* **158**, 4822-4831.

Donowitz, G.R., and Mandell, G.L. (1982). Monocyte function in patients with chronic granulomatous disease of childhood. *Blood* **60**, 1151-1158.

Dorschner, M.O., and Phillips, R.B. (1999). Comparative analysis of two nramp loci from rainbow trout. Abstract *DNA Cell Biol.* **18**, 573-583.

Dransfield, I., Cabañas, C., Craig, A., and Hogg, N. (1992). Divalent cation regulation of the function of the leukocyte integrin LFA-1. *J. Cell Biol.* **116**, 219-226.

Ehlers, S., Mielke, M.E.A., and Hahn, H. (1994). Progress in TB research: Robert Koch's dilemma revisited. *Immunology Today* **15**, 1-4.

Eibl, M.M., Mannhalter, J.W., Zielinski, C.C., and Ahmad, R. (1982a) Defective macrophage-T-cell interaction in common varied immunodeficiency. *Clin. Immunol. Immunopathol.* **22**, 316-322.

Eibl, M.M., Mannhalter, J.W., Zlabinger, G., Mayr, W.R., Tilz, G.P., Ahmad, R., and Zielinski, C.C. (1982b). Defective macrophage function in a patient with common variable immunodeficiency. *N. Eng. J. Med.* **307**, 803-806.

Eibl, M.M., Zielinski, C.C. and Mannhalter, J.W. (1983). Macrophage function in common variable immunodeficiency. Letter in reply to Ko, H.S. *N. Eng. J. Med.* **308**, 286-287.

Elices, M.J., Urry, L.A., and Hemler, M.E. (1991). Receptor functions for the intergrin VLA-3: fibronectin, collagen, and laminin binding are differentially influenced by ARG-GLY-ASP peptide and by divalent cations. *J. Cell Biol.* 112, 169-181.

Ercilla, G., Parés, A., Arriaga, F., Bruguera, M., Castillo, R., Rodés, J., and Vives, J. (1979). Primary biliary cirrhosis associated with HLA-DRw3. *Tissue Antigens* **14**, 449-452.

Ercolani, L., Florence, B., Denaro, M., and Alexander, M. (1988). Isolation and complete sequence of a functional human glyceraldehyde-3-phosphate dehydrogenase gene. *J. Biol. Chem.* **263**, 15335-15341.

Evan, G., and Littlewood, T. (1998). A matter of life and cell death. *Science* **281**, 1317-1322.

Farcasanu, I.C., Ohta, N., and Miyakawa, T. (1996). The fate of Mn^{2+} ions inside Saccharomyces cerevisiae cells seen by electron paramagnetic resonance. *Biosci. Biotech. Biochem.* 60, 468-471.

Faubion, W.A., and Gores, G.J. (1999). Death receptors in liver biology and pathobiology. *Hepatology* **29**, 1-4.

Feistauer, S.M., Penner, E., Mayr, W.R., and Panzer, S. (1997). Target platelet antigens of autoantibodies in patients with primary biliary cirrhosis. *Hepatology* **25**, 1343-1345.

Fleet, J.C. (1998). Identification of nramp2 as an iron transport protein: another piece of the intestinal iron absorption puzzle. *Nutr. Rev.* **56**, 88-89.

Fleming, M.D., Trenor III, C.C., Su, M.A., Foernzler, D., Beier, D.R., Dietrich, W.F., and Andrews, N.C. (1997). Microcytic anaemia mice have a mutation in nramp2, a candidate iron transporter gene. *Nat. Genet.* **16**, 383-386.

Fleming, M.D., Romano, M.A., Su, M.A., Garrick, L.M., Garrick, M.D., and Andrews, N.C. (1998). Nramp2 is mutated in the the anemic Belgrade (b) rat: evidence of a role for nramp2 in endosomal iron transport. *Proc. Natl. Acad. Sci. USA* **95**, 1148-1153.

Foote, S. (1999). Mediating immunity to mycobacteria. *Nat. Genet.* **21**, 345-346.

Formica, S., Roach, T.I.A., and Blackwell, J.M. (1994). Interaction with extracellular matrix proteins influences Lsh/Ity/Bcg (candidate nramp) gene regulation of macrophage priming/activation for tumour necrosis factor-α and nitrite release. *Immunology* **82**, 42-50.

Fraústo da Silva, J.J.R., and Williams, R.J.P. (1991). *The Biological Chemistry of the Elements. The Inorgamic Chemistry of Life*. Clarendon Press, Oxford. Chpt. 14.

Friend, D.S., Papahadjopoulos, D., and Debs, R.J. (1996). Endocytosis and intracellular processing accompanying transfection mediated by cationic liposomes. *Biochim. Biophys. Acta* **1278**, 41-50.

Fugger, L., Morling, N., Ryder, L.P., Platz, P., Georgsen, J., Jakobsen, B.K., Svejgaard, A., Dalhoff, K., and Ranek, L. (1989). NcoI restriction fragment length polymorphism (RFLP) of the tumour necrosis factor (TNFα) region in primary biliary cirrhosis and in healthy Danes. *Scand. J. Immunol.* **30**, 185-189.

Fugger, L., Morling, N., Ryder, L.P., Jakobsen, B.K., Andersen, V., Oxholm, P., Dalhoff, K., Heilmann, C., Karup Pedersen, F., Friis, J., Halberg, P., Spies, T., Strominger, J.L., and Svejgaard, A. (1991). Restriction fragment length polymorphism of two HLA-B-associated transcripts genes in five autoimmune diseases. *Hum. Immunol.* **30**, 27-31.

Fussey, S.P.M., Ali, S.T., Guest, J.R., James, O.F.W., Bassendine, M.F., and Yeaman, S.J. (1990). Reactivity of primary biliary cirrhosis sera with Escherichia coli dihydrolipoamide acetyltransferase (E2p): characterization of the main immunogenic region. *Proc. Natl. Acad. Sci. USA* **87**, 3987-3991.

Gailit, J., and Ruoslahti, E. (1988). Regulation of the fibronectin receptor affinity by divalent cations. *J. Biol. Chem.* **263**, 12927-12932.

Galatola, G., Secreto, P., Tabone, M., Zaffino, C., Pera, A., and Fracchia, M. (1998). Serum interferon gamma (IFN-γ) in primary biliary cirrhosis (PBC): effect of ursodeoxycholic acid (UDCA) and prednisone (PDN) therapy alone and in combination. Abstract *Hepatology* **Vol. 28**, No. 4, Part 2, p650A, 1950.

Galeotti, T., Palombini, G., and van Rossum, G.D.V. (1995). Manganese content and high-affinity transport in liver and hepatoma. *Arch. Bioch. Biophys.* **322**, 453-459.

Galle, P.R., Hofmann, W.J., Walczak, H., Schaller, H., Otto, G., Stremmel, W. Krammer, P.H., and Runkel, L. (1995). Involvement of the CD95 (APO-1/Fas) receptor and ligand in liver damage. *J. Exp. Med.* **182**, 1223-1230.

Gallin, J.I., Klimerman, J.A., Padgett, G.A., and Wolff, S.M. (1975). Defective mononuclear leukocyte chemotaxis in Chediak-Higashi Syndrome of humans, mink and cattle. *Blood* **45**,863-870.

Galperin, C., and Gershwin, M.E. (1996). Immunopathology of primary biliary cirrhosis. *Baillieres Clin. Gastroenterol.* **10**, 461-481.

Gautier, A.V., Lantier, I., and Lantier, F. (1998) Mouse susceptibility to infection by the Salmonella abortusovis vaccine strain Rv6 is controlled by the Ity/nramp1 gene and influences the antibody but not the complement responses. *Microb. Pathog.* **24**, 47-55.

Gavin, C.E., Gunter, K.K., and Gunter, T.E. (1990). Manganese and calcium efflux kinetics in brain mitochondria. *Biochem. J.* **266**, 329-334.

Gavin, C.E., Gunter, K.K., and Gunter, T.E. (1992). Mn^{2+} sequestration by mitochondria and inhibition of oxidative phosphorylation. *Toxicol. Appl. Pharmacol.* **115**, 1-5.

Gendelman, H.E., and Morahan, P.S. (1992). Macrophages in viral infections in *The Macrophage: The Natural Immune System.* Edited by Lewis, C.E., and McGee, J.O.D.. Oxford University Press, New York. Chpt. 4.

Gerdes, J., Li, L., Schlueter, C., Duchrow, M., Wohlenberg, C., Gerlach, C., Stahmer, I., Kloth, S., Brandt, E., and Flad, H.D. (1991). Immunobiochemical and molecular biologic characterization of the cell proliferation-associated nuclear antigen that is defined by monoclonal antibody Ki-67. *Am. J. Pathol.* **138**, 867-873.

Gershwin, M.E., and Mackay, I.R. (1997). Primary biliary cirrhosis: Part I. Foreword. *Semin. Liver Dis.* **17** ,1-2.

Gibbons, M.J., Lynch, P.L.M., Loughrey, C., McEneny, J., Callender, M.E., and Young, I.S. (1999). A case-control study of free radical and antioxidant activity in primary biliary cirrhosis. Abstract *Gut* **Vol. 44**, Supp. 1, pA60, W239.

Golub, M.S., Han, B., and Keen, C.L. (1996). Aluminium alters iron and manganese uptake and regulation of surface transferrin receptors in primary rat oligodendrocyte cultures. *Brain Res.* **719**, 72-77.

Gomes, M.S., and Appelberg, R. (1998). Evidence for a link between iron metabolism and nramp1 gene function in innate resistance against Mycobacterium avium. *Immunology* **95**, 165-168.

Gordon, M.A., Gleeson, D., Oppenheim, E., di Giovine, F.S., Camp, N.C., and Duff, G.W. (1996). Tumour necrosis factor genetic polymorphisms and primary biliary cirrhosis. *Hepatology* **Vol. 24**, No. 4, Part 2, p166A, 159.

Govoni, G., Vidal, S., Cellier, M., Lepage, P., Malo, D., and Gros, P. (1995). Genomic structure, promoter sequence, and induction of expression of the mouse nramp1 gene in macrophages. *Genomics*, **27**, 9-19.

Govoni, G., Vidal, S., Gauthier, S., Skamene, E., Malo, D., and Gros, P. (1996). The Bcg/Ity/Lsh locus: genetic transfer of resistance to infections in C57BL/6J mice transgenic for the Nramp1^{Gly169} allele. *Infect. Immun.* **64**, 2923-2929.

Govoni, G, Gauthier, S., Billia, F., Isove, N.N., and Gros, P. (1997) Cell-specific and inducible nramp1 gene expression in mouse macrophages in vitro and in vivo. *J. Leuk. Biol.* **62**, 277-286.

Govoni, G., and Gros, P. (1998). Macrophage NRAMP1 and its role in resistance to microbial infections. *Inflamm. Res.* **47**, 277-284.

Govoni, G., Canonne-Hergaux, F., Pfeifer, C.G., Marcus, S.L., Mills, S.D., Hackam, D.J., Grinstein, S., Malo, D., Finlay, B.B., and Gros, P. (1999). Functional expression of nramp1 in vitro in the murine macrophage line RAW264.7. *Infect. Immun.* **67**, 2225-2232.

Graham, A.M., Dollinger, M.M., Howie, S.E.M., and Harrison, D.J. (1998). Bile duct cells in primary biliary cirrhosis are 'primed' for apoptosis. *Eur. J. Gastroenterol. Hepatol.* **10**, 553-557.

Graham, A.M., Dollinger, M.M., Howie, S.E.M., and Harrison, D.J. (in press). Identification of novel alleles at a polymorphic microsatellite repeat region in the human NRAMP1 gene promoter: analysis of allele frequency in primary biliary cirrhosis. Letter *J. Med. Genet.*

Green, D.R., and Reed, J.C. (1998). Mitochondria and apoptosis. *Science* **281**, 1309-1312.

Gregory, W.L., Mehal, W., Dunn, A.N., Cavanagh, G., Chapman, R., Fleming, K.A., Daly, A.K., Idle, J.R., James, O.F., and Bassendine, M.F. (1993). Primary biliary cirrhosis: contribution of HLA class II allele DR8. *Q.J.M.* **86**, 393-399.

Gregory, W.L., Daly, A.K., Dunn, A.N., Cavanagh, G., Idle, J.R., James, O.F.W., and Bassendine, M.F. (1994). Analysis of HLA-class-II-encoded antigen-processing genes TAP1 and TAP2 in primary biliary cirrhosis. *Q.J.M.* **87**, 237-244.

Gregory, S.H., and. Wing, E.J. (1998). Neutrophil-Kupffer cell interaction in host defenses to systemic infections. *Immunol. Today* **19**, 507-510.

Griffiths, G.M. (1995). The cell biology of CTL killing. *Curr. Opin. Immunol.* **7**, 343-348.

Gros P., Skamene E., and Forget, A. (1981). Genetic control of natural resistance to Mycobacterium bovis (Bcg) in mice. *J. Immunol.* **127**, 2417-2421.

Gruenheid, S., Cellier, M., Vidal, S., and Gros, P. (1995). Identification and characterization of a second mouse nramp gene. *Genomics* **25**, 514-525.

Gruenheid, S., Pinner, E., Desjardins, M., and Gros, P. (1997). Natural resistance to infection with intracellular pathogens: the nramp1 protein is recruited to the membrane of the phagosome. *J. Exp. Med.* **185**, 717-730.

Gruenheid, S., Canonne-Hergaux, F., Gauthier, S., Hackam, D.J., Grinstein, S., and Gros, P. (1999). The iron transport protein nramp2 is an integral membrane glycoprotein that colocalizes with transferrin in recycling endosomes. *J. Exp. Med.* **189**, 831-841.

Gunshin, H., Mackenzie, B., Berger, U.V., Gunshin, Y., Romero, M.F., Boron, W.F., Nussberger, S., Gollan, J.L., and Hediger, M.A. (1997). Cloning and characterization of a mammalian proton-coupled metal-ion transporter. *Nature* **388**, 482-488.

Hackam, D.J., Rotstein, O.D., Zhang, W., Gruenheid, S., Gros, P., and Grinstein, S. (1998). Host resistance to intracellular infection: mutation of natural resistance-associated macrophage protein 1 (nramp1) impairs phagosomal acidification. *J. Exp. Med.* **188**, 351-364.

Hall, B.F., and Joiner, K.A. (1991). Strategies of obligate intracellular parasites for evading host defences. *Immunology Today* **12**, A22-A27.

Harada, K., Van de Water, J., Leung, P.S.C., Coppel, R.L., Ansari, A., Nakanuma, Y., and Gershwin, M.E. (1997a). In situ nucleic acid hybridization of cytokines in primary biliary cirrhosis: predominance of the Th1 subset. *Hepatology* **25**, 791-796.

Harada, K., Ozaki, S., Gershwin, M.E., and Nakanuma. Y. (1997b). Enhanced apoptosis relates to bile duct loss in primary biliary cirrhosis. *Hepatology* **26**, 1399-1405.

Harada, K., Van de Water, J., Leung, P.S.C., Coppel, R.L., Nakanuma, Y., and Gershwin, M.E. (1997c). In situ nucleic acid hybridization of pyruvate dehydrogenase complex-E2 in primary biliary cirrhosis: pyruvate dehydrogenase complex-E2 messenger RNA is expressed in hepatocytes but not in biliary epithelium. *Hepatology* **25**, 27-32.

Harlan, D.M., Abe, R., Lee, K.P., and June, C.H. (1995). Potential roles of the B7 and CD28 receptor families in autoimmunity and immune evasion. *Clin. Immunol. Immunopath.* **75**, 99-111.

Hartung, H.P., Pollard, J.D., Harvey, G.K., and Toyka, K.V. (1995). Immunopathogenesis and treatment of the Guillain-Barré Syndrome - Part I. *Muscle and Nerve* **18**, 137-153.

Hashimoto, E., Lindor, K.D., Homburger, H.A., Dickson, E.R., Czaja, A.J., Wiesner, R.H., and Ludwig, J. (1993). Immunohistochemical characterization of hepatic lymphocytes in primary biliary cirrhosis in comparison with primary sclerosing cholangitis and autoimmune chronic active hepatitis. *Mayo Clin. Proc.* **68**, 1049-1055.

Hattori, Y., Murakami, Y., Hattori, S., Kuroda, H., Kasai, K., and Shimoda, S.I. (1996). Ursodeoxycholic acid inhibits the induction of nitric oxide synthase. *Eur. J. Pharmacol.* **300**, 147-150.

Hazell, L.J., and Stocker, R. (1993). Oxidation of low-density lipoprotein with hypochlorite causes transformation of the lipoprotein into a high-uptake form for macrophages. *Biochem J.* **290**, 165-172.

Heathcote, J. (1996). Treatment of primary biliary cirrhosis. *J. Gastroenterol. Hepatol.* **11**, 605-609.

Heathcote, J. (1997). Autoimmune cholangitis. *Gut* **40**, 440-442.

Hewison, M., Dabrowski, M., Faulkner, L., Hughson, E., Vadher, S., Rut, A., Brickell, P.M., O'Riordan, J.L.H., and Katz, D.R. (1994). Transfection of vitamin D receptor cDNA into the monoblastoid cell line U937. *J. Immunol.* **153**, 5709-5719.

Higuchi, H., Kurose, I., Ebinuma, H., Watanabe, N., Takaishi, M., Yonei, Y., Saito, H., Miura, S., and Ishii, H. (1995). Kupffer cell induces hepatocyte apoptosis: implication of nitric oxide by fluorescence in situ hybridization. Abstract *Heptology* **Vol. 22**, No. 4, Pt 2, p227A, 484.

Hiramatsu, N., Hayashi, N., Katayama, K., Mochizuki, K., Kawanishi, Y., Kasahara, A., Fusamoto, H., and Kamada, T. (1994). Immunohistochemical detection of Fas antigen in liver tissue of patients with chronic hepatitis C. *Hepatology* **19**, 1354-1359.

Hiramatsu, K., Nakanuma, Y., Harada, K., Tsuneyama, K., Sasaki, M., Kaneko, S., and Kobayashi, K. (1998). Amplification and sequence analysis of partial bacterial 16S ribosomal RNA gene in gallbladder bile from primary biliary cirrhosis patients. Abstract *Hepatology* **Vol. 28**, No. 4, Part 2, p648A, 1942.

Hislop, W.S. (1980). Primary bilary cirrhosis: an epidemiological study. Letter *B.M.J.* **281**, 1069-1070.

Hofmeister, A., Neibergs, H.L., Pokorny, R.M., and Galandiuk, S. (1997). The natural resistance-associated macrophage protein gene is associated with Crohn's disease. *Surgery* **122**, 173-179.

Howie, S.E.M., Sommerfield, A.J., Gray, E., and Harrison, D.J. (1994). Peripheral T lymphocyte depletion by apoptosis after CD4 ligation in vivo: selective loss of $CD44^-$ and 'activating' memory T cells. *Clin. Exp. Immunol.* **95**, 195-200.

Hubbard, A.L., and Anderson, T.J. (1993). Simple 10 min preparation of fixed, embedded breast tissue for the polymerase chain reaction. *Breast* **2**, 50-51.

Hung, W.C., and Chuang, L.Y. (1996). Induction of apoptosis by sphingosine-1-phosphate in human hepatoma cells is associated with enhanced expression of bax gene product. *Biochem. Biophys. Res. Commun.* **229**, 11-15.

Invernizzi, P., Salzman, A.L., Szabó, C., Ueta, I., O'Connor, M., and Setchell, K.D.R. (1997). Ursodeoxycholate inhibits induction of NOS in human intestinal epithelial cells in vivo. *Am. J. Physiol.* **273** (*Gastrointest. Liver Physiol.* **36**) G131-G138.

James, S.P., and Jones, E.A. (1985). Abnormal natural killer cytotoxicity in primary biliary cirrhosis: evidence for a functional deficiency of cytolytic effector cells. *Gastroenterology* **89**, 165-171.

Janeway, C.A., and Travers, P. (1994). *Immunboiology The Immune System in Health and Disease*. Blackwell Scientific Publications, Oxford. Chpt 7.

Jones, D.E.J. (1996). T-cell autoimmunity in primary biliary cirrhosis. *Clin. Sci.* **91**, 551-558.

Jones, D.E.J., Palmer, J.M., Leon, M.P., Yeaman, S.J., Bassendine, M.F., and Diamond, A.G. (1997). T cell responses to tuberculin purified protein derivative in primary biliary cirrhosis: evidence for defective T cell function. *Gut* **40**, 277-283.

Jones, D.E.J., Watt, F.E., Grove, J., Newton, J.L., Daly, A.K., Gregory, W.L., Day, C.P., James, O.F.W., and Bassendine, M.F. (1999). Tumour necrosis factor-α promoter polymorphisms in primary biliary cirrhosis. *J. Hepatol.* **30**, 232-236.

Jorge, A.D., and Leuschner, U. (1996). *Primary biliary cirrhosis*. Third Edition. Falk Foundation e.V..

Jouanguy, E., Lamhamedi-Cherradi, S., Lammas, D., Doorman, S.E., Fondanèche, M.C., Dupuis, S., Döffinger, R., Altare, F., Girdlestone, J., Emile, J.F., Ducoulombier, H., Edgar, D., Clarke, J., Oxelius, V.A., Brai, M., Novelli, V., Heyne, K., Fischer, A., Holland, S.M., Kumararatne, D.S., Schreiber, R.D., and Casanova, J.L. (1999). A human IFNGR1 small deletion hotspot associated with dominant susceptibility to mycobacterial infection. *Nat. Genet.* **21**, 370-378.

Kägi, D., Ledermann, B., Bürki, K., Zinkernagel, R.M., and Hengartner, H. (1996). Molecular mechanisms of lymphocyte-mediated cytotoxicity and their role in immunological protection and pathogenesis in vivo. *Annu. Rev. Immunol.* **14**, 207-232.

Kamegaya, Y., Oda, M., Yokomori, H., Miyaguchi, S., Komatsu, H., Tsukada, N., Yonei, K., and Ishii, H. (1997). ICAM-1 expressions on small bile ducts in AMA-negative primary biliary cirrhosis. Abstract *Gastroenterology* **Vol. 112**, No. 4, pA1296.

Kaplan, M.M. (1996). Primary biliary cirrhosis. *N. Eng. J. Med.* **335**, 1570-1580.

Kimura, T., Suzuki, K., Inada, S., Hayashi, A., Isobe, M., Matsuzaki, Y., Tanaka, N., Osuga, T., and Fujiwara, M. (1996). Monoclonal antibody against lymphocyte function-associated antigen 1 inhibits the formation of primary biliary cirrhosis-like lesions induced by murine graft-versus-host reaction. *Hepatology* **24**, 888-894.

Kingsley, G. and Panayi, G.S. (1997). Joint destruction in rheumatoid arthritis: biological bases. *Clin. Exp. Rheum.* **Vol. 15**, Supp. 17, S3-S14.

Kirchhofer, D., Gailit, J., Ruoslahti, E., Grzesiak, J., and Pierschbacher, M.D. (1990). Cation-dependent changes in the binding specificity of the platelet receptor GPIIb/IIIa. *J. Biol. Chem.* **265**, 18525-18530.

Kishi, F. (1994). Isolation and characterization of human NRAMP cDNA. *Biochem. Biophys. Res. Comm.* **204**, 1074-1080.

Kishi, F., and Nobumoto, M. (1995). Identification of natural resistance-associated macrophage protein in peripheral blood lymphocytes. *Immunol. Lett.* **47**, 93-96.

Kishi, F., Yoshida, T., and Aiso, S. (1996a). Location of NRAMP1 molecule on the plasma membrane and its association with microtubules. *Mol. Immunol.* **33**, 1241-1246.

Kishi, F., Tanizawa, Y., and Nobumoto, M. (1996b). Structural analysis of human natural resistance-associated macrophage protein 1 promoter. *Mol. Immunol.* **33**, 265-268.

Kishi, F., and Tabuchi, M. (1997). Complete nucleotide sequence of human NRAMP2 cDNA. *Mol. Immunol.* **34**, 839-842.

Klion, F.M., and Schaffner, F. (1966). Electron microscopic observations in primary biliary cirrhosis. *Arch. Path.* **81**, 152-161.

Kobashi, H., Yamamoto, K., Yoshioka, T., Tomita, M., and Tsuji, T. (1994). Nonsuppurative cholangitis is induced in neonatally thymectomized mice: a possible animal model for primary biliary cirrhosis. *Hepatology* **19**, 1424-1430.

Koga, H., Sakisaka, S., Ohishi, M., Sata, M., and Tanikawa, K. (1997). Nuclear DNA fragmentation and expression of bcl-2 in primary biliary cirrhosis. *Hepatology* **25**, 1077-1084.

Koga, H., Sakisaka, S., Kawaguchi, T., Taniguchi, E., Ohishi, M., Sasatomi, K., Harada, M., and Sata, M. (1998). Involvement of Fas ligand-expressing T lymphocytes in bile duct injury of primary biliary cirrhosis. Abstract *Hepatology* **Vol. 28**, No. 4, Part 2, p543A, 1523.

Kolenbrander, P.E., Andersen, R.N., Baker, R.A., and Jenkinson, H.F. (1998). The adhesion-associated sca operon in Streptococcus gordonii encodes an inducible high-affinity ABC transporter for Mn^{2+} uptake. *J. Bacteriol.* **180**, 290-295.

Komiyama, A., Saitoh, H., Yamazaki, M., Kawai, H., Miyagawa, Y., Akabane, T., Ichikawa, M., and Shigematsu, H. (1986). Hyperactive phagocytosis by circulating neutrophils and monocytes in Chèdiak-Higashi syndrome. *Scand. J. Haematol.* **37**, 162-167.

Koukoulis, G.K., Shen, J., Iyer, A., Foster, P., Ganger, D., and Williams, J. (1995). Immunolocalization of bcl-2 and MET oncoproteins in biliary ductules and ducts of normal liver, cirrhosis and ductopenic rejection. Abstract *Hepatology* **Vol. 22**, No. 4, Part 2, p137A, 122.

Kovárová, H., Hajdúch, M., and Macela, A. (1997). Natural resistance to infection with intracellular pathogens: cross-talk between nramp1 and Lps genes. *Electrophoresis* **18**, 2654-2660.

Kovárová, H., Radzioch, D., Hadjúch, M., Sírová, M., Bláha, V., Macela, A., Stulík, J., and Hernychová, L. (1998). Natural resistance to intracellular parasites: a study by two-dimensional gel electrophoresis coupled with multivariate analysis. *Electrophoresis* **19**, 1325-1331.

Krajewski, S., Krajewska, M., Shabaik, A., Miyashita, T., Wang, H.G., and Reed, J.C. (1994). Immunohistochemical determination of in vivo distribution of bax, a dominant inhibitor of bcl-2. *Am. J. Path.* **145**,1323-1336.

Krams, S.M., Dorshkind, K., and Gershwin, M.E. (1989a). Generation of biliary lesions after transfer of human lymphocytes into severe combined immunodeficient (SCID) mice. *J. Exp. Med.* **170**, 1919-1930.

Krams, S.M., Surh, C.D., Coppel, R.L., Ansari, A., Ruebner, B., and Gershwin, M.E. (1989b). Immunization of experimental animals with dihydrolipoamide acetlyltransferase, as a purified recombinant polypeptide, generates mitochondrial antibodies but not primary biliary cirrhosis. *Hepatology* **9**, 411-416.

Krams, S.M., Van de Water, J., Coppel, R.L., Esquiviel, C., Roberts, J., Ansari, A., and Gershwin, M.E. (1990). Analysis of hepatic T lymphocyte and immunoglobulin deposits in patients with primary biliary cirrhosis. *Hepatology* **12**, 306-313.

Kröncke, K.D., Fehsel, K., and Kolb-Bachofen, V. (1997). Nitric oxide: cytotoxicity versus cytoprotection - how, why, when, and where? *Nitric Oxide* **1**, 107-120.

Kuroki, T., Seki, S., Kawakita, N., Nakatani, K., Hisa, T., Kitada, T., and Sakaguchi, H. (1996). Expression of antigens related to apoptosis and cell proliferation in chronic nonsuppurative destructive cholangitis in primary biliary cirrhosis. *Virchows Arch.* **429**, 119-129.

Kurokohchi, K., Arima, K., Yachida, M., Watanabe, S., and Nishioka, M. (1998). Analysis of co-stimulatory and other accessory molecules in patients with primary biliary cirrhosis and autoimmune hepatitis. Abstract *Hepatology* **Vol. 28**, No. 4, Part 2, p648A, 1943.

Kurose, I., Higuchi, H., Watanabe, N., Ebinuma, H., Yonei, Y., Saito, H., Miura, S., and Ishii, H. (1995). Nitric oxide and tumor necrosis factor-α mediate apoptosis of hepatoma cells induced by Kupffer cells. Abstract *Heptology* **Vol. 22**, No. 4, Part 2, p228A, 486.

Laemmli, U.K. (1970). Cleavage of structural proteins during the assembly of the head of bacteriophage T4. *Nature* **227**, 680-685.

Lang, T., Prina, E., Sibthorpe, D., and Blackwell, J.M. (1997). Nramp1 transfection transfers Ity/Lsh/Bcg-related pleiotropic effects on macrophage activation: influence on antigen processing and presentation. *Infect. Immun.* **65**, 380-386.

Le Cann, P., Tong, M.J., Werneke, J., and Coursaget, P. (1997). Detection of antibodies to hepatitis E virus in patients with autoimmune chronic active hepatitis and primary biliary cirrhosis. *Scand. J. Gastroenterol.* **32**, 387-389.

Lee, P.L., Gelbart, T., West, C., Halloran, C., and Beutler, E. (1998). The human NRAMP2 gene: characterization of the gene structure, alternative splicing, promoter region and polymorphisms. *Blood Cells Mol. Dis.* **24**, 199-215.

Leon, M.P., Spickett, G., Jones D.E.J., and Bassendine, M.F. (1995a). $CD4^+$ T cell subsets defined by isoforms of CD45 in primary biliary cirrhosis. *Clin. Exp. Immunol.* **99**, 233-239.

Leon, M.P., Kirby, J.A., Gibbs, P., Burt, A.D., and Bassendine, M.F. (1995b). Immunogenicity of biliary epithelial cells: study of the expression of B7 molecules. *J. Hepatol.* **22**, 591-595.

Leon, M.P., Bassendine, M.F., Wilson, J.L., Ali, S., Thick, M., and Kirby, J.A. (1996). Immunogenicity of biliary epithelium: investigation of antigen presentation to CD4+ T cells. *Hepatology* **24**, 561-567.

Leung, P.S.C., Van de Water, J., Coppel, R.L., Nakanuma, Y., Munoz, S., and Gershwin, M.E. (1996). Molecular aspects and the pathological basis of primary biliary cirrhosis. *J. Autoimmun.* **9**, 119-128.

Li, L., and Kaplan, J. (1998). Defects in the yeast high affinity iron transport system result in increased metal sensitivity because of the increased expression of transporters with a broad transition metal specificity. *J. Biol. Chem.* **273**, 22181-22187.

Lindgren, S., Wassmuth, R., Deppner, F., Danielsson, A., Hultcrantz, R., Lööf, L., Olson, R., Prytz, H., Sandberg-Gertzen, H., and Wallerstedt, S. (1998). A population-based study of HLA Class II polymorphism in Swedish patients with primary biliary cirrhosis. Abstract *Hepatology* **Vol. 28**, No. 4, Part 2, p540A, 1509.

Liu, J., Fujiwara, T.M., Buu, N.T., Sánchez, F.O., Cellier, M., Paradis, A.J., Frappier, D., Skamene, E., Gros, P., Morgan, K., and Schurr, E. (1995). Identification of polymorphisms and sequence variants in the human homologue of the mouse natural resistance-associated macrophage protein gene. *Am. J. Hum. Genet.* **56**, 845-853.

Liu, X.F., and Culotta, V.C. (1999a). Post-translational control of nramp metal transport in yeast - role of metal ions and the BSD2 gene. *J. Biol. Chem.* **274**, 4863-4868.

Liu, X.F., and Culotta, V.C. (1999b). Mutational analysis of Saccharomyces cerevisiae Smf1p, a member of the nramp family of metal transporters. *J. Mol. Biol.* **289**, 885-891.

Ljubuncic, P., Fuhrman, B., Oiknine, J., Aviram, M., and Bomzon, A. (1996). Effect of deoxycholic acid and ursodeoxycholic acid on lipid peroxidation in cultured macrophages. *Gut* **39**, 475-478.

Locksley, R.M., Nelson, C.S., Fankhauser, J.E., and Klebanoff, S.J. (1987). Loss of granule myeloperoxidase during in vitro culture of human monocytes correlates with decay in antiprotozoa activity. *Am. J. Trop. Med. Hyg.* **36**, 541-548.

Luettig, B., Boeker, K.H.W., Schoessler, W., Will, H., Loges, S., Schmidt, E., Worman., H.J., Gershwin, M.E., and Manns, M.P. (1998). The antinuclear autoantibodies Sp100 and gp210 persist after orthotopic liver transplantation in patients with primary biliary cirrhosis. *J. Hepatol.* **28**, 824-828.

MacDiarmid, C.W., and Gardner, R.C. (1998). Overexpression of the Saccharomyces cerevisiae magnesium transport system confers resistance to aluminium ion. *J. Biol. Chem.* **273**, 1727-1732.

Maciejewski, J., Selleri, C., Anderson, S., and Young, N.S. (1995). Fas antigen expression on $CD34^+$ human marrow cells is induced by interferon γ and tumor necrosis factor α and potentiates cytokine-mediated hematopoietic suppression in vitro. *Blood* **85**, 3183-3190.

Mackay, I.R. (1994). Molecular aspects of autoimmune liver disease in *The Liver: Biology and Pathobiology*. Edited by Arias, I.M., Boyer, J.L., Fausto, N., Jakoby, W.B., Schachter, D., and Shafritz, D.A.. Third Edition. Raven Press Ltd., New York. Chpt. 67.

MacMicking, J.D., North, R.J., LaCourse, R., Mudgett, J.S., Shah, S.K., and Nathan, C.F. (1997). Identification of nitric oxide synthase as a protective locus against tuberculosis. *Proc. Natl. Acad. Sci. USA* **94**, 5243-5248.

Malamud, A., Zaeri, N., Rubin, R., Rothstein, K., Reich, D., Manzarbeitia, C., Liang, T.J., and Munoz, S. (1997). Primary biliary cirrhosis associated with chronic hepatitis C infection: an ominous combination. Abstract *Gastroenterology* **Vol. 112**, No. 4, A1326.

Malecki, E.A., Devenyi, A.G., Beard, J.L., and Connor, J.R. (1999). Existing and emerging mechanisms for transport of iron and manganese to the brain. *J. Neurosci. Res.* **56**, 113-122.

Martinez, O.M., Villanueva, J.C., Gershwin, M.E., and Krams, S.M. (1995). Cytokine patterns and cytotoxic mediators in primary biliary cirrhosis. *Hepatology* **21**, 113-119.

Marucci, L., Baroni, G.S., Mancini, R., Benedetti, A., Jezequel, A.M., and Orlandi, F. (1993). Cell proliferation following extrahepatic biliary obstruction. Evaluation by immunohistochemical methods. *J. Hepatol.* **17**, 163-169.

Mathew, J., Hines, J.E., Toole, K., Johnson, S.J., James, O.F.W., and Burt, A.D. (1994). Quantitative analysis of macrophages in perisinusoidal cells in primary biliary cirrhosis. *Histopathology* **25**, 65-70.

Medina, E., and North, R.J. (1996). Evidence inconsistent with a role for the Bcg gene (nramp1) in resistance of mice to infection with virulent Mycobacterium tuberculosis. *J. Exp. Med.* **183**, 1045-1051.

Medina, E., Rogerson, B.J., and North, R.J. (1996). The nramp1 antimicrobial resistance gene segregates independently of resistance to virulent Mycobacterium tuberculosis. *Immunology* **88**, 479-481.

Medina, J.F., Martínez-Ansó E., Vázquez, J.J., and Prieto, J. (1997). Decreased anion exchanger 2 immunoreactivity in the liver of patients with primary biliary cirrhosis. *Hepatology* **25**, 12-17.

Medina, E. and North, R.J. (1998). Resistance ranking of some common inbred mouse strains to Mycobacterium tuberculosis and relationship to major histocompatibility complex haplotype and nramp1 genotype. *Immunology* **93**, 270-274.

Melegh, B., Skuta, G., Pajor, L., Hegedus, G., and Sumegi, B. (1998). Autoantibodies against subunits of pyruvate dehydrogenase and citrate synthase in a case of paediatric biliary cirrhosis. *Gut* **42**, 753-756.

Mella, J.G., Roschmann, E., Maier, K.P., and Volk, B.A. (1995). Association of primary biliary cirrhosis with the allele HLA-DPB1*0301 in a German population. *Hepatology* **21**, 398-402.

Menéndez, J.L., Girón, J.A., Manzano, L., Garrido, A., Abreu, L., Albillos, A., Durántez, A., and Alvarez-Mon, M. (1992). Deficient interleukin-2 responsiveness of T lymphocytes from patients with primary biliary cirrhosis. *Hepatology* **16**, 931-936.

Messer, G., Spengler, U., Jung, M.C., Honold, G., Eisenburg, J., Scholz, S., Albert, E.D., Pape, G.R., Riethmüller, G., and Weiss, E.H. (1991). Allelic variation in the TNF-β gene does not explain the low TNF-β response in patients with primary biliary cirrhosis. *Scand. J. Immunol.* **34**, 735-740.

Messmer, U.K., and Brüne, B. (1995). Nitric oxide-induced apoptosis: p53-dependent and p53-independent signalling pathways. *Biochem. J.* **319**, 299-305.

Metcalf, D. (1971). Transformation of granulocytes to macrophages in bone marrow colonies in vitro. *J. Cell Physiol.* 77, 277-280.

Metcalf, J., and James, O. (1997). The geoepidemiology of primary biliary cirrhosis. *Semin. Liver Dis.* **17**, 13-22.

Metchnikoff, E. (1989). The Nobel lectures in immunology. The Nobel prize for physiology or medicine, 1908, awarded to Elie Metchnikoff and Paul Ehrlich. In recognition of their work on immunity. *Scand. J. Immunol.* **30**, 383-398.

Mignotte, B., and Vayssiere, J.L. (1998). Mitochondria and apoptosis. *Eur. J. Biochem.* **252**, 1-15.

Mitchison, H.C., Bassendine, M.F., Hendrick, A., Bennett, M.K., Bird, G., Watson, A.J., and James, O.F.W. (1986). Positive antimitochondrial antibody but normal alkaline phosphatase: is this primary biliary cirrhosis? *Hepatology* **6**, 1279-1284.

Miyashita, T., Krajewski, S., Krajewska, M., Wang, H.G., Lin, H.K., Liebermann, D.A., Hoffman, B., and Reed, J.C. (1994). Tumor suppressor p53 is a regulator of bcl-2 and bax gene expression in vitro and in vivo. *Oncogene* **9**, 1799-1805.

Mochizuki, K., Hayashi, N., Hiramatsu, N., Katayama, K., Kawanishi, Y., Kasahara, A., Fusamoto, H., and Kamada, T. (1996). Fas antigen expression in liver tissues of patients with chronic hepatitis B. *J. Hepatol.* **24**, 1-7.

Moore, M.A.S., and Metcalf, D. (1970). Ontogeny of the haemopoietic system: yolk sac origin of in vivo and in vitro colony forming cells in the developing mouse embryo. *Br. J. Haematol.* **18**, 279-296.

Moreno-Otero, R., Civeira, M.P., Suou, T., Kanof, M.E., James, S.P., and Jones, E.A. (1994). Reduced numbers of CD8+ T cells and B cell-expression of Leu-8 antigen in peripheral blood of patients with primary biliary cirrhosis. *Hepatogestroenterology* **41**, 239-243.

Morling, N., Dalhoff, K., Fugger, L., Georgsen, J., Jakobsen, B., Ranek, L., Ødum, N., and Svejgaard, A. (1992). DNA polymorphism of HLA class II genes in primary biliary cirrhosis. *Immunogenetics* **35**, 112-116.

Nagata, S. (1997). Apoptosis by death factor. *Cell* **88**, 355-365.

Nakamura, A., Yamazaki, K., Suzuki, K., Sato, S., Sato, S., and Masuda, T. (1996). Increased mast cell and eosinophil infiltration in the liver in primary biliary cirrhosis. Abstract *Hepatology* **Vol. 24**, No. 4, Part 2, p166A, 158.

Nakanuma, Y., and Harada, K. (1993). Florid duct lesion in primary biliary cirrhosis shows highly proliferative activities. *J. Hepatol.* **19**, 216-221.

Nakanuma, Y., and Ohta, G. (1983). Quantitation of hepatic granulomas and epithelioid cells in primary biliary cirrhosis. *Hepatology* **3**, 423-427.

Nakanuma, Y., Ohta, G., Kono, N., Kobayashi, K., and Kato, Y. (1983). Electron microscopic observation of destruction of biliary epithelium in primary biliary cirrhosis. *Liver* **3**, 238-248.

Nakanuma, Y., Tsuneyama, K., Gershwin, M.E., and Yasoshima, M. (1995). Pathology and immunopathology of primary biliary cirrhosis with emphasis on bile duct lesions: recent progress. *Semin. Liver Dis.* **15**, 313-328.

Nakanuma, Y., Yasoshima, M., Tsuneyama, K., and Harada, K. (1997). Histopathology of primary biliary cirrhosis with emphasis on expression of adhesion molecules. *Semin. Liver Dis.* **17**, 35-47.

Napoli, J., Bishop, G.A., and McCaughan, G.W. (1994). Increased intrahepatic messenger RNA expression of interleukins 2, 6, and 8 in human cirrhosis. *Gastroenterology* **107**, 789-798.

Neibergs, H.L., Hofmeister, A., Rotter, J.I., Pressman, S., and Yang, H. (1997). Linkage analysis supports NRAMP as a major susceptibility locus for ulcerative colitis. Abstract *Am. J. Hum. Genetics* **Vol. 61**, Supp., No. 4, pA53, 280.

Neuberger, J. (1997). Primary biliary cirrhosis. *Lancet* **350**, 875-879.

Notas, G., Valatas, V., Xidakis, K., Kouroumalis, A., Koulentaki, M., and Kouroumalis, E. (1999). Circulating endothelin-1 and nitric oxide in primary biliary cirrhosis. Abstract *Gut* **Vol. 44**, Supp. 1, pA61, W242.

Novak, R., Braun, J.S., Charpentier, E., and Tuomanen, E. (1998). Penicillin tolerance genes of Streptococcus pneumoniae: the ABC-type manganese permease complex Psa. *Mol. Microbiol.* **29**, 1285-1296.

O'Brien, A.D., and Metcalf, E.S. (1982). Control of early Salmonella typhimurium growth in innately Salmonella-resistant mice does not require functional T lymphocytes. *J. Immunol.* **129**, 1349-1351.

Odin, J.A., Casciola-Rosen, L., and Rosen, A. (1999). Recognition of PDC-E2 by antisera from patients with primary biliary cirrhosis in apoptotic cholangiocytes versus non-cholangiocytes. *Gastroenterology* **Vol. 116**, No. 4, Part 2, pA1257, L0337.

O'Donohue, J., and Williams, R. (1996a). Primary biliary cirrhosis. *Q.J.M.* **89**, 5-13.

O'Donohue, J., and Williams, R. (1996b). Antimitochondrial antibody and primary biliary cirrhosis: can there be one without the other? *J. Hepatol.* **25**, 574-577.

O'Donohue, J., Fidler, H., Garcia-Barcelo, M., Nouri-Aria, K., Williams, R., and McFadden, J. (1998). Mycobacterial DNA not detected in liver sections from patients with primary biliary cirrhosis. *J. Hepatol.* **28**, 433-438.

Ogasawara, J., Watanabe-Fukunaga, R., Adachi, M., Matsuzawa, A., Kasugai, T., Kitamura, Y., Itoh, N., Suda, T., and Nagata, S. (1993). Lethal effect of the anti-Fas antibody in mice. *Nature* **364**, 806-809.

Ohmoto, M., Yamamoto, K., Nagano, T., Matsumoto, S., Kobashi, H., Okamoto, R., and Tsuji, T. (1997). Accumulation of multiple T-cell clonotypes in the liver of primary biliary cirrhosis. *Hepatology* **25**, 33-37.

Okamoto, R., Yamamoto, K., Ibuki, N., Yabushita, K., Matsumura, S., Okano, N., and Tsuji, T. (1998). T cell repertoire in primary biliary cirrhosis. Abstract *Hepatology* **Vol. 28**, No.4, Part 2, p650A, 1952.

Okazaki, M., Hino, K., Fujii, K., Hanada, H., Nakanishi, Y., Kanazawa, S., Kobayashi, N., and Okita, K. (1995). Immunohistochemical study of Fas antigen in liver of patients with chronic hepatitis and autoimmune liver disease. *Int. Hepatol. Comm.* **3**, 285-289.

Olivier, M., Cook, P., Desanctis, J., Hel, Z., Wojciechowski, W., Reiner, N.E., Skamene, E., and Radzioch, D. (1998). Phenotypic difference between Bcg^r and Bcg^s macrophages is related to differences in protein-kinase-C-dependent signalling. *Eur. J. Biochem.* **251**, 734-743.

Oltvai, Z.N., Milliman, C.L., and Korsmeyer, S.J. (1993). Bcl-2 heterodimerizes in vivo with a conserved homolog, bax, that accelerates programed cell death. *Cell* **74**, 609-619.

Onishi, S., Sakamaki, T., Maeda, T., Iwamura, S., Tomita, A., Saibara, T., and Yamamoto, Y. (1994). DNA typing of HLA class II genes; DRB1*0803 increases the susceptibility of Japanese to primary biliary cirrhosis. *J. Hepatol.* **21**, 1053-1060.

Orgad, S., Nelson, H., Segal, D., and Nelson, N. (1998). Metal ions suppress the abnormal taste behavior of the drosophila mutant malvolio. *J. Exp. Biol.* **201**, 115-120.

Ott, M.T., Vore, M., Barker, D.E., Strodel, W.E., and McClain, C.J. (1989). Monokine depression of bile flow in the isolated perfused rat liver. *J. Surg. Res.* **47**, 248-250.

Ottenhoff, T.H.M., Kumararatne, D., and Casanova, J.L. (1998). Novel human immunodeficiencies reveal the essential role of type-1 cytokines in immunity to intracellular bacteria. *Immunol. Today.* **19**, 491-494.

Owen-Schaub, L.B., Zhang, W., Cusack, J.C., Angelo, L.S., Santee, S.M., Fujiwara, T., Roth, J.A., Deisseroth, A.B., Zhang, W.W., Kruzel, E., and Radinsky, R. (1995). Wild-type human p53 and a temperature-sensitive mutant induce Fas/APO-1 expression. *Mol. Cell Biol.* **15**, 3032-3040.

Palmer, J.M., Jones, D.E.J., Doshi, M., Yeaman, S.J., Bassendine, M.F., and Kirby, J.A. (1998). Secretory IgA anti-PDC in saliva in primary biliary cirrhosis: a novel mechanism for tissue damage? Abstract *Hepatology* **Vol. 28**, No. 4, Part 2, p541A, 1513.

Palmer, J.M., Diamond, A.G., Yeaman, S.J., Bassendine, M.F., and Jones, D.E.J. (1999). T cell responses to the putative dominant autoepitope in primary biliary cirrhosis (PBC). *Clin. Exp. Immunol.* **116**, 133-139.

Panayiotidis, P., Ganeshaguru, K., Foroni, L., and Hoffbrand. A.V. (1995). Expression and function of the Fas antigen in B chronic lymphocytic leukemia and hairy cell leukemia. *Leukemia* **9**, 1227-1232.

Parums, D.V. (1992). Macrophages in caediovascular disease in *The Macrophage: The Natural Immune System.* Edited by Lewis, C.E., and McGee, J.O.D. Oxford University Press, New York. Chpt. 9.

Penninger, J.M., Wen, T., Timms, E., Potter, J., Wallace, V.A., Matsuyama, T., Ferrick, D., Sydora, B., Kronenberg, M., and Mak, T.W. (1995). Spontaneous resistance to acute T cell leukaemias in $TCRV_{\gamma}1.1J_{\gamma}4C_{\gamma}4$ transgenic mice. *Nature* **375**, 241-244.

Perkin-Elmer web site: http://www2.perkin-elmer.com

Pinner, E., Gruenheid, S., Raymond, M., and Gros, P. (1997). Functional complementation of the yeast divalent cation transporter family SMF by NRAMP2, a member of the mammalian natural resistance-associated macrophage protein family. *J. Biol. Chem.* **272**, 28933-28938.

Plant, J., and Glynn, A.A. (1976). Genetics of resistance to infection with Salmonella typhimurium in mice. *J. Infect. Dis.* **133**, 72-78.

Plant, J.E., Blackwell, J.M., O'Brien, A.D., Bradley, D.J., and Glynn, A.A. (1982). Are the Lsh and Ity disease resistance genes at one locus on mouse chromosome 1? *Nature* **297**, 510-511.

Pileri, S.A., Roncador, G., Ceccarelli, C., Piccioli, M., Briskomatis, A., Sabattini, E., Ascani, S., Santini, D., Piccaluga, P.P., Leone, O., Damiani, S., Ercolessi, C., Sandri, F., Pieri, F., Leoncini, L., and Falini, B. (1997). Antigen retrieval techniques in immunohistochemistry: comparison of different methods. *J. Pathol.* **183**, 116-123.

Podda, M., Bertolini, E., Battezzati, P.M., Camisaca, E., Zermiani, P., Ravizza, L., Zuin, M., Marelli, F., and Moroni, G.A. (1990). Antibodies to hepatitis C virus (anti-HCV) in primary biliary cirrhosis. Abstract *Hepatology* **Vol. 12**, No. 4, Part 2, p842, 17.

Pollack, S., Reisner, Y., Koziner, B., Good, R.A., and Hoffmann, M.K. (1985). B-cell function in common variable immunodeficiency: suppression of in vitro anti-sheep erythrocytes antibody production by T cells and monocytes. *Immunology* **54**, 89-96.

Pollack. S. and Etzioni, A. (1992). Macrophages in autoimmunity and primary immunodeficiency in *The Macrophage: The Natural Immune System.* Edited by Lewis, C.E., and McGee, J.O.D. Oxford University Press, New York. Chpt. 7.

Portmann, B.C., and MacSween, R.N.M. (1987). Diseases of the intrahepatic bile ducts in *Pathology of the Liver*. Edited by MacSweeen, R.N.M., Anthony, P.P., and Scheuer, P.J.. Second Edition. Churchill Livingstone, Edinburgh.

Prieto, J., Subirá, M.L., Castilla, A., Civeira, M.P., and Serrano, M. (1990). Monocyte disorder causing cellular immunodeficiency: a family study. *Clin. Exp. Immunol.* **79**, 1-6.

Prieto, J., Qian, C., Garcia, N., Diez, J., and Medina, J.F. (1993). Abnormal expression of anion exchanger genes in primary biliary cirrhosis. *Gastroenterology* **105**, 572-578.

Quaranta, S., Shulman, H., Paganin, S., Shoenfeld, Y., Ahmed, A., Peter, J., Leung, P.S.C., Van de Water, J., Coppel, R., Östlund, C., Worman, H.J., Rizzetto, M., Tsuneyama, K., McDonald, G.B., Rosina, F., and Gershwin, M.E. (1998). Is GVHD a model of PBC? Characterization of autoantibodies in GVHD. Abstract *Hepatology* **Vol. 28**, No. 4, Part 2, p541A, 1516.

Que, F.G., Phan, V.A., Phan, V.H., LaRusso, N.F., and Gores, G.J. (1999). GUDC inhibits cytochrome c release from human cholangiocyte mitochondria. *J. Surg. Res.* **83**, 100-105.

Rees, R.C., and Parry, H. (1992). Macrophages in tumour immunity in *The Macrophage: The Natural Immune System*. Edited by Lewis, C.E., and McGee, J.O.D. Oxford University Press, New York. Chpt. 8.

Reiner, N.E. (1994). Altered cell signaling and mononuclear phagocyte deactivation during intracellular infection. *Immunology Today* **15**, 374-381.

Rhoades, K.L., Cai, S., Golub, S.H., and Economou, J.S. (1995). Granulocyte-macrophage colony-stimulating factor and interleukin-4 differentially regulate the human tumor necrosis factor-α promoter region. *Cell. Immunol.* **161**, 125-131.

Rodrigues, V., Cheah, P.Y., Ray, K., and Chia, W. (1995). Malvolio, the Drosophila homologue of mouse NRAMP-1 (Bcg) is expressed in macrophages and in the nervous system and is required for normal taste behaviour. *E.M.B.O. J.* **14**, 3007-3020.

Roger, M., Sánchez, F.O., and Schurr, E. (1998). Comparative study of the genomic organization of DNA repeats within the 5'-flanking region of the natural resistance-associated macrophage protein gene (NRAMP1) between humans and great apes. *Mamm. Genome* **9**, 435-439.

Rojas, M., Barrera, L.F., Puzo, G., and Garcia, L.F. (1997). Differential induction of apoptosis by virulent Mycobacterium tuberculosis in resistant and susceptible murine macrophages. *J. Immunol.* **159**, 1352-1361.

Rojas, M., Barrera, L.F., and García, L.F. (1998). Induction of apoptosis in murine macrophages by Mycobacterium tuberculosis is reactive oxygen intermediates-independent. *Biochem. Biophys. Res. Comm.* **247**, 436-442.

Rojas, M., Olivier, M., Gros, P., Barrera, L.F., and García, L.F. (1999). TNF-α and IL-10 modulate the induction of apoptosis by virulent Mycobacterium tuberculosis in murine macrophages. *J. Immunol.* **162**, 6122-6131.

Roos, D., Eckmann, C.M., Yazdanbakhsh, M., Hamers, M.N., and de Boer, M. (1984). Excretion of superoxide by phagocytes measured with cytochrome c entrapped in resealed erythrocyte ghosts. *J. Biol. Chem.* **259**, 1770-1775.

Rubin, E.M., Martin, A.A., Thung, S.N., and Gerber, M.A. (1995). Morphometric and immunohistochemical characterization of human liver regeneration. *Am. J. Pathol.* **147**, 397-404.

Rudi, J., Waldherr, R., Raedsch, R., and Kommerell, B. (1995). Hepatocyte proliferation in primary biliary cirrhosis as assessed by proliferating cell nuclear antigen and Ki-67 antigen labelling. *J. Hepatol.* **22**, 43-49.

Rupprecht, A.P., and Coleman, D.L. (1991). Transfection of adherent murine peritoneal macrophages with a reporter gene using DEAE-dextran. *J. Immunol. Methods* **144**, 157-163.

Sadick, M.D. (1992). Macrophages in parasitic infection in *The Macrophage: The Natural Immune System.* Edited by Lewis, C.E., and McGee, J.O.D. Oxford University Press, Newe York. Chpt. 6.

Saibara, T., Maeda, T., Sakaeda, H., Okino, M., Onishi, S., and Ito, K. (1984). Interleukin 1 activity in primary biliary cirrhosis. Abstract (article in Japanese) *Acta Hepatol. Jpn.* **25**, 62-66.

Sakisaka, S., Koga, H., Sasatomi, K., Mimura, Y., Kawaguchi, T., and Tanikawa, K. (1997). Biliary secretion of endotoxin and pathogenesis of primary biliary cirrhosis. *Yale J. Biol. Med.* **70**, 403-408.

Sambrook, J., Fritsch, E.F., and Maniatis, T. (1989). *Molecular Cloning. A Laboratory Manual.* Second Edition. Edited by Ford, N., Nolan, C., and Ferguson, M.. Cold Spring Harbour Labortory Press, New York.

Santrach, P.J., Moore, S.B., Gores, G.J., and Dickson, E.R. (1990). Role of HLA-DRw8 in primary biliary cirrhosis (PBC): analysis by restriction fragment length polymorphism (RFLP). Abstract *Hepatology* **Vol. 112**, p938, 404.

Scheuer, P.J. (1988). *Liver Biopsy Interpretation.* Fourth Edition. Baillière Tindall, London. Chpt. 5.

Schmidt, D.M., and Ernst, J.D. (1996). Subcellular localization of the human NRAMP1 gene product. Abstract *Mol. Biol. Cell* **Vol.** 7,Supp., p152a, 883.

Schurr, E., Skamene, E., Forget, A., and Gros, P. (1989). Linkage analysis of the Bcg gene on mouse chromosome 1. Identification of a tightly linked marker. *J. Immunol.* **142**, 4507-4513.

Searle, S., and Blackwell, J.M. (1999). Evidence for a functional repeat polymorphism in the promoter of the human NRAMP1 gene that correlates with autoimmune versus infectious disease susceptibility. *J. Med. Genet.* **36**, 295-299.

Seki, T., Kiyosawa, K., Ota, M., Furuta, A., Fukushima, H., Tanaka, E., Yoshizawa, K., Kumagai, T., Mizuki, N., Ando, A., and Inoko, H. (1993). Association of primary biliary cirrhosis with human leukocyte antigen DPB1*0501 in Japanese patients. *Hepatology* **18**, 73-78.

Selvakumaran, M., Lin, H.K., Miyashita, T., Wang, H.G., Krajewski, S., Reed, J.C., Hoffman, B., and Liebermann, D. (1994). Immediate early up-regulation of bax expression by p53 but not TGFβ1: a paradigm for distinct apoptotic pathways. *Oncogene* **9**, 1791-1798.

Shaw, B. (1947) The Doctor's Dilemma in *The Doctor's Dilemma, Getting Married, and The Shewing-Up of Blanco Posnet*. Constable and Company Ltd., London. Act I, p102.

Shaw, M.A., Clayton, D., Atkinson, S.E., Williams, H., Miller, N., Sibthorpe, D., and Blackwell, J.M. (1996). Linkage of rheumatoid arthritis to the candidate gene NRAMP1 on 2q35. *J. Med. Genet.* **33**, 672-677.

Shaw, M.A., Clayton, D., and Blackwell, J.M. (1997). Analysis of the candidate gene NRAMP1 in the first 61 ARC National Repository Families for rheumatoid arthritis. *J. Rheumatol.* **24**, 212-214.

Shindo, M., Mullin, G.E., Braun-Elwert, L., Bergasa, N.V., Jones, E.A., and James, S.P. (1996). Cytokine mRNA expression in the liver of patients with primary biliary cirrhosis (PBC) and chronic hepatitis B (CHB). *Clin. Exp. Immunol.* **105**, 254-259.

Shulman, H.M., Sharma, P., Amos, D., Fenster, L.F., and McDonald, G.B. (1988). A coded histologic study of hepatic graft-versus-host disease after human bone marrow transplantation. *Hepatology* **8**, 463-470.

Si, L., Whiteside, T.L., Schade, R.R., Starzl, T.E., and Van Thiel, D.H. (1984). T-lymphocyte subsets in liver tissues of patients with primary biliary cirrhosis (PBC), patients with primary sclerosing cholangitis (PSC), and normal controls. *J. Clin. Immunol.* **4**, 262-272.

Sipos, P., Guldutuna, S., Leuschner, U., and Vallent, K. (1995). Comparitive study of superoxide production of monocytes in primary biliary cirrhosis. Abstract (article in Hungarian) *Orv. Hetil.* **136**, 2389-2392.

Sírová, M., Hovorka, O., Říha, I., Říhová, B., Baudyš, M., Kim, S.W., and Skamene, E. (1997). The in vivo antibody response against exogenous antigens is not influenced by the mouse Bcg (nramp1) gene. *Immunology* **90**, 626-631.

Skamene E., Gros, P., Forget, A., Kongshavn, P.A.L., St Charles, C., and Taylor, B.A. (1982). Genetic regulation of resistance to intracellular pathogens. *Nature* **297**, 506-509.

Skamene, E., Schurr, E., and Gros, P. (1998). Infection genomics: nramp1 as a major determinant of natural resistance to intracellular infections. *Annu. Rev. Med.* **49**, 275-287.

Smyth, M.J., and Trapani, J.A. (1995). Granzymes: exogenous proteinases that induce target cell apoptosis. *Immunol. Today.* **16**, 202-206.

Sonnenberg, A., Modderman. P.W., and Hogervost, F. (1988). Laminin receptor on platelets is the integrin VLA-6. *Nature* **336**, 487-489.

Soo, S.S., Villarreal-Ramos, B., Khan, C.M.A., Hormaeche, C.E., and Blackwell, J.M. (1998). Genetic control of immune response to recombinant antigens carried by an attenuated Salmonella typhimurium vaccine strain: nramp1 influences T-helper subset responses and protection against leishmanial challenge. *Infect. Immun.* **66**, 1910-1917.

Speert, D.P. (1992). Macrophages in bacterial infection in *The Macrophage: The Natural Immune System.* Edited by Lewis, C.E., and McGee, J.O.D. Oxford University Press, New York. Chpt. 5.

Spengler, U., Pape, G.R., Hoffmann, R.M., Johnson, J.P., Eisenburg, J., Paumgartner, G., and Riethmüller, G. (1988). Differential expression of MHC class II subregion products on bile duct epithelial cells and hepatocytes in patients with primary biliary cirrhosis. *Hepatology* **8**, 459-462.

Spengler, U., Messer, G, Jung, M.C., Honold, G., Weiss, E.H., Paumgartner, G., Riethmüller, G., and Pape, G.R. (1990). Analysis of the Nco1 polymorphism of the TNF locus in patients with primary biliary cirrhosis. Abstract *Hepatology* **Vol. 12**, No. 4, Part 2, p842, 19.

Spengler, U., Möller, A., Jung, M.C., Messer, G., Zachoval, R., Hoffmann, R.M., Eisenburg, J., Paumgartner, G., Riethmüller, G., Weiss, E.H., and Pape, G.R. (1992). T lymphocytes from patients with primary biliary cirrhosis produce reduced amounts of lymphotoxin, tumour necrosis factor and interferon-γ upon mitogen stimulation. *J. Hepatol.* **15**, 129-135.

Spengler, U., Leifeld, L., Braunschweiger, I., Dumoulin, F.L., Lechmann, M., and Sauerbruch, T. (1997). Anomalous expression of costimulatory molecules B7-1, B7-2 and CD28 in primary biliary cirrhosis. *J. Hepatol.* **26**, 31-36.

Stemerowicz, R., Hopf, U., Möller, B., Wittenbrink, C., Rodloff, A., Reinhardt, R., Freudenberg, M., and Galanos, C. (1988). Are mitochondrial antibodies in primary biliary cirrhosis induced by R(rough)-mutants of enterobacteriaceae? *Lancet* **2**, 1166-1170.

Stewart, J.J. (1998). The female X-inactivation mosaic in systemic lupus erythematosus. *Immun. Today* **19**, 352-357.

Stokkers, P.C.F., Reitsma, P.H., Tytgat, G.N.J., and van Deventer, S.J.H. (1997). A polymorphism in the NRAMP1 gene in relation to IBD. Abstract *Gastroenterology* **Vol. 112**, No. 4, pA1097.

Strasser, A. (1995). Life and death during lymphocyte development and function: evidence for two distinct killing mechanisms. *Curr. Opin. Immunol.* **7**, 228-234.

Strasser, A., and Newton, K. (1999). FADD/MORT1, a signal transducer that can promote cell death or cell growth. *Int. J. Biochem. Cell Biol.* **31**, 533-537.

Suarez, N., Walum, E., and Eriksson, H. (1995). Cellular neurotoxicity of trivalent manganese bound to transferrin or pyrophosphate studied in human neuroblastoma (SH-SY5Y) cell cultures. *Toxic. in Vitro* **9**, 717-721.

Supek, F., Supekova, L., Nelson, H., and Nelson, N. (1996). A yeast manganese transporter related to the macrophage protein involved in conferring resistance to mycobacteria. *Proc. Natl. Acad. Sci. USA* **93**, 5105-5110.

Supek, F., Supekova, L., Nelson, H., and Nelson, N. (1997). Function of metal-ion homeostasis in the cell division cycle, mitochondrial protein processing, sensitivity to mycobacterial infection and brain function. *J. Exp. Biol.* **200**, 321-330.

Takahashi, T., Tanaka, M., Inazawa, J., Abe, T., Suda, T., and Nagata, S. (1994). Human Fas ligand: gene structure, chromosomal location and species specificity. *Int. Immunol.* **6**, 1567-1574.

Takeda, A., Ishiwatari, S., and Okada, S. (1999). Manganese uptake into rat brain during development and aging. *J. Neurosci. Res.* **56**, 93-98.

Takezawa, J., and Yamada, S. (1984). Morphological studies on bile duct lesions in primary biliary cirrhosis - clinicopathological significance of granulomas. Abstract (article in Japanese) *Acta Hepatol. Jpn.* **25**, 1131-1136.

Tanaka, A., Quaranta, S., Rosina, F., and Gershwin, M.E. (1998). Polymorphism of the tumor necrosis factor-α promoter region in patients with primary biliary cirrhosis. Abstract *Hepatology* **Vol. 28**, No. 4, Part 2, p190A, 109.

Tanaka, A., Quaranta, S., Mattalia, A., Coppel, R., Rosina, F., Manns, M., and Gershwin, M.E. (1999). The tumor necrosis factor-α promoter correlates with progression of primary biliary cirrhosis. *J. Hepatol.* **30**, 826-829.

te Velde, A.A. (1994). Interaction between cytokines and monocytes/macrophages in *Immunopharmacology of Macrophages and Other Antigen-Presenting Cells.* Edited by Bruijnzeel-Koomen, C.A.F.M., and Hoefsmit, E.C.M. Academic Press, London. p13.

Thepen, T., and Havenith, C.E.G. (1994). Function of Alveolar Macrophages in *Immunopharmacology of Macrophages and Other Antigen-Presenting Cells.* Edited by Bruijnzeel-Koomen, C.A.F.M., and Hoefsmit, E.C.M. Academic Press, London. Chpt. 3.

Thompson, K., Millward-Sadler, H., and Sheron, N. (1998). Nramp deficient mice develop increased fibrosis in a carbon tetrachloride induced model. Abstract *Hepatology* **Vol. 28**, No. 4, Part 2, p188A, 102.

Thornberry, N.A., and Lazebnik, Y. (1998). Caspases: enemies within. *Science* **281**, 1312-1316.

Tokuraku, K., Nakagawa, H., Kishi, F., and Kotani, S. (1998). Human natural resistance-associated macrophage protein is a new type of microtubule-associated protein. *F.E.B.S. Lett.* **428**, 63-67.

Tovey, M.G., Gugenheim, J., Guymarho, J., Blanchard, B., Vanden Broecke, C., Gresser, I., Bismuth, H., and Reynes, M. (1991). Genes for interleukin-1, interleukin-6, and tumor necrosis factor are expressed at markedly reduced levels in the livers of patients with severe liver disease. *Autoimmunity* **10**, 297-310.

Trauth, B,C., Klas, C., Peters, A.M., Matzku, S., Moller, P., Falk, W., Debatin, K.M., and Krammer, P.H. (1989). Monoclonal antibody-mediated tumor regression by induction of apoptosis. *Science* **245**, 301-305.

Triger, D.R. (1980). Primary biliary cirrhosis: an epidemiological study. *B.M.J.* **281**, 772-775.

Tsuji, K., Watanabe, Y., Aisaka, Y., Masanaga, T., Kamiyasu, M., Kitamoto, M., Nakanishi, T., and Kajiyama, G. (1997). Detection of gp120 autoantibodies in primary biliary cirrhosis by an enzyme linked immunosorbent assay using a synthetic polypeptide. Abstract *Gastroenterology* **Vol. 112**, No. 4, pA1404.

Tsuneyama, K., Van de Water, J., Leung, P.S.C., Cha, S., Nakanuma, Y., Kaplan, M., De Lellis, R., Coppel, R., Ansari, A., and Gershwin, M.E. (1995a). Abnormal expression of the E2 component of the pyruvate dehydrogenase complex on the luminal surface of biliary epithelium occurs before major histocompatibility complex class II and BB1/B7 expression. *Hepatology* **21**, 1031-1037.

Tsuneyama, K., Van de Water, J., Van Thiel, D., Coppel, R., Ruebner, B., Nakanuma, Y., Dickson, E.R., and Gershwin, M.E. (1995b). Abnormal expression of PDC-E_2 on the apical surface of biliary epithelial cells in patients with antimitochondrial antibody-negative primary biliary cirrhosis. *Hepatology* **22**, 1440-1446.

Tsuneyama, K., Van de Water, J., Yamazaki, K., Suzuki, K., Sato, S., Takeda, Y., Ruebner, B., Yost, B.A., Nakanuma, Y., Coppel, R.L., and Gershwin, M.E. (1997). Primary biliary cirrhosis an epithelitis: evidence of abnormal salivary gland immunohistochemistry. *Autoimmunity* **26**, 23-31.

Tsuneyama, K., Yasoshima, M., Harada, K., Hiramatsu, K., Gershwin, M.E., and Nakanuma, Y. (1998). Increased CD1d expression on small bile duct epithelium and epithelioid granuloma in livers in primary biliary cirrhosis. *Hepatology* **28**, 620-623.

Underhill, J., Donaldson, P., Bray, G., Doherty, D., Portmann, B., and Williams, R. (1992). Susceptibility to primary biliary cirrhosis is associated with the HLA-DR8-DQB1*0402 haplotype. *Hepatology* **16**, 1404-1408.

Underhill, J.A., Donaldson, P.T., Doherty, D.G., Manabe, K., and Williams, R. (1995). HLA DPB polymorphism in primary sclerosing cholangitis and primary biliary cirrhosis. *Hepatology* **21**, 959-962.

Unkles, S.E., Hawker, K.L., Grieve, C., Campbell, E.I., Montague, P., and Kinghorn, J.R. (1991). crnA encodes a nitrate transporter in Aspergillus nidulans. *Proc. Natl. Acad. Sci. USA* **88**, 204-208.

Utili, R., Abernathy, C.O., and Zimmerman, H.J. (1976). Cholestatic effects of Escherichia coli endotoxin on the isolated perfused rat liver. *Gastroenterol.* **70**, 248-253.

Van de Water, J., Turchany, J., Leung, P.S.C., Lake, J., Munoz, S., Surh, C.D., Coppel, R., Ansari, A., Nakanuma, Y., and Gershwin, M.E. (1993). Molecular mimicry in primary biliary cirrhosis. Evidence for biliary epithelial expression of a molecule cross-reactive with pyruvate dehydrogenase complex-E2. *J. Clin. Invest.* **91**, 2653-2664.

Van de Water, J., Ansari, A., Prindiville, T., Coppel, R.L., Ricalton, N., Kotzin, B.L., Liu, S., Roche, T.E., Krams, S.M., Munoz, S., and Gershwin, M.E. (1995). Heterogeneity of autoreactive T cell clones specific for the E2 component of the pyruvate dehydrogenase complex in prmary biliary cirrhosis. *J. Exp. Med.* **181**, 723-733.

Van de Water, J., Gerson, L.B., Ferrell, L.D., Lake, J.R., Coppel, R.L., Batts, K.P., Wiesner, R.H., and Gershwin, M.E. (1996). Immunohistochemical evidence of disease recurrence after liver transplantation for primary biliary cirrhosis. *Hepatology* **24**, 1079-1084.

Van de Water, J., Shimoda, S., Niho, Y., Coppel, R., Ansari, A., and Gershwin, M.E. (1997). The role of T cells in primary biliary cirhosis. *Semin. Liver Dis.* **17**, 105-113.

Van Eyken, P., Sciot, R., Callea, F., Van Der Steen, K., Moerman, P., and Desmet, V.J. (1988). The development of the intrahepatic bile ducts in man: a keratin-immunohistochemical study. *Hepatology* **8**, 1586-1595.

van Furth, R., Cohn, Z.A., Hirsch, J.G., Humphrey, J.H., Spector, W.G. and Langevoort, H.L. (1972). The mononuclear phagocyte system: a new classification of macrophages, monocytes and their precursor cells. *Bull. W.H.O.* **46**, 845-852.

Van Regenmortal, M.H.V, Briand, J.P., Muller, S., and Plaué, S. (1988). Synthetic peptides as antigens in *Laboratory Techniques in Biochemistry and Molecular Biology*. Elsevier, Amsterdam. Page103.

Vassiloyanakopoulos, A.P., Okamoto, S., and Fierer, J. (1998). The crucial role of polymorphonuclear leukocytes in resistance to Salmonella dublin infections in genetically susceptible and resistant mice. *Proc. Natl. Acad. Sci. USA* **95**, 7676-7681.

Vidal, S.M., Malo, D., Vogan, K., Skamene, E., and Gros, P. (1993). Natural resistance to infection with intracellular parasites: isolation of a candidate for Bcg. *Cell* **73**, 469-485.

Vidal, S., Gros, P., and Skamene, E. (1995a). Natural resistance to infection with intracellular parasites: molecular genetics identifies nramp1 as the Bcg/Ity/Lsh locus. *J. Leuk. Biol.* **58**, 382-390.

Vidal, S., Tremblay, M.L., Govoni, G., Gauthier, S., Sebastiani, G., Malo, D., Skamene, E., Olivier, M., Jothy, S., and Gros, P. (1995b). The Ity/Lsh/Bcg locus: natural resistance to infection with intracellular parasites is abrogated by disruption of the nramp1 gene. *J. Exp. Med.* **182**, 655-666.

Vidal, S.M., Pinner, E.H., Lepage, P., Gauthier, S., and Gros, P. (1996). Natural resistance to intracellular infections. Nramp1 encodes a membrane phosphoglycoprotein absent in macrophages from susceptible (nramp1^{D169}) mouse strains. *J. Immunol.* **157**, 3559-3568.

Vierling, J.M., Nelson, D.L., Strober, W., Bundy, B.M., and Jones, E.A. (1977). In vitro cell-mediated cytotoxicity in primary biliary cirrhosis and chronic hepatitis. *J. Clin. Invest.* **60**, 1116-1128.

Vilagut, L., Vila, J., Viñas, O., Parés , A., Ginés, A, Jiménez de Anta, M.T., and Rodés, J. (1994a). Cross-reactivity of anti-Mycobacterium gordonae antibodies with the major mitochondrial autoantigens in primary biliary cirrhosis. *J. Hepatol.* **21**, 673-677.

Vilagut, L., Vila, J., Parés, A., Viñas, O., Ginés, A., Bruguera, M., Jimènez de Anta, M.T., and Rodés, J. (1994b). Mycobacterium gordonae DNA in liver tissue of patients with primary biliary cirrhosis. Abstract *J. Hepatology* **Vol. 21**, Supp. 1, pS87, P2C11/240.

Vladutiu, A.O. (1995). Role of nitric oxide in autoimmunity. *Clin. Immunol. Immunopathol.* **76**, 1-11.

Vulpe, C., and Gitschier, J. (1997). Ironing out anaemia. *Nat. Genet.* **16**, 319-320.

Wang, C.H., and Tschen, S.Y. (1997). Hepatitis E virus and primary biliary cirrhosis. *Q. J. M.* **90**, 154-155.

Wardlaw, A.C., (1992). *Practical statistics for experimental biologists.* John Wiley and Sons, Chichester UK. **Chapter 6**.

Watson, R.G.P., Angus, P.W., Dewar, M., Goss, B., Sewell, R.B., Smallwood, R.A., and the Melbourne Liver Group (1995). Low prevalence of primary biliary cirrhosis in Victoria, Australia. *Gut* **36**, 927-930.

Watson, A. (1999). The role of Fas in apoptosis induced by anticancer drugs. *Hepatology* **29**, 280-281.

Watt, F.E., Grove, J., Daly, A.K., Day, C.P., Bassendine, M.F., and Jones, D.E.J. (1997). Tumour necrosis factor -308 polymorphism and disease progression in primary biliary cirrhosis. *Gastroenterology* **Vol. 112**, No. 4, pA1414.

Weiss, S.J. (1986). Oxygen, ischemia and inflammation. *Acta Physiol. Scand.* **Vol. 126**, Supp. 548, 9-37.

West, A.H., Clark, D.J., Martin, J., Neupert, W., Hartl, F.U., and Horwich, A.L. (1992). Two related genes encoding extremely hydrophobic proteins suppress a lethal mutation in the yeast mitochondrial processing enhancing protein. *J. Biol. Chem.* **267**, 24625-24633.

Williams, M.S., Noguchi, S., Henkart, P.A., and Osawa, Y. (1998). Nitric oxide synthase plays a signaling role in TCR-triggered apoptotic death. *J. Immunol.* **161**, 6526-6531.

Woska Jr., J.R., Morelock, M.M., Jeanfavre, D.D., Caviness, G.O., Bormann, B.J., and Rothlein, R. (1998). Molecular comparison of soluble intercellular adhesion molecule (sICAM)-1 and sICAM-3 binding to lymphocyte function-associated antigen-1. *J. Biol.Chem.* **273**, 4725-4733.

Wright, S.D., Ramos, R.A., Tobias, P.S., Ulevitch, R.J., and Mathison, J.C. (1990). CD14, a receptor for complexes of lipopolysaccharide (LPS) and LPS binding protein. *Science* **249**, 1431-1433.

Wyllie, A.H. (1994). Death gets a brake. *Nature* **369**, 272-273.

Yamamoto, K., Akbar, S.M.F., Abe, M., Masumoto, T., Michitaka, K., Horiike, N., and Onji, M. (1998a). Dysfunction of antigen presenting dendritic cells in primary biliary cirrhosis; role of nitric oxide. Abstract *Hepatology* **Vol. 28**, No. 4, Part 2, p189A, 107.

Yamamoto, K., Akbar, F., Masumoto, T., and Onji, M. (1998b). Increased nitric oxide (NO) production by antigen-presenting dendritic cells is responsible for low allogeneic mixed leucocyte reaction (MLR) in primary biliary cirrhosis. *Clin. Exp. Immunol.* **114**, 94-101.

Yamazaki, M., Yasui, K., Kawai, H., Miyagawa, Y., Komiyama, A., and Akabane, T. (1984). A monocyte disorder in siblings with chronic candidiasis. A combined abnormality of monocyte mobility and phagocytosis-killing ability. *Am. J. Dis. Child.* **138**, 192-196.

Yamazaki, K., Nakadate, I., Suzuki, K., Sato, S., and Masuda, T. (1996). Eosinophilia in primary biliary cirrhosis. *Am. J. Gastroenterol.* **91**, 516-522.

Yamazaki, K., Gleich, G.J., and Kita, H. (1998). Bile acids activate eosinophils in vitro. Abstract *Hepatology* **Vol. 28**, No. 4, Part 2, p542A, 1519.

Yasoshima, M., Kono, N., Sugawara, H., Katayanagi, K., Harada, K., and Nakanuma, Y. (1998). Increased expression of interleukin-6 and tumor necrosis factor-α in pathologic biliary epithelial cells: in situ and culture study. *Lab. Invest.* **78**, 89-100.

Yonehara, S., Ishii, A., and Yonehara, M. (1989). A cell-killing monoclonal antibody (anti-Fas) to a cell surface antigen co-downregulated with the receptor of tumor necrosis factor. *J. Exp. Med.* **169**, 1747-1756.

Yoshida, T, and Kishi, F. (1997). Expression of NRAMP1 molecule in human peripheral blood leukocytes. *Immunol. Lett.* **55**, 105-108.

Yunoue, K., Nomoto, M., and Ichida, F. (1984). Histological observation on granulomas in liver. Abstract (article in Japanese) *Acta Hepatol. Jpn.* **25**, 779-787.

Zappala, F., Grove, J., Watt, F.E., Daly, A.K., Day, C.P., Bassendine, M.F., and Jones, D.E.J. (1998). No evidence for involvement of the interleukin-10 -592 promoter polymorphism in genetic susceptibility to primary biliary cirrhosis. *J. Hepatol.* **28**, 820-823.

Zhang, L., Weetman, A.P., Bassendine, M., and Oliveira, D.B.G. (1994a). Major histocompatibility complex class-II alleles in primary biliary cirrhosis. *Scand. J. Immunol.* **39**, 104-106.

Zhang, D.E., Hetherington, C.J., Gonzalez, D.A., Chen, H.M., and Tenen, D.G. (1994b). Regulation of CD14 expression during monocytic differentiation induced with 1α,25-dihydroxyvitamin D3. *J. Immunol.* **153**, 3276-3284.

Ziegler-Heitbrock, H.W.L., Thiel, E., Fütterer, A., Herzog, V., Wirtz, A., and Riethmüller, G. (1988). Establishment of a human cell line (Mono Mac 6) with characteristics of mature monocytes. *Int. J. Cancer* **41**, 456-461.

Zoller, H., Pietrangelo, A., Vogel, W., and Weiss, G. (1999). Duodenal metal-transporter (DMT-1, NRAMP-2) expression in patients with hereditary haemochromatosis. *Lancet* **353**, 2120-2123.

Zwilling, B.S., Kuhn, D.E., Wikoff, L., Brown, D., and Lafuse, W. (1999). Role of iron in nramp1-mediated inhibition of mycobacterial growth. *Infect. Immun.* **67**, 1386-1392.

9 APPENDIX A

9.1 Diagnosis of the first 227 orthotopic liver transplantation patients performed at the Scottish Liver Transplantation Unit.

Diagnosis	Total
Primary biliary cirrhosis	63
Alcoholic liver disease	33
Primary sclerosing cholangitis	22
Paracetamol overdose	22
Cryptogenic cirrhosis	14
Non AB	11
Hepatic artery thrombosis	9
Chronic rejection	9
Chronic active hepatitis	8
Primary Graft Non Function	8
Hepatitis B	5
Hepatitis C	5
Secondary biliary cirrhosis	3
Unknown cause	2
Budd Chari	2
Idiosyncratic drug reaction	2
Hepatitis A	1
Hepatoma	1
Haemangio endelthioma	1
Wilson's disease	1
Recurrent cholangitis	1
Recurrent granulomatos	1
Hepatic necrosis	1
Hepatic cell carcinoma	1
Iron overdose	1

10 APPENDIX B

10.1 Components of Solutions and Reagents

TE
10mM Tris-HCl pH 8.0
1mM EDTA

10x TBE Buffer
107.8g Tris base
7.44g EDTA
about 55.0g boric acid added until pH8.3, made up to 1litre with dH_2O

10x TBS for Immunohistochemistry
500ml 0.5M Tris pH to 7.6
Make up to 2 litres with dH_2O

Normal Saline
42.5g NaCl in 5 litres

1x TBS for Immunohistochemistry
100ml 10x TBS for Immunohistochemistry
90ml normal saline

10x TBS for Western Blotting
60g Tris base
90g NaCl
pH to 7.9, made up to 1litre with dH_2O

ABComplex Buffer
0.05M Tris-HCl pH7.6

ABComplex-HRP (DAKO, Cambridge UK)
5ml ABComplex buffer
1 drop of reagent A
1 drop reagent B
Mix well, prepare at least 30 minutes before use

ABComplex-AP (DAKO, Cambridge UK)
5ml ABComplex buffer
1 drop of reagent A
1 drop reagent B
Mix well, prepare at least 30 minutes before use

DAB (3,3'diaminobenzidine) Buffer
24ml 0.2M Tris
38ml 0.1N HCl
38ml dH_20
0.0681g imidazole
pH to 7.6

AP Buffer
0.1M Tris pH8.2

Scott's Tap Water Substitute
2g potassium carbonate
20g magnesium sulphate
made up to 1 litre in dH_2O

0.2M Phosphate Buffer pH7.3
5.6ml 0.4M sodium di-hydrogen phosphate (NaH_2PO_4-H_2O)
14.4ml 0.4M di-sodium hydrogen phosphate (Na_2HPO_4-$2H_20$)
pH to 7.3, make up to 400ml with dH_2O.

Coomasie Blue Staining Mixture
Dissolve 0.25g Coomasie blue in 10% methanol (Merck, Lutterworth UK)/7% acetic acid (Fisher Scientific, Loughborough UK) in a final volume of 100ml.

Destain Mixture
10% methanol (Merck, Lutterworth UK)
7% acetic acid (Fisher Scientific, Loughborough UK)

Protein Lysis Buffer
300mM NaCl
50mM Tris-HCl
0.5% Triton X-100
made up to 100ml with dH_2O
The following anti-proteases were added to 1ml to give a final concntration of:
1mM PMSF (phenyl methyl sulphonyl fluoride)
10μg/ml leupeptin
10μg/ml aprotinin
1.8mg/ml iodoacetamide

Stacking Gel Buffer
30.25g Tris base
2.5g SDS
pH to 6.8, made up to 500ml with dH_2O

Separating Gel Buffer
90.8g Tris base
2.5g SDS
pH to 8.8, made up to 500ml with dH_2O

10x Running Buffer
120.1g Tris base
80g glycine
20g SDS
made up to 2 litres with dH_2O

12% Separating Gel
11.1ml 30% acrylamide (Flowgen, Lichfield UK)
9.25ml separating gel buffer
2ml 1% ammonium persulphate
20µl TEMED
14.7ml dH_2O

4.5% Stacking Gel
1.5ml 30% acrylamide (Flowgen,Lichfield UK)
2.5ml stacking gel buffer
300µl 1% ammonium persulphate
10µl TEMED
5.7ml dH_2O

Sample Buffer
10ml stacking gel buffer
2g SDS
5ml 2-mercaptoethanol
10ml glycerol (Fisher Scientific, Loughborough UK)
5mg bromophenol blue
made up to 100ml with dH_2O

TBST
500µl Tween 20 in 1litre of 1x TBS

Blocking Solution
3g Marvel low fat dried milk
100ml TBST

Alkaline Carbonate Stock Solution
20g sodium carbonate
4g NaOH

Alkaline Carbonate Working Solution
5ml 1% copper sulphate
5ml 2% sodium potassium tartrate
490ml alkaline carbonate stock solution

Folin-coicalteau reagent
Dilute 1:1 with dH_2O before use

Transfer Buffer
35.8g di-sodium hydrogen phosphate
4l dH_2O
1l methanol (Merck, Lutterworth UK)
Make up fresh before use

NBT/BCIP Chromogen Substrate
66µl NBT stock (50mg NBT in 1ml 70% dimethylformamide)
33µl BCIP stock (50mg BCIP in 1ml 100% dimethylformamide
990µl AP buffer

TMB Buffer
25.7ml 0.2M di-sodium hydrogen phosphate (Na_2HPO_4-$2H_20$)
24.3ml 0.1M citric acid
50.0ml dH_2O
pH to 5

TMB Chromogen Substrate
1 TMB tablet
10ml TMB buffer
2µl 30% H_2O_2

OPD Buffer
25.7ml 0.2M di-sodium hydrogen phosphate (Na_2HPO_4-$2H_20$)
24.3ml 0.1M citric acid
50.0ml dH_2O
pH to 5

OPD Chromogen Substrate
1 OPD tablet
10ml OPD buffer
4µl 30% H_2O_2

6% Denaturing Polyacrylamide Gel
47.25g urea
54.375ml Milli-Q dH_2O
5.625ml 10x TBE
16.875ml 40% acrylamide/bis (19:1)
75µl TEMED
750µl 10% APS

3x Acrylamide Gel Loading Solution
10mM NaOH
95% formamide
0.05% bromophenol blue
0.05% xylene cyanol FF

GMEM
10ml of 10x stock GMEM (Life Technologies, Paisley UK) was diluted in 90ml sterile dH_2O.
3.7ml stock sodium bicarbonate solution was added to buffer the medium.
Filter sterilised before use.

Supplemented RPMI-1640 Medium
Unless stated otherwise RPMI-1640 medium was used for tissue culture experiments supplemented with:
100U/ml penicillin
100µg/ml streptomycin
2mM L-glutamine
10% FCS
All purchased from Life Technologies, Paisley UK

Heat Treated NHS
Normal human serum was obtained from the Scottish National Blood Transfusion Service and heated for 1 hour at 56°C to inactivate complement components.

Crystal Violet
2% acetic acid (Fisher Scientific, Loughborough UK) coloured pale violet with gentian violet.

Dense BSA
3.72ml PBS
0.58ml 1N NaOH (0.574g NaOH in 14.35ml dH_2O)
1.3ml dH_2O
2.12g BSA was poured carefully onto the top of the PBS/NaOH/dH_2O in a 25ml beaker which was covered with foil and left overnight to dissolve. The mixture was swirled gently then centrifuged for 5 minutes at 300g to ensure all the BSA was in solution.
Filter sterilised before use and stored at 4°C.

X-Gal Stain
20mM sodium di-hydrogen phosphate (NaH_2PO_4)
80mM di-sodium hydrogen phosphate (Na_2HPO_4)
3mM $K_3Fe(CN)_6$
3mM $K_4Fe(CN)_6$
1mg/ml X-Gal (Promega, Southampton UK)
1M $MgCl_2$
Prepared in dH_2O
Filtered prior to use.

DEPC Treated dH_2O
1ml DEPC in 1 litre dH_2O left overnight then autoclaved.

10x Ligation Buffer (Promega, Southampton UK)
300mM Tris-HCl pH7.8
100mM $MgCl_2$
100mM DTT
10mM dATP

L-Broth
10g NaCl
10g Bacto-tryptone (Becton Dickinson UK Ltd., Oxford UK)
5g Bacto-yeast extract (Becton Dickinson UK Ltd., Oxford UK)
pH to 7.5 with 5N NaOH made up to 1 litre with dH_20, autoclaved

L-Amp plates
7.5g Bacto agar (Becton Dickinson UK Ltd., Oxford UK)
500ml L-broth
autoclaved and cooled to 50°C, 50μg/ml ampicillin added, poured into Petri dishes and allowed to set

SOC Medium
20g Bacto-tryptone (Becton Dickinson UK Ltd., Oxford UK)
5g Bacto-yeast extract (Becton Dickinson UK Ltd., Oxford UK)
0.5g NaCl
made up to 1 litre with dH_2O, autoclaved
prior to use add 10ml 1M $MgCl_2$
10ml 1 M $MgSO_4$
10ml 2M glucose solution
Filter sterilise before use

Sequenase PCR Product Sequencing Kit (Amersham Pharmacia Biotech, Little Chalfont UK) contained:

Exonuclease
10U/μl in 20mM Tris-HCl pH7.5, 5mM 2-mercaptoethanol, 50% glycerol

SAP
2U/µl in 25mM Tris-HCl pH 7.6, 1mM $MgCl_2$, 0.1mM $ZnCl_2$, 50% glycerol

Sequenase Version 2.0 DNA Polymerase
1.6U/ µl with inorganic pyrophosphatase (2U/ml) in 20mM Tris-HCl pH7.5, 2mM DTT, 0.1mM EDTA, 50% glycerol

Sequenase Reaction Buffer
200mM Tris-HCl pH 7.5
100mM $MgCl_2$
250mM NaCl

Termination Mixes for dGTP
ddG Termination Mix
80µM dGTP
80µM dATP
80µM dCTP
80µM dTTP
8µM ddGTP
50mM NaCl

ddC, ddA and ddT Termination Mixes for dGTP
as above replacing ddGTP with ddCTP, ddATP and ddTTP.

Labeling Mix for dGTP 5x concentrate
7.5µM dGTP
7.5µM dCTP
7.5µM dTTP

Termination Mixes for 7-deaza-dGTP
ddG Termination Mix
80µM 7-deaza-dGTP
80µM dATP
80µM dCTP
80µM dTTP
8µM ddGTP
50mM NaCl

ddC, ddA and ddT Termination Mixes for 7-deaza-dGTP
as above replacing ddGTP with ddCTP, ddATP and ddTTP.

Labeling Mix for 7-deaza-dGTP 5x concentrate
7.5µM 7-deaza-dGTP
7.5µM dCTP
7.5µM dTTP

Mn Buffer
0.15M Sodium isocitrate
0.1M $MnCl_2$

Stop Solution
95% formamide
20mM EDTA
0.05% bromophenol blue
0.05% xylene cyanol FF

20x Glycerol Tolerant Gel Buffer
216g Tris base
72g taurine
4g $Na_2EDTA.2H_2O$
made up to 1 litre with dH_2O

6% Glycerol Tolerant Polyacrylamide Gel
15ml 40% acrylamide/bis (19:1)
42g urea
5ml 20x glycerol tolerant buffer
made up to 100ml with dH_2O
1ml 10% APS and 25µl added to polymerise gel immediately before pouring

6% Formamide Glycerol Tolerant Polyacrylamide Gel
15ml 40% acrylamide/bis (19:1)
42g urea
30ml deionized formamide
5ml 20x glycerol tolerant buffer
made up to 100ml with dH_2O
1ml 10% APS and 80µl added to polymerise gel immediately before pouring

T7 Sequenase version 2.0 DNA sequencing kit (Amersham Pharmacia Biotech, Little Chalfont UK)
Reagents are as for **Sequenase PCR Product Sequencing Kit** except:

T7 Sequenase Version 2.0 DNA Polymerase
13U/µl in 20mM KPO_4 pH7.4, 1mM DTT, 0.1 mMEDTA, 50% glycerol

DetectaGene Green *lacZ* Expression Kit (Cambridge Bioscience, Cambridge UK) contained:

Detectagene Green Substrate Reagent
10mM CMFDG in 1:1 (v/v) water/DMSO

Propidium Iodide
150µM propidium iodide in water

11 APPENDIX C

11.1 Sequence of phNRAMP1 (D38171) plasmid insert.

The *HindIII* and *NheI* restriction enzymes used to characterise phNRAMP1 (**5.2.2.1**) cut after base 434 and 273, respectively. *NheI* was also used to construct the whole *NRAMP1* cDNA as described in **5.2.4**. The *MscI* restriction enzyme used to clone the whole *NRAMP1* cDNA in the pCIneo plasmid cuts after base 2128.
The enzymes recognise the following sites and cut at the position shown by the vertical slash; n represents any base.

HindIII	a|agctt ttcga|a	*NheI*	g|gtagc cgatc|g
MscI	tgg|cca acc|ggt		

```
1    cgcttcagcc tgcggaagct atgggccttc acggggcctg
41   gcttcctcat gagcattgct ttcctggacc caggaaacat
81   cgagtcagat cttcaggctg gcgccgtggc gggattcaaa
121  cttctctggg tgctgctctg ggccaccgtg ttgggcttgc
161  tctgccagcg actggctgca cgtctgggcg tggtgacagg
201  caaggacttg ggcgaggtct gccatctcta ctaccctaag
241  gtgccccgca ccgtcctctg gctgaccatc gagctagcca
281  ttgtgggctc cgacatgcag gaagtcatcg gcacggccat
321  tgcattcaat ctgctctcag ctggacgaat cccactctgg
361  ggtggcgtcc tcatcaccat cgtggacacc ttcttcttcc
401  tcttcctcga taactacggg ctgcggaagc tggaagcttt
441  ttttggactc cttataacca ttatggcctt gacctttggc
481  tatgagtatg tggtggcgcg tcctgagcag ggagcgcttc
521  ttcggggcct gttcctgccc tcgtgcccgg gctgcggcca
561  ccccgagctg ctgcaggcgg tgggcattgt tggcgccatc
601  atcatgcccc acaacatcta cctgcactcg gccctggtca
641  agtctcgaga gatagaccgg gcccgccgag cggacatcag
681  agaagccaac atgtacttcc tgattgaggc caccatcgcc
721  ctgtccgtct cctttatcat caacctcttt gtcatggctg
761  tctttgggca ggccttctac cagaaaacca accaggctgc
801  gttcaacatc tgtgccaaca gcagcctcca cgactacgcc
841  aagatcttcc ccatgaacaa cgccaccgtg gccgtggaca
881  tttaccaggg gggcgtgatc ctgggctgcc tgttcggccc
921  cgcggccctc tacatctggg ccataggtct cctggcggct
961  gggcagagct ccaccatgac gggcacctac gcgggacagt
1001 tcgtgatgga gggcttcctg aggctgcggt ggtcacgctt
1041 cgcccgtgtc ctcctcaccc gctcctgcgc catcctgccc
1081 accgtgctcg tggctgtctt ccgggacctg agggacttgt
1121 cgggcctcaa tgatctgctc aacgtgctgc agagcctgct
1161 gctcccgttc gccgtgctgc ccatcctcac gttcaccagc
1201 atgcccaccc tcatgcagga gtttgccaat ggcctgctga
1241 acaaggtcgt cacctcttcc atcatggtgc tagtctgcgc
1281 catcaacctc tacttcgtgg tcagctatct gcccagcctg
1321 ccccaccctg cctacttcgg ccttgcagcc ttgctggccg
1361 cagcctacct gggcctcagc acctacctgg tctggacctg
1401 ttgccttgcc cacggagcca cctttctggc ccacagctcc
1441 caccaccact tcctgtatgg gctccttgaa gaggaccaga
1481 aaggggagac ctctggctag gcccacacca gggcctggct
```

```
1521 gggagtggca tgtatgacgt gactggcctg ctggatgtgg
1561 agggggcgcg tgcaggcagc aggatggagt gggacagttc
1601 ctgagaccag ccaacctggg ggctttaggg acctgctgtt
1641 tcctagcgca gccatgtgat taccctctgg gtctcagtgt
1681 cctcatctgt aaaatggaga cgccaccacc cttgccatgg
1721 aggttaagca ctttaacaca gtgtctggca cttgggacaa
1761 aaacaaacaa acaaacaaaa aacatttcaa aaggtattta
1801 ttgagcacct gcaggcgtga cctgacagcc caagggtggg
1841 tggggtgagg gcttgaggac ttgggcggga cacaggctcc
1881 aaactggagc ttgaaatagt gtctgatgaa tgttaaatta
1921 tctatctatc tatttattta tttatttgag acagggaaag
1961 ggtctccctc tgttgccaag gctggagtgc agtggcgcaa
2001 tcttaactca ttgcaacctc caccttctgg gttcaagcga
2041 ttctctttat tcagccccgg gagtggcgcg cgccaccacg
2081 cccagctaat ttgtgtattt tcagcagaga cggggtttgc
2121 catgctggcc aggctggtct cgaactgctg gattcaagtg
2161 atccgcccat ctccgtctcc caaagtgctg ggaattacag
2201 gcgtgagcca ccaaaacccg gcctgattaa agttaaataa
2241 atacg
```

11.2 Sequence of 5'NRAMP37 (D50403) plasmid insert.

Vector sequence at the 5' and 3' end of the *NRAMP1* sequence is shown in bold. The anchor primer used by Kishi when using the 5'-RACE method to define the extreme 5' end of *NRAMP1* is underlined. The *EcoRI* restriction enzyme used to characterise 5'NRAMP1 cuts after base 1 and 713. The *NheI* restriction enzyme used to characterise 5'NRAMP1 and construct the whole *NRAMP1* cDNA as described in **5.2.2.3** and **5.2.4** cuts after base 571.

The enzymes recognise the following sites and cut at the position shown by the vertical slash; n represents any base.

NheI g|gtagc
cgatc|g

EcoRI g|aattc
cttaa|g

```
1   gaattcggct tctggttcgg cccacctctg aaggttccag
41  aatcgatagt ggattcgcgg caccagtgcc cagagagggg
81  gtgcaggctg aggagctgcc cagagcaccg ctcacactcc
121 cagagtacct gaagtcggca tttcaatgac aggtgacaag
161 ggtccccaaa ggctaagcgg gtccagctat ggttccatct
201 ccagcccgac cagcccgacc agcccagggc cacagcaagc
241 acctcccaga gagacctacc tgagtgagaa gatccccatc
281 ccagacacaa aaccgggcac cttcagcctg cggaagctat
321 gggccttcac ggggcctggc ttcctcatga gcattgcttt
361 cctggaccca ggaaacatcg agtcagatct tcaggctggc
401 gccgtggcgg gattcaaact tctctgggtg ctgctctggg
441 ccaccgtgtt gggcttgctc tgccagcgac tggctgcacg
481 tctgggcgtg gtgacaggca aggacttggg cgaggtctgc
521 catctctact accctaaggt gccccgcacc gtcctctggc
561 tgaccatcga gctagccatt gtgggctccg acatgcagga
601 agtcatcggc acggccattg cattcaatct gctctcagct
641 ggacgaatcc cactctgggg tggcgtcctc atcaccatcg
681 tggacacctt cttcttcctc ttcctcgaag ccgaattc
```

12 APPENDIX D

12.1 Abbreviated names used for MM6 and U937 transfected clones

For clarity and simplicity when writing this thesis the MM6 and U937 transfected clones have been identified by abbreviations of the names used during laboratory work and in my laboratory books. If reference is to be made between this thesis and my books or stocks of frozen cells the full names of the clones discussed in this thesis are given below.

12.1.1 MM6 Clones Transfected with the pCIneo/NRAMP1 Plasmid

B4	A3C3,96^{1}B4
B6	A3C3,96^{1}B6
D12	A3C3,96^{2}D12
F12	A3C3,96^{1}F12

12.1.2 MM6 Clones Transfected with the pCIneo Plasmid

M/pB2	M/p4, 96^{1}B2
M/pB10	M/p4, 96^{1}B10
M/pC6	M/p4, 96^{2}C6
M/pF2	M/p6, 96^{1}F2
M/pF7	M/p4, 96^{2}F7
M/pG3	M/p4, 96^{1}G3

12.1.3 U937 Clones Transfected with the pCIneo/NRAMP1 Plasmid

2	U/N1,96^{1}E6
4	U/N1,96^{2}E10
5	U/N1,96^{4}D2
18	U/N6,96^{1}D7
27	U/N6,96^{3}B11

12.1.4 U937 Clones Transfected with the pCIneo Plasmid

39	U/p,96^{2}F9

13 LIST OF PUBLICATIONS

Graham, A.M., Dollinger, M.M., Howie, S.E.M., and Harrison, D.J. (1998). Bile duct cells in primary biliary cirrhosis are 'primed' for apoptosis. *Eur. J. Gastroenterol. Hepatol.* **10**, 553-557.

Graham, A.M., Dollinger, M.M., Howie, S.E.M., and Harrison, D.J. (in press). Identification of novel alleles at a polymorphic microsatellite repeat region in the human NRAMP1 gene promoter: analysis of allele frequency in primary biliary cirrhosis. Letter *J. Med. Genet.*

Graham, A.M., Dollinger, M.M., Howie, S.E.M., and Harrison, D.J. (1998). NRAMP1 polymorphisms in patients with liver disease. Abstract *J. Path.* **Vol. 184**, Suppl., pA36.

Dollinger, M.M., Howie, S.E.M., Plevris, J.N., Graham, A.M., Hayes, P.C., and Harrison, D.J. (1998). Intrahepatic proliferation of 'naive' and 'memory' T cells during liver allograft rejection: primary immune response within the allograft. *F.A.S.E.B. J.* **12**, 939-947.

Dollinger, M.M., Plevris, J.N., Graham, A.M., Howie, S.E.M., Hayes, P.C., and Harrison, D.J. (1998). Aberrant expression of p53 and Ki-67 during acute and chronic rejection following orthotopic liver transplantation. *Gut* **Vol. 40**, Suppl. 1, W67.

Dollinger, M.M., Plevris, J.N., Graham, A.M., Howie, S.E.M., Hayes, P.C., and Harrison, D.J. (1997). Bax and bcl-x expression during acute and chronic rejection following orthotopic liver transplantation. *Gut* **Vol. 41**, Suppl. 3, A238.

Dollinger, M.M., Plevris, J.N., Graham, A.M., Howie, S.E.M., Hayes, P.C., and Harrison, D.J. (1997). Intrahepatic proliferation of CD4+ T lymphocytes during acute and chronic rejection following orthotopic liver transplantation. *Hepatology* **Vol.26**, No. 4, Part 2, 451.

Dollinger, M.M., Howie, S.E.M., Graham, A.M., Plevris, J.N., Hayes, P.C., and Harrison, D.J. (1998). Intra-graft proliferation of naive and memory T lymphocytes during hepatic allograft rejection. *J. Path* **Vol. 184**, Suppl., A9.

LIPPINCOTT
WILLIAMS & WILKINS

A **Wolters Kluwer** Company

09/17/99

ALEXANDRA M GRAHAM
87 RANKIN DRIVE
EH9 3DG EDINBURGH
ENGLAND, U.K.

Invoice # P33028862 Customer # 000107305474 FEE: 0.00
Re: , EUROPE JNL GASTRO HEP
Spec Mat: 1998;10(7):553-557 Ph.D. thesis

CONDITIONS OF AGREEMENT

Permission is granted upon the return of this signed agreement to Lippincott Williams & Wilkins (LWW). Please sign and date this form and return with payment (if applicable) in the enclosed envelope. Please retain a copy for your files. This permission is subject to the following conditions:

1) A credit line will be prominently placed and include: for books - the author(s), title of book, editor, copyright holder, year of publication; for journals - the author(s), title of article, title of journal, volume number, issue number and inclusive pages.

2) The requestor warrants that the material shall not be used in any manner which may be considered derogatory to the title, content, or authors of the material or to LWW.

3) Permission is granted for one time use only as specified in your correspondence. Rights herein do not apply to future reproductions, editions, revisions, or other derivative works.

4) Permission granted is non-exclusive, and is valid throughout the world in the English language only.

5) LWW cannot supply the requestor with the original artwork or a "clean copy."

6) The requestor agrees to secure written permission from the author (for book material only).

7) Permission is valid if the borrowed material is original to a LWW imprint (Lippincott-Raven Publishers, Williams & Wilkins, Lea & Febiger, Harwal, Igaku-Shoin, Rapid Science, Little Brown and Company, Harper & Row Medical American Journal of Nursing Co, and Urban & Schwarzenberg - English Language).

8) Payment can be made via credit card (Amex, VISA, Discover and MC) or by check.

Card # _____ Exp Date: _____

Requestor accepts: _____ Date: 26/9/99

Bile duct cells in primary biliary cirrhosis are 'primed' for apoptosis

Alexandra M. Graham, Matthias M. Dollinger, Sarah E.M. Howie and David J. Harrison

Objective **Primary biliary cirrhosis (PBC) is characterized by progressive, immune-mediated destruction of bile ducts (< 75 μm diameter) and secondary changes related to cholestasis which may involve apoptosis. In this study we sought to examine the protein expression of genes involved in apoptosis in biliary epithelium of PBC cases.**

Design **In order to investigate the susceptibility of biliary epithelial cells to apoptosis and their ability to proliferate, we examined the expression of a number of apoptosis related proteins in early and late stage PBC and histologically normal liver control tissue using immunohistochemistry.**

Methods **Liver biopsies from 15 early (stages I and II) and 14 late (stages III and IV) cases of PBC and 15 normal cases were examined immunohistochemically for expression of p53, CD95/Fas, bax, bcl-x, bcl-2 and the proliferation marker Ki-67.**

Results **CD95/Fas, bax and bcl-x were identified in biliary epithelium in 8/15, 11/15 and 8/15 normal biopsies. Weak expression of bcl-2 was found, but p53 was not identified. In cases of PBC surviving bile ducts showed strong bax and bcl-x expression. Inflammatory infiltrates were strongly bcl-2 positive. In cases showing a marked ductular reaction there was increased reactivity for bax and bcl-x in ductules. No change in CD95/Fas or p53 expression was seen. An increase in Ki-67 positive biliary epithelial cells was seen in PBC cases, indicating cell cycle activity.**

Conclusions **Bile duct epithelium constitutively expresses several genes involved in the execution of apoptosis but these cells also retain the ability to proliferate.**

Eur J Gastroenterol Hepatol 10:553–557 © 1998 Lippincott-Raven Publishers

Keywords: apoptosis, bax, bcl-2, Fas, primary biliary cirrhosis

University Department of Pathology, Edinburgh, UK

Correspondence to A.M. Graham, University Department of Pathology, Medical School, Teviot Place, Edinburgh, EH8 9AG, UK.
Tel: 0044 131 650 2960; Fax: 0044 131 650 6528;
e-mail: ag@srv4.med.ed.ac.uk

Received 2 June 1997 **Revised** 24 November 1997
Accepted 19 January 1998

European Journal of Gastroenterology & Hepatology 1998, **10**:553–557

0954–691X © 1998 Lippincott-Raven Publishers

Introduction

Primary biliary cirrhosis (PBC) is a chronic, slowly progressive cholestatic liver disease characterized by destruction of bile ducts of < 75 μm diameter [1]. The destruction is thought to be the result of apoptosis of biliary epithelial cells, triggered by autoimmune mechanisms [reviewed in References 2 and 3]. The aetiology remains unknown although various factors such as HLA type [4] and microbiological infection have been invoked [5–8]. One of the major diagnostic criteria for PBC is the presence of high titres of anti-mitochondrial antibodies in patients' sera, frequently specific for the E2-subunit of pyruvate dehydrogenase complex (PDC-E2) [reviewed in Reference 9]. However, the precise role of autoantibodies in pathogenesis has not been established.

$CD8^+$ T lymphocytes are present in inflammatory infiltrates within the livers of PBC patients [10–13]. They are centred around small bile ducts and may initiate damage directly through apoptosis induced via CD95/Fas and CD95L/Fas ligand or perforin mediated cytotoxic mechanisms [14]. Thus, cellular components of the immune response around the targeted bile ducts may release cytokines, generating an environment which increases the neighbouring biliary epithelial cells' sensitivity to apoptosis. Tumour necrosis factor alpha (TNFα) [15], interferon gamma (IFNγ) [16] and transforming growth factor beta (TGFβ) [17–19] have been shown to cause apoptosis of hepatocytes and mRNA for each has been detected in human PBC liver [20–22].

The reason why biliary epithelial cells are specifically targeted in this disease and are vulnerable to death as an initiating event is unknown, but it does not appear to be the result of aberrant MHC Class II expression or antigen presentation by these cells as such changes occur late in the disease [23,24].

To test the hypothesis that in PBC the sensitivity of biliary epithelial cells to apoptosis is altered we examined the expression of a number of apoptosis related proteins in the bile ducts and liver of early and late stage PBC and normal control tissue. p53, Fas/CD95 and members of the bcl-2 family have been shown to interact with one another, for example p53 transcriptionally regulates Fas/CD95 and bax [25–27], and members of the bcl-2

family homo- and heterodimerize [reviewed in Reference 28]. The proliferative status of biliary epithelial cells was examined using the MIB-1 antibody against Ki-67 [29].

Methods

Biopsies

The diagnosis of PBC was made after full clinical, serological and histological assessment. Fifteen cases showed predominantly histological features seen in stage I or II (14 women, one man) and 14 showed stage III or IV (13 women, one man) according to the proposed model of disease progression reported by Scheuer [30]. Fifteen control liver samples were obtained from patients during routine lymphoma staging, psoriasis patients prior to commencing methotrexate therapy, or laparotomy during resection of colon cancer (six women, nine men). All liver tissue in the control group was reported as histologically normal and there was normal liver biochemical and synthetic function. Clinical details of the PBC cases are shown in Table 1.

Immunohistochemistry protocols

Liver tissue was fixed in 10% buffered formalin and processed to paraffin. Sections of 3 μm thickness were cut onto Dako ChemMate Capillary Gap Microscope Slides (75 mm). Sections were dewaxed in xylene and rehydrated through descending alcohols. Pre-treatment with trypsin (ICN Biomedicals Inc.) (0.1% trypsin, 0.1% calcium chloride (Sigma), pH 7.8 at 37°C for 17 min) was required with the anti-bcl-x (Autogen Bioclear UK Ltd, dilution 1/100) and anti-bax (Autogen Bioclear UK Ltd, dilution 1/200) antibodies. Microwave antigen retrieval (2 × 5 min at 1000 W; slides immersed in 1.05 g citric acid (BDH Chemicals Ltd)/500 ml H_2O, pH 6.0) was required for the anti-bcl-2 (Dako UK, dilution 1/50), anti-CD95/Fas (Immunotech UK, dilution 1/200) and anti-Ki-67 (Immunotech UK, dilution 1/100) antibodies. p53 (Dako UK) was used at 1/100 dilution. All sections were washed in running tap water then phosphate buffered saline (Oxoid)/0.1% Tween 20 (Sigma) prior to loading onto a Dako Techmate 500 automated immunocytochemistry stainer according to the manufacturer's instructions using a streptavidin/biotin and horseradish peroxidase detection system with 3′,3′-diaminobenzidine as chromogen. Negative controls omitting primary antibody were included.

Table 1 Clinical data assessing liver function of patients at time of liver biopsy. Median and (range) values of bilirubin, alanine aminotransferase, alkaline phosphatase and albumin of PBC patients at time of biopsy

Stage	Bilirubin	Alanine amino-transferase	Alkaline phosphatase	Albumin
Normal range	5–17 μM	< 35 U/l	< 130 U/l	40–50 g/l
Histological early disease (Stage I, II)	11 (5–60)	69.5 (27–194)	200 (104–891)	41.5 (29–44)
Histological late disease (Stage III, IV)	56.5 (13–256)	87 (20–945)	402.5 (115–1368)	32 (22–43)

Fig. 1

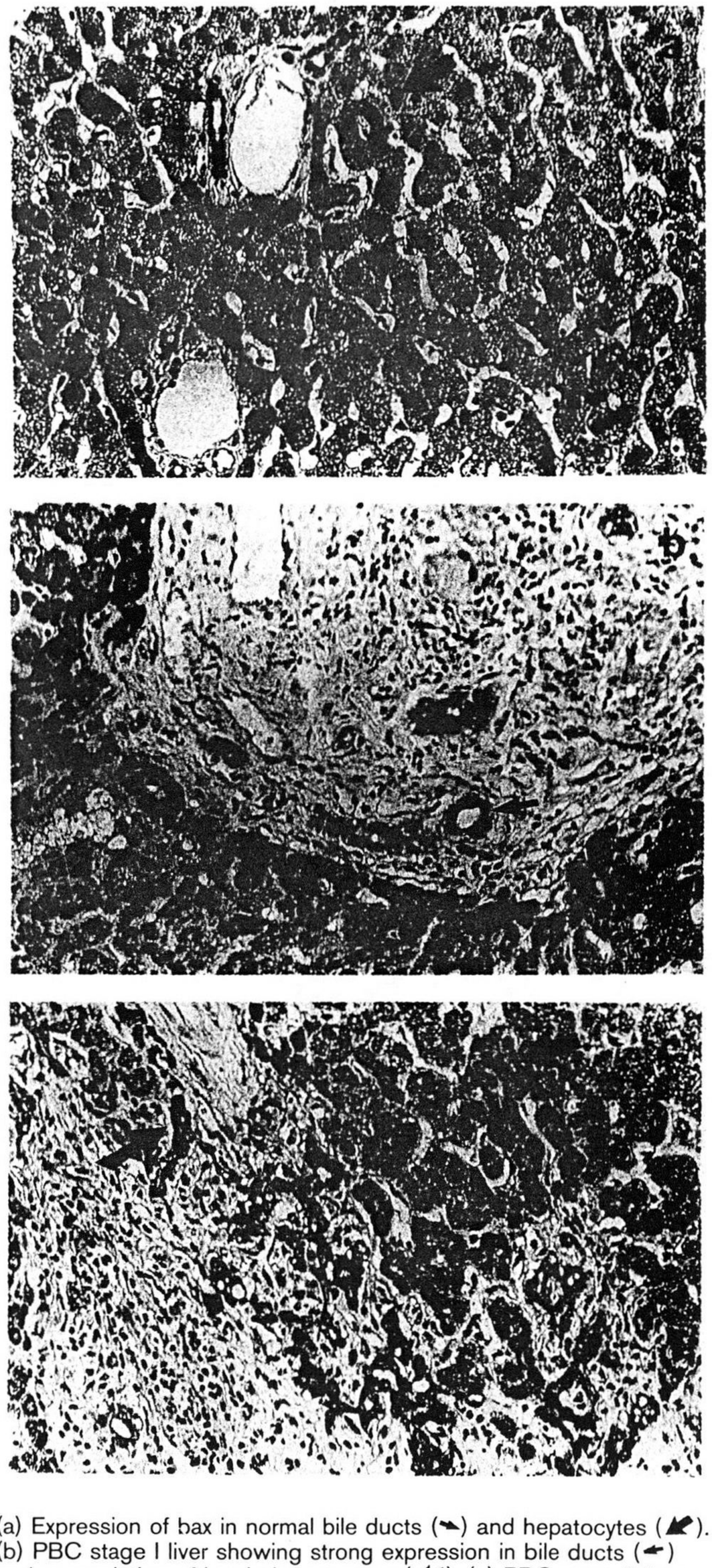

(a) Expression of bax in normal bile ducts (➘) and hepatocytes (🡅). (b) PBC stage I liver showing strong expression in bile ducts (🡄) and upregulation of bax in hepatocytes (🡅). (c) PBC stage II liver showing upregulation of bax in 'metaplastic ductules' (🡅) and hepatocytes (🡅). Original magnification × 20.

Analysis of results

It was noted that the intensity of immunostaining for bcl-2, bax, bcl-x and Fas/CD95 was homogeneous with little variation between cells within a single duct or between ducts. For this reason biopsies were scored as follows by three independent observers: strong (that is,

clearly visible granular stain at low power examination (× 4)); moderate (definite but weak immunopositivity visible at low power but needing confirmation by high power microscopic examination (× 25)); or weak/negative (equivocal staining, not consistently greater than in negative control section where primary antibody was omitted). Where inter-observer discrepancies were observed results were recorded after discussion of the individual case.

When Ki-67 or p53 were present they produced clear, discrete nuclear staining. Cases were scored positive if one or more nuclei of biliary epithelial cells was stained and negative if no positive cells were seen. Thereafter an estimate was made of the proportion of individual biliary epithelial cells stained.

Bile ducts were classified as small (<75 μm) or large (>75 μm) by measurement using the HOME (Highly Optimized Microscope Environment) semi-automated computer system.

Fig. 2

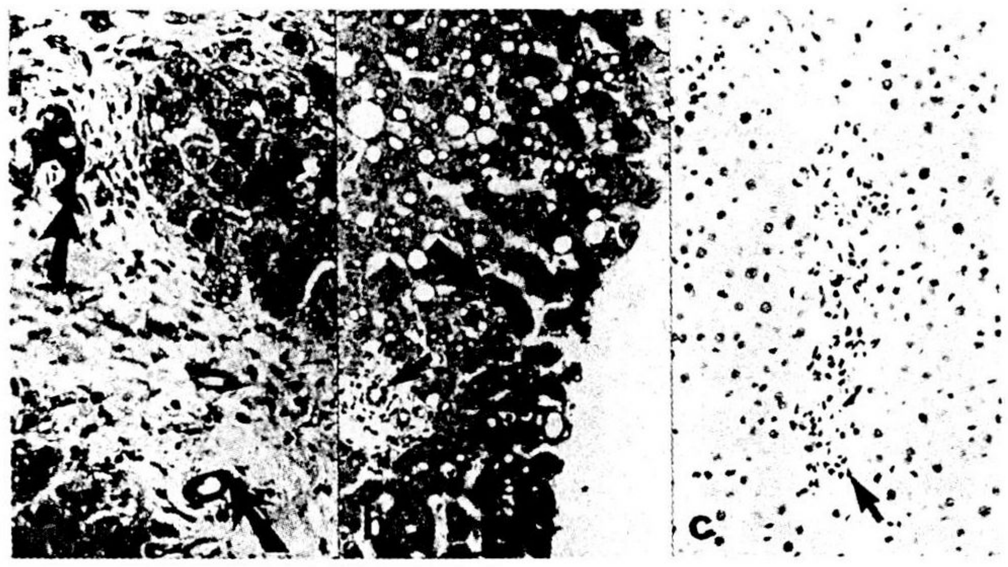

Expression of bcl-x in (a) PBC stage IV liver hepatocytes ( ) and 'metaplastic ductules' bile ducts ( ) showing upregulation, compared with (b) histologically normal liver showing only mild steatosis; hepatocytes ( ) and bile ducts ( ). (c) Negative control omitting primary antibody on histologically normal liver section; bile duct ( ). Original magnification × 20.

Results

Normal liver

bax (Fig. 1a) and bcl-x (Fig. 2b) were expressed uniformly in both hepatocytes and bile ducts but were not detected in Kupffer cells or endothelial cells. Moderate bax expression was seen in bile ducts < 75 μm in 11/15 sections (Table 2) and moderate bcl-x expression in 8/15 sections (Table 3). Only 3/15 cases expressed detectable bcl-2 in biliary epithelium. bcl-2 was not detected in hepatocytes. Eight of fifteen cases showed moderate staining of biliary epithelium with the anti-Fas/CD95 antibodies. In all cases hepatocytes were positive, the staining pattern being granular as previously reported in paraffin embedded tissue [31,32]. p53 was not detected and biliary epithelial cells did not express Ki-67.

PBC liver

Residual bile ducts showed strong staining of bax (Table 2, Fig. 1b) and bcl-x (Table 3) which appeared more intense than in normal liver. bax and bcl-x were expressed strongly in 'metaplastic' biliary ductules (Figs 1c and 2a). Lymphocytes showed intense expression of bcl-2. bcl-2 expression seen in surviving biliary epithelial cells was weak and inconsistent, similar to normal liver. No change in Fas/CD95 staining was noted. p53 was not expressed. In PBC cases up to 8% of biliary epithelial cells in large ducts and in residual small ducts expressed Ki-67 (Fig. 3). The number of positive nuclei seen was greatest in ducts > 75 μm in sections showing early stage PBC. Areas of ductal 'metaplasia' remained Ki-67 negative.

Table 2 **Results of bax immunocytochemistry in bile ducts < 75 μm and > 75 μm in normal and early and late stage PBC liver biopsy material. The figures are the number of cases with detectable strong, moderate and weak/negative expression. Expression when detected was homogeneous and uniform. *n*, total number of sections**

	bax (< 75 μm)				bax (> 75 μm)			
Stage	Strong	Moderate	Weak/negative	*n*	Strong	Moderate	Weak/negative	*n*
Normal	0	11	4	**15**	0	10	2	**12**
Early	14	1	0	**15**	12	0	0	**12**
Late	6	4	4	**14**	8	3	3	**14**

Table 3 **Results of bcl-x immunocytochemistry in in bile ducts < 75 μm and > 75 μm in normal and early and late stage PBC liver biopsy material. The figures are the number of cases with detectable strong, moderate and weak/negative expression. Expression when detected was homogeneous and uniform. *n*, total number of sections**

	bcl-x (< 75 μm)				bcl-x (> 75 μm)			
Stage	Strong	Moderate	Weak/negative	*n*	Strong	Moderate	Weak/negative	*n*
Normal	0	8	7	**15**	0	8	4	**12**
Early	14	0	1	**15**	11	0	1	**12**
Late	13	1	0	**14**	13	1	0	**14**

Fig. 3

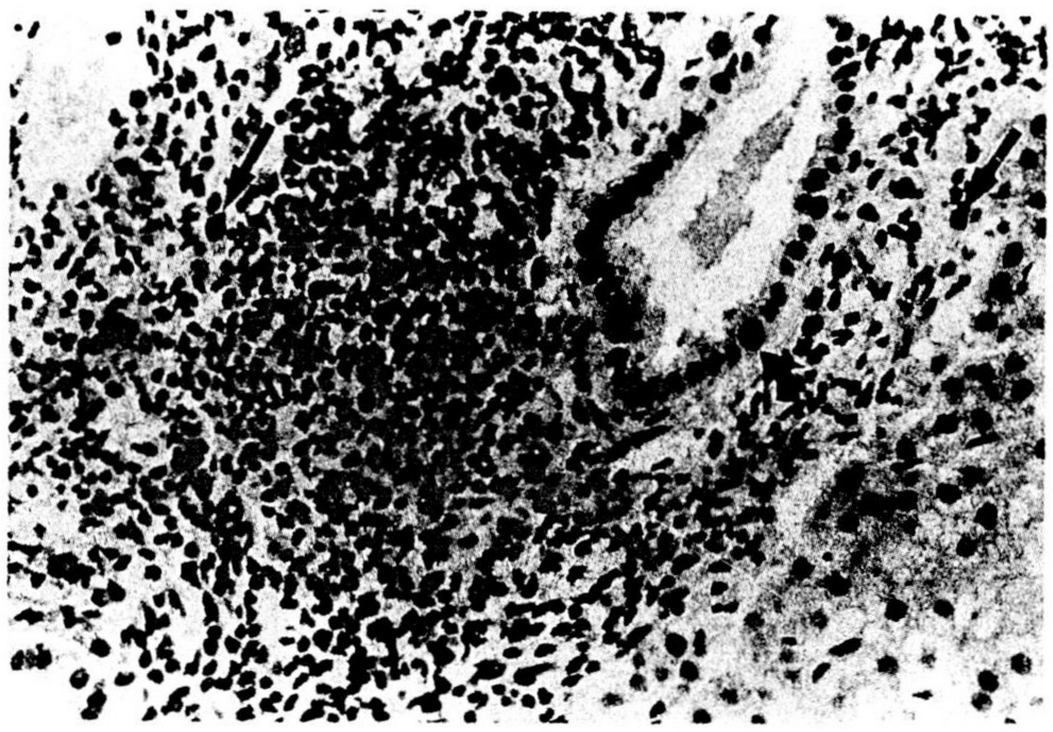

Proliferating biliary epithelial cell (↖) and infiltrating cells (↙) expressing Ki-67 in PBC stage I liver. Original magnification × 20.

Discussion

We have shown that bile ducts constitutively express pro-apoptotic proteins, particularly bax, and the apoptotic regulator bcl-x. In contrast the anti-apoptotic protein bcl-2 is barely expressed and thus appears to play little part in regulating apoptosis in biliary epithelial cells in the cases we have studied. In addition to having a phenotype that allows apoptosis there is evidence that biliary cells retain the ability to proliferate, as shown by the positive Ki-67 staining seen in PBC liver. This supports the observation of Nakanuma and Harada [33] who showed increased proliferative activity of epithelial cells in affected ducts. Charlotte *et al.* [34] have reported that normal bile ductules and small bile duct epithelium, but not large bile duct epithelium or hepatocytes, show weak expression of bcl-2 as detected immunohistochemically. However, Kuroki *et al.* [35] found no bcl-2 expression in biliary epithelium of normal or PBC livers, and other studies have shown more prominent bcl-2 staining in ductules at the borders of cirrhotic nodules relative to normal liver [36]. The absence of bcl-2 expression we report in hepatocytes is consistent with previous observations [34,37]. We have shown weak expression of Fas/CD95 in bile ducts supporting the findings of Kuroki *et al.* [35] and confirm its presence in hepatocytes [31,38–40]. The antiserum used against Fas/CD95 did not detect increased levels of Fas in the PBC livers. The presence of TNFα and IFNγ in PBC liver [20–22] might suggest an accompanying elevation in Fas expression. However, many of the experiments showing increased Fas expression by TNFα and IFNγ are *in vitro* studies using high doses of cytokine [41,42]. PBC is a chronic disease and levels of these cytokines present in the liver have not been quantified. Any changes that they may induce in Fas expression might not be sufficient for detection by immunohistochemistry, or in this disease these pleiotropic cytokines may be exerting other effects on the disease state independent of Fas.

Apoptosis of biliary epithelial cells in PBC has been shown [32,43,44] and this may be associated with the presence of cytotoxic $CD8^+$ T cells [10,11,13]. How these cells may be inducing apoptosis is unknown but a Fas-mediated mechanism is unlikely in view of the low level of expression we have seen. Such mechanisms have been invoked in a number of inflammatory diseases of the liver, especially viral hepatitis [31,38–40] and ligation of constitutively expressed Fas/CD95 on hepatocytes by antibodies results in rapid apoptosis [45–47].

Both bax and bcl-x proteins appeared to be upregulated in biliary epithelium in PBC cases. The expression of bax is induced by p53 [25,26] and the protein heterodimerizes with bcl-2, inhibiting the anti-apoptotic effect of bcl-2 [48]. We did not see upregulation of p53, suggesting p53-independent induction of bax and bcl-x may be occurring, as has been reported by others [49]. The bcl-x gene codes for two splice variants, full length bcl-x_l protein and a smaller bcl-x_s [50]. bcl-x_l protects cells from apoptosis and bcl-x_s blocks the protective effect of bcl-2 and bcl-x_l, acting as an 'anti-anti-apoptosis' protein. It is the relative ratio of homo- and heterodimeric forms of these interactive proteins which affects the apoptotic pathway. The polyclonal serum against bcl-x used does not discriminate between the long and short forms and hence we cannot draw any conclusions as to their relative ratios and role in regulating cell death in PBC biliary epithelial cells.

We have shown that the presence of proteins involved in executing apoptosis in biliary epithelial cells in PBC is consistent with previous reports of apoptosis of these cells [32,41,42]. We do not know what causes this apoptosis but we have also shown these cells are capable of regeneration. It may be that a change in the balance between apoptosis and regeneration of biliary epithelial cells during the course of disease contributes to the ultimate loss of bile ducts in PBC. However, because of the prolonged time course of this chronic disease and the secondary effects and immune response resulting from bile duct loss, intervention of apoptosis is unlikely to be a therapeutic target in the treatment of PBC.

Acknowledgements

This work was supported by the Wellcome Trust and the Sir Stanley and Lady Davidson Research Trust.

References

1 O'Donohue J, Williams R. Primary biliary cirrhosis. *Q J Med* 1996; **89**:5–13.
2 Schulte-Herman R, Bursch W, Grasl-Kraupp B. Active cell death (apoptosis) in liver. *Prog Liver Diseases* 1995; **13**:1–35.
3 Patel T, Gores GJ. Apoptosis and hepatobiliary disease. *Hepatology* 1995; **21**:1725–1741.

4 Gregory WL, Mehal W, Dunn AN,Cavanagh G, Chapman R, Fleming KA. Primary biliary cirrhosis: contribution of HLA class II allele DR8. *Q J Med* 1993; **86**:393–399.

5 Stemerowicz R, Hopf U, Moller B, Wittenbrink C, Rodloff A, Reinhardt R. Are antimitochondrial antibodies in primary biliary cirrhosis induced by R (rough)-mutants of Enterobacteriaceae? *Lancet* 1988; **ii**:1166–1170.

6 Hopf U, Moller B, Stemerowicz R, Lobeck H, Rodloff A, Freudenberg M. Relation between *Escherichia coli* R (rough)-forms in gut, lipid A in liver, and primary biliary cirrhosis. *Lancet* 1989; **ii**:1419–1422.

7 Burroughs AK, Rosenstein IJ, Epstein O, Hamilton-Miller JMT, Brumfitt W, Sherlock S. Bacteriuria in primary biliary cirrhosis. *Gut* 1994; **25**:133–137.

8 Vilagut L, Vila J, Viñas O, Parés A, Ginés A, Jiménez de Anta MT, Rodés J. Cross-reactivity of anti-*Mycobacterium gordonae* antibodies with the major mitochondrial autoantigens in primary biliary cirrhosis. *J Hepatol* 1994; **21**:673–677.

9 Coppel RL, Gershwin ME. Primary biliary cirrhosis: the molecule and the mimic. *Immunol Rev* 1995; **144**:17–49.

10 Si L, Whiteside TL, Schade RR, Starz TE, Van Thiel DH. T-lymphocyte subsets in liver tissues of patients with primary biliary cirrhosis (PBC), patients with primary sclerosing cholangitis (PSC), and normal controls. *J Clin Immunol* 1984; **4**:262–272.

11 Krams SM, Van de Water J, Coppel RL, Esquivel C, Roberts J, Ansari A, Gershwin ME. Analysis of hepatic T lymphocyte and immunoglobulin deposits in patients with primary biliary cirrhosis. *Hepatology* 1990, **12**:306–313.

12 Björkland A, Festin R, Mendel-Hartvig I, Nyberg A, Lööf L, Tötterman TH. Blood and liver infiltrating lymphocytes in primary biliary cirrhosis: increase in activated T and natural killer cells and recruitment of primed memory T cells. *Hepatology* 1991; **13**:1106–1111.

13 Hashimoto E, Lindor KD, Homburger HA, Dickson ER, Czaja AJ, Wiesner RH, Ludwig J. Immunohistochemical characterization of hepatic lymphocytes in primary biliary cirrhosis in comparison with primary sclerosing cholangitis and autoimmune chronic active hepatitis. *Mayo Clin Proc* 1993; **68**:1049–1055.

14 Kojima H, Shinohara N, Hanaoka S, Someya-Shirota Y, Takagaki Y, Ohno H. Two distinct pathways of specific killing revealed by perforin mutant cytotoxic T lymphocytes. *Immunity* 1994; **1**:357–364.

15 Leist M, Gantner F, Bohlinger I, Germann PG, Tiegs G, Wendel A. Murine hepatocyte apoptosis induction *in vitro* and *in vivo* by TNF-alpha requires transcriptional arrest. *J Immunol* 1994; **153**:1778–1788.

16 Morita M, Watanabe Y, Akaike T. Protective effect of hepatocyte growth factor on interferon-gamma-induced cytotoxicity in mouse hepatocytes. *Hepatology* 1995; **21**:1585–1593.

17 Lin J-K, Chou C-K. *In vitro* apoptosis in the human hepatoma cell line induced by transforming growth factor β_1. *Cancer Res* 1992; **52**:385–388.

18 Oberhammer FA, Pavelka M, Sharma S, Tiefenbacher R, Purchio AF, Bursch W, Schulte-Hermann R. Induction of apoptosis in cultured hepatocytes and in regressing liver by transforming growth factor β_1. *Proc Natl Acad Sci USA* 1992; **89**:5408–5412.

19 Fukuda K, Kojiro M, Chiu J-F. Induction of apoptosis by transforming growth factor-β1 in the rat hepatoma cell line McA-RH7777: a possible association with tissue transglutaminase expression. *Hepatology* 1993; **18**:945–953.

20 Tovey MG, Gugenheim J, Guymarho J, Blanchard B, Vanden Broeke C, Gresser I. Genes for interleukin-1, interleukin-6, and tumor necrosis factor are expressed at markedly reduced levels in the livers of patients with severe liver disease. *Autoimmunity* 1991; **10**:297–310.

21 Martinez OM, Villanueva JC, Gershwin ME, Krams SM. Cytokine patterns and cytotoxic mediators in primary biliary cirrhosis. *Hepatology* 1995; **21**:113–119.

22 Shindo M, Mullin GE, Braun-Elwert L, Bergasa NV, Jones EA, James SP. Cytokine mRNA expression in the liver of patients with primary biliary cirrhosis and chronic hepatitis B. *Clin Exp Immunol* 1996; **105**:254–259.

23 Tsuneyama K, Van de Water J, Leung PSC, Cha S, Nakanuma Y, Kaplan M. Abnormal expression of the E2 component of the pyruvate dehydrogenase complex on the luminal surface of biliary epithelium occurs before major histocompatibility complex class II and B1/B7 expression. *Hepatology* 1995; **21**:1031–1037.

24 Spengler U, Leifield L, Braunschweiger I, Dumoulin FL, Lechmann M, Sauerbruch T. Anomalous expression of costimulatory molecules B7–1, B7–2 and CD28 in primary biliary cirrhosis. *J Hepatol* 1997; **26**:31–36.

25 Miyashita T, Krajewski S, Krajewska M, Wang HG, Lin HK, Liebermann DA. Tumor suppressor p53 is a regulator of *bcl-2* and *bax* gene expression *in vitro* and *in vivo*. *Oncogene* 1994; **9**:1799–1805.

26 Selvakumaran M, Lin H-K, Miyashita T, Wang HG, Krajewski S, Reed JC. Immediate early up-regulation of bax expression by p53 but not TGFβ1: a paradigm for distinct apoptotic pathways. *Oncogene* 1994; **9**:1791–1798.

27 Owen-Schaub LB, Zhang W, Cusack JC, Angelo LS, Santee SM, Fujiwara T. Wild-type human p53 and a temperature-sensitive mutant induce Fas/APO-1 expression. *Mol and Cell Biol* 1995; **15**:3032–3040.

28 Wyllie AH. Death gets a brake. *Nature* 1994; **369**:272–273.

29 Gerdes J, Li L, Schlueter C, Duchrow M, Wohlenberg C, Gerlach C. Immunobiochemical and molecular biologic characterization of the cell proliferation-associated nuclear antigen that is defined by monoclonal antibody Ki-67. *Am J Pathol* 1991; **138**:867–873.

30 Scheuer PJ. *Liver Biopsy Interpretation*. 4th Edn. London: W.B. Saunders; 1988.

31 Mochizuki K, Hayashi N, Hiramatsu N, Katayama K, Kawanishi Y, Kasahara A. Fas antigen expression in liver tissues of patients with chronic hepatitis B. *J Hepatol* 1996; **24**:1–7.

32 Nakanuma Y, Ohta G, Kono N, Koayashi K, Kato Y. Electron microscopic observation of destruction of biliary epithelium in primary biliary cirrhosis. *Liver* 1983; **3**:238–248.

33 Nakanuma Y, Harada K. Florid duct lesion in primary biliary cirrhosis shows highly proliferative activities. *J Hepatol* 1993; **19**:216–221.

34 Charlotte F, L'Hermine A, Martin N, Geleyn Y, Nollet M, Gaulard P, Zafrani ES. Immunohistochemical detection of bcl-2 protein in normal and pathological human liver. *Am J Pathol* 1994; **144**:460–465.

35 Kuroki T, Seki S, Kawakita N, Nakatani K, Hisa T, Kitada T, Sakaguchi H. Expression of antigens related to apoptosis and cell proliferation in chronic nonsuppurative destructive cholangitis in primary biliary cirrhosis. *Virchows Arch* 1996; **429**:119–129.

36 Koukoulis GK, Shen J, Iyer A, Foster P, Ganger D, Williams J. Immunolocalization of bcl-2 and MET oncoproteins in biliary ductules and ducts of normal liver, cirrhosis and ductopenic rejection. *AASLD Meeting*, Chicago 1995; Abstract.

37 Krajewski S, Krajewska M, Shabaik A, Miyashita T, Wang HG, Reed JC. Immunohistochemical determination of in-vivo distribution of bax, a dominant inhibitor of bcl-2. *Am J Path* 1994; **145**:1323–1336.

38 Hiramatsu N, Hayashi N, Katayama K, Mochizuki K, Kawanishi Y, Kasahara A. Immunohistochemical detection of Fas antigen in liver tissue of patients with chronic hepatitis C. *Hepatology* 1994; **19**:1354–1359.

39 Galle PR, Hofmann WJ, Walczak H, Schaller H, Otto G, Stremmel W. Involvement of the CD95 (APO-1/Fas) receptor and ligand in liver damage. *J Exp Med* 1995; **182**:1223–1230.

40 Okazaki M, Hino K, Fujii K, Hanada H, Nakakishi Y, Kanazawa S. Immunohistochemical study of Fas antigen in liver of patients with chronic hepatitis and autoimmune liver disease. *Int Hepatol Comm* 1995; **3**:285–289.

41 Maciejewski J, Selleri C, Anderson S, Young NS. Fas antigen expression on CD34+ human marrow cells is induced by interferon gamma and tumour necrosis factor and potentiates cytokine-mediated hematopoietic suppression *in vitro*. *Blood* 1995; **85**:3183–3190.

42 Panayiotidis P, Ganeshaguru K, Foroni L, Hoffbrand AV. Expression and function of the FAS antigen in B chronic lymphocytic leukemia and hairy cell leukemia. *Leukemia* 1995; **9**:1227–1232.

43 Bernuau D, Feldmann G, Degott C, Gisselbrecht C. Ultrastructural lesions of bile ducts in primary biliary cirrhosis *Hum Path* 1981; **12**:782–793.

44 Koga H, Sakisaka S, Ohishi M, Sata M, Tanikawa K. Nuclear DNA fragmentation in biliary epithelial cells and in hepatocytes in primary biliary cirrhosis. *AASLD Meeting*, Chicago 1995; Abstract.

45 Trauth BC, Klas C, Peters AM, Matzku S, Moller P, Falk W. Monoclonal antibody-mediated tumour regression by induction of apoptosis. *Science* 1989; **245**:301–305.

46 Yonehara S, Ishii A, Yonehara M. A cell-killing monoclonal antibody (anti-Fas) to a cell surface antigen co-downregulated with the receptor of tumour necrosis factor. *J Exp Med* 1989; **169**:1747–1756.

47 Ogasawara J, Watanabe-Fukunaga R, Adachi M, Matsuzawa A, Kasugai T, Kitamura Y. Lethal effect of the anti-Fas antibody in mice. *Nature* 1993; **364**:806–809.

48 Oltvai ZN, Milliman CL, Korsmeyer SJ. bcl-2 heterodimerizes *in vivo* with a conserved homolog, bax, that accelerates programmed cell death. *Cell* 1993; **74**:609–619.

49 Hung WC, Chiuang LY. Induction of apoptosis by sphingosine-1-phosphate in human hepatoma cells is asssociated with enhanced expression of bax gene product. *Biochem Biophys Res Commun* 1996; **229**:11–15.

50 Boise LH, González-García M. bcl-x, a bcl-2-related gene that functions as a dominant regulator of apoptotic cell death. *Cell* 1993; **74**:597–608.